

INFORMATION TO USERS

This manuscript has been reproduced from the microfilm master. UMI films the text directly from the original or copy submitted. Thus, some thesis and dissertation copies are in typewriter face, while others may be from any type of computer printer.

The quality of this reproduction is dependent upon the quality of the copy submitted. Broken or indistinct print, colored or poor quality illustrations and photographs, print bleedthrough, substandard margins, and improper alignment can adversely affect reproduction.

In the unlikely event that the author did not send UMI a complete manuscript and there are missing pages, these will be noted. Also, if unauthorized copyright material had to be removed, a note will indicate the deletion.

Oversize materials (e.g., maps, drawings, charts) are reproduced by sectioning the original, beginning at the upper left-hand corner and continuing from left to right in equal sections with small overlaps. Each original is also photographed in one exposure and is included in reduced form at the back of the book.

Photographs included in the original manuscript have been reproduced xerographically in this copy. Higher quality 6" x 9" black and white photographic prints are available for any photographs or illustrations appearing in this copy for an additional charge. Contact UMI directly to order.

UMI

A Bell & Howell Information Company
300 North Zeeb Road, Ann Arbor MI 48106-1346 USA
313/761-4700 800/521-0600

Glaciation and Neotectonic Deformation on the
Western Olympic Peninsula, Washington

by

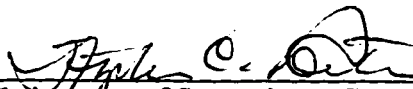
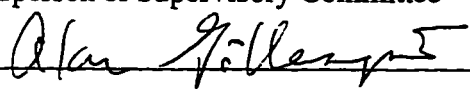
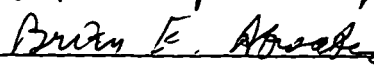
Glenn David Thackray

A dissertation submitted in partial fulfillment
of the requirements for the degree of

Doctor of Philosophy

University of Washington

1996

Approved by 
Chairperson of Supervisory Committee



Program Authorized
to Offer Degree Department of Geological Sciences

Date December 19, 1996

UMI Number: 9716931

**UMI Microform 9716931
Copyright 1997, by UMI Company. All rights reserved.**

**This microform edition is protected against unauthorized
copying under Title 17, United States Code.**

UMI
300 North Zeeb Road
Ann Arbor, MI 48103

Doctoral Dissertation

In presenting this dissertation in partial fulfillment of the requirements for the Doctoral degree at the University of Washington, I agree that the Library shall make its copies freely available for inspection. I further agree that extensive copying of this dissertation is allowable only for scholarly purposes, consistent with "fair use" as prescribed in the U.S. Copyright Law. Requests for copying or reproduction of this dissertation may be referred to University Microfilms, 1490 Eisenhower Place, P.O. Box 975, Ann Arbor, MI 48106, to whom the author has granted "the right to reproduce and sell (a) copies of the manuscript in microform and/or (b) printed copies of the manuscript made from microform."

Signature *Alan J. Fink*

Date 12/13/96

University of Washington

Abstract

Glaciation and Neotectonic Deformation on the
Western Olympic Peninsula, Washington

by Glenn Thackray

Chairperson of the Supervisory Committee:
Professor Stephen C. Porter
Department of Geological Sciences

The Quaternary stratigraphic and geomorphic sequence on the western Olympic Peninsula records mountain glaciation and coastal tectonic deformation. The sequence includes drift from six glacier advances during the last (Wisconsinan) glacial cycle and from two glaciations that preceded the last interglaciation. The Lyman Rapids drift records the most extensive Wisconsinan advance. Stratigraphic and chronologic evidence suggest that the advance dates to early or middle Wisconsin time (isotope stage 4 or 3) or to the last interglaciation (IS 5b). The Hoh Oxbow and Twin Creeks drifts record five Hoh valley advances, constrained by radiocarbon dates of plant matter from lacustrine sediments, outwash, and till. Hoh Oxbow advances occurred between 39,000 and ca. 36,000 (Hoh Oxbow Ø), between 29,000 and 27,000 (Hoh Oxbow I), and between ca. 23,000 and 19,500 ¹⁴C yr BP (Hoh Oxbow II). Twin Creeks readvances occurred between 19,100 and ca. 18,300 ¹⁴C yr BP (Twin Creeks I) and possibly ca. 14,000 ¹⁴C yr BP (Twin Creeks II). Maximum glaciation did not necessarily coincide with maximum cooling previously inferred from local pollen records: correlation of the glacier and pollen records suggests an approximately inverse relationship between glacier extent and stadial temperature depression, suggesting strong dependence of glacier mass balance on Pacific moisture sources.

Coastal bluffs expose a pre-last interglacial sediment sequence, a last-interglacial wave-cut surface, and a post-last-interglacial outwash/alluvium sequence. Outwash deposition dominated sedimentation near valley mouths, while non-glacial detritus from adjacent uplands was dominant between the Queets and Hoh rivers. Patterns of the three parts of the stratigraphic sequence define a broad syncline. The wave-cut surface and associated cover sediments, inferred from stratigraphic evidence to have originated during IS 5e or 5c, most clearly define the syncline. Net uplift rates for the wave-cut surface over the inferred 125,000 and 105,000 yr since formation range from 0 to 0.5

mm/yr. Magnetically reversed sediment in the pre-last-interglacial sequence suggests little or no net uplift of sediments deposited before 780,000 yr BP.

TABLE OF CONTENTS

	<i>Page</i>
LIST OF FIGURES.....	viii
LIST OF TABLES	ix
CHAPTER 1: DISCIPLINARY CONTEXT AND PHYSICAL SETTING	1
INTRODUCTION.....	1
SIGNIFICANCE OF PROJECT	1
SIGNIFICANCE OF GLACIAL RECORD	3
SIGNIFICANCE OF NEOTECTONIC RECORD.....	4
PROJECT SETTING	7
BEDROCK GEOLOGY	8
METHODS OF STUDY.....	9
MAPPING OF DRIFT UNITS.....	9
STRATIGRAPHIC DESCRIPTION	10
DATING OF GLACIAL AND NONGLACIAL DEPOSITS	10
CHAPTER 2:GLACIAL GEOLOGY OF THE QUEETS AND HOH RIVER VALLEYS.....	11
INTRODUCTION.....	11
NOMENCLATURE.....	11
INFLUENCE OF VALLEY PHYSIOGRAPHY ON GLACIAL GEOLOGY.....	13
DESCRIPTION OF DRIFTS AND CHRONOLOGIC CONTROL	15
WOLF CREEK DRIFT.....	15
Morphology	15
Seacliff Stratigraphy.....	16
Chronology.....	18
WHALE CREEK DRIFT.....	18
Morphology	19
Queets Valley.....	19
Hoh Valley	19
Snahapish and Clearwater Valleys.....	20
Stratigraphy	21
Chronology.....	21
LYMAN RAPIDS DRIFT.....	22
Queets Valley.....	22
Morphology	22
Stratigraphy	25
Snahapish and Clearwater Valleys.....	25
Hoh Valley	26
Morphology	26
Stratigraphy	27
Chronology of Lyman Rapids Glaciation.....	29
HOH OXBOW DRIFT	29
Queets Valley.....	32
Morphology	32
Stratigraphy	33
Hoh Valley	33
Morphology	33
Stratigraphy	35
Chronology of Hoh Oxbow Glaciation	38

Summary of Hoh Oxbow Glaciation—Three Advances Or Two?	42
TWIN CREEKS DRIFT.....	44
Morphology	44
Stratigraphy	45
Chronology.....	47
SUMMARYEXTENT AND CHRONOLOGY OF GLACIER ADVANCES DURING THE LAST GLACIAL CYCLE.....	47
GLACIER RECONSTRUCTIONS AND PALEO-EQUILIBRIUM LINE ALTITUDES	49
COMPARISON OF WESTERN OLYMPIC GLACIAL RECORD WITH OTHER CLIMATIC PROXY RECORDS	51
LOCAL AND REGIONAL CLIMATIC PROXY RECORDS.....	51
Pollen And Beetle Records	51
Other Olympic Mountain Glacial Sequences	54
Regional Ice-Sheet And Mountain Glacier Records	55
Discussion.....	56
MARINE OXYGEN ISOTOPE AND SEDIMENT RECORDS.....	57
Discussion.....	60
CONCLUSIONS	60
CHAPTER 3: COASTAL STRATIGRAPHY AND NEOTECTONIC DEFORMATION.....	62
INTRODUCTION.....	62
PREVIOUS STRATIGRAPHIC WORK	62
NOMENCLATURE.....	64
COASTAL STRATIGRAPHY	64
STRATIGRAPHIC FRAMEWORK.....	64
DETAILED STRATIGRAPHIC FRAMEWORK AND SECTIONS.....	67
Hoh River to Abbey Island.....	67
South Hoh Section	67
Lateral Correlations.....	70
Abbey Island to Steamboat Creek	71
Destruction Island Viewpoint Section.....	73
Age of the Wave-Cut Surface	76
Age of Lyman Rapids Outwash.....	76
Lateral Correlations.....	77
Steamboat Creek to Browns Point.....	78
Beach Trail 4 Section.....	78
Lateral Correlations.....	81
Browns Point to Beach Trail 2.....	82
North Kalaloch Section	82
Lateral Correlations.....	85
Beach Trail 2 to Queets River	85
Queets River to Whale Creek North.....	85
Whale Creek North to Raft River	88
Whale Creek Section	88
Lateral Correlations.....	92
COASTAL STRATIGRAPHIC EVOLUTION.....	94

NEOTECTONIC DEFORMATION.....	97
KALALOCH SYNCLINE	97
Deformation of the Steamboat Creek Formation.....	98
DEFORMATION RATES.....	100
Age of the Wave-cut Surface:	
Summary of Evidence.....	100
North Limb of Syncline.....	106
South Limb of Syncline.....	110
DISCUSSION.....	112
Secular Uplift Rates	113
POSSIBLE ORIGINS OF THE KALALOCH SYNCLINE.....	113
SUMMARY.....	114
FUTURE RESEARCH.....	115
CHAPTER 4: QUATERNARY STRATIGRAPHIC AND GEOMORPHIC	
EVOLUTION OF THE WESTERN OLYMPIC PENINSULA.....	117
INTRODUCTION.....	117
INTERACTION BETWEEN QUATERNARY GLACIAL	
CYCLES AND TECTONIC DEFORMATION.....	117
GEOMORPHIC AND STRATIGRAPHIC EVOLUTION OF THE	
RIVER VALLEYS	118
THE LAST INTERGLACIATION (IS 5).....	118
THE LAST GLACIAL CYCLE (IS 4 THROUGH IS 2)	120
GEOMORPHIC AND STRATIGRAPHIC EVOLUTION OF THE	
COASTAL ZONE.....	126
THE LAST INTERGLACIATION (IS 5).....	128
THE LAST GLACIAL CYCLE (IS 4 THROUGH IS 2)	128
THE HOLOCENE AND THE FUTURE.....	129
LIST OF REFERENCES.....	131
POCKET MATERIALS:	
PLATE 1: Quaternary Geologic Map of the Hoh, Queets, and Lower	
Clearwater Valleys, Washington	
PLATE 2: Stratigraphic Cross-Section, Hoh River to Raft River	

LIST OF FIGURES

<i>Number</i>	<i>Page</i>
1.1 Map showing location of project area	2
1.2 Map showing geographic relationship to the Cascadia Subduction Zone.....	5
2.1 Map of western Olympic Peninsula, showing locations mentioned in text.....	12
2.2 Longitudinal profiles of Queets valley outwash valley trains.....	24
2.3 Longitudinal profiles of Hoh valley outwash valley trains	28
2.4 Correlated sections in the middle Hoh River valley	36
2.5 Correlated sections in the South Fork Hoh valley	46
2.6 Glacier time-distance diagrams for the last glacial cycle (IS 4 through IS 2)	48
2.7 Reinterpretation of Heusser's (1972) pollen sequence	52
2.8 Correlation of western Olympic chronology with north-Atlantic records.....	58
3.1 Map of central Olympic Coast.....	63
3.2 Generalized stratigraphic framework between the Hoh and Raft Rivers	65
3.3 Sketch of stratigraphic sequence between the Hoh River and Abbey Island area	68
3.4 Stratigraphic section 1.9 km south of the Hoh River.....	69
3.5 Sketch of stratigraphic sequence between Abbey Island area and Steamboat Creek.....	72
3.6 Destruction Island Viewpoint area.....	74
3.7 Stratigraphic section 150 m south of Destruction Island Viewpoint.....	75
3.8 Sketch of stratigraphic sequence between Steamboat Creek and Brown's Point.....	79
3.9 Stratigraphic section at outlet of Beach Trail 4.....	80
3.10 Sketch of stratigraphic sequence between Brown's Point and Beach Trail 2	83
3.11 Stratigraphic section 2.0 km north of Kalaloch	84
3.12 Sketch of stratigraphic sequence between Beach Trail 2 and Queets River	86
3.13 Sketch of stratigraphic sequence between Queets River and Whale Creek ...	87
3.14 Sketch of stratigraphic sequence between Whale Creek and Raft River	89
3.15 Seacliff exposure 2.1 km north of Whale Creek.....	90
3.16 Stratigraphic section 0.4 km north of Whale Creek	91
3.17 Seacliff below Destruction Island Viewpoint.....	99
3.18 Seacliff 0.3 km north of Whale Creek	101
3.19 Seacliff 0.8 km south of Whale Creek	102
3.20 Uplift rates (mm/yr) inferred from tide gauges and leveling.....	103
3.21 Observed deformation of buried wave-cut surface and profile of geodetically measured coastal uplift.....	104
3.22 Schematic cross-section showing projection of wave-cut surface	108
3.23 Uplift rate comparisons for north limb of the Kalaloch syncline.....	109
3.24 Uplift rate comparisons for south limb of the Kalaloch syncline	111
4.1a Schematic map of project area ca. 125,000 yr BP (IS 5e).....	119
4.1b Schematic map of project area prior to Lyman Rapids advance.....	121
4.2a Schematic map of project area during Lyman Rapids advance.....	122
4.2b Schematic map of project area ca. 40,000 yr BP (IS 3).....	123
4.2c Schematic map of project area ca. 27,000 yr BP (IS 3).....	125
4.2d Schematic map of project area ca. 18,000 yr BP (IS 2).....	127

LIST OF TABLES

<i>Number</i>		<i>Page</i>
2.1	Limiting dates for the Lyman Rapids drift.....	30
2.2	Limiting dates for the Hoh Oxbow and Twin Creeks drifts	39
2.3	Estimated ELA's and Δ ELA's for stadial advances of the last glacial cycle.....	50

ACKNOWLEDGMENTS

This project began in the fall of 1991 at the encouragement of Steve Porter, to whom I am indebted for guidance, constructive criticism, and practical assistance in and out of the field. The other members of my supervisory committee—Brian Atwater, Alan Gillespie, Larry Bliss, David Montgomery, and Richard Stewart—also deserve great thanks for helping to focus and hone the project and its results.

At the outset, the project was designed partly to fit the needs of the state map program of the Washington Division of Geology and Earth Resources. While funding for the program collapsed before this project really got underway, DGER personnel were very helpful throughout. In particular, Wendy and Alsea Gerstel spent many cold and/or wet days (plus a nice one every now and then) helping out in the field, as well as providing much encouragement and logistical assistance. DGER's Josh Logan also provided help, good humor, and some exquisite chanterelle mushrooms during a particularly miserable field excursion.

The original thrust of the project was to document the glacial sequence and construct a detailed radiocarbon chronology for the last glaciation. During the summer of 1993, it appeared that the chronology would be less detailed (and thus less interesting) than had been hoped. With my optimism for the project beginning to fade, two events took place that would reinvigorate the project: 1) I took note of tectonic deformation of the coastal sequence, first described decades earlier, and 2) I ran into Frank Pazzaglia, then at Yale University. At Frank's encouragement, the project was refocussed to include a treatment of the tectonic as well as the glacial history of the area. Ever since, our collaboration has been a very fruitful one, and I am indebted to Frank for his comradery, inspiration, and advice. The new, dual focus led to broader interest in the project as well as new funding possibilities.

Several other people have provided invaluable assistance through the course of the project. Maria Hansler, Alison Wiens, James Thackray, Maya Thackray, Garren Mayer, Julie Williams, Rebecca Bendick, and Robert Virtue provided assistance in the field. Leon Sawyko assisted with laboratory work. Ted Reid and Dawn Welsh (Idaho State University) and Harvey Greenberg (University of Washington) shepherded the glacial-geologic map from hand-drawn to digitized GIS format. Participants in a 1994 Geological Society of America field trip and a 1996 Friends of the Pleistocene field trip provided invaluable feedback at important points in the project.

The project has been completed in the two years since I joined the faculty of Idaho State University. I am indebted to my colleagues, particularly Tom Ore and Dave Rodgers, for placing and retaining faith in me, for freeing my time up as much as possible to work on the project, and for imposing the right amount and right kind of good-natured, constructive prodding to "get the thing done."

The project has been funded by NSF grant EAR 9405659, by student research grants from the Geological Society of America and the Society of Sigma Xi, and by the Graduate Support Fund and Richard Fuller and George Goodspeed Fellowships in the University of Washington Department of Geological Sciences.

CHAPTER 1 DISCIPLINARY CONTEXT AND PHYSICAL SETTING

INTRODUCTION

Glaciation, sea-level fluctuation, and tectonic deformation have dominated the Quaternary history of the western Olympic Peninsula. Large valley glaciers have advanced repeatedly down the major river valleys of the Olympic western slope, delivering copious amounts of sediment to the coastal lowlands. The fall and rise of sea level coincident with the glacial cycles has allowed the construction and subsequent erosion of broad outwash fans and thick valley fills, as well as the cutting of shorelines and wave-washed surfaces and the deposition of marine sediments. Neotectonic deformation has warped the strata and landforms along the coast, revealing older portions of the Quaternary sequence and their telltales of tectonic processes. The complex interplay of these diverse processes has left an extensive stratigraphic and geomorphic record, which is revealed in river valleys and along the Pacific coast.

The western Olympic Peninsula (Figure 1.1) is unique in the conterminous United States in its preservation of such a detailed record of glaciation and neotectonic glaciation. This dissertation describes the sediments and landforms of the area, and interprets their record in terms of the climatic and tectonic processes that have operated and continue to operate in the region. The dissertation consists of four chapters. Chapter 1 introduces the physiographic, geologic, tectonic, and climatic setting of the study area, and discusses the disciplinary context of the project. Chapter 2 describes the glacial morphologic and stratigraphic record preserved in the Hoh and Queets river valleys and adjacent seacliffs, and from that record synthesizes the glacial and climatic history of the Olympic western slope. Chapter 3 describes in detail the coastal stratigraphic sequence between the Hoh and Raft rivers and the structures that deform that sequence. Those structures are interpreted in light of Cascadia Subduction Zone processes. Finally, Chapter 4 summarizes the combined influences of glaciation, sea-level fluctuation, and tectonic deformation on the development of the western Olympic landscape.

SIGNIFICANCE OF PROJECT

While the records of glaciation and neotectonic deformation on the western Olympic Peninsula are physically intertwined, the contributions of the two principal

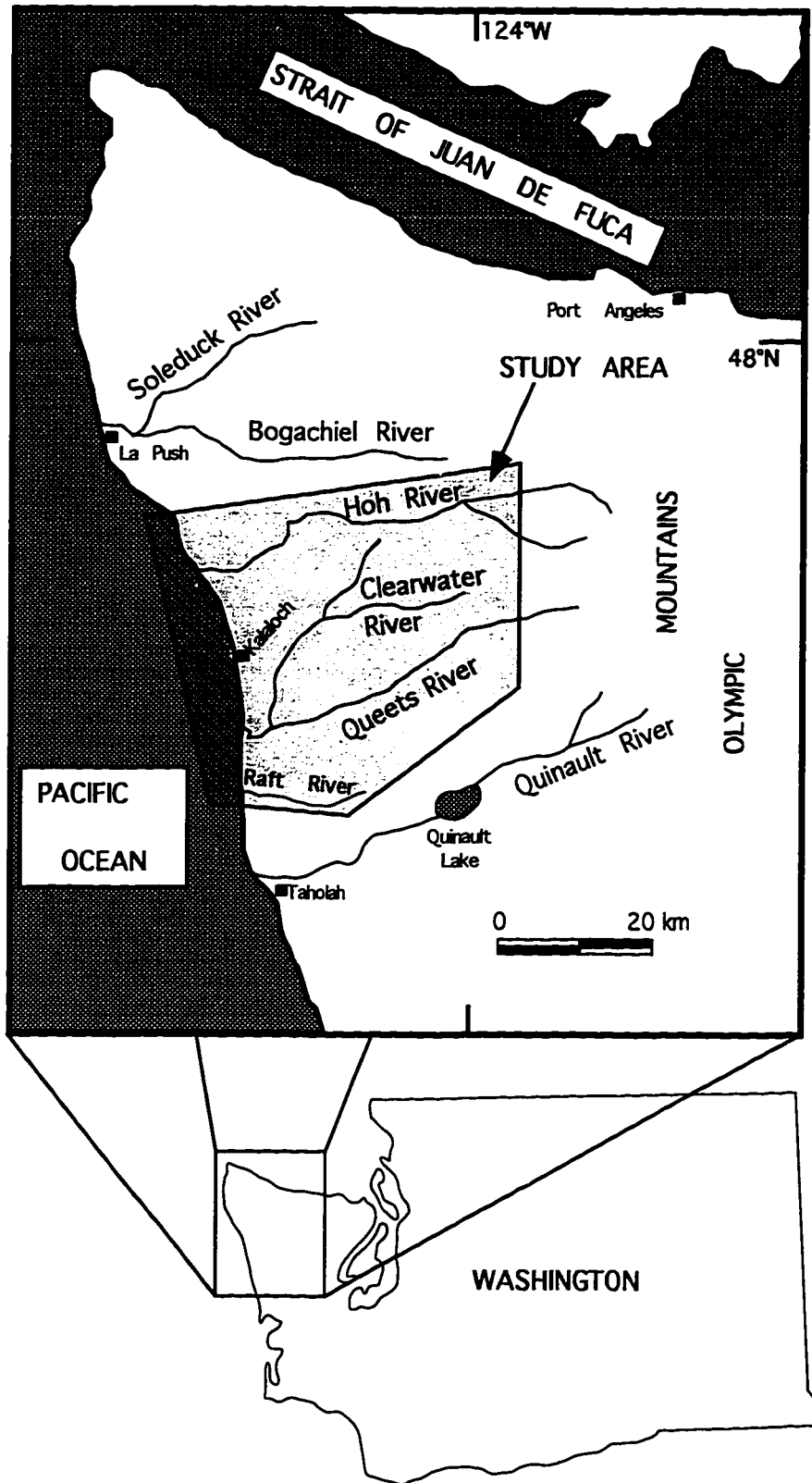


Figure 1.1: Map showing location of project area

project foci lie in distinct fields. The glacial record holds significance for the understanding of climate during glacial ages. The neotectonic record contributes to the understanding of tectonic processes and seismic hazards on the Cascadia subduction zone.

SIGNIFICANCE OF GLACIAL RECORD

The importance of mountain glacier records lies in the sensitivity of mountain glaciers to climatic variations. Temperate mountain glaciers respond rapidly to climatic changes, and can leave geomorphic and sedimentary records of high-frequency climatic oscillations. Although terrestrial glacial records are, by their nature, imperfect and potentially ambiguous, multiple glacial events sometimes can be discerned. Further, the relative magnitude of the corresponding climatic changes can be estimated through the reconstruction of snowline elevations (i.e., equilibrium-line altitudes).

Despite decades of glacial geologic research in western North America, chronologic data for mountain glacier fluctuations remains quite limited, and important gaps in knowledge persist. Most chronologic control is limited to relative-age methods [e.g., Colman and Pierce (1983, 1986)]; to experimental geochronologic methods such as cosmogenic isotope dating [e.g., Cerling (1990), Gosse et al. (1995), Phillips et al. (1990), Swanson (1994)] and cation-ratio and radiocarbon dating of rock varnish (Dorn et al., 1987; cf. Bierman and Gillespie, 1994); to minimum-limiting radiocarbon ages from bogs and lakes behind moraines; or to sparse maximum-limiting radiocarbon ages on samples within and beneath till. The limited chronologic control leaves important questions unanswered: How often and at what times did mountain glaciers advance during the last glaciation? Were the mountain-glacier maxima synchronous locally and regionally? Were the mountain-glacier maxima synchronous with ice-sheet maxima?

These questions have special relevance in the Pacific Northwest. During the Fraser Glaciation (late Wisconsin), Cascade Range glaciers appear to have reached their maximum extents several thousand years earlier than did the Cordilleran ice sheet (Waitt and Thorson, 1983). Stratigraphic evidence and limited chronologic data suggest that at least some Cascade glaciers reached their maximum extent about 18,000 ^{14}C yr BP (Evans Creek Stade), while the detailed Puget Lowland ice-sheet chronology indicates an ice-sheet maximum (Vashon Stade) about 14,000 ^{14}C yr BP. Carson (1970) described stratigraphic evidence indicating that mountain glaciers originating in the southeastern Olympic Mountains similarly had maxima nonsynchronous with those of

the Cordilleran ice sheet, during the Fraser Glaciation and at least one earlier glaciation. Were the western Olympic glacier maxima also nonsynchronous with those of the ice sheet? If so, did they readvance during the Vashon Stade and/or during late-glacial time?

The setting of glacial landforms and sediments on the western Olympic Peninsula is conducive to the construction of a mountain-glacier chronology. The large valley glaciers descended repeatedly onto the broad coastal lowlands, leaving a voluminous geomorphic and stratigraphic record. That record is well preserved and is exposed in seacliffs, stream cuts, and road cuts, albeit masked by dense vegetation in most areas. Furthermore, the glaciers descended into a relatively mild, maritime region, where woody vegetation persisted during glacial times (Heusser, 1964, 1972). Wood is common in glacial and nonglacial sediments of the project area. Numerous finite radiocarbon ages obtained in this and other studies provide substantial chronologic data for glacier fluctuations. Paleomagnetic polarity measurements of fine-grained glacial and non-glacial sediments augment the radiocarbon chronology.

The unique sedimentologic setting of the Olympic coast has also produced a nearly unrivaled interglacial-glacial stratigraphic sequence. Non-glacial and glacial sediments of the last interglacial-glacial cycle (IS 5d through IS 2) overlie an early last-interglacial (IS 5e) wave-cut surface in coastal exposures. This sequence provides a glimpse of apparent middle- and late-last interglacial landscape stability and of the interglacial-glacial transition.

SIGNIFICANCE OF NEOTECTONIC RECORD

The Olympic coast neotectonic record contributes to a growing body of knowledge concerning the Cascadia subduction zone and its geologic processes. This convergent margin (Figure 1.2) has received much research attention in the past decade, largely because of the recognized potential for large earthquakes. A lack of historic large earthquakes long caused the Cascadia subduction zone to be viewed as a benign feature relative to many of its counterparts around the world. Heaton and Kanamori (1984), however, likened the Cascadia subduction zone to seismogenic zones elsewhere and concluded that it may be capable of generating great earthquakes (magnitude > 8). Thereafter, several workers [e.g., Atwater (1987, 1992), Darienzo and Peterson (1990), Darienzo (1991), Nelson (1992)] found geologic evidence of past coseismic subsidence and tsunami activity in coastal marshes of Washington and Oregon,

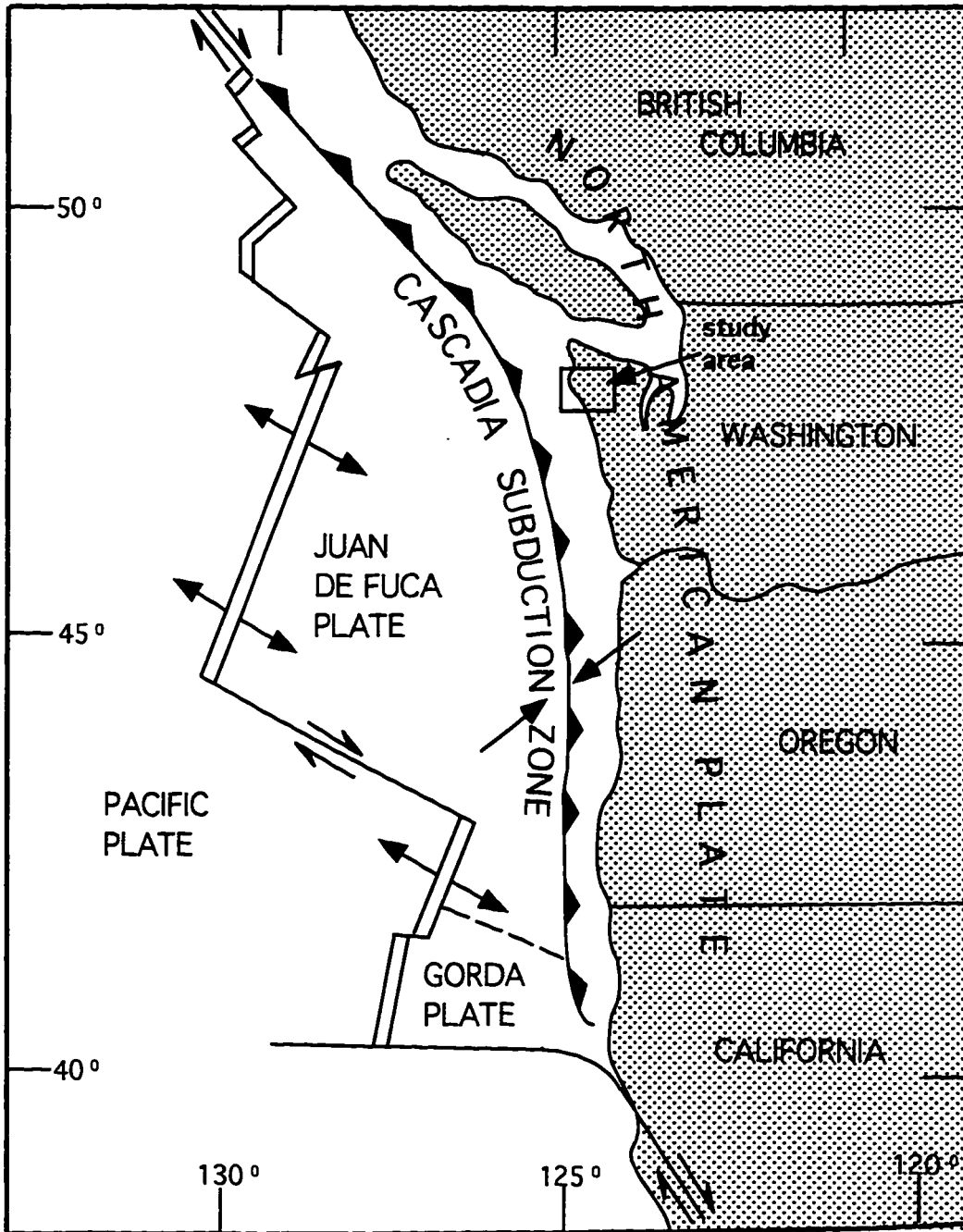


Figure 1.2: Map showing geographic relationship of study area to the Cascadia Subduction Zone.

respectively, while Adams (1990) attributed Holocene turbidites in the Cascadia channel to recurrent earthquakes along the subduction zone. While some workers have suggested that subduction is occurring aseismically along the Cascadia margin [e.g., Ando and Balasz, (1979), West and McCrumb (1988)], geologic evidence (including that noted above) and geodetic evidence [e.g., Mitchell et al. (1994), Savage et al. (1991), Holdahl et al. (1989)] suggest that the interface is locked and that a great-earthquake hazard exists.

The Olympic Peninsula represents a unique section of the Cascadia convergent margin. There, a broad arch in the downgoing Juan de Fuca plate (Crosson and Owens, 1987) has caused rapid uplift of an accretionary wedge to form the Olympic Mountains (Brandon and Calderwood, 1990; Brandon and Vance, 1992; Brandon, 1994). The slab arch may also have implications for seismic hazards. The seismogenic part of the plate boundary—the "stick-slip" zone of Hyndman and Wang (1993) and the equivalent "locked" zone of Savage et al. (1991)—may be broader and may extend closer to the coast in the Olympic section than in other sections of the coast. In addition, the Olympic Mountains engender a coastal sedimentologic setting unique along the Cascadia subduction zone: only there has voluminous glacial sedimentation inundated the coastal zone, providing an extensive subaerial stratigraphic record in which the Quaternary deformation can be directly observed and interpreted.

The Olympic coast neotectonic record provides deformational data on intermediate time scales and in an intermediate geographic position relative to other data sources. Considerable geologic work has been conducted off the Olympic coast [e.g., Boyer and Lingley (1991), Wagner et al. (1986), Wagner and Tomsen (1987), Kulm et al. (1993), McNeill et al. (1994b, 1995)], in unglaciated western Olympic valleys (Pazzaglia and Brandon, in review), and in the Olympic Mountains [e.g., Tabor and Cady (1978a), Brandon and Calderwood (1990), Brandon and Vance (1992), Brandon (1994)]. The coastal tectonic information resulting from this project fills the gap between offshore and alpine studies.

The coastal neotectonic data also bridges a temporal gulf, between decadal-scale data of geodetic studies and the million-year-scale data of plate-motion and fission-track studies. A wealth of geodetic data from tide gauges, releveling surveys, and strain-rate measurements reveal patterns of differential uplift, subsidence, and contraction (Mitchell et al., 1994; Holdahl et al., 1987, 1989; Savage et al., 1991). On longer time scales, paleomagnetic studies constrain plate movements over million-year intervals

(Riddihough, 1984), and fission-track dating provides long-term uplift rate estimates for the Olympic Mountains (Brandon and Vance, 1992; Brandon, 1994). The Olympic coast neotectonic record, in contrast, provides deformation-rate estimates on 10,000- to 100,000-yr time scales. The relationship of these intermediate-scale rates to geodetic rates permits estimates of the relative proportions of elastic (pre-seismic) and permanent deformation.

PROJECT SETTING

The study area, on the western slope of the Olympic Peninsula (Figure 1.1), is dominated by the Olympic Mountains, a 7700 km², domal uplift fringed by coastal and riverine lowlands. The Olympic Mountains comprise a steep, mountainous terrain, incised by a radial drainage network. The highest peaks rise to nearly 2500 m near Mt. Olympus, in the approximate center of the peninsula. To the northwest, west, and south, altitudes decline rapidly to a relatively low-relief piedmont and coastal plain. To the north, east and southeast, however, altitudes remain high through the Bailey Range and the eastern Olympic upland to the edge of the Puget and Juan de Fuca lowlands.

The Olympic Peninsula is dominated by a maritime climate of high annual precipitation and moderate temperatures. Moisture-laden Pacific air masses deliver large amounts of precipitation in the period between October and March, when 80 percent of the annual precipitation falls (Spicer, 1986). Along the Pacific coast, annual precipitation ranges from 1780 to 2540 mm, rising to more than 3175 mm in the rainforest-clad valleys tens of kilometers inland. The Mt. Olympus area receives 4800 to 5080 mm of annual precipitation, a maximum for the continental United States (LaChapelle, 1959, 1960; Spicer, 1986). To the northeast, annual precipitation decreases markedly, amounting to only 460 mm in the continental mesoclimate of the Olympic rain shadow. This steep precipitation gradient exerts strong influences on present glacier distribution (Spicer, 1986; see below) and probably controlled Pleistocene glaciation in similar fashion. Summer temperatures range daily from 10 to 24° C in the coastal lowlands, and winter temperatures from -2° to 7° C (Spicer, 1986).

The Olympic Mountains harbor 266 active glaciers (Spicer, 1986), nourished at relatively low altitudes by the prodigious precipitation of Pacific air masses. Most are small cirque glaciers and perennial ice patches protected on north-facing slopes. On the Mt. Olympus massif, however, several glaciers extend beyond their cirques as valley glaciers. The 5 km² Blue Glacier, largest of the Olympic glaciers, descends the east and

north slopes of Mt. Olympus to 1200 m altitude at the head of the Hoh River valley. Mean altitudes of Olympic glaciers range from 1400 to 2100 m, with a steep, southwest-to-northeast gradient of approximately 12 m/km. This gradient reflects the steep decrease in annual precipitation across the range. Major topographic saddles at the heads of two major west-slope valleys (Queets and Quinault) permit the penetration of moist air masses further into the range, supporting glaciers at lower altitudes.

BEDROCK GEOLOGY

The Olympic Mountains are composed of two lithologic assemblages, the peripheral rocks and the core rocks (Tabor and Cady, 1978a, 1978b). The peripheral rocks comprise the upper plate of the Olympic subduction complex. The basement of this structural lid includes Eocene sandstone, argillite, and conglomerate (Blue Mountain Formation), interlayered with lower and middle Eocene basaltic rocks (Crescent Formation). The basement complex underlies an Eocene to Miocene forearc-basin sedimentary cover. As a package, this upper-plate volcanic and sedimentary sequence is folded into a horseshoe-shaped belt ringing the Olympic uplift on the south, east, and north sides, and is separated from the core rocks by the peripheral fault. The peripheral rocks are unmetamorphosed and stratigraphically continuous, standing in sharp contrast to the core rocks.

The core rocks comprise the exposed accretionary wedge of the Olympic subduction complex. The core rock assemblage consists of penetratively deformed and stratigraphically incoherent early(?) Eocene to middle Miocene litharenite, greywacke, argillite, conglomerate, and minor carbonate rocks and basalt. These rocks exhibit mild metamorphism of pumpellyite and low greenschist grade (Tabor and Cady, 1978a).

Uplift of the Olympic subduction complex appears to be driven by a combination of accretionary wedge thickening and the development of an arch in the subducting Juan de Fuca plate (Brandon and Calderwood, 1990; Crosson and Owens, 1987). Uplift began in middle to late Miocene time: clasts of Olympic lithology in the late-Miocene Montesano Formation (Bigelow, 1987) indicate an initial emergence of the complex about 12 million yr BP (Brandon and Calderwood, 1990). Zircon fission-track dates for, and metamorphic assemblages within, the core rocks indicate that the highest parts of the peninsula were initially accreted to the wedge 17 million years ago, at a depth of 12 km. The accretion-depth and initial-emergence data allow a secular uplift rate estimate of about 1 mm/yr (Brandon and Vance, 1992).

METHODS OF STUDY

The current project concentrates on glacial landforms and deposits in the Queets and Hoh river valleys and on coastal landforms and deposits at the mouths of those valleys (Figure 1.1). Project goals have been accomplished through mapping of drift units, stratigraphic description of glacial and nonglacial units, and radiometric and paleomagnetic dating of glacial and nonglacial sediments.

MAPPING OF DRIFT UNITS

The project has employed a variety of methods to produce a map of drift units (Plate 1). Topographic-map interpretation, air-photo interpretation, and field observations have been used to delineate areas covered by glacial deposits (till, outwash, lacustrine sediment) and to determine the distribution of moraines and related outwash. Mapping has been done on 7.5-minute (1:24,000-scale) and 15-minute (1:62,500-scale) topographic quadrangles and with 1:44,000- and 1:12,000-scale aerial photographs. The final map (Plate 1) was compiled on a 1:100,000-scale metric base and digitized onto a shaded relief image derived from 7.5-minute digital elevation models. Correlations among landforms have been established through stratigraphic and morphologic relationships, degree of soil formation, and erosional modification. A loess cover of probable late-Wisconsin (IS 2) age diminishes the value of soil profiles for resolution of early and late Wisconsin surfaces (these surfaces can be readily distinguished through morphologic relationships). However, soils on older surfaces are distinct enough to separate pre-last-interglacial (pre-IS 5) surfaces from one another and from Wisconsin-age surfaces. Weathering-rind analysis proved of limited use in the Queets and Hoh valleys, though Pazzaglia and Brandon (in review) succeeded in differentiating terrace surfaces therewith in the Clearwater River valley (Chapter 2).

Although the thick vegetative cover has hindered mapping in many respects, two aspects of that cover have aided the project. First, intensive logging during the 1970's and 1980's exposed glacial landforms for the 1991 to 1995 field project, and generated an extensive network of access roads. Second, surviving vegetative cover provides clues to underlying deposits: areas underlain by outwash tend to support dense forest, whereas those underlain by till or lacustrine sediment are poorly drained and support cedar swamps and treeless bogs. This distinction has proven especially useful in the Hoh valley.

STRATIGRAPHIC DESCRIPTION

Glacial and nonglacial deposits were examined in seacliffs, stream cuts, road cuts, and gravel pits. Seacliffs and high stream-cut exposures were most valuable for describing and interpreting the stratigraphic sequence produced by glacier fluctuations. Deep stratigraphic exposures are uncommon in the river valleys, but enough have been found to piece together the sequence of glacial units and to relate radiocarbon dates to the morphologic sequence (Chapter 2). Roadcuts and gravel pits normally are too shallow to expose thick stratigraphic sections. They have been used to link deeper stream-cut sections, to examine sediment variability in glacial-fluvial units, and to confirm mapping of drift units.

DATING OF GLACIAL AND NONGLACIAL DEPOSITS

Radiocarbon, thermoluminescence, and paleomagnetic methods provide chronologic control for the glacial-interglacial deposits and landforms. More than 100 samples of wood and other plant matter have been collected from coastal and inland exposures. From this suite, 59 samples have been submitted for radiocarbon dating. Submitted samples have been selected on the basis of their relevance to the sequence (e.g., limiting ages for outwash units and moraines) and the likelihood of obtaining finite ages [e.g., samples thought to be of middle- or late-Wisconsin age (IS 3 and 2), based on sequence relationships and existing dates]. Conventional radiocarbon dating has been performed by the University of Washington's Quaternary Isotope Laboratory and by Beta Analytic, Inc. Accelerator mass spectrometry (AMS) dates have been provided by the National Science Foundation-University of Arizona AMS Facility.

Thermoluminescence dates and paleomagnetic data have been used to constrain ages of sediments older than the limit of radiocarbon dating (ca. 55,000 ^{14}C yr BP). Thermoluminescence dating has focused on sand and mud deposits thought to date from the last interglaciation (IS 5), based on stratigraphic relationships and infinite radiocarbon ages. Glenn Berger of the Desert Research Institute (University of Nevada) collected the samples and performed the analyses. Paleomagnetism samples collected from silty glacial and nonglacial sediments provide broad age control [e.g., greater than or less than ca. 780,000 yr BP (Baksi et al., 1992)] on selected units. Harry Rowe and John Geissman of the University of New Mexico conducted the analyses.

CHAPTER 2 GLACIAL GEOLOGY OF THE QUEETS AND HOH RIVER VALLEYS

INTRODUCTION

The geomorphic and surficial stratigraphic records in the Queets and Hoh valleys were studied with the aims of delineating drift units, constructing a chronology for the last (Wisconsin) glacial cycle, and estimating paleoclimatic parameters for glacial events. Five drift units have been described and mapped, and a framework of limiting dates has been obtained through radiocarbon, thermoluminescence, and paleomagnetic methods. Two pre-last interglacial drifts are present, and three Wisconsinan drifts preserve evidence of six distinct advances. In both valleys, early and middle Wisconsin drifts are more extensive than late Wisconsin drift.

NOMENCLATURE

The glacial-geologic map (Plate 1) shows the distribution of five principal drifts. These drifts are informally designated allostratigraphic units, defined by data from topographic maps, aerial photographs, and field investigation. The breadth of the mapped area, dense vegetation, and rarity of stratigraphic exposures prompted the use of allostratigraphic, rather than lithologic units; i.e., a map of morphologic units was deemed more informative than a map of deposits inferred from morphology and random field observations. The mapped morphologic units nevertheless can be interpreted in terms of their lithologic composition.

The five drift units are assigned local names, derived from geographic features in their terminal moraine areas. The two oldest, the Wolf Creek and Whale Creek drifts, are named for streams in the coastal plain south of the Queets River (Figure 2.1), whereas the Lyman Rapids drift is named for a stretch of the Queets River between the Salmon River and Matheny Creek. The Hoh Oxbow drift's principal terminal moraine lies in the Hoh Oxbow area of the Hoh valley, while the youngest drift is named for Twin Creeks, a set of small Hoh River tributaries.

Each drift does not necessarily represent a distinct glaciation. For example, the two oldest drifts may contain multiple units that are morphologically and pedologically indistinguishable. Conversely, the Hoh Oxbow and Twin Creeks drifts represent distinguishable stades of the same glaciation. This contrast reflects the greater exposure

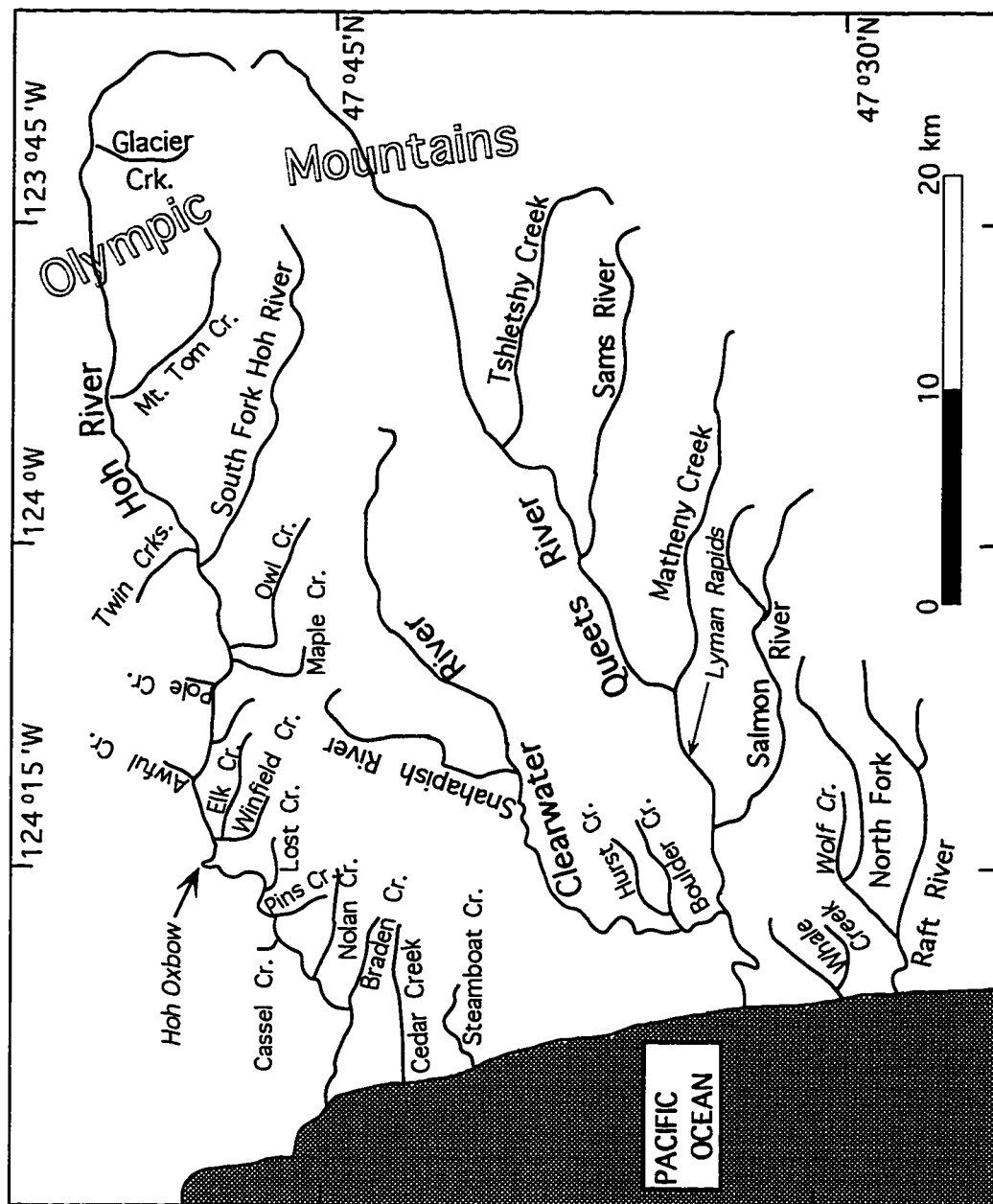


Figure 2.1: Map of western Olympic Peninsula, showing locations mentioned in text

area and less-altered character of younger drifts, as well as the focus of this project on records of the last glaciation.

Each drift is divided into two or more morphologic units. End moraines and outwash terraces are identified for each drift. Ground moraine is mapped for the Lyman Rapids and Hoh Oxbow drifts, while drift-mantled bedrock on the south edge of the lower Hoh valley is included in the Wolf Creek drift.

The local units are correlated with time-stratigraphic units in the Puget Lowland (e.g., Possession, Fraser) and American Midwest (late, middle, and early Wisconsin), and with marine oxygen isotope stages or events [abbreviated, e.g., IS 1, IS 4, IS 5e, as designated by Imbrie et al. (1984) and Martinson et al. (1987)].

Unless otherwise noted, all radiocarbon dates are quoted in uncalibrated ^{14}C years. Omission of aberrant dates tightens the radiocarbon chronology considerably: where dates are stratigraphically reversed in an exposure (i.e., an older date stratigraphically above a younger date), the younger date is disregarded in favor of the older date. In this setting (moist, heavily vegetated, no carbonate bedrock), the younger sample is more likely to be contaminated with modern carbon than is the older sample to be contaminated with older carbon. In most cases, the older date in a reversed sequence is supported by other dates. Unless noted, all existing dates are included in figures and tables.

INFLUENCE OF VALLEY PHYSIOGRAPHY ON GLACIAL GEOLOGY

Physiographic contrasts between the Queets and Hoh valleys have caused development of strongly differing drift morphologies (Plate 1). The Queets valley glaciers were confined to a narrow (≤ 4 km wide), bedrock-walled valley extending from the valley head to a point approximately 25 km from the coast; there, the valley broadens onto the coastal plain, bounded on its north side by a low bedrock ridge separating the Queets and Clearwater valleys. Thus, the glaciers were able to spread southward, largely unconstrained by bedrock, to form broad (ca. 8-km- to 12-km-wide) lobes. The result is a series of nested moraines and inset terraces, large portions of which have escaped erosion because the Queets River is confined to a relatively narrow portion of the coastal plain. A series of steep-sided, nested lateral moraines mantles the bedrock ridge north of the river. South of the river lies a series of more subdued end moraines and broad outwash terraces. Longitudinal profiles of valley trains in this

physiographic setting are mostly smooth and graded, and steepen upvalley toward moraines.

The Hoh valley is bounded by bedrock along most of its course. The river merges with its southern fork 33 km inland and emerges into a valley slightly broader (3 km) than above. The valley further widens 26 km from the coast, reaching 7 km at its widest point. The glaciers were largely bordered by bedrock valley walls most of the way to the modern coastline. In addition, tributary valleys and bedrock outliers channeled glacier ice and outwash away from the main valley in several places. The result is a much more complex morphologic pattern, relative to the Queets valley, of nested but discontinuous terminal moraines, limited lateral moraines, inset valley trains, outwash fans, ground moraine, and drift-mantled bedrock. Valley trains exhibit irregular and non-graded (non-equilibrium) longitudinal profiles, particularly where outwash fans from small distributary lobes of the glacier coalesce with the main valley train. Finally, the bedrock-constrained valley partly enabled a Hoh valley glacier to flow past the modern coastline on at least one occasion, preserving a stratigraphic record of that glaciation now exposed in seacliffs.

The contrasting morphologic patterns in the two major valleys complement one another in interpreting the sequence. The well-preserved and less-complex Queets valley glacial morphology has proven most useful for defining drift units and their sequence. Greater erosion in the Hoh valley has produced a better-exposed stratigraphic record, which can be related to the glacial morphology.

The drainage of the two valleys was confluent during at least three glaciations. The Snahapish River valley (Figure 2.1), an anomalous tributary to the Hoh valley, channeled ice and/or meltwater southwestward into the lower Clearwater valley. The Clearwater River, a Queets River tributary, has deposited thick gravel fills during glacial episodes in response to sediment-laden meltwater input from the Snahapish valley and base-level fluctuations in the Queets valley. The result is a series of thick gravel fills, now represented by a series of terraces, in the lower Clearwater and Snahapish valleys. The Clearwater-Snahapish terrace sequence, which has been studied in detail by F.J. Pazzaglia (personal communication, 1993-1995; Pazzaglia and Brandon, in review), aids in the correlation of drifts between the Queets and Hoh valleys (Thackray and Pazzaglia, 1994, 1996).

DESCRIPTION OF DRIFTS AND CHRONOLOGIC CONTROL

The two oldest Pleistocene units—the Wolf Creek and Whale Creek drifts—predate the last interglaciation. The younger drifts—Lyman Rapids, Hoh Oxbow, and Twin Creeks—postdate the last interglaciation, having been deposited during the last (Wisconsin) glacial cycle.

WOLF CREEK DRIFT

The Wolf Creek drift is poorly exposed inland from the coast and was not studied in detail. The drift is identified in two areas of the Queets valley, in two areas of the Hoh valley, and in seacliff exposures south of the Hoh River.

Morphology

In its type area on the coastal plain between the Queets and Raft river valleys, the Wolf Creek drift includes a prominent end moraine, cut by Wolf Creek, plus the deeply dissected remnants of an outwash terrace between Wolf Creek and the coastline (Plate 1). The end-moraine crest lies 10 to 35 m above surrounding outwash terraces. Its large initial volume and the gentle surrounding topography likely contributed to its preservation as an identifiable feature through the inferred >780,000 yr since its construction (see below), as did partial isolation from fluvial erosion.

Additional Wolf Creek outwash terraces may lie south of the Raft River. Moore (1965) delineated broad areas of his Humptulips drift in the Raft River area, and the two units may be correlative. That portion of his map is very generalized, however, and the Humptulips drift was not examined during this study. No stratigraphic exposures in Wolf Creek landforms were found in the Raft River area, but braided-stream gravels exposed in the lower portions of seacliffs between the Raft River and the Whale Creek area might belong to the Wolf Creek drift. A diamicton on the Salmon River (SE1/4, SW1/4, SW1/4, Section 36, T24N, R12W) may also correlate with the Wolf Creek drift.

Wolf Creek drift mantles the ridge separating the Queets and Clearwater valleys. The drift straddles the drainage divide in the upper reaches of Hurst, Boulder, and Shale creeks (sections 1, 2, and 11 of T24N R12W). A bouldery diamicton exposed in this area exhibits a thick (≥ 2.5 m) weathering profile, far thicker than profiles on other drifts. Together, this drift and the southern lateral moraines define a former glacier more than 12 km wide.

Wolf Creek drift has also been mapped in Snahapish and Hoh valleys. Drift that mantles hills at the southern end of the Snahapish valley is provisionally correlated with Wolf Creek drift. At the southern edge of the lower Hoh valley, drift covering smoothed bedrock hills has also been mapped as Wolf Creek drift. Exposure is poor in both areas; therefore, neither deposits nor weathering profiles have been described.

Seacliff Stratigraphy

Seacliffs stretching 8 km from the Hoh River south to the Steamboat Creek area expose a basal drift sequence that is correlated provisionally with the Wolf Creek drift. The reasoning behind this correlation is two-fold. First, the basal drift sequence contains till and glacial-marine drift, indicating that at least one advance of the Hoh valley glacier extended beyond the modern shoreline. Second, no end moraines or outwash terraces of Wolf Creek character (i.e., thick weathering profile, deep dissection) were identified in the Hoh valley; therefore, it is likely that the glacier extended beyond the modern coastline. This supposition is supported by the greater length of Pleistocene glaciers in the Hoh valley relative to the Queets valley, where the Wolf Creek end moraine extends to within 6 km of the coastline. Glacier-length ratios (Hoh valley/Queets valley) for the Lyman Rapids and Hoh Oxbow advances are 1.12 and 1.42, respectively. Extrapolation of these ratios suggests that the Wolf Creek glacier in the Hoh valley terminated between the modern coastline and 17 km offshore.

The basal drift sequence includes till, glacial-marine drift, glacial-lacustrine drift, and outwash, all lying beneath a wave-cut surface that separates pre-last-interglacial from post-last-interglacial deposits. The basal drift sequence is part of the Steamboat Creek Formation, an informal unit described in Chapter 3. Exposures of the sediments are excellent, but discontinuous. Thus, the individual drift types can be readily observed, but the stratigraphic relationships between them cannot be.

Diamictons interpreted as tills are exposed adjacent to a small, unnamed creek south of Destruction Island Viewpoint (SW1/4, NE1/4, Section 8, T25N, R13W) and in a seacliff approximately 1.1 km north of Abbey Island (NW1/4, SW1/4, SW1/4, Section 29, T26N, R13W). Both till exposures were described previously by Heusser (1974). The Destruction Island Viewpoint diamicton extends 3 m above beach level; is clast-rich (up to 75% by volume) with boulders as large as 2 m diameter; has a grey, sand- and clay-rich matrix; and contains blocks of laminated mud and pebbly mud lying at angles up to 30° from horizontal. The blocks are interpreted as proglacial or

supraglacial pond or lake deposits incorporated into the till by the advancing glacier; such blocks are common in tills throughout the study area. The diamicton extends only 25 m laterally and is overlain by approximately 8 m of braided-stream gravel (see below). The diamicton north of Abbey Island extends 3.5 m above beach level; contains lithic clasts (40% by volume), with cobbles and boulders as large as 30 cm; has a silty and sandy matrix; and contains blocks of laminated mud similar to those described above. It also contains detrital wood, for which Heusser (1974) reported an age of >47,000 ^{14}C yr BP. This diamicton is exposed over only 25 m lateral distance, and is overlain by 2 m of horizontally stratified gravel and 4 m of stratified sand that may represent lacustrine deposition. Diamictons exposed between this exposure and the Abbey Island area resulted from slumping of modern seacliffs, but their overall character suggests they may have been derived from till in the seacliff stratigraphic section.

Another diamicton in the basal drift sequence is interpreted as glacial-marine drift. The diamicton is exposed 2 km north of Abbey Island (0.9 km north of the till exposure described above) and 1.9 km southeast of the Hoh River (SE1/4, NE1/4, NE1/4, Section 30, T26N, R13W). It is at least 12.8 m thick, extending to 19.2 m above sea level. About 15% of the diamicton is evenly distributed lithic clasts as large as 5 cm in diameter, in addition to gravel lenses as much as 100 cm wide and 30 cm thick. It has a grey, sandy silty clay matrix and contains shells of the bivalve *Mytilus*, some of which are articulated and in apparent growth position. The glacial-marine drift is overlain by 2.1 m of cross-bedded medium sand, which may represent a beach or intertidal environment.

Between the till and glacial-marine drift north of Abbey Island lies an exposure of interbedded sand and mud that appears to represent a lacustrine environment. The exposure is located 1.5 km north of Abbey Island (NE1/4, NE1/4, SE1/4, Section 30, T26N, R13W). The unit is 5.7 m thick, and extends to 20 m above sea level. The alternating sand and silt layers are 0.5 to 5 cm thick and are internally laminated; some of the sand beds, which dominate the upper third of the unit, contain ripple cross-laminae. The bedded and laminated character of the sediments and the lack of marine fossils indicate a lacustrine depositional environment. The near-rhythmic alternation of sand and mud is suggestive of the fluctuating meltwater flux of a glacial-lacustrine environment. Poor exposures above the lacustrine deposits appear to contain braided-stream gravel.

Braided-stream gravels, interpreted as outwash, dominate the basal drift sequence in the 4 km of seacliffs between Abbey Island and the Steamboat Creek area. The gravel is at least 10 m thick and consists of cobbles and pebbles, with rare boulders, and a sandy matrix. Cobbles dominate, with sparse pebble-dominated interbeds and sand lenses. Stratification is crude, though cut-and-fill structures are apparent in places. The gravel contains logs (mostly in the upper third of the unit) and twigs in sand lenses near the base. The gravel is strongly stained and iron-cemented, forming vertical cliffs in most exposures. The broad lateral extent of the gravel, its sedimentologic features indicative of a braided-stream depositional environment, and its spatial association with the till suggest deposition as outwash. Florer (1972) described pollen from the gravel suggestive of interglacial conditions, contradicting this stratigraphic interpretation. It is possible, however, that the pollen was reworked from pre-existing sediments—the fine organic matter observed in the current study was concentrated in clasts.

Chronology

Aside from the soil profile described previously, no direct chronologic data exist for Wolf Creek landforms; however, limited chronologic data have been obtained from the seacliff exposures described above. The glacial-lacustrine deposits north of Abbey Island and silty overbank sediments in the outwash near Destruction Island Viewpoint (Chapter 3) have yielded reversely magnetized samples, suggesting that the drift was deposited more than about 780,000 yr BP (the approximate age of the Brunhes-Matuyama reversal; Baksi et al., 1992).

WHALE CREEK DRIFT

Whale Creek drift has been mapped principally in the Queets valley, where large end moraines and broad outwash terraces are preserved. Limited Whale Creek outwash terraces, but no moraines, have been identified in the Hoh valley. An ice-proximal outwash terrace is mapped in the lower Snahapish valley, and thick alluvial fills correlated with the Whale Creek drift (Plate 1) have been mapped by F.J. Pazzaglia (personal communication, 1993-1995; Thackray and Pazzaglia, 1996) in the lower Clearwater valley.

Morphology

Queets Valley

In the Queets valley and adjacent coastal plain, Whale Creek drift covers extensive areas south of the Queets River and includes a prominent lateral moraine on the north side of the valley (Plate 1). In the southern area, two end moraines and outwash terraces are present. The two moraines exhibit similar morphology and pedologic development, and therefore are mapped as a single drift.

The southern lateral moraine extends more than 9 km along the southern and southwestern edge of the Salmon River valley (Figure 2.1), controlling the valley's arcuate trend. The lateral moraine bifurcates 14 km inland from the coastline, with the two moraine branches extending westward and west-northwestward (as terminal moraines) across the coastal plain. The moraines exhibit diffuse topography, but rise above the generally flat outwash surfaces beyond them. Small areas of ground moraine were mapped adjacent to the end moraines.

A prominent Whale Creek lateral moraine also extends more than 16 km along the north side of the Queets valley. It turns southwestward as a 3-km-long terminal moraine, truncated by the Queets River and associated with a broad area of apparent ground moraine. The northern and southern lateral moraines outline a former glacier about 9 km wide.

The outwash terraces associated with the end moraines cover broad areas of the coastal plain. They are only moderately dissected, much less so than the adjacent Wolf Creek terraces. Drainage is moderately integrated, and is marked by shallow stream cuts (deeper in proximity to major rivers and the coastline) and boggy ground. The result is a broad area of gently undulating outwash terrain. At their seaward edge, the terraces are truncated by a paleoshoreline, inferred to have been cut during the last-interglacial sea-level highstand (IS 5e). The paleoshoreline separates Whale Creek terraces from the younger Lyman Rapids and Hoh Oxbow terraces that parallel the coastline.

Hoh Valley

Whale Creek outwash terraces cover limited areas of the lower Hoh valley (Plate 1). Whale Creek moraines have not been identified there. This limited morphologic expression is likely due to the narrow breadth of the Hoh valley and the lack of a broad

coastal plain. The laterally migrating lower Hoh River likely eroded most of the Whale Creek landforms prior to subsequent glacier expansion (Chapter 4).

Three areas south of, and one area north of, the Hoh River contain Whale Creek outwash terraces. The three southern areas are separated by younger outwash terraces filling the Cedar Creek and mainstem Hoh valleys. As in the Queets valley, a paleoshoreline separates the seaward edge of the Whale Creek terrace from younger and lower coastal outwash terraces. Immediately landward of the paleoshoreline, the Whale Creek terrace exhibits nearly circular to oblong bogs (400 to 800 m in diameter or maximum length) surrounded by 12- to 20-m-high ridges. Small creeks drain the semicircular bogs truncated by the paleoshoreline. The kettle-like morphology of the surface suggests dead-ice terrain, implying that the Whale Creek glacier may have reached near or beyond the modern shoreline and that the outwash is a recessional deposit. Till from this inferred advance may be represented in the seacliff sequence by a coarse gravel lag, containing boulders as large as 2 m diameter, that marks the buried wave-cut surface discussed in detail in Chapter 3. Glacier-length ratios (see above) suggest that the Whale Creek glacier might have terminated as far as 13 km offshore.

Snahapish and Clearwater Valleys

The southern end of the Snahapish River valley contains two small Whale Creek outwash terraces (Plate 1). Gravel in the largest, upvalley terrace contains many coarse cobbles and boulders. The coarseness and the lack of Whale Creek terraces upvalley suggests that the outwash is an ice-proximal deposit. In addition, the freshest set of faceted spurs in the Snahapish valley declines in elevation southward, converging approximately with the outwash terrace. Thus, the terrace may mark an outwash head.

A thick alluvial fill in the lower Clearwater River valley, represented morphologically as the second-highest terrace in a series of seven mapped by Pazzaglia (personal communication, 1993-1995; Thackray and Pazzaglia, 1996), appears to be related to the Whale Creek glaciation. Weathering-rind data from the Clearwater gravel fill, the coarse Snahapish outwash described above, and from Whale Creek outwash on the south side of the Queets valley, form a population distinct from those of other outwash/fill units. These data support correlations of terraces based on altitudinal gradients. The terrace relationships indicate that the lower Clearwater River deposited the thick fill in response to sediment input from the Snahapish valley ice lobe, coupled

with downstream base level changes resulting from outwash deposition in the Queets valley.

Stratigraphy

Logging, coastal erosion, and intense weathering have limited the abundance of Whale Creek drift exposures. Most areas mapped as Whale Creek drift were extensively logged over the last two to three decades and now support a cover of dense, second-growth vegetation. Coastal erosion during the last (and perhaps previous) interglaciation(s) likely removed Whale Creek deposits from the upper portion of the stratigraphic sections, and intense weathering has made the outwash gravel unsuitable for road metal. Hence, stratigraphic exposures are limited to rare, shallow gravel pits and road cuts.

Outwash thus exposed south of the Queets River is typically cobble-pebble gravel, with a sparse, sandy matrix. Clasts are subrounded to rounded greywacke sandstone. Weathering profiles typically are 1.5 to 2 m thick and, particularly on terrace surfaces, have clay-rich B horizons that impede surface drainage and lead to gleyed profiles.

Chronology

Direct age control is lacking for the Whale Creek drift, but correlation with IS 6 is inferred. Whale Creek outwash terraces are truncated by a paleoshoreline between the Queets and Raft rivers and between the Hoh River and Brown's Point, indicating that the drift predates the last interglaciation. Dissection, drainage development, and weathering profiles suggest that the Whale Creek glaciation dates to the glaciation immediately preceding the last interglaciation (IS 6), rather than to previous glaciations.

Thermoluminescence dates from seacliff exposures (Chapter 3) suggest that the buried wave-cut surface and (by inference) the paleoshoreline date to IS 7, rather than to IS 5. If valid, the dates suggest that the Whale Creek drift dates to IS 8 or earlier. Reasons exist to doubt the thermoluminescence dates, however, and stratigraphic relationships indicate that the buried wave-cut surface dates to IS 5.

LYMAN RAPIDS DRIFT

Landforms consisting of Lyman Rapids drift cover large areas in the Queets and Hoh valleys. This drift is the most extensive in the Queets valley and includes the dominant coastal terraces at the mouths of both valleys. Lyman Rapids outwash also fills the Snahapish valley, and correlative nonglacial gravel fills a portion of the lower Clearwater valley. The Lyman Rapids drift likely is of early or middle Wisconsin (IS 4 or 3) age, but might also date to late-last interglacial time (i.e., IS 5b).

Queets Valley

Morphology

Five Lyman Rapids terminal and/or recessional moraines, two prominent lateral moraines, limited dead-ice terrain, and extensive outwash terraces are found in the Queets valley (Plate 1). Drift of two phases of this glaciation can be discerned there: the maximum phase (Lyman Rapids I) and a less-extensive later phase (Lyman Rapids II). The most prominent Lyman Rapids I terminal moraine (Plem₁, Plate 1), the projection of which would cross the Queets River in the vicinity of Lyman Rapids, is a broad, low-relief feature approximately 1 km wide. A similar recessional moraine lies approximately 1 km upvalley (south side of valley only), while remnants of two narrower and less-well preserved end moraines lie within 2 km downvalley. The principal terminal moraine and the recessional moraine connect with lateral moraines on both sides of the valley. The southern lateral moraine abuts a bedrock outlier in the Matheny Creek-Salmon River area. The northern lateral moraine is the lowest of three moraines marking the ridge that bounds the Queets valley (see discussion of older drifts above). Together, the lateral moraines and principal terminal moraine outline a former glacier approximately 8 km wide. Dead-ice terrain extends approximately 2 km upvalley of the principal moraine on both sides of the river.

Extensive outwash terraces (Plo₁, Plate 1) extend downvalley from the principal terminal moraine (Plem₁). A broad terrace covers much of the area between the moraine and the Salmon River, upvalley from moraines of Whale Creek drift. The now-incised valley train narrowed to 1.8 km where constrained by Whale Creek landforms (south side of valley) and bedrock of Kalaloch Ridge (north side of valley), then widened near the valley mouth to cover the coastal area. The coastal outwash terrace south of the river is about 1.5 km wide between the paleoshoreline described above and the modern shoreline, where the sediments forming the terrace are well exposed in seacliffs. A

coastal outwash terrace also lies north of the Queets River mouth, filling the 1.5-km-wide zone between the coastline and bedrock hills of Kalaloch Ridge. The outwash is exposed in seacliffs stretching 8 km north of the Queets River mouth, but is covered in the Kalaloch area by as much as 9 m of loess and locally derived sediment (Chapter 3). Approximately 6.5 km north of the Queets River mouth, a morphologic boundary is arbitrarily drawn where the locally derived sediment thickens northward to more than ca. 2 m and forms the coastal terrace.

Figure 2.2 shows the longitudinal profile of the Lyman Rapids outwash valley train. The profile is mostly smooth and graded, steepening toward the principal terminal moraine described above. The smooth profile reflects the largely unconstrained valley in which the meltwater streams deposited the thick fill, and contrasts strongly with valley-train profiles in the Hoh valley.

The Lyman Rapids II drift includes terminal-moraine remnants lying approximately 12 km upvalley from the principal Lyman Rapids I moraine, as well as outwash terraces. The outwash terraces are best preserved in the Tacoma Creek area on the north side of the valley. Lyman Rapids II terraces lie at elevations between those of adjacent Lyman Rapids I and Hoh Oxbow terraces.

Interpretation of this intermediate drift as a younger member of the Lyman Rapids drift, rather than as an older member of the Hoh Oxbow drift, is based on two characteristics. First, the surface morphology and vegetation on Lyman Rapids II terraces, as observed on aerial photographs, are similar to Lyman Rapids I terraces. Small patches of apparent boggy ground, represented by light-colored patches on aerial photographs, mark both sets of terraces. Hoh Oxbow terraces lack such a surface morphology, which may result from poorly integrated, shallowly incised drainage or from pedogenic clay accumulation. Second, a broad area (up to 5 km original width) of Hoh Oxbow outwash terraces lies inset between Lyman Rapids II outwash terraces (Plate 1). Such extensive erosion of the Lyman Rapids II outwash likely required more time than can be accounted for between Hoh Oxbow advances.

Figure 2.2 shows the longitudinal profile of the Lyman Rapids II outwash valley train. The profile steepens smoothly upvalley to the terminal moraine. The downvalley extrapolation of the profile, beyond the Tacoma Creek area, projects below the Lyman Rapids I valley-train profile.

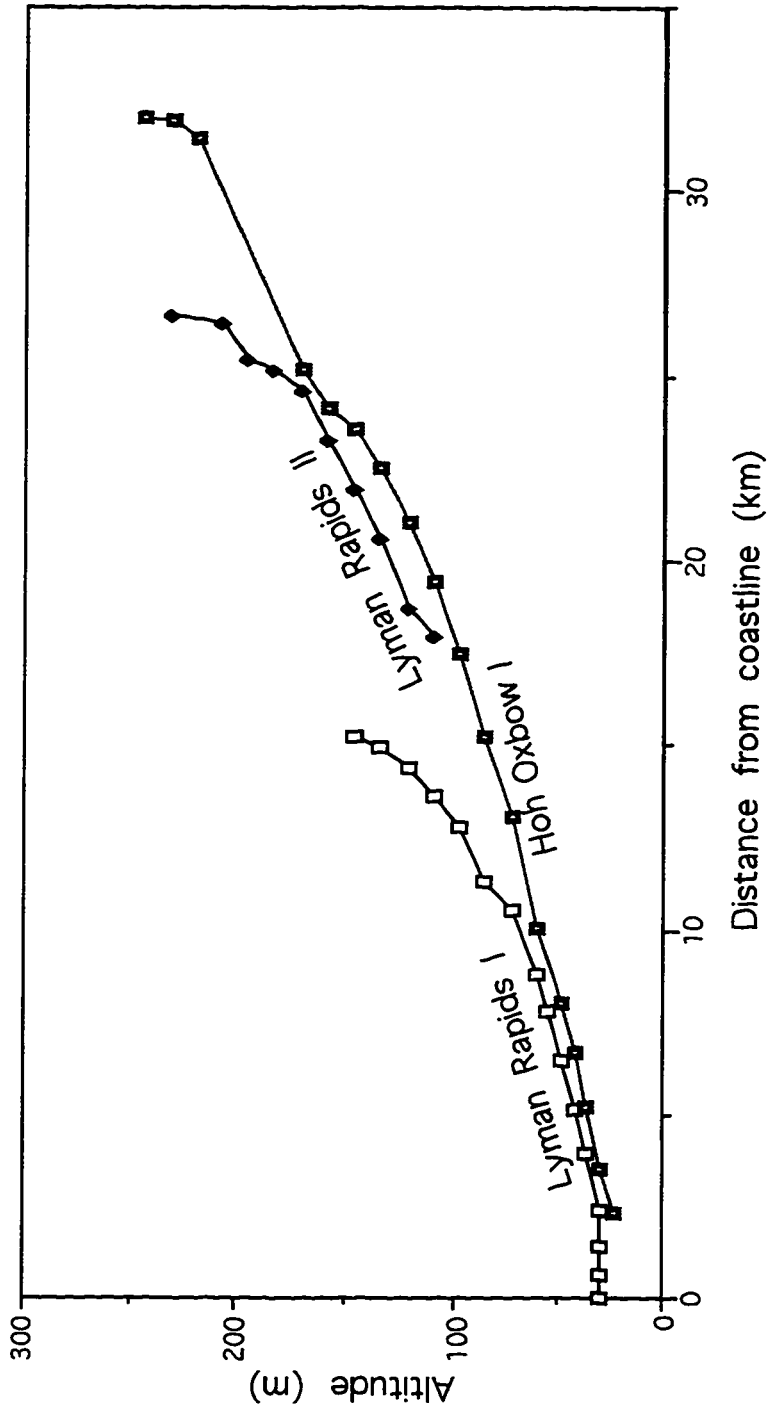


Figure 2.2: Longitudinal profiles of outwash valley trains in the Queets valley.

Stratigraphy

Exposures of Lyman Rapids drift are limited in the Queets valley, where Lyman Rapids till was observed in two exposures. A terrace-edge landslide (E1/2, E1/2, NE1/4, Section 20, T24N, R11W), approximately 3 km upvalley from the Queets valley Lyman Rapids I terminal moraine (Plem₁), exposes basal till. It contains 40 percent lithic clasts, mostly subangular pebbles and cobbles in a clayey sand matrix. The till contains wood as large as 30 cm in diameter, which yielded a radiocarbon date of >59,700 ¹⁴C yr BP (QL-4737). Two till units separated by fluvial sand are exposed adjacent to Sams Rapids (SE1/4, Section 32, T25N, R10W), approximately 3 km upvalley from the younger Lyman Rapids terminal moraine (Plem₂, Plate 1). The tills are similar, containing 50 to 60 percent lithic clasts, as large as 40 cm, in a silty sand matrix.

Several gravel pits in the lower Queets valley expose Lyman Rapids outwash. The outwash is moderately sorted, crudely to moderately well bedded, pebble- and cobble-dominated sandy gravel. Pebble- and cobble-dominated zones alternate in irregular fashion both vertically and horizontally. Cut-and-fill stratification is common and clasts are dominantly subrounded to rounded. Outwash is also exposed in seacliffs both north and south of the Queets River mouth (Chapter 3).

Snahapish and Clearwater Valleys

Extensive Lyman Rapids outwash terraces also exist in the Snahapish valley (Plate 1). An outwash head at the north end of the Snahapish valley marks the lateral extent of the Hoh valley glacier in that area. A valley train slopes southward from the outwash head, filling the Snahapish valley, and controls the southerly flow of the extremely underfit Snahapish River.

Thackray and Pazzaglia (1996) used weathering rind data to correlate fill terraces in the lower Clearwater valley (Plate 1) with the Snahapish valley outwash fill surface to the north and the lower Queets valley Lyman Rapids terraces to the south. As in the case of the Whale Creek drift, outwash apparently was transported through a narrow canyon from the Snahapish valley to the lower Clearwater valley. The nonglacial Clearwater River thus deposited a thick fill in its lower valley, in response to sediment-laden meltwater influx from the Snahapish valley and to base level changes at its confluence with the Queets River.

Hoh Valley

Morphology

The morphology of Lyman Rapids drift in the Hoh valley (Plate 1) is complicated by valley physiography. As described in the introduction to this chapter, lateral erosion in the relatively narrow Hoh valley and the influence of bedrock outliers on ice and meltwater channeling have produced a much more complicated morphology there than in the Queets valley. Only Lyman Rapids I drift has been recognized in the Hoh valley.

One extensive Lyman Rapids terminal moraine is recognized in the Hoh valley, but it is split into three parts by intervening bedrock masses. In the main valley, the terminal moraine lies about 4 km downvalley from the Hoh Oxbow area and about 12 km upvalley from the modern coastline. The moraine is about 0.8 km wide and stands well above surrounding landforms of Hoh Oxbow drift. Its surface is marked by several kettle ponds, some of which are associated with ice-contact stratified drift. A smaller moraine lies approximately 2 km south of the main portion, and separated from it by a bedrock outlier.

A third portion of the Lyman Rapids terminal moraine lies on the low drainage divide between the Hoh and Bogachiel valleys. It has a breadth similar to, but less relief than, the moraine in the main valley. Heusser (1974, 1978) reported limiting radiocarbon dates for associated bog peat, and suggested that the moraine was constructed between ca. 30,000 and 59,000 ^{14}C yr BP (given potential contamination, the latter date should be considered $\geq 59,000$ ^{14}C yr BP). Apparent dead-ice terrain lies on the Hoh valley side of the terminal moraine. Together, the three portions of the Lyman Rapids terminal moraine complex outline a large glacier which, on encountering the narrow lower Hoh valley and its surrounding bedrock masses, bifurcated into two major lobes and one minor one.

The bifurcation of the Hoh valley glacier also influenced the pattern of outwash deposition. An outwash valley train filled the lower Hoh valley and likely spread westward beyond the constricted valley and onto the broad plain exposed by low glacial sea level (Chapter 4). In addition, meltwater streams emanating from the minor southern moraine built an outwash fan in the Nolan Creek area (Figure 2.1, Plate 1). The fan merged with the main valley train and filled the Cedar Creek valley before reaching the broad coastal plain. The outwash valley train is preserved mainly as small terraces, particularly on the south side of the valley, because of erosion and subsequent

infilling with Hoh Oxbow outwash. In the coastal area, the Lyman Rapids terrace extends only as far south as Cedar Creek, where Hoh Oxbow outwash covers Lyman Rapids outwash and forms the terrace surface. Outwash valley trains from the Hoh-Bogachiel divide moraine likely merged with Bogachiel valley outwash trains, but that valley was not mapped during this project.

The Lyman Rapids longitudinal valley-train profile is shown in Figure 2.3. The influence of the Nolan Creek fan is clearly seen as a bulge in the center of the profile, but the profile is otherwise smooth and steepens to the main terminal moraine.

Stratigraphy

Stratigraphic exposures of Lyman Rapids drift have been observed only at and downvalley from the terminal moraine, located in the Lost Creek area (Plate 1, Figure 2.1), and at an outwash head in the Snahapish valley. As described below, however, the Lyman Rapids terminal moraine dammed the valley and strongly influenced subsequent sedimentation.

Lyman Rapids till has been observed only in the terminal moraine area, in the bank of Lost Creek at the Highway 101 crossing (SE1/4, SE1/4, Section 5, T26N, R12W). That till contains 20% lithic clasts, dominantly coarse cobbles and boulders, in a grey, clayey silt matrix. Blocks of dropstone-bearing, laminated slackwater sediments are included. Basal till may be present beneath the post-Lyman Rapids lake beds upvalley from the moraine, but it has not been observed.

Outwash is exposed in the lower Hoh valley, along the coast (Chapter 3), and in the Snahapish valley. Approximately 3 km downvalley from the main-valley Hoh terminal moraine, a gravel pit cut into a Lyman Rapids terrace near Pins Creek exposes distal to proximal outwash. The pit walls reveal crudely bedded, moderately sorted sandy gravel about 9 m thick. Clasts are dominantly subrounded to rounded. Much of the outwash is pebble- and cobble-dominated, but coarsens upward to a 2.5-m-thick, boulder-dominated section. This coarse section is overlain abruptly by a 1-m-thick bed of pebble-dominated gravel, in turn overlain by approximately 1 m of loamy soil. The grain-size relationships in the gravel suggest deposition by increasingly energetic meltwater streams as the glacier approached its maximum extent, followed by the superjacent deposition of finer gravel during the initial stages of retreat.

A gravel pit cut into the Snahapish valley outwash head exposes ice-proximal outwash of the Hoh valley glacier. The outwash consists of poorly sorted sandy gravel,

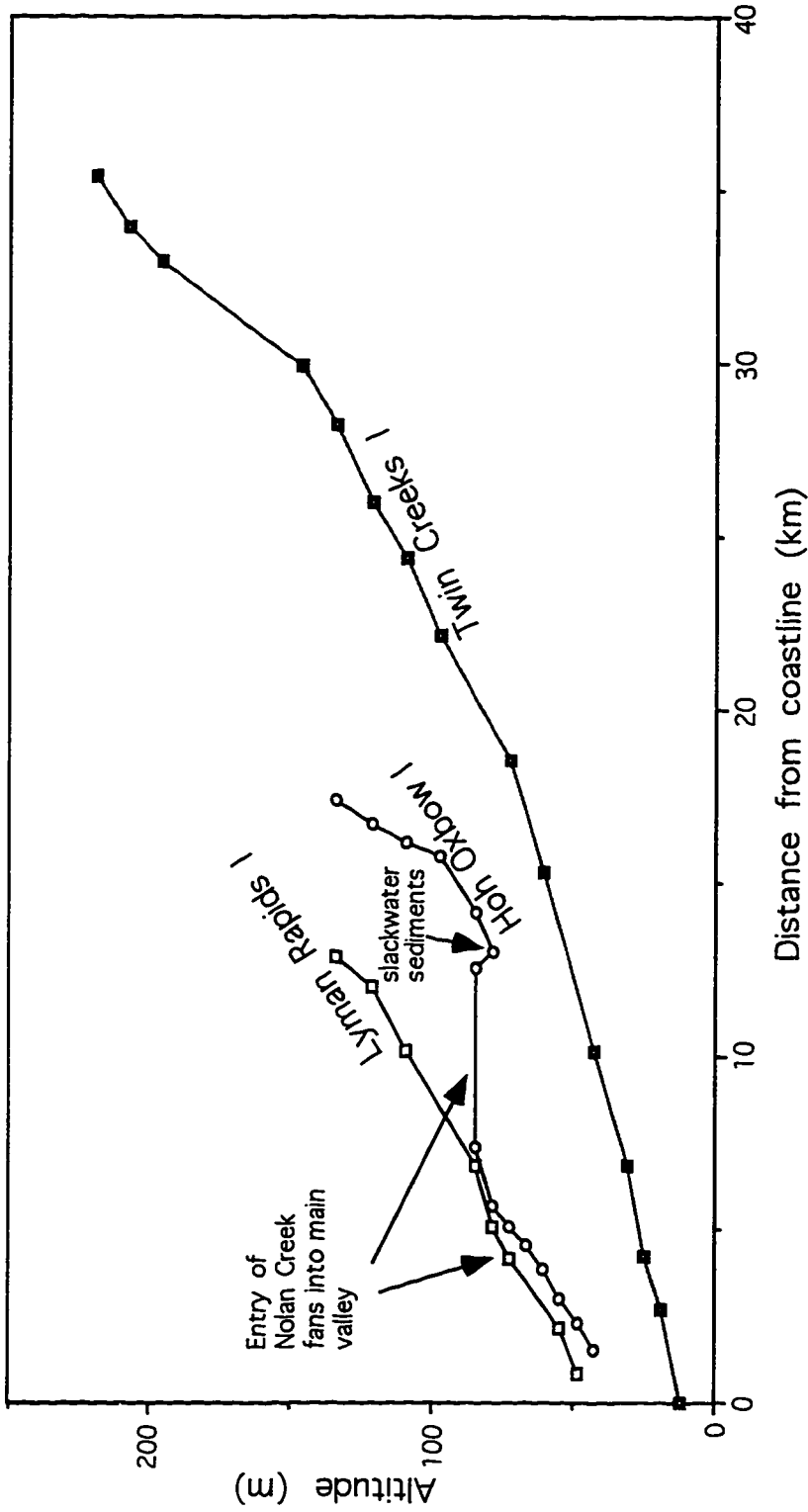


Figure 2.3: Longitudinal profiles of outwash valley trains in the Hoh valley. Note bulges in Lyman Rapids I and Hoh Oxbow I profiles due to sediment input of Nolan Creek outwash fans. Elevation data for Hoh Oxbow II and Twin Creeks II valley trains are insufficient to construct profiles.

with gravel clasts ranging in size from 2 to at least 150 cm. The clasts are subangular to subrounded and consist mostly of greywacke. The pit walls exhibit cut-and-fill structures, as well as bedding delineated by abrupt changes in dominant grain size.

Chronology of Lyman Rapids Glaciation

Limiting radiocarbon dates and seacliff stratigraphic relationships constrain the age of the Lyman Rapids drift. Lyman Rapids outwash buries a last-interglacial (IS 5e or 5c) wave-cut surface and associated interglacial sediments in seacliff exposures (Chapter 3). Therefore, the Lyman Rapids drift clearly postdates the sea-level highstand of the last interglaciation. Several "infinite" radiocarbon dates within and beneath Lyman Rapids outwash and till are the only maximum dates for the glacial advance (Table 2.1). Lacustrine sediments deposited in lakes upvalley from Lyman Rapids moraines have provided numerous minimum limiting dates, while several additional minimum dates have been obtained from cored bogs on terraces and from sediments overlying Lyman Rapids drift in seacliffs. Table 2.1 includes all dates with a stratigraphic or geomorphic relationship with Lyman Rapids drift.

The limiting dates in Table 2.1, together with the seacliff stratigraphic relationships, indicate that the Lyman Rapids drift was deposited during early or middle Wisconsin time (IS 4 or 3), or during a latter substage of the last interglaciation (i.e., IS 5b). The ca. 51,000 and 54,000 ^{14}C yr BP dates from the Queets valley, if finite, represent the closest minimum limiting dates, and allow for an early or middle Wisconsin age (IS 4 or 3). It is also conceivable that the Lyman Rapids drift was deposited during IS 5b. The buried wave-cut surface dates to IS 5e or 5c, and the actual amount of time represented by sediments between the wave-cut surface and Lyman Rapids outwash cannot be determined. However, at Destruction Island Viewpoint and elsewhere (Chapter 3), those intervening sediments include interglacial peat and paleosols, while sediments separating Lyman Rapids and Hoh Oxbow outwash were minimally altered by pedogenesis. That is, more time seems to be represented by sediments beneath the Lyman Rapids outwash than above, arguing for a younger rather than an older age.

HOH OXBOW DRIFT

The Hoh Oxbow drift represents the maximum extent of middle to late Wisconsin glaciation (IS 3 to IS 2), which was less extensive than that represented by

Table 2.1: Limiting dates for the Lyman Rapids drift. Table includes all dates with a stratigraphic or geomorphic relationship to the Lyman Rapids drift.

<u>Maximum Limiting Dates</u>		<u>Location</u>	<u>Material/relationship</u>
<u>Date, 14C yr BP/Reference</u>			
>59,700 (QL-4736)		Sams Rapids, Queets valley	Wood in outwash below LR or older till
>59,700 (QL-4737)		Mud Creek, Queets valley	Wood in LR till
>49,468 (AA-18410)		Seacliff 1 km north of Ruby Beach	Wood, silt bed within LR outwash
>48,230 (AA-16692)		Seacliff south of Whale Creek	Wood in peat bed within LR outwash
>44,498 (AA-16693)		Seacliff north of Whale Creek	Wood in silt bed within LR outwash
>42,430 (Beta-61320)		Seacliff north of Whale Creek	Wood in silt bed within LR outwash
>48,000 (Florer, 1972)		Seacliff near Destruction Is. Viewpoint	Interglacial peat beneath LR outwash
>33,700 (Florer, 1972)		Seacliff near Destruction Is. Viewpoint	Interglacial peat beneath LR outwash
<u>Minimum Limiting Dates</u>		<u>Location</u>	<u>Material/relationship</u>
<u>Date, 14C yr BP/Reference</u>			
>49,000 (AA-15379B)		Seacliff 0.8 km north of Kalaloch	Wood, silt bed overlying LR outwash
>49,000 (AA-15389)		Awful Creek, Hoh valley	Wood, lake beds behind LR moraine
>49,000 (AA-15390)		Morgan's Crossing, Hoh valley	Wood, lake beds behind LR moraine
>49,000 (AA-15394)		Red Creek/High Banks, Hoh valley	Wood, lake beds behind LR moraine
>49,000 (AA-15392)		Pole Creek, Hoh valley	Wood, lake beds behind LR moraine
*54,200+2500/-1900 (QL-4735)		Queets Ranger Station area, Queets v.	Wood, lake beds behind LR moraine
*51,400+1800/-1500 (QL-4789)		Queets Ranger Station area, Queets v.	Wood, lake beds behind LR moraine
44,109 ± 2014 (AA-18403)		Huelsdonk Ranch/Maple Crk., Hoh v.	Wood, lake beds behind LR moraine
43,300 ± 2300/-1800 (QL-4790)		Awful Creek, Hoh valley	Wood, lake beds behind LR moraine
41,900 ± 2000/-1600 (QL-4788)		Queets Ranger Station area, Queets v.	Wood, lake beds behind LR moraine
40,629 ± 1332 (AA-18415)		Seacliff 0.5 km north of Whale Creek	Wood, mud above LR outwash
40,050 ± 1200/-1000 (QL-4791)		Red Creek/High Banks, Hoh valley	Wood, lake beds behind LR moraine
39,700 ± 1,300 (AA-15388)		Awful Creek, Hoh valley	Wood, lake beds behind LR moraine
39,400 ± 1000/-800 (QL-4792)		Morgan's Crossing, Hoh valley	Wood, lake beds behind LR moraine
36,860 ± 925 (AA-18416)		Seacliff 0.5 km north of Whale Creek	Seeds, mud above LR outwash
36,760 ± 840 (AA-15383)		Seacliff near Destruction Is. Viewpoint	Wood, sand bed above LR outwash

Table 2.1 (continued)

<u>Date, ¹⁴C yr BP/Reference</u>	<u>Location</u>	<u>Material/relationship</u>
36,256 ± 807 (AA-18413)	Moses Prairie, Queets valley	Stems, bog atop LR outwash terrace
35,219 ± 883 (AA-18417)	Seacliff 0.5 km north of Whale Creek	Stems, mud above LR outwash
35,100 +1700/-1400 (QL-4793)	Pole Creek, Hoh valley	Wood, lake beds behind LR moraine
33,182 ± 756 (AA-16694)	Moses Prairie, Queets valley	Seeds, bog atop LR outwash terrace
30,340 ± 260 (Beta-61321)	Seacliff 0.8 km north of Kalaloch	Wood, peat bed above LR outwash
29,556 ± 1187 (AA-18404)	Huelsdonk Ranch/Maple Crk., Hoh v.	Stems(?), lac. behind LR/HO moraine
27,270 ± 380 (AA-15381)	Huelsdonk Ranch/Maple Crk., Hoh v.	Seed, lake beds behind LR moraine
15,180 ± 230 (AA-15380)	Seacliff north of Whale Creek	Seeds, silt beds above LR outwash

* Denotes closest limiting dates after younger, stratigraphically reversed dates are disregarded (see text)

Key to dating facilities: AA = NSF-Arizona AMS facility
 QL = Quaternary Isotope Laboratory, University of Washington
 Beta = Beta Analytic, Inc.

the Lyman Rapids drift. A still-less extensive readvance is represented by the Twin Creeks drift, described below. Hoh Oxbow landforms are most prevalent in the Hoh valley, where they occupy large areas upvalley from the Lyman Rapids limit. The bulk of morphologic, stratigraphic, and chronologic information for the Hoh Oxbow drift has been obtained from the Hoh valley. In the Queets valley, a single moraine and valley train has been identified, and the landforms cover small areas relative to their Hoh valley counterparts.

Queets Valley

Morphology

Only the Hoh Oxbow I drift has been mapped in the Queets valley. This contrast with the Hoh valley is due in part to geologic factors, described below, but may also reflect poorer access and exposure within the unroaded and unlogged land of Olympic National Park.

A single Hoh Oxbow end moraine has been identified in the Queets valley (Plate 1). That moraine lies on the south side of the valley in the Sams River area; it forms the southern edge of the tributary valley and extends partially across the main valley. An outwash valley train stretches downvalley from the moraine. The outwash filled the relatively narrow bedrock-walled valley immediately downvalley from the moraine, and spread across the coastal plain 3 km downvalley. A few small terrace remnants have been mapped nearly to the coastline. A longitudinal profile of the former outwash surface (Figure 2.2) shows two separate graded sections. The upper section, stretching from the end moraine to the area of the Lyman Rapids II end moraine, likely represents constriction or partial damming of the valley by the latter moraine. The meltwater stream apparently formed one profile graded to that temporary base level, and a second, longer profile graded to sea level.

An apparent fan-delta fill terrace stretches more than 7 km upvalley from the single Hoh Oxbow end moraine. The terrace is broad (1 to 1.7 km wide), and lies at a nearly constant elevation along its entire length. It spans the mouths of two major, formerly glaciated tributaries (Sams River and Tshletshy Creek), and several minor ones. Delta foreset beds are exposed at the mouth of Tshletshy Creek (Figure 2.1), and possible delta foresets are minimally exposed on the terrace riser between Tshletshy Creek and Sams River (T. Abbe, personal communication, 1994). Lake beds in the Sams River area coarsen upward into gravels in the lower portion of the stratigraphic

sequence. The fan-delta surface serves as evidence of a major lake, apparently dammed behind the Hoh Oxbow moraine. The lake may be responsible for the absence of late-phase Hoh Oxbow and Twin Creeks landforms in the Queets valley. The glacier likely terminated at or in the lake during those readvances, precluding the construction of moraines and outwash valley trains.

Stratigraphy

A sequence of apparent middle Wisconsin (IS 3) lacustrine strata is exposed from the Matheny Creek area at least as far upvalley as the Queets Ranger Station area, a distance of 6.6 km. The lacustrine sediments are exposed solely in river-bank exposures, where they are overlain disconformably by coarse gravels that form low terraces.

The lacustrine strata consist of grey, bedded and laminated silt, clay, and very fine sand. They contain rare detrital wood. In places, the beds and laminae are rhythmites, with alternating fine and coarse layers. Some outcrops display isoclinal to asymmetric overturned folds with wavelengths of 10 to 100 cm. Such outcrops are interspersed with those exposing flat-lying lacustrine sediment; thus, the deformation is likely a result of slumping, rather than tectonic or glacial-tectonic processes.

Hoh Oxbow outwash is exposed in several gravel pits south of the Queets River. It is similar to the Lyman Rapids outwash described above. Exposures of the entire stratigraphic sequence are lacking; therefore, the relationship of the outwash to the underlying lacustrine sequence cannot be ascertained.

Lacustrine sediments are well exposed along Sams River, a short distance upvalley from the Hoh Oxbow end moraine (Phem₁ on Plate 1). These strata were deposited later than those discussed above. The younger lacustrine strata consist of rhythmically laminated grey silt with very fine sand partings. The lacustrine sediments are 20-25 m thick and grade upward into sand and gravel. Delta foresets at the mouth of Tshletshy Creek likely relate to the same lacustrine episode (see above).

Hoh Valley

Morphology

Two members (I and II) of the Hoh Oxbow drift have been recognized in Hoh valley landforms. These members represent distinct advances, and evidence of a probable earlier, less extensive advance (Hoh Oxbow Ø) has been recognized only in

the stratigraphy. The maximum-phase (Hoh Oxbow I) terminal moraine (P_{hem1}, Plate 1) lies in the Hoh Oxbow area. As with the Lyman Rapids terminal moraine a short distance downvalley, this Hoh Oxbow moraine is split into two portions by a bedrock outlier south of the Hoh Oxbow area. In the area immediately south of the Hoh Oxbow, the moraine impinges upon a steep-fronted, bedrock-cored hill. The hill may represent a low bedrock ridge that impeded the glacier's downvalley movement. A prominent dead-ice moraine lies 3.5 km upvalley from the terminal moraine, with much of the intervening area marked by dead-ice terrain (P_{hdiu}). Apparent flow till is present near Elk Creek, and outwash covers the area immediately upvalley from the terminal moraine. Morphologically, the dead-ice terrain consists of poorly drained ground with numerous closed depressions as large as 500 by 200 m. A cross-section through a small depression in the latter area shows collapse features in outwash, indicating that recessional outwash buried stranded ice blocks.

The morphology of the Hoh Oxbow I outwash fill is complicated by the valley morphology. The two ice lobes, separated by the bedrock outlier, created distinct outwash fans that merged in the Pins Creek/Nolan Creek area (Figure 2.1, Plate 1). In that area, the fan from the southern lobe has a higher surface elevation than do the fan remnants in the main valley. A longitudinal profile stretching from the main-valley Hoh Oxbow I moraine to the coast (Figure 2.3) shows the influence of the southern-lobe fan. Coupled with a linear, cross-valley oriented Lyman Rapids outwash terrace, the Nolan Creek fan apparently ponded meltwater in the Pins Creek area. The ponding is evidenced by slackwater beds atop terraces on both sides of the Hoh River. Further downvalley, the outwash fill again split into two portions. One portion filled the main valley and is represented by outwash terraces reaching to the mouth of the Hoh River. The other portion filled a minor drainage to the south: in the Braden Creek area, meltwater from the edge of the Nolan Creek fan spilled over a divide and into the Cedar Creek drainage. Outwash terraces occupy the Cedar Creek valley and extend to the coast. In seacliff exposures south of Cedar Creek, Hoh Oxbow outwash overlies Lyman Rapids outwash (Chapter 3). Hoh Oxbow I outwash is not present between the Abbey Island area and the Hoh River mouth; instead, Lyman Rapids outwash dominates that area.

The Hoh Oxbow II drift includes end moraines (P_{hem2}) and dead-ice terrain (P_{hdiu}) lying upvalley from Hoh Oxbow I moraines, and outwash terraces (P_{ho2}) largely inset below Hoh Oxbow I terraces (Plate 1). On the south side of the river, two

closely spaced, narrow end moraines lie about 5 km upvalley of the Hoh Oxbow I moraine. A single moraine was mapped on the north side. Dead-ice terrain occupies a broad area upvalley the moraines, and also lies downvalley from the southern moraines. An outwash terrace, however, covers a 0.5- to 1.5-km-wide swath stretching from the southern moraines to the Winfield Creek area. This area appears to have been a meltwater channel that funneled water and sediment from the southern lateral edge of the glacier to a point at which it could enter the main river channel. The former channel is clearly represented on aerial photographs as a well-drained area supporting dense forest, in strong contrast to the surrounding poorly drained, sparsely forested dead-ice terrain. Downvalley from the Winfield Creek area, the outwash fill is represented by small terraces that are inset below Hoh Oxbow I and Lyman Rapids terraces. Stratigraphic and chronologic evidence (below) suggests that the Hoh Oxbow II landforms represent a readvance, rather than a recessional stillstand.

Stratigraphy

The stratigraphic sequence in the middle portion of the Hoh valley, upstream from the Lyman Rapids glacial limit, consists of middle Wisconsin (IS 3) lacustrine sediments overlain by middle and late Wisconsin (IS 3 and 2) Hoh Oxbow outwash and till (Figure 2.4). The lacustrine sediments consist of bedded and laminated silt, sandy silt, and clayey silt, commonly with fine sand partings. Stratification is locally rhythmic. Interbeds of sand and fine gravel are also present (Figure 2.4, sections 1, 2, and 5). Wood samples from the lake beds have yielded radiocarbon dates ranging from >49,000 (several samples) to $27,270 \pm 380$ ^{14}C yr BP (AA-15381).

A particularly gravel-rich lacustrine sequence is exposed in the Huelsdonk Ranch area (Figure 2.4, section 5). The 19-m-thick lacustrine section there contains clast-supported, sandy pebble-gravel beds as thick as 1.5 m; matrix-supported, gravel-rich silt beds as thick as 2.5 m; and common silt beds with rare gravel clasts. One of the matrix-supported, gravel-rich silt beds contains boulders as large as 80 cm, indicating ice-rafting. Radiocarbon dates indicate that the gravel-bearing lacustrine sediments were deposited ca. 29,560 ^{14}C yr BP. Wood from a slackwater bed in overlying outwash yielded a radiocarbon date of 29,160 ^{14}C yr BP.

The relationship of the Huelsdonk Ranch lacustrine sequence to the downvalley lacustrine sequence is ambiguous. It is unclear whether the Huelsdonk Ranch sequence (Figure 2.4, section 5) is the upward continuation of the lacustrine sequence observed

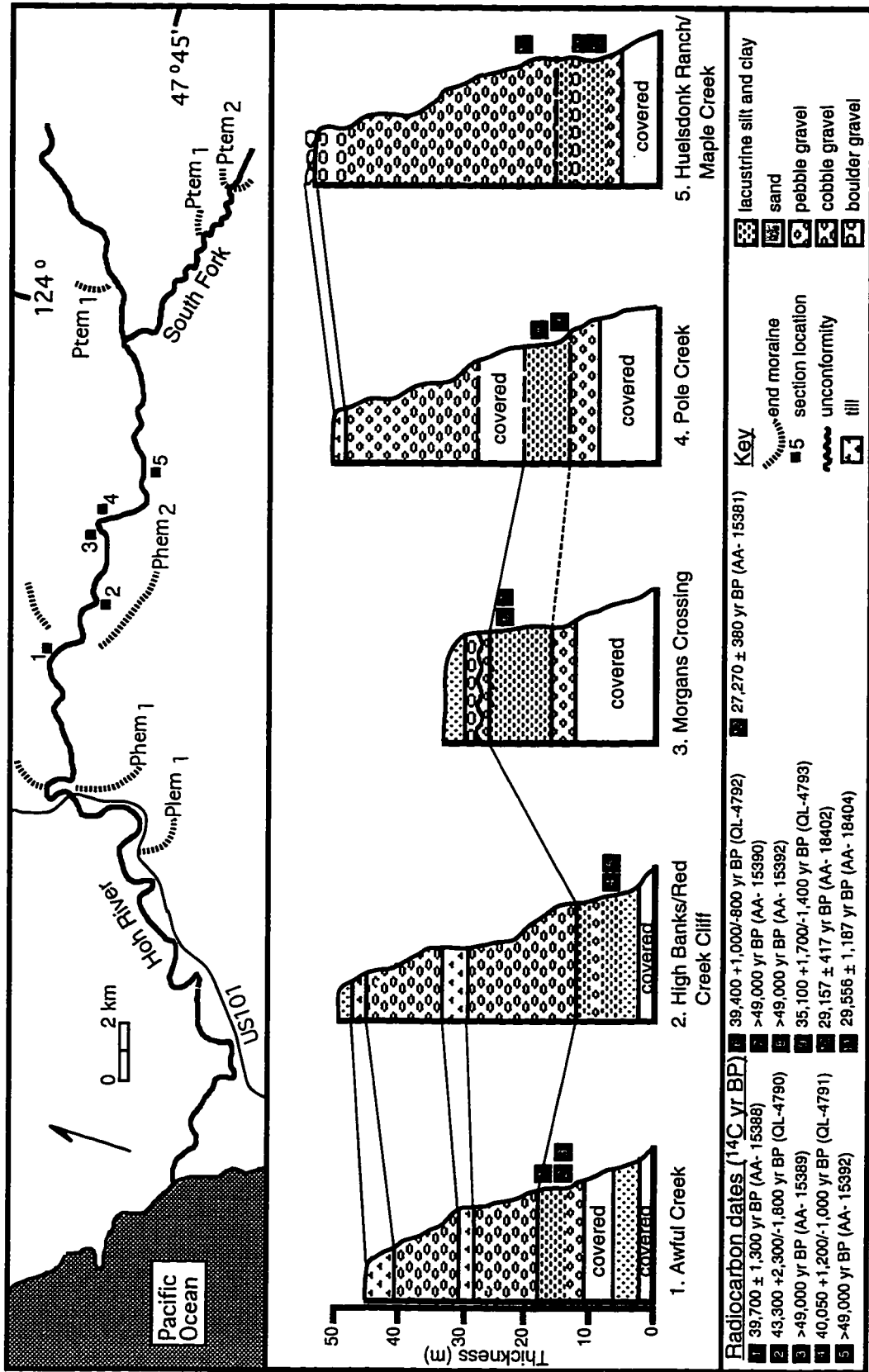


Figure 2.4: Correlated sections in the middle Hoh River valley, showing middle to late Wisconsin (IS 3 to IS 2) stratigraphy and chronology. Possible correlations between sections 3/4/5 and 1/2 are discussed in the text. Sections are not correlated to a common datum.

elsewhere in the middle Hoh valley (Figure 2.4, sections 1-4), or if it represents a distinct lacustrine episode following an initial middle Wisconsin (IS 3) advance. A ca. 44,000 ^{14}C yr BP date on wood from nearby sub-outwash lacustrine sediments suggests there are indeed two distinct lacustrine sequences. Furthermore, chronologic data elsewhere in the valley suggest initial outwash deposition (and thus an initial glacier advance) shortly after 39,000 ^{14}C yr BP. Conversely, none of the downvalley lacustrine sections contains ice-rafted detritus or upward-coarsening sediment that would indicate the approach of the Hoh valley glacier. This suggests the lacustrine-outwash contact is unconformable in the downvalley sections, with the upper portion of the sequence having been eroded. Thus, the Huelsdonk Ranch section may merely be the only conformable section observed. In either case, the Huelsdonk Ranch section and other evidence downvalley (see below) indicate a glacier advance into the middle Hoh valley, commencing between 29,560 and 29,160 ^{14}C yr BP.

As noted, outwash and till overlie the lacustrine sediments throughout the middle Hoh valley. These deposits are best exposed in the "High Banks" cliff (Figure 2.4, section 2), located approximately 7 km upvalley from the Hoh Oxbow area. Two outwash-till sequences are present. The lower outwash is 18 m thick and consists of grey, pebble-cobble gravel with no apparent upward increase in grain size. It is overlain by 3 to 6 m of grey, clast-rich till. Lithic clasts (70%) are mostly pebbles and cobbles, with rare striated boulders. The till is in turn overlain by 12 m of reddish outwash. This upper outwash consists mostly of reddish, pebble-cobble gravel, but coarsens upward to cobble-pebble gravel with rare boulders. A 3-m-thick bed of grey till overlies that outwash. The till in turn is overlain by a thin (< 1 m) bed of fluvial sand and 0.5 m of loess. This upper till apparently underlies much of the surrounding area, which is characterized by poorly drained, boggy ground (see geomorphology discussion above).

The High Banks stratigraphic relationships point to two distinct glacier advances. The outwash separating the two till units suggests that the glacier retreated well upvalley before readvancing to deposit the upper outwash and till.

A similar sequence is exposed at Awful Creek (Figure 2.4, section 1), which lies within 1 km (downvalley) of the High Banks exposure. The two sections differ principally in their top few meters. Instead of an upper till bed, the Awful Creek exposure is capped by poorly sorted, bouldery outwash or ice-contact stratified drift. This ice-proximal deposit may have been deposited as the glacier constructed the nearby

Hoh Oxbow II end moraine (Phem2, Plate 1) or as the glacier advanced to construct the Hoh Oxbow I landforms (see below).

Upvalley from the High Banks exposure, the Pole Creek and Huelsdonk Ranch areas (Figure 2.4, sections 4 and 5) expose a simpler outwash/till sequence. A single, 2.5-m-thick till unit is exposed within 3 m of the top of the Pole Creek section, underlain by at least 11 m of outwash. A lower till unit is not exposed there. However, the Pole Creek section is a composite of two exposures—one at the edge of the highest terrace and the other at the edge of a lower, erosional terrace—and the lower till may be present in the unexposed portion of the section. In the Huelsdonk Ranch area, which lies only 1.5 km upvalley from Pole Creek, a lower till is clearly absent. An upper till has not been observed in section, but boulders as large as 2 m litter the terrace. The terrace appears to be an erosional surface cut into the till/outwash sequence, with the boulders concentrated as a lag.

Chronology of Hoh Oxbow Glaciation

Hoh valley lacustrine strata have yielded much of the chronologic data pertaining to the Hoh Oxbow drift (Table 2.2). The Lyman Rapids moraine at Lost Creek (Plate 1, Figure 2.1) is inferred to have dammed the valley, maintaining a several-kilometer-long lake for several thousand years. The Queets valley was similarly dammed by a moraine in the Lyman Rapids area, but only three dates have been obtained from lacustrine strata there. Outwash-related dates from the Hoh valley and adjacent seacliffs augment the lacustrine dates.

As noted, the lacustrine-outwash relationship in the middle Hoh valley is ambiguous. Dates on lacustrine and other strata suggest two middle Wisconsin (IS 3) advances, shortly after ca. 39,000 ¹⁴C yr BP and between 29,560 and 26,660 ¹⁴C yr BP. However, it is not clear that there are two distinct lacustrine sequences, and it is possible that evidence suggesting a ca. 39,000 ¹⁴C yr BP advance merely reflects an unconformity between lacustrine strata and outwash in some exposures (Figure 2.4, sections 1-4). The ensuing discussion emphasizes the two-advance interpretation.

Radiocarbon dates beneath the oldest outwash in four of five stratigraphic sections (Figure 2.4, sections 1-4) range from >49,000 to 35,100 ¹⁴C yr BP. The *closest* maximum limiting dates (omitting stratigraphically reversed dates, as discussed in the introduction to this chapter) range from 40,050 to 39,400 ¹⁴C yr BP (Figure 2.4, dates 4, 1, and 6). These dates suggest a glacier expansion into the middle Hoh valley

Table 2.2: Limiting radiocarbon dates for the Hoh Oxbow and Twin Creeks drifts. Several maximum dates are also listed in Table 2.1 as minimum dates for the Lyman Rapids drift.

ca. 39,000 14C yr BP Hoh Oxbow Ø advance		
<u>Date, 14C yr BP/Ref.</u>	<u>Location</u>	<u>Material/relationship</u>
>49,000 (AA-15389)	Awful Creek, Hoh valley	Wood, lake beds beneath HO outwash
>49,000 (AA-15394)	Red Creek/High Banks, Hoh valley	Wood, lake beds beneath HO outwash
>49,000 (AA-15392)	Pole Creek, Hoh valley	Wood, lake beds beneath HO outwash
>49,000 (AA-15390)	Morgan's Crossing, Hoh valley	Wood, lake beds beneath HO outwash
43,300 ± 2300/-1800 (QL-4790)	Awful Creek, Hoh valley	Wood, lake beds beneath HO outwash
*40,050 ± 1200/-1000(QL-4791)	Red Creek/High Banks, Hoh valley	Wood, lake beds beneath HO outwash
*39,700 ± 1300 (AA-15388)	Awful Creek, Hoh valley	Wood, lake beds beneath HO outwash
*39,400 ± 1000/-800 (QL-4792)	Morgan's Crossing, Hoh valley	Wood, lake beds beneath HO outwash
35,100 ± 1700/-1400 (QL-4793)	Pole Creek, Hoh valley	Wood, lake beds beneath HO outwash

Minimum Limiting Dates
None

ca. 29,000 14C yr BP Hoh Oxbow I advance		
<u>Date, 14C yr BP/Ref.</u>	<u>Location</u>	<u>Material/relationship</u>
36,760 ± 840 (AA-15383)	Seacliff near Destruction Is. Viewpoint	Wood, sand bed beneath HO outwash
*29,556 ± 1187 (AA-18404)	Huelsdonk Ranch/Maple Crk., Hoh v.	Stems(?), lac. behind HO/LR moraine
*†29,157 ± 417 (AA-18402)	Huelsdonk Ranch/Maple Crk., Hoh v.	Wood near base of HO outwash
*28,352 ± 504 (AA-18409)	Seacliff near Destruction Is. Viewpoint	Wood, peat bed beneath HO outwash
*†28,010 ± 320 (AA-15382)	Owl Creek, Hoh valley	Wood near base of HO outwash in trib.
27,270 ± 380 (AA-15381)	Huelsdonk Ranch/Maple Crk., Hoh v.	Seed, lake beds beneath HO outwash

Table 2.2 (continued)

<u>Minimum Limiting Dates</u>	<u>Location</u>	<u>Material/relationship</u>
<u>Date, ¹⁴C yr BP/Ref.</u>		
*26,661 ± 343 (AA-18414)	Cassel Crk., Hoh valley	Wood, fine seds. above HO outwash
15,600 ± 240 (Heusser, 1974)	Elk Creek bog, Hoh valley	peat, bog in HO dead-ice terrain
14,480 ± 600 (Heusser, 1974)	upper Elk/Winfield Crk, Hoh valley	peat, bog in HO dead-ice moraine
ca. 23,000 ¹⁴C yr BP Hoh Oxbow II advance		
<u>Maximum Limiting Dates</u>		
None		
<u>Minimum Limiting Dates</u>		
<u>Date, ¹⁴C yr BP/Ref.</u>	<u>Location</u>	<u>Material/relationship</u>
19,324 ± 165 (AA-18407)	South Fork Hoh valley, confluence area	Wood, lake beds above till
19,274 ± 154 (AA-18408)	South Fork Hoh valley, confluence area	Wood, lake beds above till
19,169 ± 162 (AA-18406)	South Fork Hoh valley, confluence area	Wood, lake beds above till
19,067 ± 329 (AA-18405)	South Fork Hoh valley, Line Creek area	Wood, lake beds (above till?)
18,800 ± 800 (Heusser, 1974)	upper Clear Creek area, Hoh valley	peat, bog in HO dead-ice terrain
ca. 18,300 ¹⁴C yr BP Twin Creeks I advance		
<u>Maximum Limiting Dates</u>		
<u>Date, ¹⁴C yr BP/Ref.</u>	<u>Location</u>	<u>Material/relationship</u>
19,324 ± 165 (AA-18407)	South Fork Hoh valley, confluence area	Wood, lake beds above till
19,274 ± 154 (AA-18408)	South Fork Hoh valley, confluence area	Wood, lake beds above till
19,169 ± 162 (AA-18406)	South Fork Hoh valley, confluence area	Wood, lake beds above till
19,067 ± 329 (AA-18405)	South Fork Hoh valley, Line Creek area	Wood, lake beds (above till?)
*?18,274 ± 195 (AA-16700)	South Fork Hoh valley, Line Creek area	Wood in TC I (?) till

Table 2.2 (continued)

<u>Minimum Limiting Dates</u>	<u>Location</u>	<u>Material/relationship</u>
None		
Twin Creeks II advance		
<u>Maximum Limiting Date</u>		
<u>Date, ¹⁴C yr BP/Ref.</u>		
18,274 ± 195 (AA-16700)	South Fork Hoh valley, Line Creek area	Wood in TCI (?) till
<u>Minimum Limiting Dates</u>		
None		

* Denotes closest limiting dates after filtering process (see text)

† Denotes date on wood within outwash, therefore may reflect syn-depositional rather than pre-depositional age

Key to dating facilities: AA = NSF-Arizona AMS facility
 QL = Quaternary Isotope Laboratory, University of Washington
 Beta = Beta Analytic, Inc.

shortly after ca. 39,000 ¹⁴C yr BP. This advance (designated Hoh Oxbow Ø) is not expressed in the morphologic sequence (Plate 1), and was probably less extensive than the subsequent ca. 29,000 ¹⁴C yr BP advance.

Radiocarbon dates of lacustrine strata in the Huelsdonk Ranch/Maple Creek area, and of outwash elsewhere, indicate a ca. 29,200 to 26,700 ¹⁴C yr BP glacier expansion (Hoh Oxbow I) into the middle Hoh valley. The gravel-rich lacustrine sequence near Huelsdonk Ranch (Figure 2.4, section 5) yielded dates of 27,270 and 29,560 ¹⁴C yr BP (Figure 2.4, dates 12 and 13). The younger date is disregarded because it is out of sequence. A silty interbed in the overlying outwash yielded a 29,160 ¹⁴C yr BP date (Figure 2.4, date 10), and outwash at the mouth of Owl Creek (Figure 2.1, Table 2.2) yielded a date of 28,010 ¹⁴C yr BP. The closest maximum limiting date on Hoh Oxbow I outwash in a seacliff exposure at Destruction Island Viewpoint (Chapter 3) is 28,350 ¹⁴C yr BP. The closest minimum limiting date for Hoh Oxbow I outwash is 26,660 ¹⁴C yr BP, from an outwash terrace at Cassel Creek in the lower Hoh valley (Figure 2.1). Florer (1972) reported bracketing dates of 27,900 and 23,150 ¹⁴C yr BP for Quillayute valley outwash at LaPush (Table 2.2).

The Hoh Oxbow II drift is constrained by a basal bog date and by lacustrine dates in the South Fork Hoh valley. A bog in dead-ice terrain near Clear Creek (4.2 km upvalley of the terminal moraine) yielded a basal date of 18,800 ¹⁴C yr BP (Heusser, 1974). Lacustrine strata directly overlying till in the South Fork valley yielded three dates ranging from 19,320 to 19,170 ¹⁴C yr BP (Table 2.2). These dates indicate a mean minimum age of ca. 19,250 ¹⁴C yr BP. Direct maximum ages are lacking, but it is likely that the advance culminated well before 19,250 ¹⁴C yr BP—the glacier retreated at least 19 km before the ca. 19,250 ¹⁴C yr BP lacustrine strata were deposited. In the case of the Hoh Oxbow I advance, nearly 3,000 ¹⁴C yr passed between deposition of ice-rafted boulders (29,560 ¹⁴C yr BP) and the accumulation of supra-outwash organic sediment (26,700 ¹⁴C yr BP). Thus the Hoh Oxbow II glacier likely advanced into the middle Hoh valley between 23,000 and 20,000 ¹⁴C yr BP and retreated before 19,500 ¹⁴C yr BP.

Summary of Hoh Oxbow Glaciation—Three Advances Or Two?

The ambiguity in the Hoh valley glacial record, noted above, can be summarized as follows with regard to morphologic and stratigraphic evidence:

- a. *Two-advance interpretation*: Major advances occurred ca. 29,200 ¹⁴C yr BP (Hoh Oxbow I) and ca. 23,000 to 19,500 ¹⁴C yr BP (Hoh Oxbow II). Advance outwash was deposited atop 29,560 ¹⁴C yr BP lacustrine strata, conformably at Huelsdonk Ranch/Maple Creek and unconformably elsewhere. The glacier advanced over its outwash to the Hoh Oxbow area, depositing the sequence-capping till (inferred) at Huelsdonk Ranch and Pole Creek (Figure 2.4, sections 5 and 4), and the lower till at High Banks and Awful Creek (sections 2 and 1). The glacier constructed the Hoh Oxbow I terminal moraine before retreating upvalley from the High Banks area. It then readvanced between ca. 23,000 and 19,500 ¹⁴C yr BP, depositing the upper advance outwash and till at High Banks and the upper advance outwash and ice-proximal outwash at Awful Creek. The glacier constructed the Hoh Oxbow II terminal moraine before retreating upvalley from the Twin Creeks I glacial limit (see below).
- b. *Three advance interpretation*: Major advances occurred ca. 39,000 ¹⁴C yr BP (Hoh Oxbow Ø), ca. 29,200 ¹⁴C yr BP (Hoh Oxbow I), and ca. 23,000 to 19,500 ¹⁴C yr BP (Hoh Oxbow II). Advance outwash was deposited conformably atop lacustrine strata (now exposed at Pole Creek, Morgan's Crossing, High Banks, and Awful Creek) shortly after 39,400 ¹⁴C yr BP. The glacier advanced beyond Awful Creek, depositing the lower till there and at the High Banks. The glacier likely terminated upvalley from the Hoh Oxbow, with morphologic evidence subsequently eroded during the more extensive Hoh Oxbow I advance. The glacier retreated upvalley from the Huelsdonk Ranch area before readvancing ca. 29,200 ¹⁴C yr BP to deposit ice-rafted boulders and outwash there, the upper outwash and till at High Banks, and the upper outwash and ice-contact stratified drift at Awful Creek. It constructed the Hoh Oxbow I moraine adjacent the Hoh Oxbow before retreating an unknown distance upvalley. Dead-ice terrain formed upvalley of the moraine during and after that retreat. The glacier subsequently readvanced over previously deposited sediment (and the previously constructed dead-ice terrain) to construct the Hoh Oxbow II moraine near Awful Creek. Outwash deposition of this advance may have been limited to the lateral channel upvalley from Winfield Creek (see above) and to the then-entrenched main river valley.

Although either scenario is plausible, given available data, the three-advance interpretation is favored by the bulk of the evidence. In subsequent discussions, a ca. 39,000 ¹⁴C yr BP advance is assumed.

TWIN CREEKS DRIFT

Landforms and sediments representing a major glacial readvance are present in the Hoh valley. End moraines constructed during this readvance lie well upvalley of Hoh Oxbow end moraines, and a distinct stratigraphic sequence is exposed in the South Fork Hoh valley and adjacent parts of the main valley. For these reasons, the drift is considered distinct and is given a separate designation—Twin Creeks drift. Landforms consisting of Twin Creeks drift have not been recognized in the Queets valley, and probably were not constructed for reasons discussed above.

Morphology

Two phases of the Twin Creeks readvance are represented by landforms and sediments in the main Hoh and South Fork valleys. A Twin Creeks II end moraine/outwash head (Ptem₁, Plate 1) lies on the north side of the main valley, adjacent to Twin Creeks. This arcuate form spans only the northern half of the main valley, perhaps because a delta (see below) building from the South Fork valley into the main valley partially plugged the latter and forced the glacier terminus to occupy only the north side.

A correlative outwash head lies about 4 km up the South Fork valley. The glacier terminus is represented morphologically by the upvalley limit of the highest outwash terraces (Pto₁), and stratigraphically by till and ice-contact stratified drift (described below). An end moraine has not been recognized.

Outwash valley trains from the two outwash heads merge in the confluence area, and broad fill terraces stretch a short distance (2.3 km) downvalley from the confluence area. Narrower, largely erosional terraces downvalley, inset below Hoh Oxbow terraces and stretching nearly to the coastline, are correlated with the Twin Creeks I fill terraces (Figure 2.3). The river eroded into the Hoh Oxbow sequence before depositing 2 to 5 m of outwash.

A series of Twin Creeks II landforms have been mapped in the South Fork valley. A prominent end moraine (Ptem₂) lies 2 km upvalley of the Twin Creeks I outwash head and inset outwash terraces mark (Pto₂) the South Fork and main valleys. Stratigraphic relationships indicate that the late-phase outwash surface largely represents regrading of main phase landforms, with only 1 to 5 m of fresh gravel deposited above

the unconformity. A Twin Creeks II moraine has not been identified in the main Hoh valley.

Stratigraphy

Excellent exposures of Twin Creeks drift in the South Fork valley, plus additional exposures in the main Hoh valley, provide stratigraphic details and limiting radiocarbon dates. Dates from lacustrine beds in the South Fork valley also serve as minimum ages for the Hoh Oxbow II drift.

Till, outwash, and a variety of lacustrine sediments typify the South Fork stratigraphy. Till at the base of the confluence section (Figure 2.5, section 1) likely correlates with the Hoh Oxbow II drift (see above). The overlying lacustrine sequence extends into the main Hoh valley, and was deposited in a lake inferred to have been dammed behind the Hoh Oxbow II moraine (Ptem₂, Plate 1). In the confluence area, the lacustrine sequence consists of laminated silt with pebble dropstones, overlain by sandy and gravelly, upward-coarsening delta foreset and bottomset beds. Wood from the laminated silty sediment yielded three radiocarbon dates clustered around ca. 19,250 ¹⁴C yr BP (Table 2.2). The lacustrine sequence within 2 km of the Twin Creeks I outwash head (Figure 2.5, section 3) consists of thick sequences of silty sediment with variable amounts (20 to 70 percent) of lithic clasts. The lithic clasts are dominantly pebbles and cobbles, but boulders are also present. The sediment is vaguely bedded and appears to represent lacustrine deposition close to the ice margin, with delivery of abundant ice-rafted detritus. A wood sample from near the base of the clast-rich lacustrine sequence has a radiocarbon age of 19,070 ¹⁴C yr BP (Table 2.2).

Thick outwash caps the sequence downvalley from the outwash head, forming the broad terrace along the north valley edge that merges with the main-valley outwash terrace in the confluence area. In most exposures, including sections 1 and 2 on Figure 2.5, the outwash is thick (up to 25 m) and coarsens upward from pebble-cobble gravel to boulder-dominated gravel. The top 10 m of the outwash head section (Figure 2.5, section 3) contains bouldery till and ice-contact stratified drift.

A stratigraphic section near the Twin Creeks II terminal moraine (Ptem₂, Plate 1), contains sediments deposited during both Twin Creeks advances (Figure 2.5, section 5). Lacustrine silt at the base of the section coarsens upward to ice-proximal lacustrine sediment, similar to that observed downstream from the Twin Creeks I terminal moraine (Figure 2.5, section 3). The lacustrine sediment is overlain by till

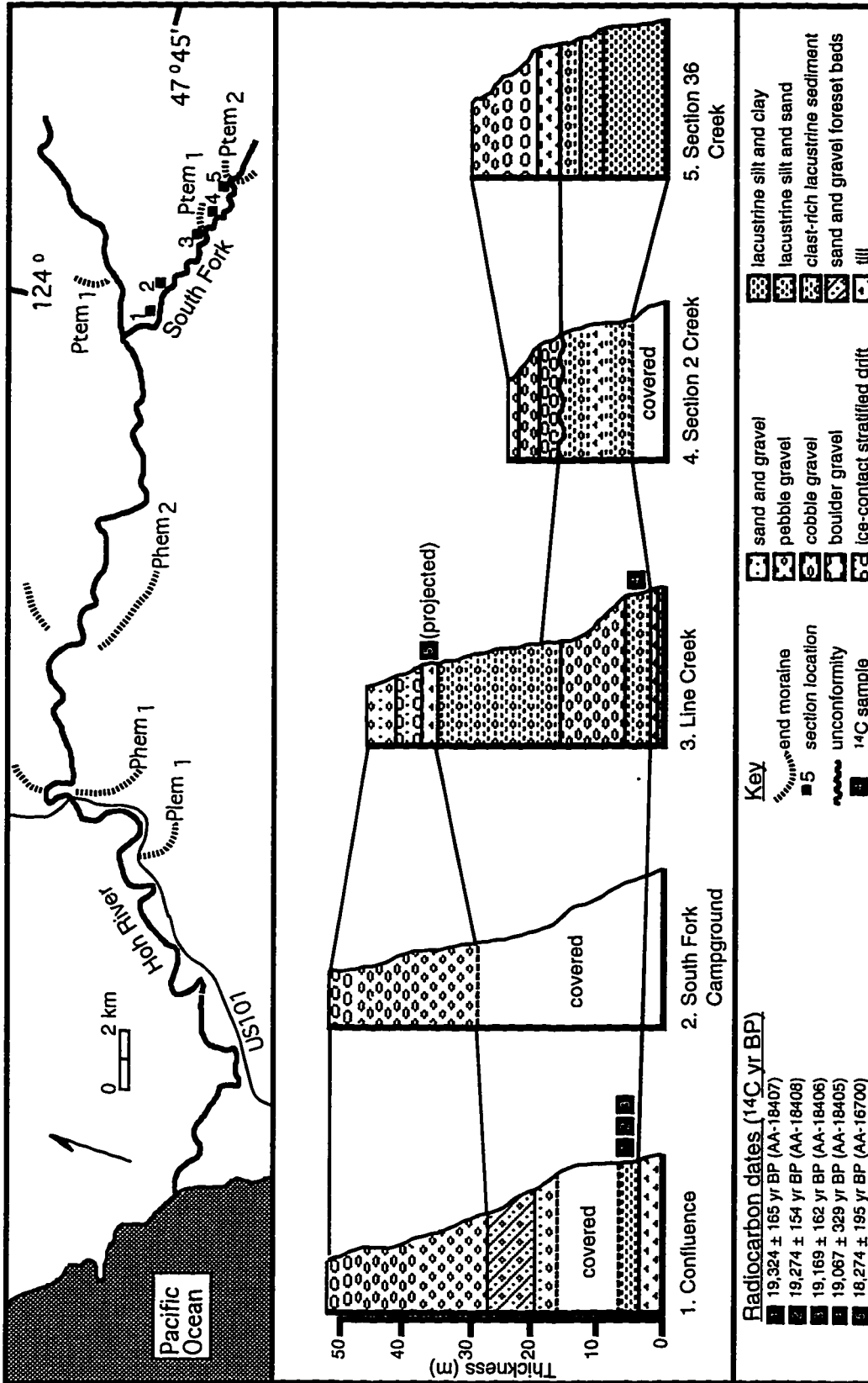


Figure 2.5: Correlated sections in the South Fork Hoh valley, showing late Wisconsin (IS 2) stratigraphy and chronology. Sections are not correlated to a common datum.

inferred to have been deposited during the Twin Creeks I advance. The till is overlain, in turn, by several meters of bouldery gravel, which was likely deposited during the readvance to the nearby Twin Creeks II moraine. Overlying cobble- and pebble-dominated gravel may be recessional outwash.

The outwash fill terrace overlying the section described above correlates downvalley with a series of erosional terraces. A typical terrace is represented in Figure 2.5, section 4. The terrace is cut into till and ice-proximal lacustrine sediment similar to that in sections 3 and 5. The erosional surface is capped by a boulder-cobble lag concentrate. The lag concentrate is in turn overlain by 4 m of fining-upward fluvial gravel.

Chronology

Drift of the two Twin Creeks readvances has yielded sparse chronologic data. The lacustrine dates from the South Fork valley cited above suggest that the first readvance began after ca. 19,250 ^{14}C yr BP. The 19,070 ^{14}C yr BP date is from clast-rich lacustrine strata that appear to signal the advance of the glacier into the lake. A date of 18,270 ^{14}C yr BP on till from the Line Creek area (Table 2.2), near the outwash head/moraine of the Twin Creeks I drift, may be a close maximum limiting date for that readvance. Thus, the Hoh Oxbow II and Twin Creeks I advances are separated by only 1,000 to ca. 4,000 ^{14}C yr. As noted, however, the advances are morphologically and stratigraphically distinct.

SUMMARY: EXTENT AND CHRONOLOGY OF GLACIER ADVANCES DURING THE LAST GLACIAL CYCLE

At least six distinct advances and readvances took place during the last glacial cycle (IS 4 through IS 2). The advances are summarized on time-distance diagrams in Figure 2.6.

The Lyman Rapids drift records the maximum advance of the last glacial cycle. The glaciers reached within 15 km of the coastline in both valleys, and the resulting outwash terraces dominate the lower valleys.

The maximum middle to late Wisconsin (IS 3 to IS 2) advance (Hoh Oxbow I) took place between ca. 29,200 and 26,700 ^{14}C yr BP. The spatial difference between Lyman Rapids and Hoh Oxbow I advances is much greater in the Queets than in the Hoh valleys, owing largely to contrasts in valley morphology. An earlier, less

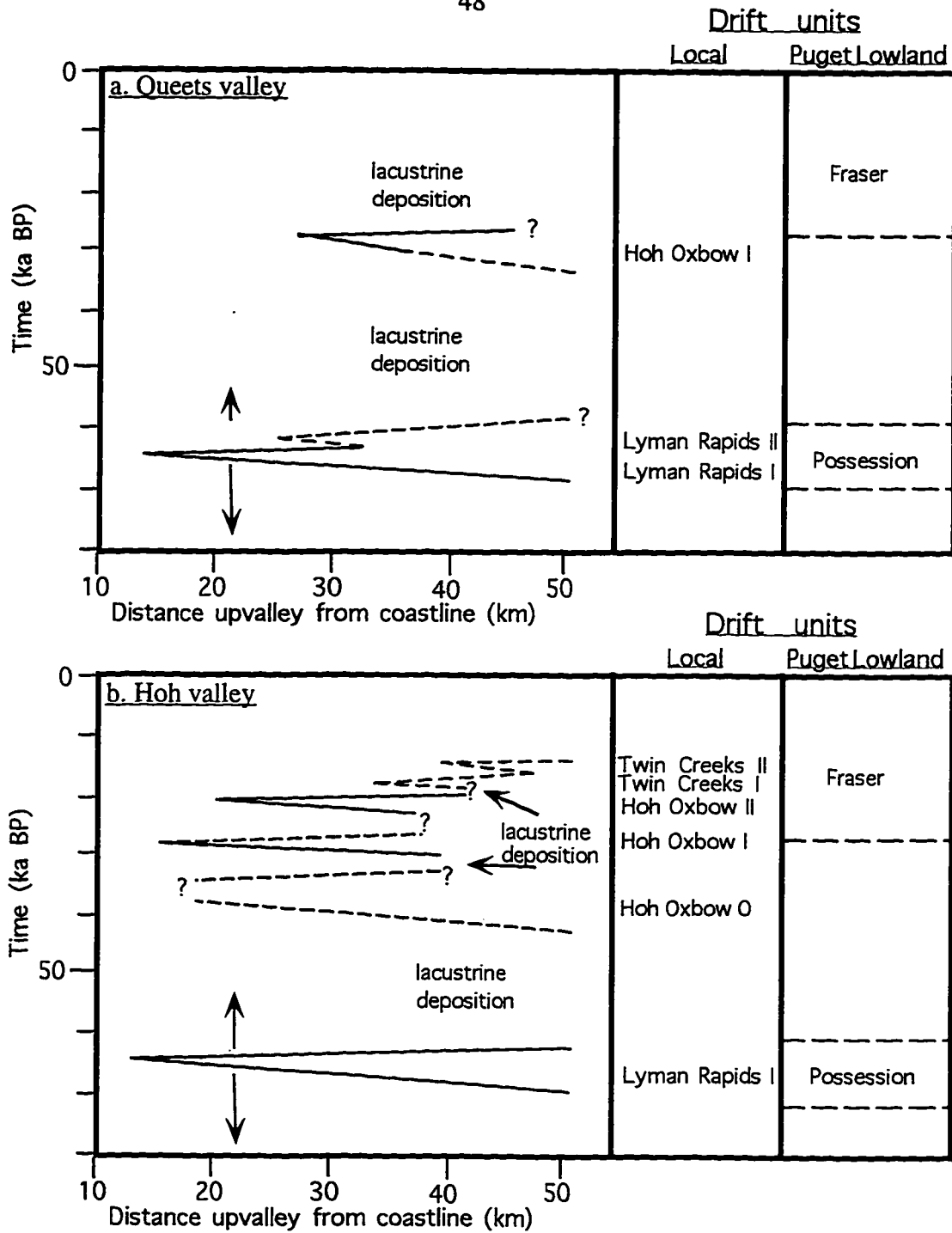


Figure 2.6: Glacier time-distance diagrams for the last glacial cycle, based on mapped drift limits and inferred ages. Question mark indicates uncertain glacier position at peak of advance or retreat. Time scale is in uncalibrated radiocarbon years from 0 to ca. 55,000 yr BP, and is correlated to marine oxygen isotope time scale beyond ca. 55,000 yr BP. Age of Lyman Rapids advance(s) is uncertain, as designated by arrows. The advance(s) may have occurred as late as ca. 52,000 radiocarbon yr BP, or as early as ca. 90,000 yr BP (IS 5b).

extensive, ca. 39,000 ^{14}C yr BP advance (Hoh Oxbow Ø) is reflected in the Hoh valley stratigraphic sequence.

Three subsequent readvances, represented only in the Hoh valley record, occurred after ca. 23,000 ^{14}C yr BP. The Hoh glacier readvanced between ca. 23,000 and 19,500 ^{14}C yr BP (Hoh Oxbow II), then retreated well up both the main Hoh and South Fork valleys before readvancing to deposit the Twin Creeks drift, probably ca. 18,270 ^{14}C yr BP. The Twin Creeks II advance occurred thereafter, perhaps coincidentally with the ca. 14,000 ^{14}C yr BP Puget Lowland ice-sheet maximum.

GLACIER RECONSTRUCTIONS AND PALEO-EQUILIBRIUM LINE ALTITUDES

Maps of inferred glacier topography in the Hoh and Queets valleys were drawn for each stage of the last glacial cycle, with the aim of estimating paleo-equilibrium line altitudes (ELA's). Glacial-geologic and topographic data were utilized in reconstructing the glaciers. Terminal and lateral moraines delimit outlines and elevations within the ablation zones of the glaciers, while valley and cirque morphologies aid reconstruction in the upper reaches. An assumed accumulation area ratio (AAR) of 0.6 (Porter, 1976) was applied to the glacier area-altitude distribution in order to calculate ELA's. Limited lateral moraine preservation and/or exposure, as well as uncertainties regarding tributary ice contribution to trunk glaciers, introduced considerable potential error into the reconstructions and, thus, into the ELA calculations. Nonetheless, the results (Table 2.3) are instructive.

The most striking aspect of these data is the strong contrast in ELA's and ELA depressions (ΔELA 's) between the Hoh and Queets drainages. Calculated ELA's for the main Queets valley and most tributaries are higher than, and ΔELA 's less than, for the main Hoh valley and its tributaries. These discrepancies may reflect contrasts in topographic, geologic, and/or glaciologic factors, or errors in glacier reconstruction. The principal ice accumulation areas for both drainages lie on the Mt. Olympus massif and surrounding uplands. However, the Hoh drainage receives ice from the northern slope, and the Queets drainage from the southern slope, of the massif. Thus, the ELA contrasts may reflect, in part, the greater snow and ice preservation capability of the upper Hoh drainage. Furthermore, Pleistocene AAR's may have been higher for the Hoh valley than for Queets valley. The upper Hoh valley is bounded by a much greater proportion of high, steep topography than is the upper Queets valley. The steep, rocky

Table 2.3: Estimated paleo-equilibrium line altitudes (ELA's) and ELA depressions (Δ ELA's) for stadial advances of the last glacial cycle.

	<u>Drift Name/Stadial Event</u>				
	<u>Lyman Rapids I</u>	<u>Hoh Oxbow I</u>	<u>Hoh Oxbow II</u>	<u>Twin Creeks I</u>	<u>Twin Creeks II</u>
<u>Hoh drainage</u>					
	<u>ELA 1/ΔELA²</u>	<u>ELA/ΔELA</u>	<u>ELA/ΔELA</u>	<u>ELA/ΔELA</u>	<u>ELA/ΔELA</u>
Hoh River	280 m/1408 m	350 m/1338 m	640 m/1048 m	920 m/768 m	no data
S. Fork Hoh R.	380 m/1308 m	480 m/1208 m	650 m/1038 m	660 m/1028 m	680 m/1008m
Mt. Tom Creek	810 m/878 m	830 m/858 m	830 m/858 m	830 m/858 m	no data
<u>Queets drainage</u>					
Queets River	540 m/1087 m	920 m/707 m	no data	no data	no data
Tshletshy Crk.	710 m/917 m	715 m/912 m	no data	no data	no data
Sams River	575 m/1052 m	600 m/1027 m	no data	no data	no data
Matheny Creek	615 m/1012 m	610 m/1017 m	no data	no data	no data

Notes:

1. Estimated uncertainty is ± 100 to ± 200 m. ELA's could not be calculated for the Hoh Oxbow \emptyset advance because end moraines are not preserved.
2. The ELA depression relative to modern (Δ ELA) is based on comparisons with drainage-wide median altitudes of modern glaciers (Spicer, 1988).
3. The small apparent ELA differences between stadial events in most tributaries (Mt. Tom Creek, Tshletshy Creek, Sams River, Matheny Creek) likely reflect a lack of data constraining downvalley ice extent, rather than climatic factors.

slopes bounding the upper Hoh valley might have contributed greater amounts of lithic debris to the glacier, potentially inhibiting ablation. As noted by Clark et al. (1994), debris cover on a glacier can greatly decrease the AAR. Thus, it is conceivable that the assumed AAR of 0.6 is too large for the former Hoh glaciers, reducing ELA estimates and increasing apparent ELA depressions. The estimated Queets valley ELA depressions of 700 to 1100 m are more in line with ELA depression estimates for the Washington Cascades (e.g., Porter et al., 1983) than are the Hoh ELA depressions.

COMPARISON OF WESTERN OLYMPIC GLACIAL RECORD WITH OTHER CLIMATIC PROXY RECORDS

Comparison of the western Olympic glacial chronology with other climate proxy records lends insight into regional and global climatic processes. Available comparisons include local (western Olympic Peninsula) and regional (western Washington) pollen records, a local beetle record, regional glacial records, marine sediment and oxygen-isotope records, and ice core records.

LOCAL AND REGIONAL CLIMATIC PROXY RECORDS

Pollen And Beetle Records

Heusser (1964, 1972, 1973, 1974, 1978) and Florer (1972) described pollen records from several western Olympic sites. Heusser (1972) documented the longest pollen record, preserved in the silt/peat seacliff sequence near Kalaloch (Chapter 3). He extrapolated his ca. 17,000 to 42,000 ^{14}C yr BP radiocarbon time scale back to 70,000 yr BP by assuming uniform sedimentation rates. The pollen data indicate cold episodes (Figure 2.7a), represented by increased *Graminae* pollen and decreased arboreal pollen, between ca. 52,000 and 48,000 ^{14}C yr BP, ca. 39,000 and 33,000 ^{14}C yr BP, ca. 25,000 and 21,000 ^{14}C yr BP, and ca. 19,000 and 16,000 ^{14}C yr BP.

Three factors suggest that a reinterpretation of Heusser's (1972) time scale is warranted. First, the current coastal stratigraphic study (Chapter 3) indicates that the beginning of Heusser's pollen record may be ca. 125,000 yr old. Second, the propensity for modern carbon contamination in the moist local climate suggests that Heusser's bulk-sediment radiocarbon dates may underestimate the ages of the cold episodes, particularly those older than 25,000 ^{14}C yr BP. Third, pollen in the lower third of Heusser's section (Figure 2.7a) indicate coldest temperatures above 12°C. These temperatures are 1 to 2°C warmer than during later stadial episodes, suggesting

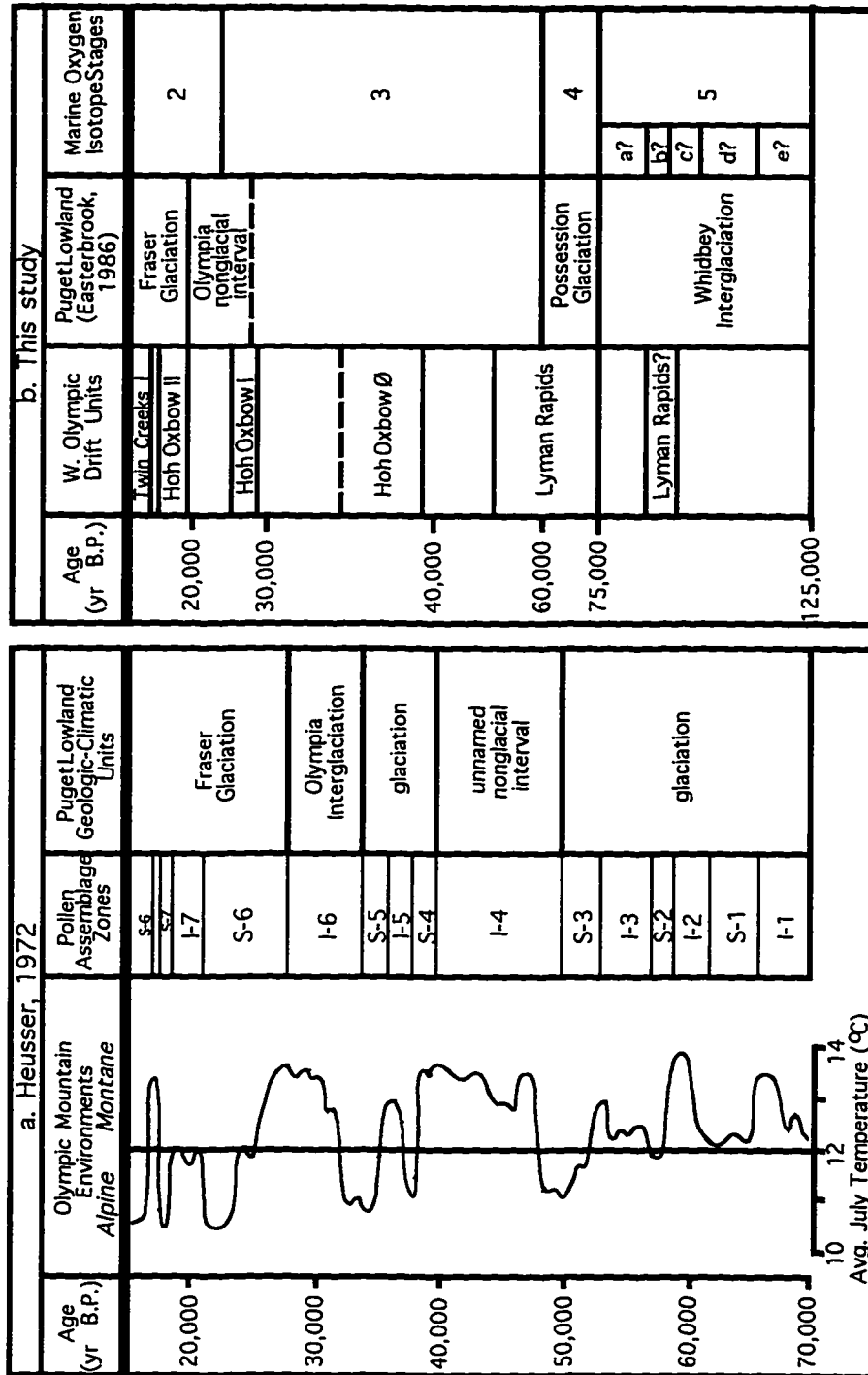


Figure 2.7: Reinterpretation of Heusser's (1972) pollen sequence from the Kalaloch silt/peat section. Reinterpreted time scale (right) follows Heusser's time scale to 25,000 14 C yr BP; from 25,000 to 40,000 14C yr BP, time scale is adjusted to dates of Hoh valley drift units, correlated to temperature minima and stadial (e.g., S-4) pollen assemblage zones; remainder assumes a ca. 52,000 to 75,000 yr BP age for the Lyman Rapids drift and a ca. 125,000 yr BP age for basal beach sediments [IS 3, 4 and 5e of Imbrie et al. (1984) and Martinson et al. (1987)]. Heusser (1972) correlated his older glaciations to the Salmon Springs Glaciation. Those names are here deleted, as the type Salmon Springs drift is now known to be >800,000 yr old (Easterbrook, 1986).

that the older portion of the record reflects interglacial rather than glacial conditions. Reinterpretation of Heusser's time scale (Figure 2.7b) suggests that his cold episodes correlate, respectively, with the Lyman Rapids advance, the post-ca. 39,000 ^{14}C yr BP, ca. 29,000 to 26,000 ^{14}C yr BP, and ca. 23,000 to 19,500 ^{14}C yr BP Hoh Oxbow advances, and the post-18,300 ^{14}C yr BP Twin Creeks advances. This reinterpretation suggests that the glacial record correlates broadly with the pollen record.

Heusser (1972) used modern vegetational community equivalents to construct his temperature curve for the Kalaloch pollen sequence (Figure 2.7a). He estimated average July temperatures of 10° to 11° C (3° to 4° C cooler than modern temperatures) for the cold episodes. The inferred temperature minima decrease successively from the oldest cold episode to the youngest, suggesting that stadial climatic cooling intensified through the last glacial cycle. Relative ice volumes inferred from the glacial stratigraphic and geomorphic record (Figure 2.6) generally decrease through the same succession of stadial episodes. Such a relationship suggests that lesser ice volumes in later stades of the last glacial cycle reflected less precipitation through the successively colder stadial episodes.

Heusser et al. (1980) developed vegetation-climate transfer-functions for four pollen types, in order to estimate more rigorously temperature and precipitation for the Kalaloch sequence. The resulting temperature curve reflects the general pattern of the earlier curve, but does not reveal the general decrease in peak stadial temperatures discussed above. The transfer function-derived estimates do show a strong correlation between Pleistocene precipitation and temperature, however, with colder temperatures corresponding to times of lower precipitation.

Pollen data elsewhere on the western Olympic Peninsula indicate similar climatic conditions for the last glacial cycle, although suspect chronologic control render comparisons difficult. Florer's (1972) pollen spectra from a seacliff sequence at LaPush show warming, then cooling conditions from ca. 34,000 to 28,000 ^{14}C yr BP, followed by outwash deposition. The inferred cool conditions prior to 34,000 and around 28,000 ^{14}C yr BP may correspond to the ca. 39,000 and 29,000 ^{14}C yr BP glacier expansions documented by the Hoh Oxbow drift. Cold, dry conditions are suggested after ca. 23,000 ^{14}C yr BP. Pollen from a bog at Humptulips, on the southwestern Olympic Peninsula (Heusser, 1964), suggest that the warmest and wettest middle Wisconsin (IS 3) climatic conditions existed between ca. 30,000 and 25,000 ^{14}C yr BP. Cold, dry conditions prevailed between about 20,000 and 15,000 ^{14}C yr BP.

Heusser (1978) described pollen from two sites on the Hoh-Bogachiel divide that indicate cold, dry, tundra/park tundra conditions shortly prior to ca. 60,000 ¹⁴C yr BP (correlating with the Lyman Rapids advance of this study?) and after ca. 20,000 ¹⁴C yr BP. Ameliorated conditions prevailed between 30,000 and 25,000 ¹⁴C yr BP. Heusser (1974) also reported cold, dry conditions in the Hoh valley between ca. 19,000 and 10,000 ¹⁴C yr BP.

In summary, correlation between middle and late Wisconsin (IS 3 and 2) pollen and glacier records is inconsistent and perhaps obscured by poor chronologic control. The most consistent feature of the various pollen records is the inferred cold, dry climate that prevailed for several thousand years after ca. 20,000 ¹⁴C yr BP. Pollen studies elsewhere in the Pacific Northwest [e.g., Hicock et al. (1982), Barnosky (1984), Whitlock (1992), Worona and Whitlock (1995)] also suggest cold, dry conditions for this interval. The relative dryness of this period is a likely cause for the relatively low western Olympic ice volumes reflected in the glacial-geologic record.

Cong and Ashworth's (1996) beetle study on the Kalaloch silt/peat sequence produced a climate record similar to that of Heusser (1972). They concluded that July temperatures between ca. 48,000 and 40,000 ¹⁴C yr BP were only ca. 1° C cooler than today. Beetle assemblages prevalent between ca. 28,000 and 17,000 ¹⁴C yr BP suggest a treeless environment 3° C cooler than today.

Other Olympic Mountain Glacial Sequences

Drift units in the Queets and Hoh valleys can be correlated broadly with drifts described elsewhere on the Olympic Peninsula. Moore (1965) described three drifts on the southwestern Olympic Peninsula. Moore's descriptions of weathering profiles suggest that his Humptulips drift correlates with the Wolf Creek and/or Whale Creek drifts, and that his Chow Chow drift correlates with the Lyman Rapids, Hoh Oxbow, and/or Twin Creeks drifts.

Carson (1970) described several drifts on the south-central Olympic Peninsula. Weathering profiles suggest that the Helm Creek and Mobray drifts correlate with the Wolf Creek and/or Whale Creek drifts. Carson subdivided sediments and landforms of the last glaciation (Grisdale drift) into six members. Weathering characteristics and relationships with the ca. 14,000 ¹⁴C yr BP Vashon drift suggest that his Grisdale I through III drifts and Grisdale IV through VI drifts may correlate with the Lyman Rapids drift and Hoh Oxbow/Twin Creeks drifts, respectively. A lack of radiocarbon

dates there and on the southwestern Olympic Peninsula limits evaluation of synchrony across the Olympic Mountains.

Regional Ice-Sheet And Mountain Glacier Records

The Cordilleran ice sheet record in the Puget Lowland (summarized by Easterbrook, 1986) documents advances correlative in part with the western Olympic record. Stratigraphic and aminostratigraphic data suggest that the Possession drift was likely deposited during the early Wisconsin (IS 4) glaciation, and may correlate with the Lyman Rapids drift. This advance likely reached the central Puget Lowland (Haase, 1987), but was less extensive than the late-Wisconsin Vashon advance. A possible middle-Wisconsin (IS 3) drift, representing the Oak Harbor stade of Easterbrook (1976), is bracketed by radiocarbon ages of ca. 35,000 and 27,000 ^{14}C yr BP. There is, however, no evidence from the Fraser Lowland or the Okanogan Plateau for such an advance. Numerous radiocarbon dates bracket the Vashon till, deposited during the late-Wisconsin (IS 2) Fraser Glaciation. This was the most extensive ice-sheet advance of the last glacial cycle (IS 4 through 2) and reached its maximum extent ca. 14,000 ^{14}C yr BP.

Glacial deposits have been described in several parts of the Washington Cascade Range [e.g., Mackin (1941), Crandell and Miller (1974), Porter (1976)], but chronologic data are few. Drift of the Evans Creek stade defines the mountain glacier maximum near Mt. Rainier, and is overlain in some valleys by lacustrine sediments associated with the Vashon stade ice-sheet advance. Thus, the alpine maximum preceded the ice-sheet maximum. The Evans Creek advance may have been contemporaneous with the ca. 22,000 ^{14}C yr BP alpine advance (Coquitlam drift) in southern British Columbia (Clague et al., 1980), as well as with the ca. 23,000 to 19,500 ^{14}C yr BP Hoh Oxbow II advance described above. Halstead (1968), reported maximum dates of ca. 21,100 and 19,200 for an advance of the Cowichan glacier on southern Vancouver Island.

Late-glacial advances in the Washington Cascades, represented by the Hyak drift (Porter, 1976) and the McNeeley I drift (Crandell and Miller, 1974; Heine, 1996), preceded deposition of organic matter dated between ca. 11,300 and 11,000 ^{14}C yr BP. Such advance(s) may correspond with the Twin Creeks II advance recorded in the western Olympic sequence, or with yet unrecognized advances. Forthcoming

radiocarbon and cosmogenic dates (T. Swanson, personal communication) may permit more detailed comparisons between the Cascade and western Olympic glacial records.

The above comparisons suggest that western Olympic Peninsula glacial advances correlated, at least in part, with those of the Cordilleran ice sheet and Cascade alpine glaciers. However, the relative extents of the successive advances were in contrast in the different areas.

Discussion

Western Olympic glacier fluctuations apparently corresponded to local climatic fluctuations, as reflected in pollen records, but their relative extents did not match those of other glaciers in western Washington. The Pleistocene Olympic glaciers likely were sensitive to moisture availability, having reached their greatest extents during stadial periods when the climate was milder and wetter. Modern Olympic glaciers are also sensitive to moisture availability: the largest and lowest glaciers occupy the western, oceanward portion of the Olympic uplift, with median elevations (Spicer, 1988) and the glaciation threshold (Porter, 1977) rising steeply to the northeast. Modern glacier distribution is also strongly influenced by the moisture funneling effect of major western river valleys (Spicer, 1988).

The apparent asynchrony of western Olympic glacier fluctuations with Cordilleran Ice Sheet fluctuations may be a result of contrasts in response time, or merely of contrasting preservation of sedimentary records. The smaller mass of the mountain glaciers allows more rapid response to short-lived climatic fluctuations. Thus, the Olympic glaciers advanced and retreated markedly during IS 3 stadial events lasting as little as 2,000 to 3,000 ^{14}C yr, while the ice sheet may not have fluctuated significantly. In fact, the Cordilleran ice sheet had coalesced and begun to advance into the northern Georgia Depression by ca. 28,800 ^{14}C yr BP, the approximate time of the Hoh Oxbow I advance. Within the limits of stratigraphic and chronologic control, it appears to have expanded slowly until ca. 14,000 ^{14}C yr BP, when it reached its maximum [chronology summarized by Booth (1987)]. Thus, the ice sheet may have integrated into one advance the four successive stadial events recorded in the Olympic record (Hoh Oxbow I through Twin Creeks II advances). Conversely, the ice sheet may have fluctuated in response to each stadial event, with evidence of early fluctuations having been eroded during the subsequent 14,000 ^{14}C yr BP maximum advance. That maximum advance is likely related to the modeled northward shift of the jet stream

between 18,000 and 12,000 ^{14}C yr BP (Thompson et al., 1993), which would have brought ice-sheet nourishing precipitation to southwestern British Columbia.

The apparent asynchrony of Olympic and Cascade alpine glacier maxima is perplexing. At face value, the asynchrony suggests that a) the two ranges experienced strongly contrasting local climatic conditions, or b) contrasts in glacier mass balance factors in the two ranges caused contrasting responses to similar climatic variation. The former seems unlikely, given the proximity of the ranges. The latter is more conceivable. Pleistocene Olympic glaciers may have been more dependent on voluminous precipitation, satisfied by proximity to the Pacific Ocean, than were Cascade glaciers. During IS 3, a more northerly jet-stream track and prevailing westerly winds likely delivered greater precipitation to the region than was delivered during IS 2. Circulation models suggest that the jet stream was displaced southward during the last glacial maximum, and that the ice-sheet anticyclone brought dry easterly winds to the Pacific Northwest (Thompson et al., 1993). Cascade glaciers, *if* less dependent on voluminous precipitation (i.e., more dependent upon colder temperatures), would have been less affected by the precipitation contrasts and may not have responded strongly to the IS 3 stadial events. Conversely, the western Olympic and Cascade glaciers may have responded to the same sequence of stadial episodes, with the downvalley extents reversed because of a) minor mass-balance contrasts that created the small ELA differences necessary, and/or b) differences in ice flow or other factors.

The reliability of regional correlations and of the inference of asynchrony is limited by available chronologic data. Additional dates are needed, particularly with respect to glacier fluctuations in the Cascade Range, to assess these hypotheses.

MARINE OXYGEN ISOTOPE AND SEDIMENT RECORDS

The western Olympic glacial record appears to correspond with both first-order (i.e., Milankovitch-related) and second-order fluctuations in the deep-sea oxygen isotope record. The Twin Creeks I advance correlates, at least broadly, with the global ice-volume peak of IS 2. On the other hand, all three Hoh Oxbow advances and the Twin Creeks II advance occurred during periods of lesser global ice volume during IS 3 and IS 2.

The western Olympic chronology suggests a correlation between local glacier advances and second-order climatic fluctuations recorded largely in the North Atlantic region (Figure 2.8). Several studies [e.g., Heinrich (1988), Broecker et al. (1992),

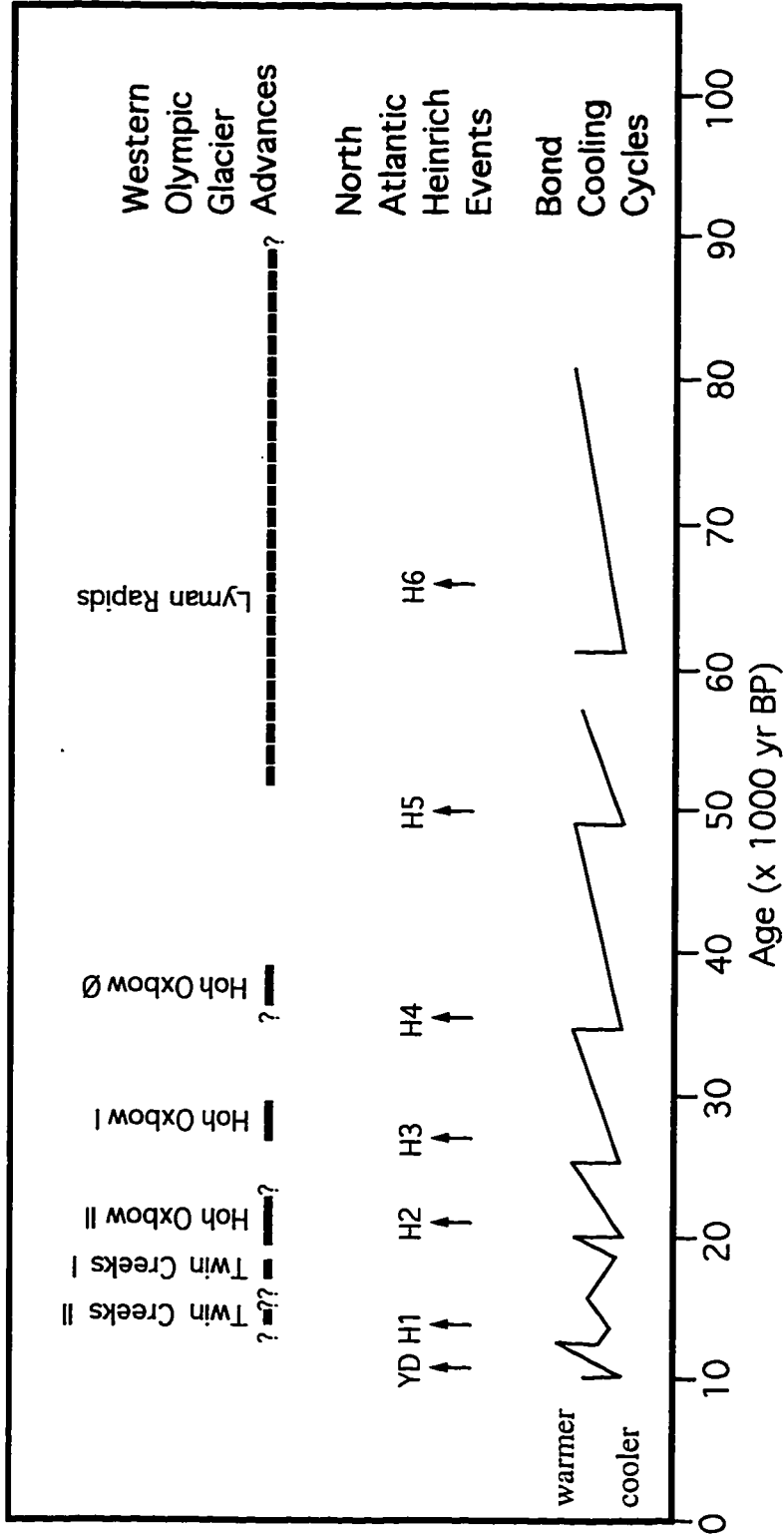


Figure 2.8: Suggested correlation of western Olympic glacial chronology with north-Atlantic Heinrich ice-rafter events and Bond cooling cycles, reflected in marine- and ice-core oxygen-isotope data (Bond et al., 1993). Time scale, from Bond et al. (1993), is based on uncalibrated radiocarbon dates to 35,500 yr BP. For >35,500 yr BP, time scale is based on correlations of oxygen isotope peaks and Heinrich events, coupled with linear interpolation. Ages of western Olympic glacier advances are in uncalibrated radiocarbon yr for Twin Creeks II through Hoh Oxbow Ø advances. Potential age range of Lyman Rapids advance based on minimum limiting radiocarbon dates and stratigraphic interpretation.

Bond et al. (1992), Bond et al. (1993), Grousset et al. (1993)] have documented episodic iceberg rafting events (Heinrich events) there that correlate with marked cold periods. Bond et al. (1993) correlated foraminiferal and sediment data ($\delta^{18}\text{O}$ ratios, percent *Neogloboquadrina pachyderma* [s.], Heinrich ice-rafted detritus layers) with $\delta^{18}\text{O}$ ratios from the Greenland GRIP summit core. They demonstrated that bundles of millennial-scale Dansgaard-Oeschger cooling cycles comprise longer-term cooling cycles ("Bond cycles"), the culminations of which coincide with Heinrich iceberg-discharge events.

With the exception of Twin Creeks I, the Olympic chronology suggests that advances of the last glacial cycle correspond with Bond cycles and Heinrich events. Hoh Oxbow \emptyset and I glacier expansions into the middle Hoh valley, taken as the dates of initial outwash deposition (ca. 39,000 and 29,200 ^{14}C yr BP, respectively), occurred approximately two-thirds through successive Bond cycles. The ca. 26,700 ^{14}C yr BP Hoh Oxbow I culmination coincides with the culmination of the corresponding Bond cycle and thus with Heinrich event 3 (H3). Though the timing of Hoh Oxbow \emptyset retreat is unconstrained, the correspondence of the expansion with the Bond cooling cycle suggests the culmination correlated with H4. Timing of the Hoh Oxbow II advance phase is also unconstrained. However, minimum dates suggest that the advance occurred between 23,000 and 19,500 ^{14}C yr BP and may thus have corresponded with H2. The Twin Creeks II advance has no direct chronologic constraint, but it is suspected to correspond with the ca. 14,000 ^{14}C yr BP Cordilleran ice-sheet maximum [and with Domerie advance of Porter (1976) in the Washington Cascades]. Thus, the Twin Creeks II advance may correlate with H1. Finally, the Lyman Rapids advance occurred between the sea-level highstand of the last interglaciation (seacliff stratigraphic evidence) and ca. 52,000 ^{14}C yr BP (minimum date from lacustrine strata) and therefore might correlate with H6 or H5.

In summary, the number and general timing of advances in the western Olympic chronology suggests a correspondence with North Atlantic climatic cycles. The correlation of the Hoh Oxbow I advance with H3 and the corresponding Bond cycle is strong, and lends support to the other correlations.

Discussion

It is evident that western Olympic glaciers have not responded only to Milankovitch forcing. They have responded also to another forcing mechanism, not yet understood, that has affected mountain glaciers and other climatically sensitive archives.

The western Olympic record adds to a growing body of evidence showing that mountain glaciers are much more sensitive to short-term climatic excursions than are ice sheets, and that they can record second-order climatic fluctuations. In their review of mountain glacier fluctuations, Gillespie and Molnar (1995) emphasize that mountain glaciers respond to regional climates. In the case of the western Olympic glacier record, the regional climatic variations appear to mirror more widespread variations. But, as in the discussion of regional correlations above, evaluation of global climatic variations and their underlying causes requires much better chronologic control than now exists.

CONCLUSIONS

The western Olympic glacial record provides a new chronology for alpine glaciation in the maritime Pacific Northwest. This record is unique for the North American Cordillera, in terms both of the chronologic detail and the number of documented advances during the last glacial cycle, and should serve as an important reference for studies in other parts of western North America.

Specific conclusions that can be drawn from this study include:

1. Two pre-last interglacial glaciations are documented in the geomorphic and stratigraphic record. The Wolf Creek drift has yielded reversely magnetized samples, and, therefore may have been deposited during an early Pleistocene glaciation (>780,000 yr ago). The Whale Creek drift may have been deposited during the glaciation (IS 6) immediately preceding the last interglaciation.
2. Six glacier advances and readvances occurred during the last glacial cycle (IS 5b or 4 through IS 2), and their chronology suggests partial correlation with north-Atlantic Heinrich (H) events and Bond cooling cycles (Bond et al., 1993):
 - a. Lyman Rapids: between 90,000 yr BP (IS 5b) and ca. 52,000 ¹⁴C yr BP
 - b. Hoh Oxbow Ø: between ca. 39,000 and 36,000 ¹⁴C yr BP (H4?)
 - c. Hoh Oxbow I: between ca. 29,200 and 26,700 (H3)

- d. Hoh Oxbow II: ca. 23,000 to 19,500 ¹⁴C yr BP (H2)
- e. Twin Creeks I: ca. 18,300 ¹⁴C yr BP
- f. Twin Creeks II: after ca. 18,300 ¹⁴C yr BP; ca. 14,000 ¹⁴C yr BP
Vashon Stade? (H1?)

3. Estimated ELA depressions for the six glacier advances in the main Hoh and Queets valleys are:

- a. Lyman Rapids: 1408 m (Hoh)/1087 m (Queets)
- b. Hoh Oxbow Ø: insufficient morphologic data
- c. Hoh Oxbow I: 1338 m (Hoh)/707 m (Queets)
- d. Hoh Oxbow II: 1048 m (Hoh)
- e. Twin Creeks I: 768 m (Hoh)
- f. Twin Creeks II: 1008 m (South Fork Hoh only)

Greater ELA depressions in the Hoh valley may reflect topographic, glaciologic, and/or geologic contrasts, or errors in glacier reconstructions.

- 4. Comparison with local pollen records suggests that the western Olympic glaciers reached successive maxima during times that were wetter and slightly warmer (mean July temperature) than during the last glacial maximum. The magnitude of western Olympic glacier advances, therefore, was likely more strongly influenced by moisture availability than by temperature.
- 5. Within the limits of available chronologic data, the Olympic glacial record is at least partially asynchronous with the Puget Lobe of the Cordilleran Ice Sheet and with Cascade mountain glaciers.
- 6. Correlation of western Olympic glacial events with North Atlantic cooling cycles and iceberg discharge events suggests that the Olympic glaciers responded to regional climatic fluctuations that were linked to broader Northern Hemisphere climatic variations.

CHAPTER 3 COASTAL STRATIGRAPHY AND NEOTECTONIC DEFORMATION

INTRODUCTION

Coastal stratigraphy offers a wealth of information for understanding interglacial-glacial cycles and neotectonic deformation in the project area. The stratigraphic sequence provides a view, unique in the conterminous United States, of coastal sedimentologic activity spanning an entire interglacial-glacial cycle. Additionally, the interglacial-glacial sequence reveals details of deformational processes that are less perceptible in portions of the Cascadia convergent margin that lack such a sequence.

This chapter describes and interprets the varied stratigraphic sequence revealed in excellent seacliff exposures between the Hoh and Raft rivers. The vertical stratigraphic succession includes interspersed evidence of glacial-fluvial inundation, interglacial marine transgression, and late-interglacial and interstadial landscape stabilization. Lateral stratigraphic variability is due principally to decreasing importance of outwash away from river mouths and the increasing dominance of sediments from local uplands. The magnitude and direction of tectonic deformation appears to be variable through the Brunhes magnetic-polarity chron, and helps to constrain magnitudes of permanent and flexural (elastic) deformation recorded in geodetic measurements.

PREVIOUS STRATIGRAPHIC WORK

Previous workers have studied stratigraphic, palynologic, and tectonic aspects of the Quaternary coastal stratigraphy. Rau (1973, 1980) studied the coastal geology between Point Grenville and LaPush and described the Quaternary stratigraphy in reconnaissance detail. Florer (1972) described the sediments and pollen of several coastal stratigraphic sections, naming three stratigraphic units and correlating pollen assemblage zones with Puget Lowland geologic-climate units. Heusser (1972) described the stratigraphy and palynology of a thick section of fine-grained sediment at Browns Point (Figure 3.1 for location names). From pollen data, he inferred a paleotemperature curve for the past 70,000 yr. The expanded stratigraphic study described here suggests that Heusser's record may instead span 125,000 yr (Chapter 2). Heusser also correlated his pollen assemblage zones with the Puget Lowland glacial-

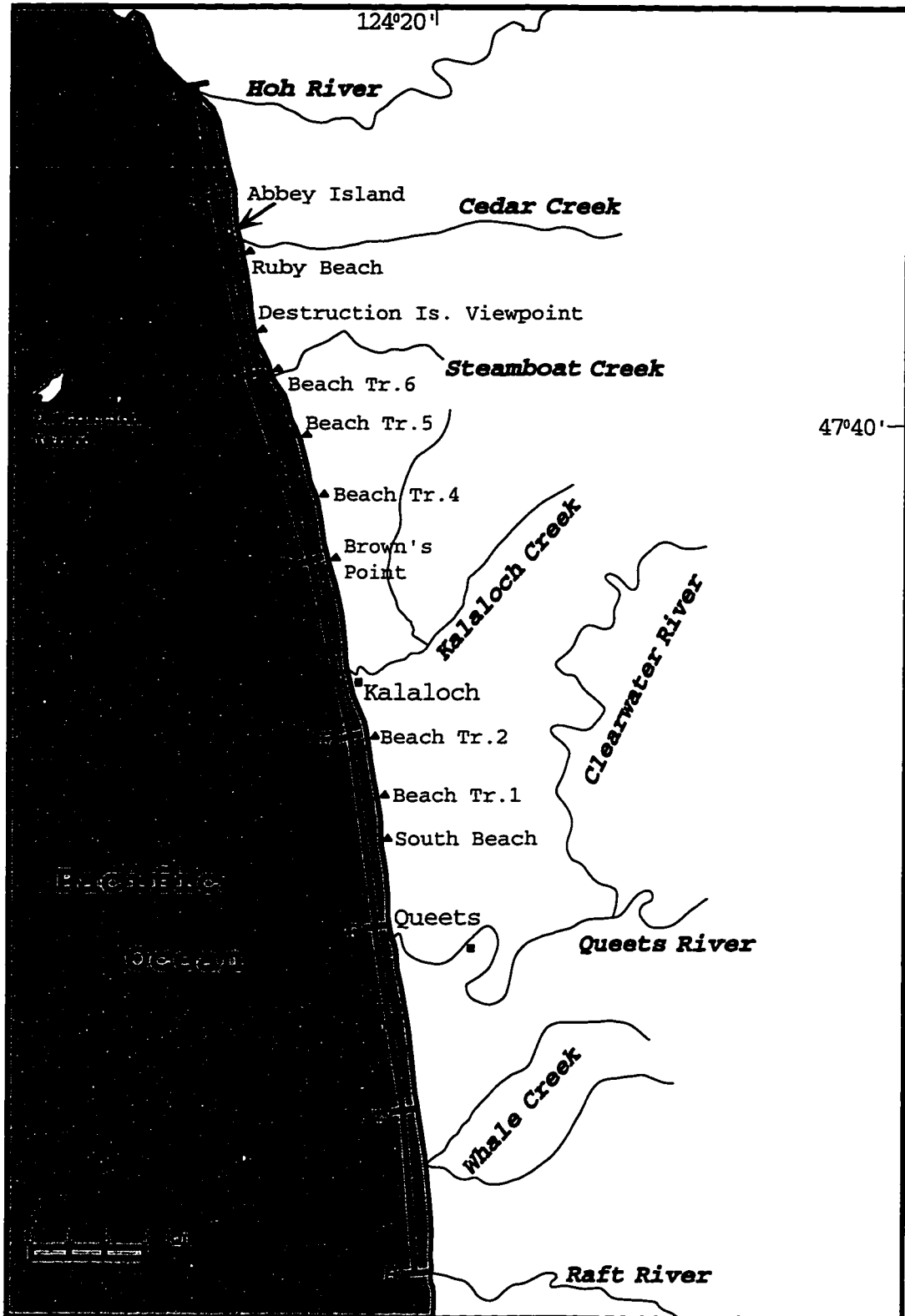


Figure 3.1: Map of central Olympic Coast, showing locations mentioned in the text and locations of stratigraphic sketches A-B through G-H.

climatic sequence. Such correlations with Puget Lowland geologic climatic units by both Florer and Heusser are problematic, principally because of insufficient local chronologic control and of subsequent geochronologic revisions of the Puget Lowland stratigraphy (Easterbrook, 1986).

Recent stratigraphic work has focused on fossil beetles and neotectonics. Cong and Ashworth (1996) studied fossil beetles from the middle and upper portions of the Browns Point section. Their paleoclimatic interpretations based on beetle assemblages agree well with interpretations based on pollen. McCrory (1992, 1994a, 1994b) has made a reconnaissance study of neotectonics of much of the coastal stratigraphy described here, with more detailed work to the south of this project area.

NOMENCLATURE

Informal time-stratigraphic units and lithostratigraphic units are used in this report. The local time-stratigraphic units are correlated, where appropriate, with time-stratigraphic units in the Puget Lowland (e.g., Possession, Fraser) and American Midwest (late, middle, and early Wisconsin) and with marine oxygen isotope stages or events [abbreviated, e.g., IS 1, IS 4, IS 5e, as designated by Imbrie et al. (1984) and Martinson et al. (1987)]. Division of the coastal sequence into time-stratigraphic and lithostratigraphic units is complicated by marked lateral variability. Lateral variability of sediments—principally locally derived, fine-grained sediments juxtaposed with coarse glacial-fluvial sediments (outwash)—necessitated the designation of multiple, coeval units. Furthermore, the same lateral variability of sedimentation produced strongly contrasting stratigraphic sections. Sections dominated by outwash are more clearly divisible into distinct units than are those dominated by fine-grained, locally derived detritus. Thus, several stratigraphic units in the former span the same stratigraphic interval as a single unit in the latter. Finally, the basal portion of the sequence—which predates the last interglaciation—has been treated as one informal unit (the Steamboat Creek Formation, below). That unit includes a variety of glacial and nonglacial sediments that may not be coeval from area to area.

COASTAL STRATIGRAPHY

STRATIGRAPHIC FRAMEWORK

The coastal stratigraphy (Figure 3.2) consists of three principal components: an older sequence and a younger sequence, separated by a wave-cut surface and associated

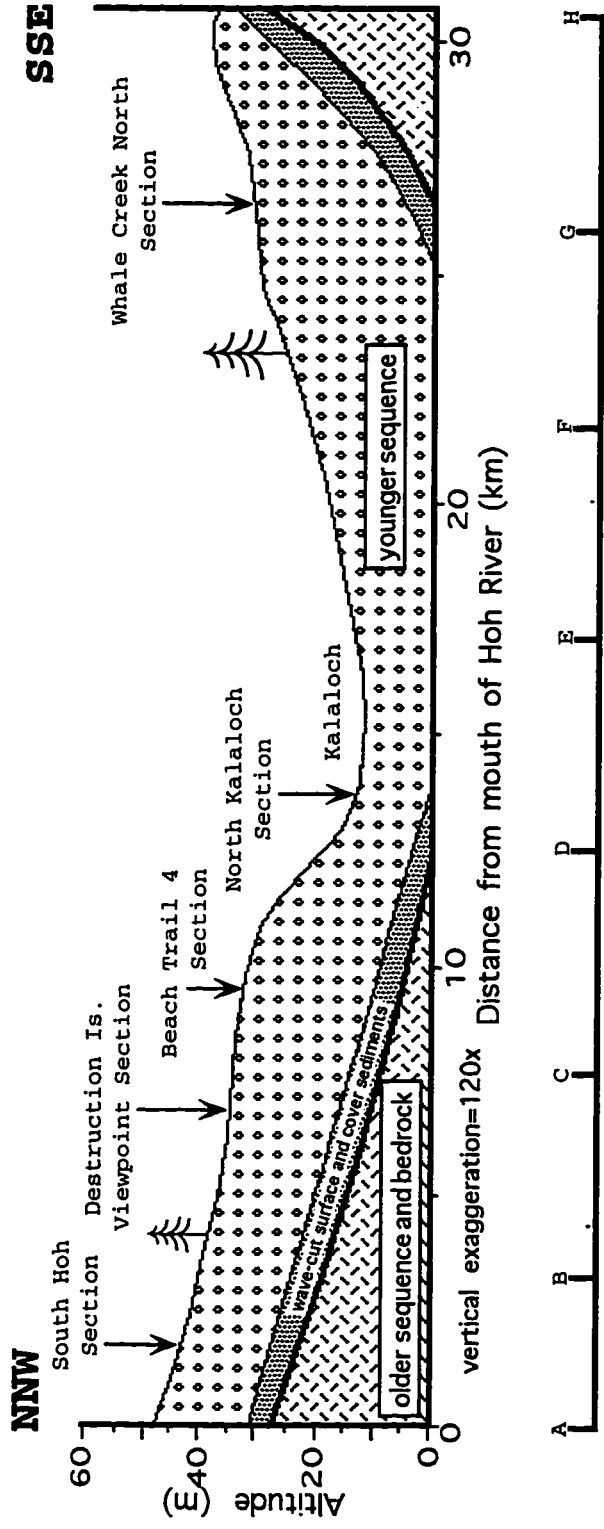


Figure 3.2: Generalized stratigraphic framework between the Hoh and Raft Rivers (profile A-H in Figure 3.1), showing three principal components of the stratigraphic sequence: older sequence (Steamboat Creek Formation), wave-cut surface, and younger sequence (Lyman Rapids outwash, Hoh Oxbow outwash, and Browns Point Formation). Locations of detailed stratigraphic sections and correlation sketches A-B through G-H area also shown.

cover sediments. The older sequence, consisting of glacial and nonglacial sediments, forms the base of exposed stratigraphic sections (except where Tertiary bedrock predominates) between the Hoh River and Browns Point, and between Whale Creek and the Raft River. Between Browns Point and Whale Creek, the older sequence lies below beach level, having subsided tectonically in the axial zone of the Kalaloch syncline [named by Baldwin (1939)]. Most strata in the older sequence dip between 0° and 11°, but reach 90° at an exposure between Whale Creek and the Raft River. Magnetically reversed sediments indicate that at least portions of the older sequence were deposited more than 780,000 yr BP [Baksi et al (1992) dated the Brunhes-Matuyama reversal at $783,000 \pm 11,000$ yr BP; that date is here rounded to 780,000 yr BP]. The older sequence is here named (informally) the Steamboat Creek Formation, after the typical exposures near Steamboat Creek (Figure 3.1). This unit is a revision and extension of the Steamboat Creek gravel, an informal unit designated by Florer (1972) and included in this redefined formation. The Steamboat Creek Formation also includes the portion of the informal Joe Creek silt (Florer, 1972) exposed in the Whale Creek area.

The wave-cut surface truncates the Steamboat Creek Formation, as well as Miocene- and Pliocene-age bedrock. In some areas, most notably between Ruby Beach and Beach Trail 4, the wave-cut surface is marked by a cobble-boulder lag. Where cut across bedrock, the surface is marked by ancient pholad clam borings. The wave-cut surface is everywhere overlain by horizontally bedded sand and gravel that was deposited in a beach and/or intertidal environment. Although direct radiometric ages are lacking, stratigraphic relationships with the overlying sequence suggest that the wave-cut surface and cover sediments originated during the last-interglacial sea-level highstand (IS 5e; see below).

The younger sequence consists of glacial and nonglacial sediments deposited during latter substages of the last interglaciation (IS 5d through 5a) and the last glacial cycle (IS 4 through 2). The younger sequence is subdivided into three informal units of formation rank. Within several kilometers of the Queets and Hoh river mouths, this sequence consists principally of outwash. The outwash is assigned to two time-stratigraphic units—the Lyman Rapids outwash and Hoh Oxbow outwash—corresponding to allostratigraphic units of the same names in Chapter 2. Between Kalaloch and Beach Trail 5 (Figure 3.1), the sequence is dominated by silt, clay, and peat deposits. Florer (1972) named these sediments the "Kalaloch silts." That name is

not used here because the sequence is dominated by silt only in the Kalaloch area. That sedimentary package is called here the Browns Point Formation, an informal lithostratigraphic unit.

DETAILED STRATIGRAPHIC FRAMEWORK AND SECTIONS

Detailed description and lateral correlation of stratigraphic units allows the construction of a detailed stratigraphic framework and the synthesis of a Pleistocene sedimentologic history for the project area. The stratigraphic framework described below is based upon dozens of measured stratigraphic sections, coupled with other detailed observations. This framework is presented in a sequence of seven stratigraphic sketches (with key measured sections), each sketch covering a portion of coastline between the Hoh and Raft Rivers and showing observed and inferred stratigraphic relationships. The stratigraphic sketches are combined as Plate 2.

Hoh River to Abbey Island

Seacliffs between the Hoh River and the area north of Abbey Island (Figures 3.1 and 3.3) expose the thickest stratigraphic sections and the greatest variety of Steamboat Creek sediments in the study area.

South Hoh Section

A stratigraphic section 1.9 km southeast of the Hoh River characterizes the stratigraphic framework and principal units in this area (Figure 3.4). The bottom 12.8 m of the section consists of a grey diamicton, interpreted as glacial-marine drift and inferred to be possibly correlative with the Wolf Creek Drift in Chapter 2. The glacial-marine drift is included in the Steamboat Creek Formation and has been observed only at this locality. The few exposures of the Steamboat Creek Formation in this area also include glacial-lacustrine sediments and till. Transitions between drift types are not exposed, so their stratigraphic relationships are unknown.

Beach and intertidal sediments overlie the glacial-marine drift. Cross-bedded medium sand, 2.1 m thick and suggestive of a beach or intertidal environment, lies between the glacial-marine drift and the approximate level of the wave-cut surface. The wave-cut surface is less apparent in this section than in most. A cobble-boulder lag marks the apparent surface, as in areas to the south where it is more clearly defined, but the surface is both overlain and underlain by beach/intertidal sand. Here the cover

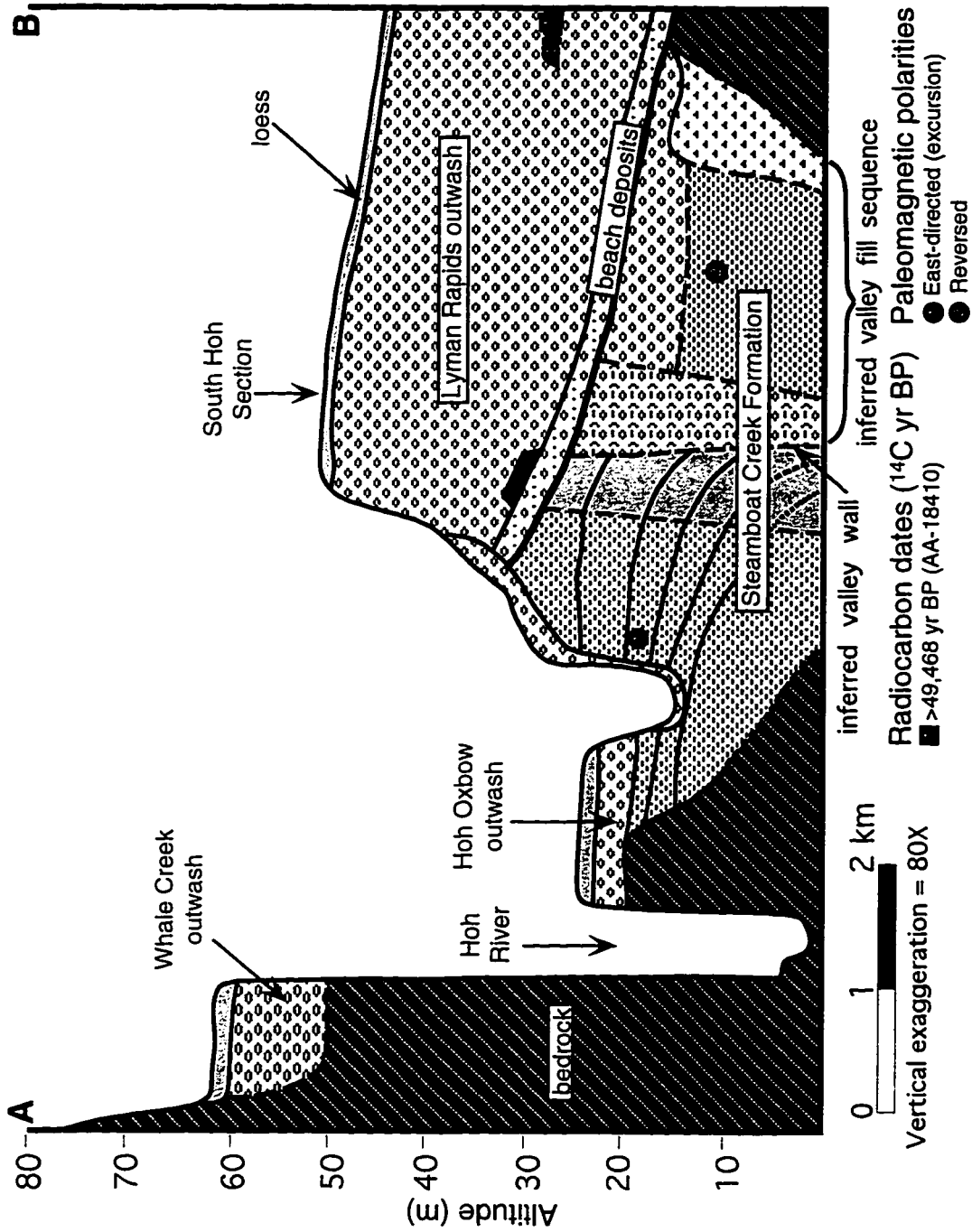


Figure 3.3: Sketch of stratigraphic sequence between the Hoh River and Abbey Island area (A-B on Figure 3.2), showing stratigraphic correlations and chronologic control.

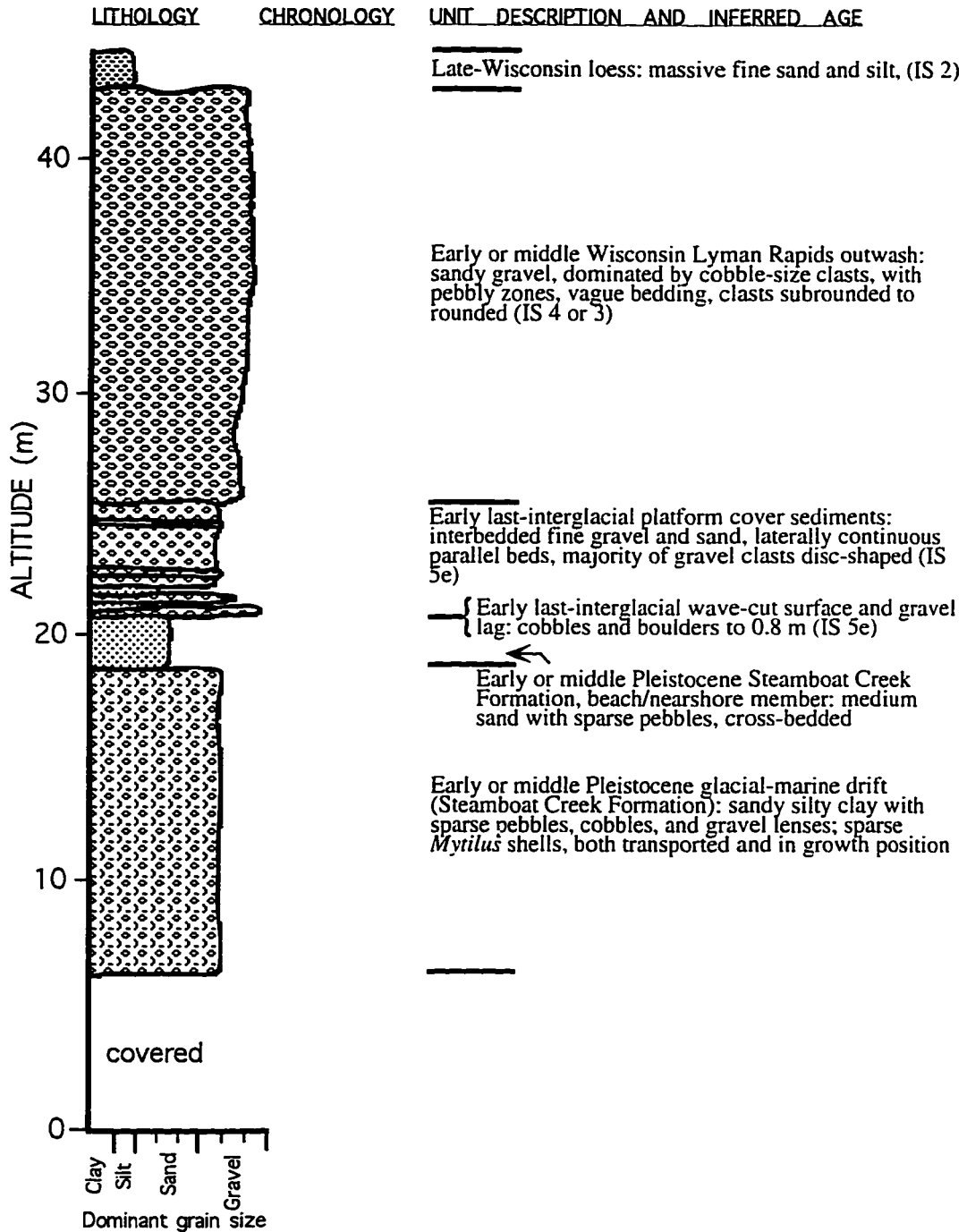


Figure 3.4: Stratigraphic section 1.9 km south of the Hoh River (S 1/2, NE1/4, NE1/4, Sec. 30, T.26N., R.13W.; Figure 3.2). No chronologic data have been obtained for this section.

sediments are 4.5 m thick. Organic-rich, fine-grained sediments and paleosols, which overlie the beach deposits in many sections, are absent here.

The younger sequence is represented in this section only by Lyman Rapids outwash and loess. Seventeen meters of moderately coarse outwash overlies the beach deposits. The outwash consists of clast-supported pebble-cobble gravel, with sparse sand matrix. Vague bedding is defined largely by alternating dominance of pebbles and cobbles, as is characteristic of most outwash in the coastal study area. Cut-and-fill features are present, as are lenses of sand and fine gravel. A 1.5-m-thick layer of pedogenically altered yellowish-brown silt, interpreted as loess, caps the section.

Lateral Correlations

A valley margin/valley fill relationship can be inferred between two portions of the Steamboat Creek Formation. The southern third of Figure 3.3 includes the inferred valley fill, consisting of glacial-marine drift (Figure 3.4), glacial-lacustrine drift, and till. As noted, these sediments appear in isolated exposures, and any inferred relationships between them cannot be verified. They represent one or more glacial cycles.

The middle third of Figure 3.3 includes the inferred valley wall sequence, consisting of glacial-lacustrine sediments and eolian sand. These sediments are interbedded, with the former being dominant to the north and the latter dominant to the south. Southerly bedding dips increase gradually in dip from north to south, i.e., from 6° to 13° over 300 m lateral distance. At the southernmost exposure of the inferred valley-wall sequence (Sec. 19/30 boundary, T.26N., R.13W.), stratal dips increase from 13° to as much as 30° within 150 m lateral distance. Liquefaction structures, minor graben-like features, and ancient slump structures cut the sequence at several places within the immediate area. An undetermined component of the stratal inclination likely is tectonic in origin (see below). However, the markedly steepened stratal inclinations, liquefaction features, graben-like structures, and ancient slump features suggest that a portion of the deformation is related to ancient mass-wasting activity. R.L. Logan (personal communication, 1994) notes that such features mark areas of modern valley-margin mass-wasting activity elsewhere in western Washington.

Available geochronologic evidence suggests that the Steamboat Creek Formation in this area is of Early Pleistocene age. The glacial-lacustrine sediments of the inferred valley-fill sequence yielded two magnetically reversed samples, suggesting that the sediments are more than 780,000 yr old (Baksi et al., 1992). Till and glacial-marine

drift of the valley-fill sequence may be of similar antiquity, or could be significantly older or younger. If the valley-margin/valley-fill inference is correct, the former sequence must be older than the latter. Four samples from the valley-margin glacial-lacustrine sediments yielded an east-directed magnetic polarity (excursion), which yields little geochronologic information.

The wave-cut surface and cover sediments rise northward from 16 m to more than 30 m through this section of the coastline. They are truncated at a terrace edge approximately 1.1 km south of the Hoh River. The wave-cut surface is marked, with local exceptions, by a cobble or cobble-boulder lag. Fine-grained sediment and peat overlie the cover sediments at some locations in this area, and by stratigraphic position correlate with those at Destruction Island Viewpoint (see below). They were likely deposited more widely, but were subsequently eroded by meltwater streams during the Lyman Rapids glaciation.

The outwash described above dominates this section of the coastline. It is as much as 26 m thick where not partially or completely removed by subsequent erosion near the Hoh River mouth and does not thin significantly north of Ruby Beach. The outwash is locally broken by silty and peaty interbeds. Its upper surface forms a prominent coastal terrace along most of this coastline section. Only one radiocarbon date exists from the outwash in this area. A sample of wood from a peaty interbed at the south end of the area (Figure 3.3) yielded an age of $>49,468$ ^{14}C yr BP (AA-18410). Dates from elsewhere in this unit, coupled with correlations of the coastal terrace with landforms in the Hoh valley, indicate that the outwash is part of the Lyman Rapids drift (Chapter 2). This drift was deposited during the early part of the last glacial cycle and likely correlates with IS 4, IS 3, or, perhaps, IS 5b (see below).

Within 1.1 km south of the Hoh River mouth, the stratigraphic sequence has been modified by erosion. A flight of narrow terraces, ranging from 30 to 12 m altitude, marks this area. The terraces are largely erosional (including at least one broad strath), with minimal fresher, aggraded sediment capping them. A 24-m-high terrace correlates with the ca. 29,200 to 26,700 ^{14}C yr BP Hoh Oxbow I drift (Chapter 2).

Abbey Island to Steamboat Creek

Seacliffs between Steamboat Creek and the area north of Abbey Island (Figures 3.1 and 3.5) display less variation in the Steamboat Creek Formation, but reveal much

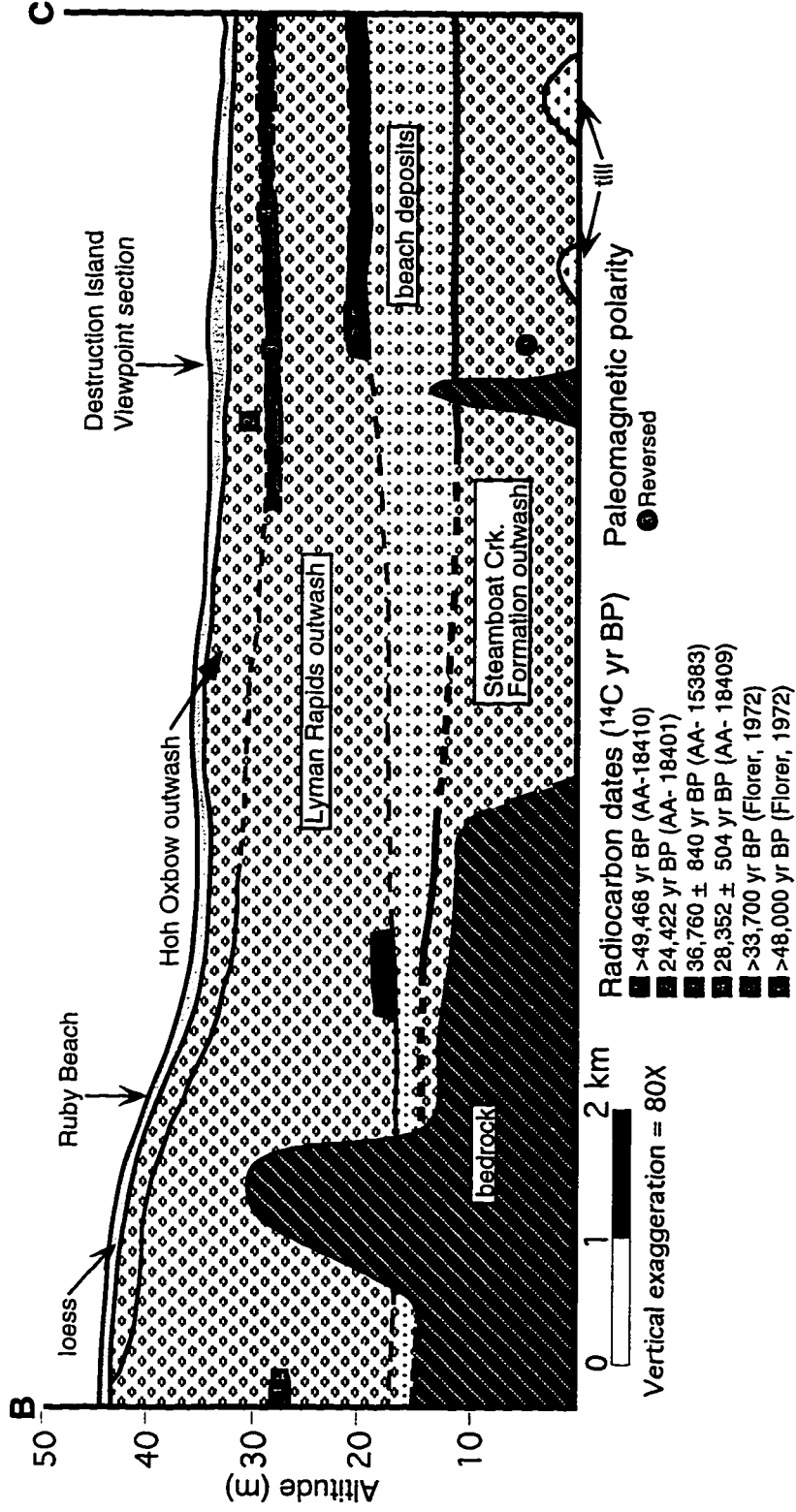


Figure 3.5: Sketch of stratigraphic sequence between Abbey Island area and Steamboat Creek (B-C on Figure 3.2), showing stratigraphic correlations and chronologic control.

lateral variation in the younger sequence. A stratigraphic section at Destruction Island Viewpoint typifies this portion of the coastline.

Destruction Island Viewpoint Section

The Destruction Island Viewpoint area, located 6.7 km south of the Hoh River (Figures 3.1 and 3.2), contains some of the best-exposed sections in the entire study area (Figure 3.6). The measured section (Figure 3.7) is the most complete in the immediate area, and provides data in support of several important stratigraphic interpretations.

The basal Steamboat Creek Formation at this section includes more than 10 m of outwash and a small volume of exposed till. The outwash consists of crudely bedded, pebble and cobble gravel with sparse detrital wood. It is deeply stained and firmly cemented with iron oxides. The outwash dominates the Steamboat Creek Formation in the 9.6 km of seacliffs between Abbey Island and the Steamboat Creek area, and represents the original Steamboat Creek gravels of Florer (1972). Both south and north ends of the Destruction Island Viewpoint exposure includes 3 to 5 m of till below the outwash (not shown on section).

The wave-cut surface truncates the basal outwash, forming a clearly defined unconformity approximately 11.5 m above sea level (Figure 3.6). The surface is marked by a coarse gravel lag that includes polished boulders as large as 2 m diameter. Ancient pholad clam borings indent a nearby bedrock knob at the same level. Nine meters of horizontally bedded sand and gravel beach deposits cover the wave-cut surface and lag.

The base of the younger sequence consists of 2.5 m of organic-rich sediments and paleosols lying atop the beach deposits. Half-meter-thick intervals at the top and bottom of the unit are brown, sandy clay. Though clear horizonation is lacking, these two clay-rich intervals appear to represent paleosols. The lower paleosol developed in the top of the beach deposits described above. The middle 1.5 m of the unit consists of interlaminated brown sand and silty sand. Discontinuous laminae may have been disrupted by pedogenic processes and/or bioturbation. Overall, the unit contains abundant organic matter, including rooted stumps (particularly at the top) and detrital wood, cones, and seeds. Thin peat horizons are also present. Taken as a whole, this unit appears to have accumulated during a period of extremely slow sedimentation, probably adjacent to small creeks that drained the higher outwash surface lying 1.5 km

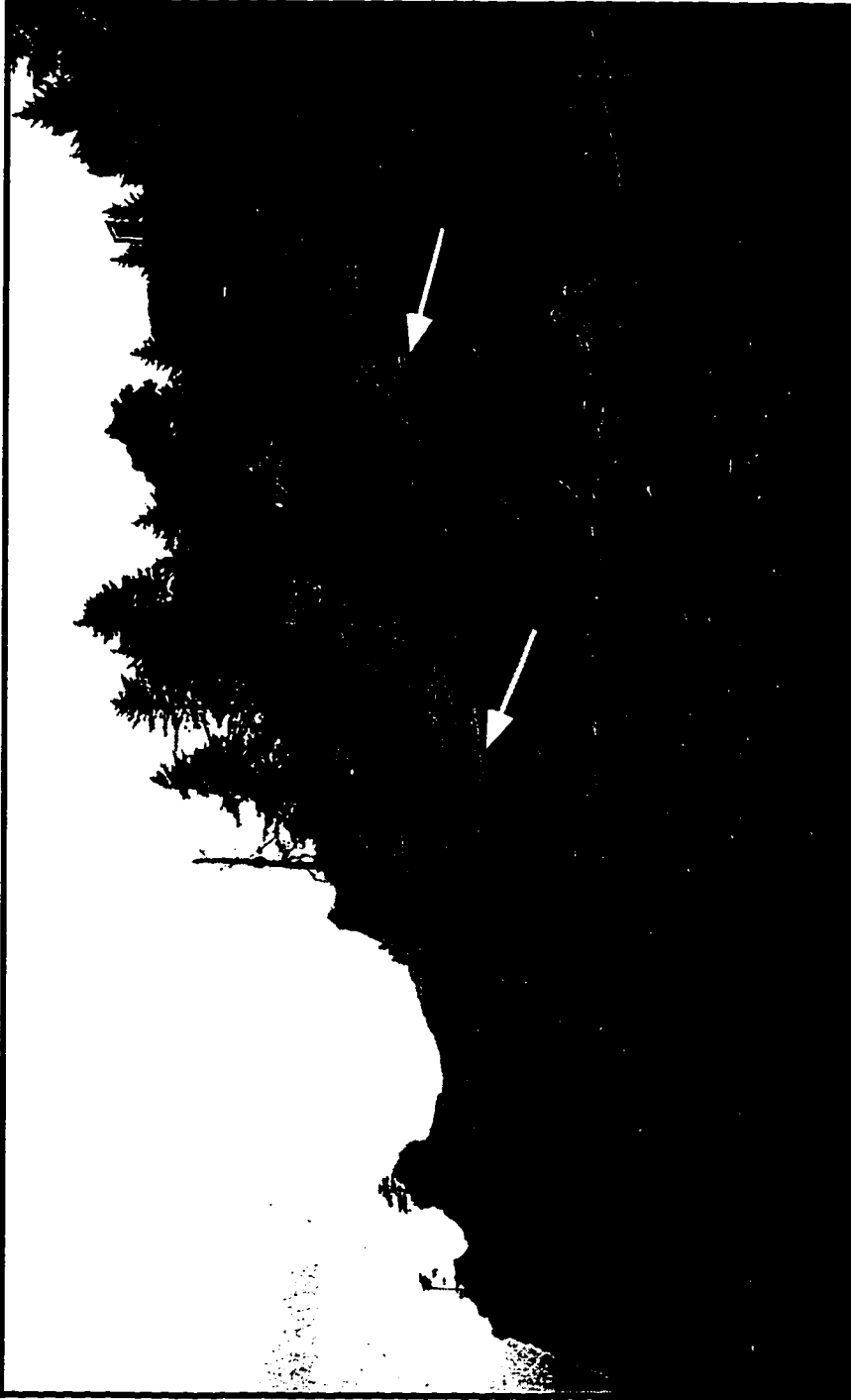


Figure 3.6: Destruction Island Viewpoint area. Note prominent wave-cut surface (arrows), which separates the Steamboat Creek Formation (below) from beach sediments, interglacial overbank sediments, and outwash (above).

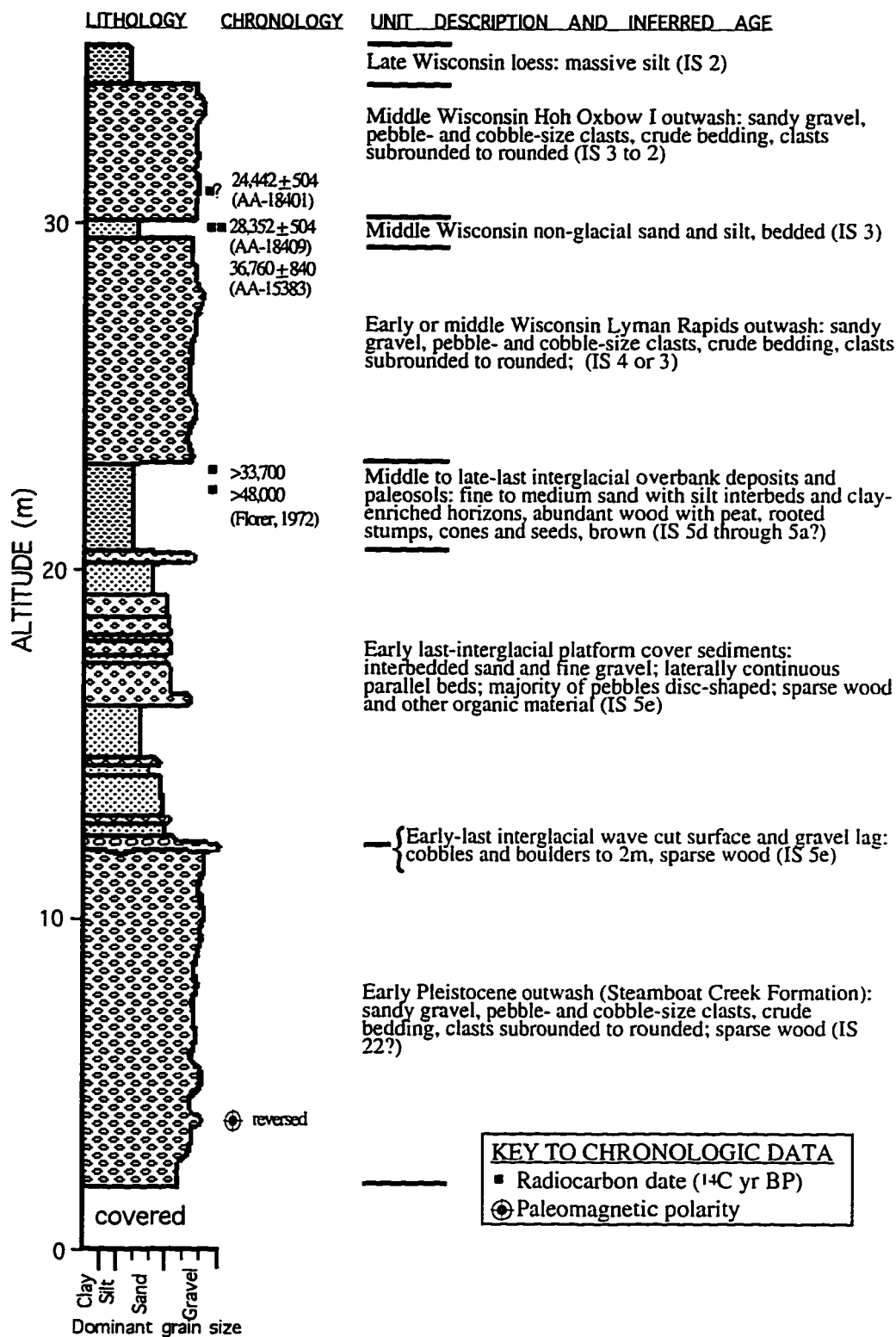


Figure 3.7: Stratigraphic section 150 m south of Destruction Island Viewpoint (SE1/4, NE1/4, NW1/4, Sec. 8, T.25N., R.13W.; Figure 3.2).

landward. It likely represents a period of late-interglacial landscape stabilization following abandonment by marine waters and preceding glacial-fluvial inundation. The two paleosols, in particular, suggest that the unit may represent a considerable period of time. Fossil pollen spectra from this unit indicate vegetation similar to the modern coastal forest (Florer, 1972), further indicating interglacial deposition.

As in the South Hoh section, thick outwash (11 m) and loess (1.5 m) cap the sequence. In this portion of the coast, however, a 0.5-m-thick bed of fine sand separates the outwash into two distinct units (see below). The upper unit forms a terrace that is part of the Hoh Oxbow drift, while the lower unit correlates with the Lyman Rapids drift (Chapter 2).

Age of the Wave-Cut Surface

The stratigraphic succession and palynological and geochronologic data from this exposure support the age interpretation of the wave-cut surface, which is inferred to date to IS 5e, rather than to IS 7, IS 5c, or IS 5a. If it were an IS 7 wave-cut surface, one would expect to see much better developed paleosol(s) between its cover sediments and the Lyman Rapids (IS 4) outwash, because of an extended period without substantial sedimentation during IS 6 and 5. If the wave-cut surface were an IS 5a feature, the interglacial paleosols and peat between the cover sediments and Lyman Rapids outwash should not be present. This argument does not preclude the possibility that the wave-cut surface formed during IS 5c, as the paleosols and peat conceivably represent substages 5b and 5a. However, Steamboat Creek incises the same stratigraphic sequence 1 to 1.5 km inland from the Destruction Island Viewpoint area, and an IS 5e wave-cut surface (expected near 36 m altitude if the seacliff wave-cut surface were IS 5c) is absent. Lacking direct geochronologic data for the wave-cut surface, the most reasonable interpretation of available data indicates that it dates to IS 5e.

Age of Lyman Rapids Outwash

As discussed in Chapter 2, the age of the Lyman Rapids drift is uncertain. Chronologic data indicate it is older than ca. 52,000 ¹⁴C BP, suggesting an IS 4 or early IS 3 age. However, if the wave-cut surface dates to IS 5e, the Lyman Rapids outwash conceivably originated during IS 5b. The stratigraphic sequence in Figure 3.7 suggests an IS 4 or IS 3 age is more likely than IS 5b. The sediments underlying the outwash

(2.5 m- thick paleosols, peat, overbank sediments) appear to represent considerably more time than do those overlying the outwash (0.5 m-thick sand). Thus, the stratigraphic data more strongly suggest a younger age than an older age.

Lateral Correlations

The Steamboat Creek Formation is not exposed within 1.5 km north of Ruby Beach. The wave-cut surface is instead cut on bedrock. At Ruby Beach, pebble-cobble gravel of the Steamboat Creek Formation fills shallow depressions in the bedrock. That gravel correlates with Steamboat Creek Formation outwash at Destruction Island Viewpoint (Figure 3.7), but exposures are lacking in the 1.6 km separating the two localities. Most of the Steamboat Creek Formation between Ruby Beach and Steamboat Creek consists of outwash. South of Steamboat Creek, the wave-cut surface largely bevels bedrock, and the Steamboat Creek Formation is not exposed.

The wave-cut surface descends from 16 m altitude north of Abbey Island to 11 m at Steamboat Creek. At most locations, it is marked by a cobble-boulder lag and is readily apparent in outcrop. Beach sand and gravel cover the wave-cut surface to a depth of as much as 8 m. Where thinner, they appear to have been eroded prior to deposition of the Lyman Rapids outwash. The overlying silt/peat/paleosol unit is discontinuous through this area, and also appears to have been locally eroded.

The younger-sequence outwash varies laterally through this section of coastline. The Lyman Rapids outwash (Figure 3.7) comprises the entire upper part of the section (except for the omnipresent loess) between the Hoh River and the north end of this section, and forms the extensive terrace stretching south from the Hoh River. In the Abbey Island area, however, a second body of outwash appears above the Lyman Rapids outwash and thickens southward. In the seacliffs near Abbey Island, the upper outwash is only 1 m thick and is separated from the Lyman Rapids outwash by a 2-m-thick unit of laminated clay and silt. Three km south, at Destruction Island Viewpoint, the upper outwash is 4 m thick and is separated from the Lyman Rapids outwash by a 0.5- to 1.5-m-thick bed of silt and sand. Terrace relationships in the Ruby Beach area demonstrate that the upper outwash reached the coastal area via Cedar Creek (Chapter 2), and that it correlates with the Hoh Oxbow I drift.

A variety of geochronologic data exist for this section of coastline. Overbank silt within outwash of the Steamboat Creek Formation at Destruction Island viewpoint (Figure 3.7) has a reversed polarity, suggesting that it is more than 780,000 years old

(Baksi et al., 1992). The silt/peat unit yielded radiocarbon dates of >33,700 and >48,000 ^{14}C yr BP (Florer, 1972). Detrital wood from the sand bed between outwash units yielded radiocarbon dates of $36,760 \pm 840$ ^{14}C yr BP (AA-15383) and $28,352 \pm 504$ (AA-18409) ^{14}C yr BP.

Steamboat Creek to Browns Point

Infrequent exposures between Steamboat Creek and Browns Point (Figure 3.1) document the southward transition from stratigraphic sections dominated by Hoh valley outwash to those dominated by peat and locally derived sediments (Figure 3.8). The fine-grained sediments of this area promote slumping and limit exposures; thus, the correlations between sections are more speculative than elsewhere.

Beach Trail 4 Section

The Beach Trail 4 area (Figure 3.1) displays stratigraphy typical of this area. Miocene bedrock lies at the base of the section (Figure 3.9), and the Steamboat Creek Formation is absent. The wave-cut surface, marked by ancient pholad clam borings, truncates the bedrock at only 2.7 m altitude. The sand and gravel cover sediments extend to 7 m altitude. Dominated here by gravel, the cover sediments fill irregularities in the erosional surface. The younger sequence between Beach Trail 5 and Browns Point comprises the Browns Point Formation. This lithostratigraphic unit, which reaches its maximum thickness at Browns Point, includes gravel, but clay, silt, and peat dominate. Most of the gravel clasts consist of easily weathered, unmetamorphosed sedimentary lithologies characteristic of bedrock on Kalaloch Ridge, which lies a short distance to the east. Only one gravel bed (noted on Figure 3.9) contains relatively unweathered, hard, well-rounded clasts characteristic of Hoh River outwash. Radiocarbon dates indicate that the gravel bed was deposited >47,000 ^{14}C yr BP, as was most of the section. On the basis of stratigraphic position, the gravel bed likely correlates with the Lyman Rapids drift.

As a whole, the section indicates that sediment deposited after the last-interglacial sea-level highstand (IS 5e) was dominated by detritus from adjacent uplands. The area was isolated from the Hoh valley sediment source except during the Lyman Rapids glaciation, and the numerous peat beds indicate that sedimentation was likely sporadic. The Browns Point section, described by Heusser (1972), consists

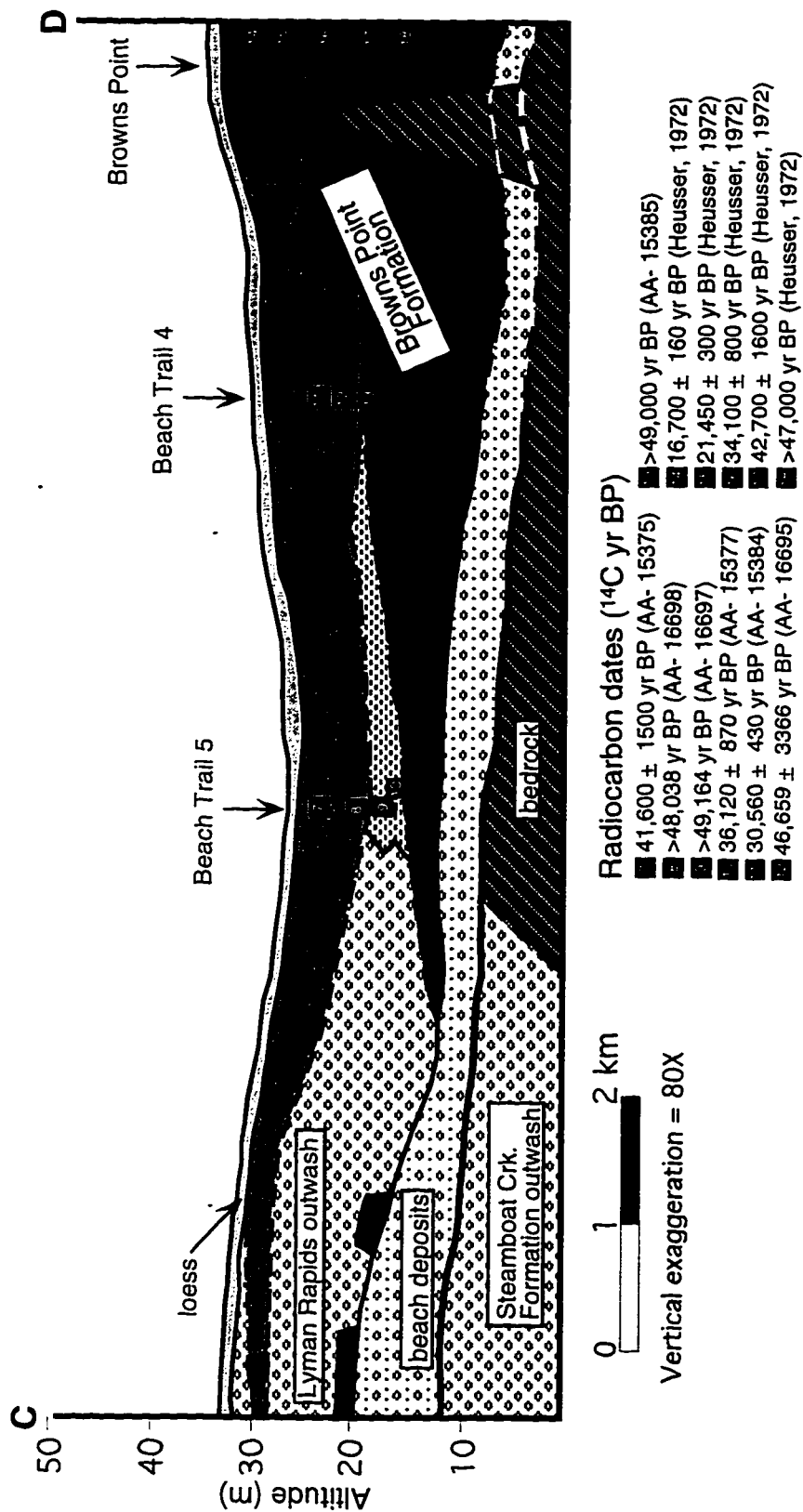


Figure 3.8: Sketch of stratigraphic sequence between Steamboat Creek and Brown's Point (C-D on Figure 3.2), showing stratigraphic correlations and chronologic control. See key to lithologies in Figure 3.10.

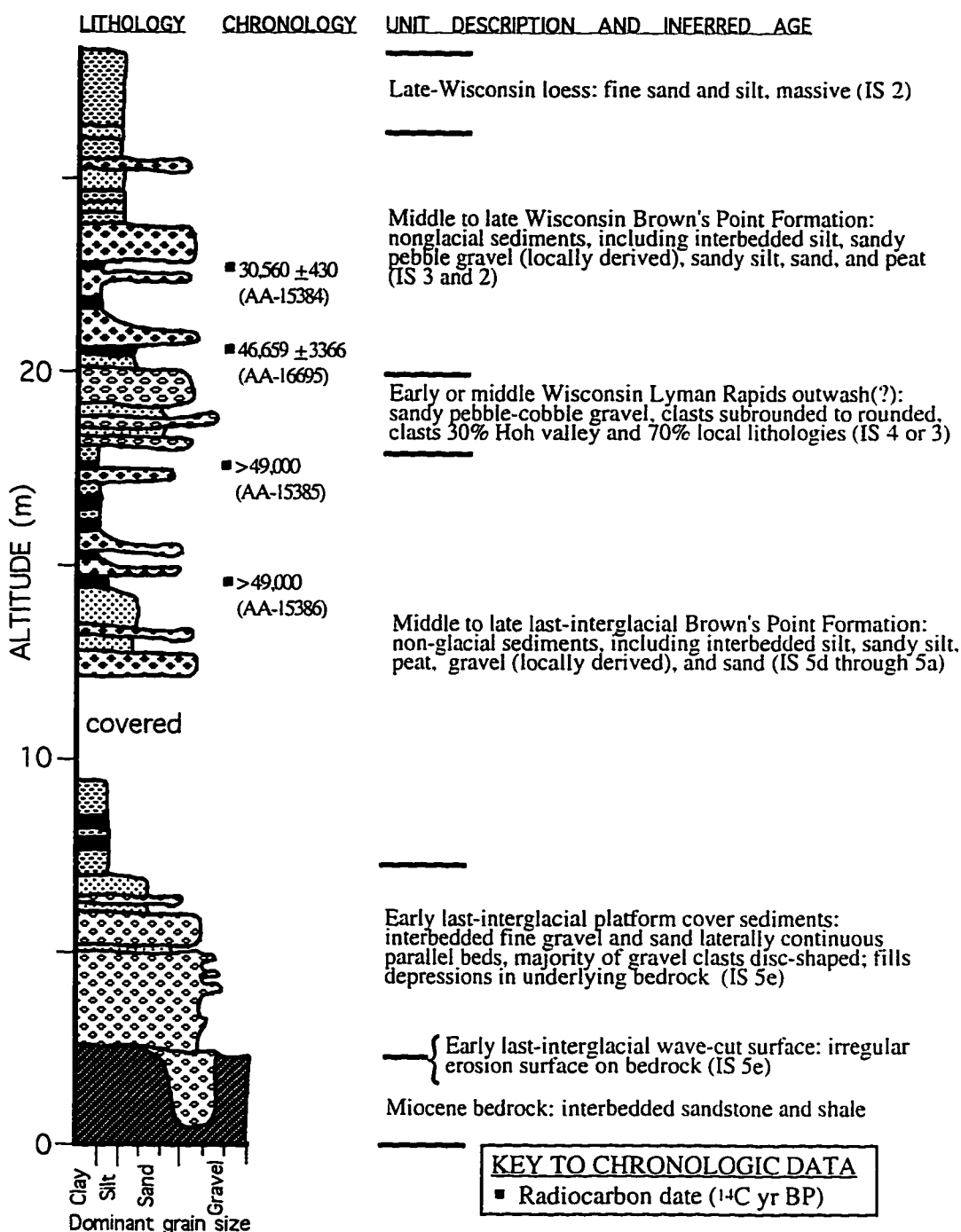


Figure 3.9: Stratigraphic section at outlet of Beach Trail 4 (SE1/4, SE1/4, SW1/4, Sec. 21, T.25N., R.13W.; Figure 3.2). Chronology consists of AMS radiocarbon dates.

almost solely of silt, clay, and peat, and contains only rare beds of locally derived gravel.

Lateral Correlations

The wave-cut surface, cut almost solely on Miocene bedrock, descends southward from 11.8 m at Steamboat Creek to beach level (1 to 2 m altitude) between Beach Trail 4 and Browns Point (Figure 3.8). It then rises to approximately 5 m on the south side of Browns Point and subsequently descends below sea level south of Browns Point. The high altitude of the wave-cut surface around Browns Point, a bedrock headland, is anomalous in the otherwise smooth southward descent. The modern shoreline apparently coincides with the early last-interglacial (IS 5e) paleoshoreline at Browns Point, while to the north and south the paleoshoreline lies 0.5 to 1.5 km inland from the modern shoreline. Therefore, the high wave-cut surface altitude at Browns Point is likely related to paleoshoreline proximity rather than tectonic deformation. To the north and south, the exposed wave-cut surface (at the modern shoreline) lies several meters below its inferred altitude at the paleoshoreline.

Four to 5 m of beach sand and gravel overlies the wave-cut surface, a substantially thinner section than to the north. The relatively thin unit here may be a result of the more limited supply of preexisting outwash from which the beach sediments could be derived.

Both outwash units thin substantially between Steamboat Creek and Beach Trail 5, where neither outwash unit is clearly represented; because exposure is poor between the two locations, stratigraphic correlations cannot be directly demonstrated. Above the beach sand and gravel, the Beach Trail 5 section is dominated by silt and peat. Much of the silt in the middle portion contains sandy interbeds, suggesting the unit may have been deposited on the fringe of outwash fans. Two graded beds near the top of the section contain pebbles of Hoh valley lithology, and may also represent distal outwash. A peat bed within the interbedded silt and sand unit yielded a radiocarbon date of $36,120 \pm 870$ ^{14}C yr BP (AA-15377). Dates on peat and wood from overlying beds, however, are substantially older ($>49,160$ ^{14}C yr BP [AA-16697], $>48,040$ ^{14}C yr BP [AA-16698], and $41,600 \pm 1500$ ^{14}C yr BP [AA-15375]). These dates suggest that most of the interbedded silt and sand may correlate with Lyman Rapids drift, and that the uppermost, graded, cobble-bearing bed may correlate with the Hoh Oxbow drift.

No gravel beds are exposed south of Beach Trail 4, suggesting that this area represents the southernmost extent of Hoh River outwash. The Browns Point section, described by Heusser (1972), lacks gravel of either Hoh or Queets River lithologies. The section was deposited adjacent to an interfluvium between the two meltwater/outwash systems.

Browns Point to Beach Trail 2

South of Browns Point (Figure 3.1), the entire stratigraphic sequence and the coastal terrace descend toward the axis of the Kalaloch syncline (Figure 3.10). The wave-cut surface descends below beach level on the south edge of Browns Point, as do the sand and gravel cover sediments approximately 300 m farther south.

The stratigraphic sequence changes markedly between Browns Point and Beach Trail 2. The silt and peat sequence thins to between 5 and 10 m, and Queets River outwash appears 1.3 km south of Browns Point.

North Kalaloch Section

A stratigraphic section 2 km north of Kalaloch (Figure 3.11) is the most complete in the area. The basal 1.4 m consists of sandy gravel containing hard, well-rounded clasts characteristic of Queets valley outwash. A 5.6-m-thick sequence of silt, peat, clay, and sand overlies the outwash. That sequence, in turn, is overlain by 2 m of pebble gravel, 1.1 m of fluvial sand, and 0.6 m of silty clay. The gravel is very different in character from that lower in the section. Clasts are dominantly subangular, and consist of poorly indurated, deeply weathered lithologies. Like the gravels at Beach Trail 4 and Browns Point, these gravels were apparently derived from bedrock on Kalaloch Ridge (1.5 km east of the coastline) and were likely deposited by Kalaloch Creek.

Radiocarbon dates have been obtained for two wood samples from this exposure (Figure 3.11). The uppermost sample yielded an age of $30,340 \pm 260$ ^{14}C yr BP (Beta-61321), whereas the lower sample has an infinite age of $>49,000$ ^{14}C yr BP (AA-15379B). These dates, together with stratigraphic correlations to exposures nearer the Queets River mouth, indicate that the basal outwash correlates with the Lyman Rapids drift and that the silt-peat-clay-sand sequence accumulated during IS 3 and, probably, IS 2.

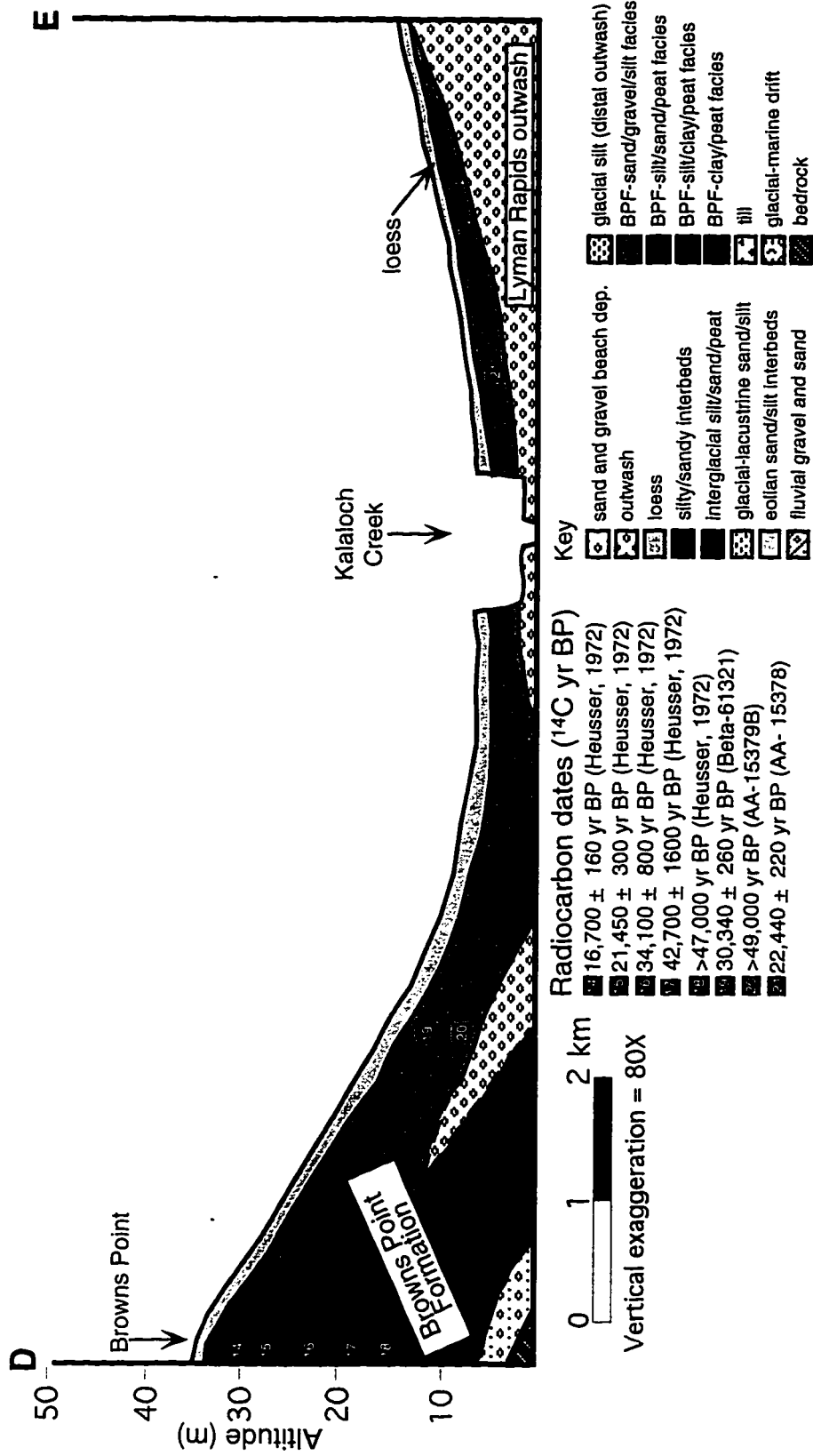


Figure 3.10: Sketch of stratigraphic sequence between Brown's Point and Beach Trail 2 (D-E on Figure 3.2), showing stratigraphic correlations and chronologic control. Key includes all lithologies in stratigraphic sketch series.

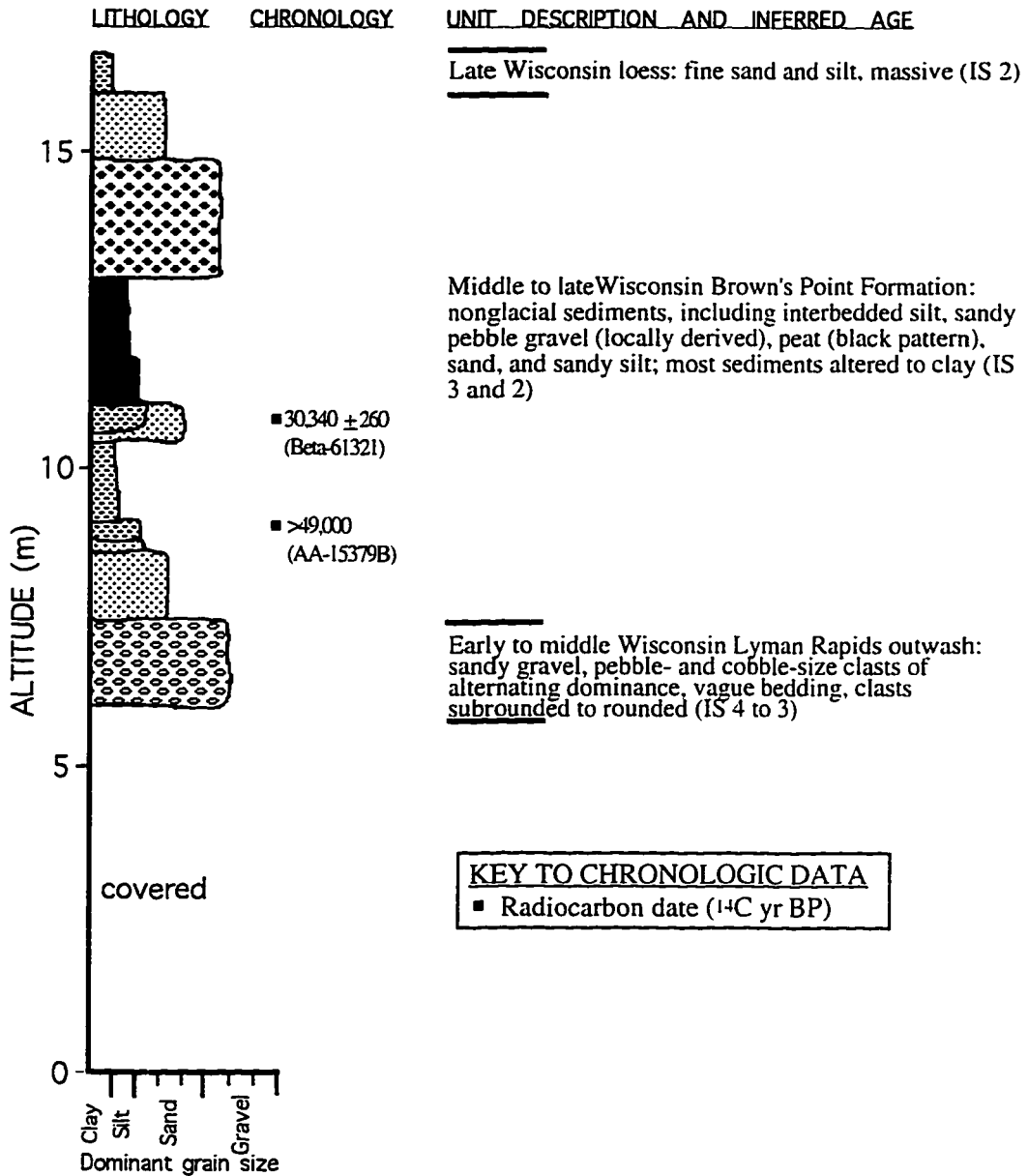


Figure 3.11: Stratigraphic section 2.0 km north of Kalaloch (SE1/4, SW1/4, Sec. 33, T.25N., R.13W.; Figure 3.2). Chronology consists of AMS (AA-) and conventional radiocarbon dates (Beta-).

Lateral Correlations

As to the north, the fine-grained sediments promote slumping, resulting in poor exposure, and stratigraphic correlations are tentative. The outwash descends southward below beach level approximately 1.6 km north of Kalaloch, but reappears approximately 0.3 km south of Kalaloch on the south limb of the syncline. At Kalaloch, the exposed stratigraphic section is as little as 5 m thick and consists of silt, peat, and locally derived gravel and sand. As the outwash rises southward, the silt/peat/local gravel sequence thins, and pinches out 1.3 km south of Kalaloch.

The silt/peat/local gravel sequence in the Kalaloch area was deposited following the Lyman Rapids glaciation (IS 4). Radiocarbon dates of $30,340 \pm 260$ ^{14}C yr BP (Beta-61321) and $>49,000$ ^{14}C yr BP (AA-15379B) from the North Kalaloch section and $22,440 \pm 220$ ^{14}C yr BP (AA-15378) from the upper peat at Kalaloch, indicate that the sequence was deposited during IS 3 and IS 2. The time span represented by the exposed portion of this sequence is thus considerably shorter than that represented by the Browns Point section described by Heusser (1972).

Beach Trail 2 to Queets River

Seacliffs between Beach Trail 2 and the Queets River (Figure 3.12) expose only beach sediment, outwash, and loess. The outwash terrace rises southward. The altitude increase is a result both of uplift on the south limb of the Kalaloch syncline and of the depositional gradient of the outwash fill surface, which slopes away from the Queets River mouth. At two locations, beach sand and gravel are exposed beneath the outwash. These sediments are likely the wave-cut surface cover sediments.

At the mouth of the Queets River, two low terraces are inset within the main outwash body. The terraces are mainly erosional, rather than constructional, and have only thin veneers (1- to 3-m-thick) of fluvial gravel deposited above the erosional surface. They originated during middle and/or late Wisconsin (IS 3 and/or IS 2) glaciations.

Queets River to Whale Creek North

Thick outwash with silty interbeds typifies the stratigraphic sequence between the Queets River and the area north of Whale Creek (Figures 3.1 and 3.13). The outwash is as thick as 25 m. It is generally dominated by pebble and cobble gravel, but

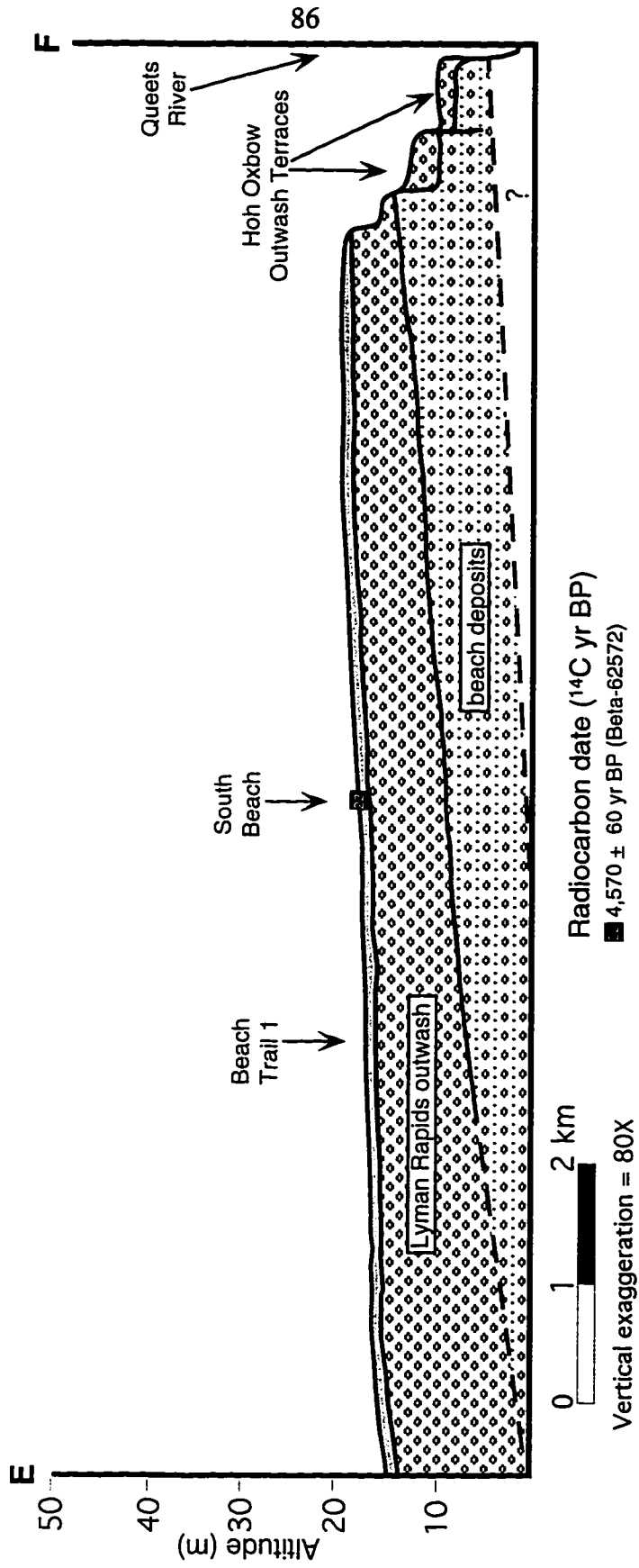


Figure 3.12: Sketch of stratigraphic sequence between Beach Trail 2 and the Queets River (E-F on Figure 3.2), showing stratigraphic correlations and chronologic control. See Figure 3.10 for key to lithology symbols.

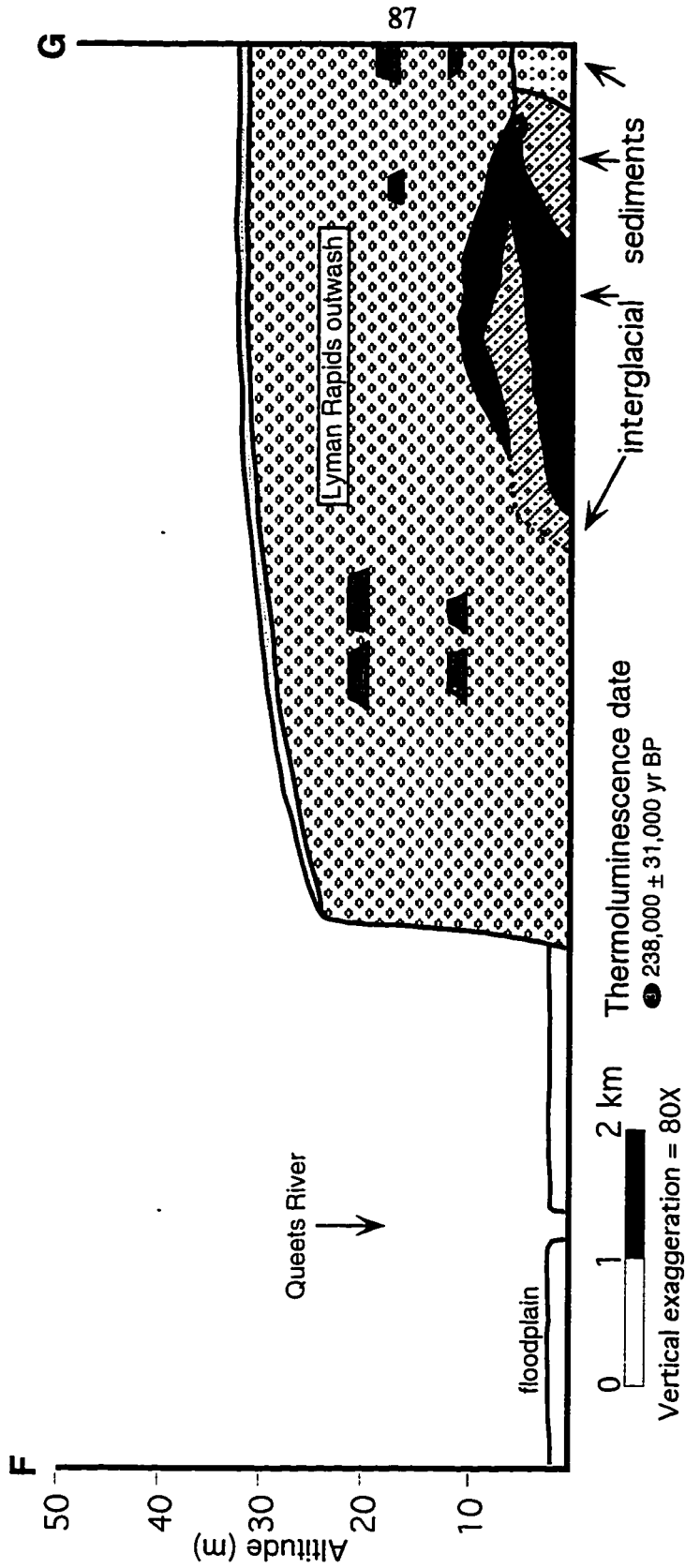


Figure 3.13: Sketch of stratigraphic sequence between the Queets River and the area north of Whale Creek (F-G on Figure 3.2), showing stratigraphic correlations and chronologic control.

locally by sand. Laterally discontinuous silty interbeds can be correlated by altitude over 2 km laterally. Three such beds have been recognized. They contain abundant wood, including in-situ stumps, and were likely deposited on the floodplains of meltwater streams. Subsequent scouring by aggrading streams has disrupted the continuity of the beds. Radiocarbon dates from seacliffs near Whale Creek (see below) indicate that the outwash accumulated before about 42,000 ¹⁴C yr BP. The outwash forms the prominent coastal terrace that is part of the Lyman Rapids drift.

Seacliffs in this area also expose a unique portion of the last-interglacial sequence. The wave-cut surface ascends southward from beach level about 0.5 km north of Whale Creek (Figure 3.14). The overlying beach sand and gravel also rise southward, but at the north end of their exposure they terminate at a 4-m-deep paleo-channel (Figure 3.13). The paleo-channel is filled with fluvial gravel, which is capped by mud and woody peat. This channel-fill sequence correlates northward with a sequence that consists of two 3- to 4-m-thick, silt-rich beds separated by a 1- to 4-m-thick bed of pebble gravel. The lower silt-rich bed contains peat, detrital wood, and spruce cones. The upper bed contains a series of large, *in-situ* stumps that are the apparent remnants of a last-interglacial forest (Figure 3.15; age inferred from character of unit and stratigraphic relationship to the wave-cut surface). The interglacial sequence terminates northward at a channel cut filled with Lyman Rapids outwash.

Whale Creek North to Raft River

Seacliffs stretching from the area north of Whale Creek to the Raft River (Figure 3.1) expose the wave-cut surface and both the Steamboat Creek Formation and the Lyman Rapids outwash (Figure 3.14). The wave-cut surface rises southward above modern beach level about 0.5 km north of Whale Creek. It rises steeply, relative to the north limb of the syncline, reaching 31 m altitude at the Raft River.

Whale Creek Section

A stratigraphic section 0.4 km north of Whale Creek includes Steamboat Creek Formation sediments characteristic of the area, as well as the wave-cut surface and younger sequence (Figure 3.16).

The Steamboat Creek strata dip approximately 11° north. In the vicinity of the exposure, various sediments are present in beds as thick as 3 m: silt and clay (both laminated and massive), peat, and fluvial sand and fine gravel. The gravel is poorly

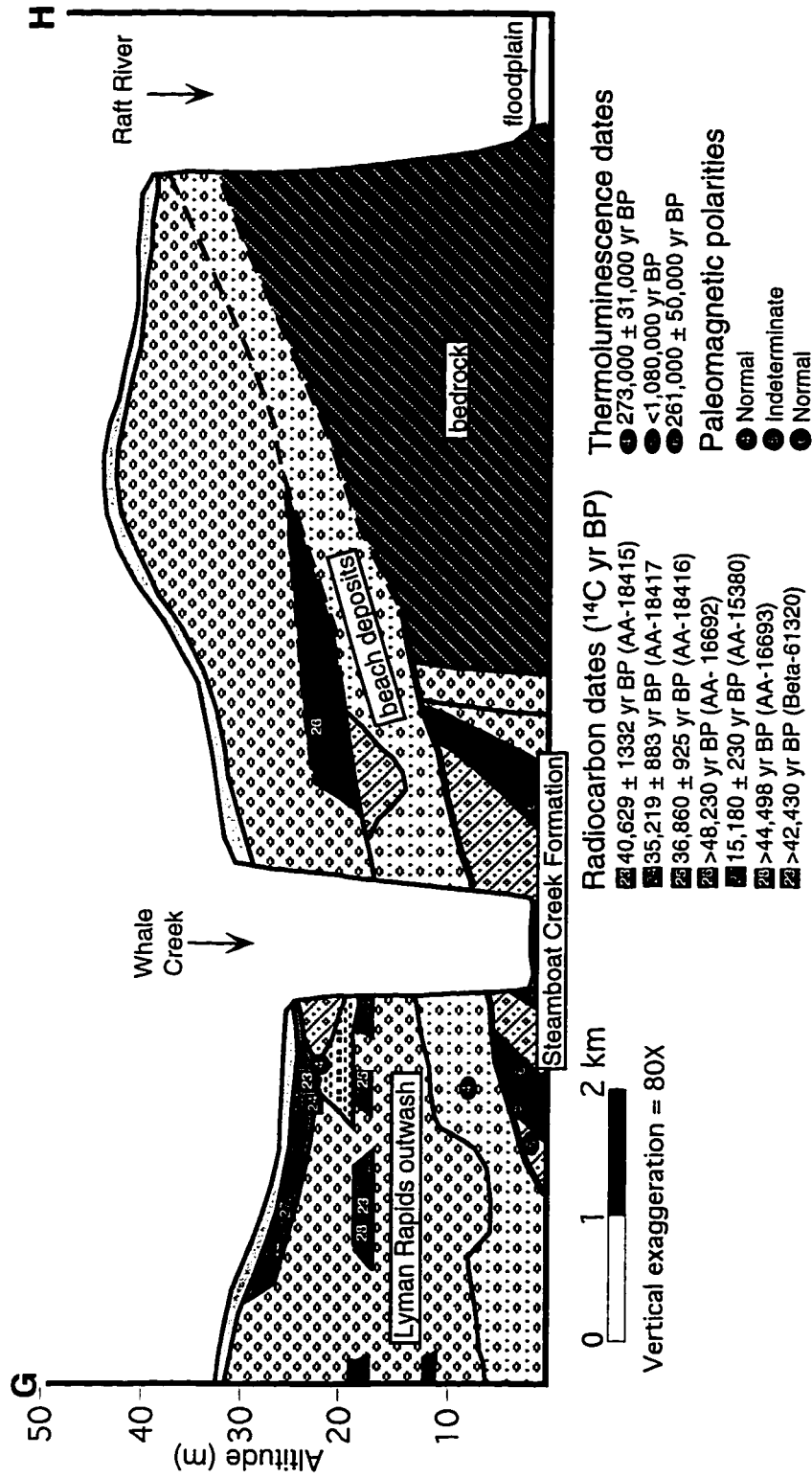


Figure 3.14: Sketch of stratigraphic sequence between the area north of Whale Creek and the Raft River (G-H on Figure 3.2), showing stratigraphic correlations and chronologic control. See Figure 3.10 for key to lithologic symbols.



Figure 3.15: Seacliff exposure 2.1 km north of Whale Creek. Note two thick peat beds at right (arrows), separated by fluvial gravel. Upper peat bed contains in-situ stumps and is overlain by Lyman Rapids outwash.

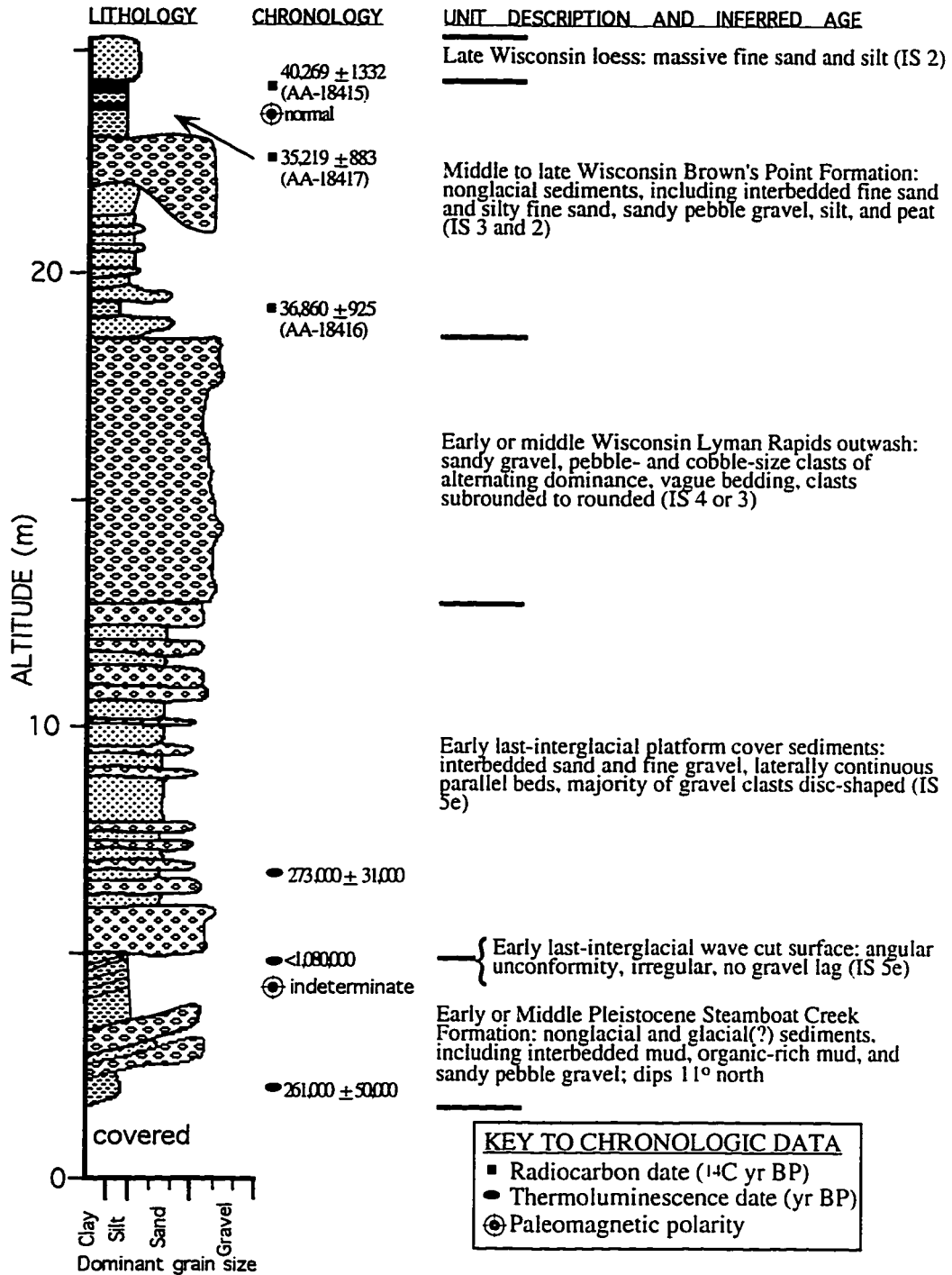


Figure 3.16: Stratigraphic section 0.4 km north of Whale Creek (NW1/4, SE1/4, SW1/4, Sec. 9, T.23N., R.13W.; Figure 3.2).

bedded generally, but locally displays cut-and-fill stratification; in these respects, it is similar to outwash gravel elsewhere in the older and younger sequences. However, its limited vertical extent and its interbedding with silt, clay, and peat suggest that such an interpretation is unwarranted. The fine-grained sediments and peat likely accumulated in terrestrial slackwater environments. They contain terrestrial plant fossils and lack marine diatoms.

The wave-cut surface marks an angular unconformity in this area. Thus, it is very clearly defined despite its lack of a cobble-boulder lag. Sand and gravel beach deposits cover the wave-cut surface to a thickness of 7.8 m. Gravel dominates the lower and upper thirds of the unit, while sand dominates the middle third.

A 6.3-m-thick unit of gravelly outwash overlies the beach deposits. The gravel is dominated by pebbles, except for sparse, cobble-dominated zones, and includes sand lenses only near its top. Silt and peat units are not associated with the outwash at this locality, but seacliff sections within 0.3 km to the north include silt and peat units both below and within the outwash.

The top 6.3 m of the section is dominated by fine-grained sediments. Interbedded fine sand and silt generally grade upward to silt with peat interbeds, but a pebble-gravel bed interrupts that trend. Pollen spectra from the base of this unit indicate stable, mild conditions, but progressive cooling is indicated by pollen spectra from the upper portion (Florer, 1972). The expansion of an alpine plant assemblage characterizes the top of the unit, suggesting a glaciation. Fine sand and silt, interpreted as loess, cap the section. Radiocarbon dates of $40,630 \pm 1332$ ^{14}C yr BP (AA-18415), $35,220 \pm 883$ ^{14}C yr BP (AA-18417), and $36,860 \pm 925$ ^{14}C yr BP (AA-18416), while stratigraphically reversed, indicate a middle Wisconsin (IS 3) age for this unit. It appears to have accumulated in a depression or abandoned meltwater channel in the top of the Lyman Rapids outwash.

Lateral Correlations

Exposures of the Steamboat Creek Formation extend about 0.5 km north and 0.8 km south of Whale Creek. South of that area, the wave-cut surface is poorly exposed and/or cut on bedrock. Where exposed, the Steamboat Creek Formation includes beds of silt-rich sediment, peat, and fluvial gravel and sand. An exposure 0.8 km south of Whale Creek contains thick (8 m) beds of cobble-rich gravel that may be outwash. A normally magnetized sample collected from the Steamboat Creek Formation

0.7 km south of Whale Creek suggests that the sediments are either less than 780,000 years old (Brunhes normal polarity chron) or greater than 2,500,000 years old (Gauss normal polarity chron). It is also conceivable that the sediments were deposited during one of the normal subchrons (e.g., Jaramillo) of the Matuyama reversed chron.

Thermoluminescence samples were collected from exposures in this area to test the applicability of the method to the sequence. Thermoluminescence dates of $238,000 \pm 31,000$ yr BP (above wave-cut surface), $273,000 \pm 31,000$ yr BP (above wave-cut surface), and $261,000 \pm 50,000$ yr BP (below wave-cut surface; Figures 3.13, 3.14, 3.15, and 3.16) suggest that the wave-cut surface formed during IS 7. The similarity of the dates from both above and below the wave-cut surface, however, suggest that sediments above the wave-cut surface were merely recycled—without having their thermoluminescence signal reset—as preexisting sediments were eroded by wave action. That is, the dates on sediments overlying the wave-cut surface may reflect the age of an immediate sediment source rather than the timing of their own deposition. Forman and Ennis (1992) and Kaufman et al. (1996) found that the variability of bleaching in waterlain sediments, caused by the light-filtering effects of water and turbidity, can lead to substantial thermoluminescence age overestimates. They encountered age overestimates of 5,000 to 40,000 yr for Late Pleistocene and Holocene mud-flat and glacial-marine sediments in Alaska and Spitsbergen.

If the wave-cut surface indeed formed during IS 7, then the outwash overlying the beach sediments was deposited during IS 6 and/or the last glacial cycle. The broad coastal outwash terrace in this area has been correlated with the Lyman Rapids drift. Radiocarbon dates from seacliff exposures, from a bog on the terrace, and from lacustrine sediments behind Lyman Rapids moraines indicate an early or middle Wisconsin (IS 4 or 3) age for the Lyman Rapids drift (Chapter 2). Thus, at least the upper portion of the thick outwash exposed in seacliffs north of Whale Creek was deposited during IS 4 or 3. Though there are several silt-clay beds within the outwash sequence, all are grey and indicative of short-lived hiatuses in outwash deposition. That is, there are no horizons within the outwash sequence that are suggestive of an extended period of interglacial weathering. The stratigraphic evidence thus indicates that the entire body of outwash accumulated during IS 4 or 3 and that the wave-cut surface dates to IS 5.

The younger sequence consists of silt-rich sediments, outwash, and loess. Silt-rich sediments and peat overlie the beach sand and gravel in some sections. These

sediments are as much as 5 m thick in an exposure 0.8 km south of Whale Creek (Figure 3.16), with multiple peaty horizons. The uppermost peat yielded an AMS radiocarbon date of $>48,230$ ^{14}C yr BP (AA-16692).

The Lyman Rapids outwash described above thins considerably south of Whale Creek (Figures 3.13 and 3.14) and is only about 5 m thick at the mouth of the Raft River. The thinning likely results from a combination of sedimentologic and tectonic influences. The outwash thins with distance from its major source (the Queets River), and the southward-ascending bedrock contact left limited space for gravel deposition. In the Raft River area, the outwash forms a broad coastal terrace that can be traced upvalley. Although the Raft River originates on the coastal plain, meltwater may have spilled into its valley from the Queets drainage and constructed an outwash valley train.

COASTAL STRATIGRAPHIC EVOLUTION

The coastal stratigraphy reflects a variety of sedimentologic regimes, including glacial-fluvial aggradation during glaciations, marine transgression during interglacial sea-level highstands, and landscape stabilization during non-highstand interglacial and interstadial episodes. Overprinted on these climate-related regimes is the variable influence of meltwater streams with varying distance from major valley mouths.

Evidence of the earliest sedimentologic episodes is preserved in the Steamboat Creek Formation, which lies beneath the wave-cut surface. In the northern half of the coastal study area, this formation consists mostly of glacial-lacustrine and glacial-marine drift, till, and outwash. Eolian sand is also present, but it is unclear whether the sand represents glacial or nonglacial conditions. Obscured stratigraphic relationships between most exposures of Steamboat Creek Formation drift preclude determining the number of glaciations involved, but an inferred valley margin/valley fill relationship between two portions of the Steamboat Creek Formation south of the Hoh River (Figure 3.3) indicates that at least two glaciations are represented. At least some of the glacial sediments were deposited during the Matuyama Reversed-Polarity Chron, and therefore most likely represent Early Pleistocene glaciation. Till and glacial-marine drift indicate that at least one glacier advanced past the location of the modern coastline and calved in marine water. The large lag boulders marking the wave-cut surface between the Hoh River and Beach Trail 4 suggest that the eroded portion of the sequence included till (the outwash does not

contain such large boulders) and, thus, that the Hoh glacier may have advanced past the location of the modern shoreline while depositing the Whale Creek drift (Chapter 2).

The Steamboat Creek Formation in the southern part of the study area (Whale Creek-Raft River) includes sediments that appear to be of both glacial (braided stream gravel) and nonglacial (peat, estuarine muds) origin. It is not possible to evaluate temporal relationships with Steamboat Creek Formation sediments in the northern half of the study area.

The coastal stratigraphic evolution can be more precisely inferred for strata above the wave-cut surface. This surface is interpreted as an early last-interglacial (IS 5e) feature, representing erosion by wave action as sea level rose to its highstand. Although radiometric dates supportive of this interpretation are lacking, continuity with the overlying sequence indicates that the surface formed during the last interglaciation (rather than a previous one). Furthermore, the presence of overlying interglacial sediments precludes an IS 5a origin, and a lack of an IS 5e erosion surface inland argues against a 5c interpretation.

As sea level rose to its highstand, the coastline eroded landward, past the position of the modern seacliff. Coastline recession terminated at paleo-seacliffs variably preserved ca. 1.5 km from the modern coastline. Horizontally bedded gravel and sand accumulated in beach and intertidal environments. Those sediments were likely derived locally from seacliffs that retreated landward.

Sea-level recession stranded the surface formed by the horizontally bedded sand and gravel overlying the wave-cut surface. In most of the coastal study area (excepting the Beach Trail 4 to Kalaloch section and a 1 to 2 km section between the Queets River and Whale Creek), the coastal landscape then stabilized. Thin soils formed on the stranded beach sand and gravel, and peat accumulated locally. Abundant fossil wood indicates that portions, at least, of the new coastal terrace supported forest. Pollen data from the Steamboat Creek area (Florer, 1972) support this interpretation. Small amounts of fine-grained sediment (clay, silt, and fine sand) were eroded from the outwash terraces landward of the paleo-seacliff and deposited on the coastal terrace by low-gradient streams. These conditions apparently prevailed through the rest of the interglaciation (IS 5d through 5a). In the Beach Trail 4-Browns Point-Kalaloch portion of the coastline, sedimentation rates were somewhat greater because of the higher, bedrock cored hills adjacent to the modern coastline. The accumulated interglacial sediments are thus thicker there than in the other areas described above.

An extensive glaciation followed. This glaciation is represented by the Lyman Rapids drift. The Queets valley glacier advanced to within 13 km of the coastline, filling the lower valley with a broad valley train. Outwash as thick as 25 m aggraded at the location of the modern coastline. Discontinuous but laterally extensive silty interbeds characterize the outwash along a 4.3 km stretch of coastline north of Whale Creek. The interbeds contain detrital and in-situ wood (stumps), indicating that lateral portions of the Queets valley outwash fan stabilized temporarily during the aggradational phase. The Hoh valley glacier advanced to within 12 km of the modern coastline, also constructing an extensive outwash valley train and aggrading thick outwash now exposed at the coastline. At both valley mouths, outwash surfaces constructed during this glaciation are preserved as the most extensive coastal terraces.

As the glaciation waned, rivers incised into the outwash valley trains, forming outwash terraces. The terrace surfaces stabilized and accumulated silt and fine sand in some areas, perhaps via eolian deposition into ponded water. North of Whale Creek, the Lyman Rapids outwash is capped by as much as 6 m of fine-grained sediment (Figure 3.16). In the Hoh River coastal sequence, 0.5 to 3 m of fine sediment accumulated on the outwash terrace before ca. 28,000 ^{14}C yr BP.

An additional glacial event is recorded in the Hoh coastal sequence. A less-extensive glacier advance, represented by the Hoh Oxbow I drift (ca. 29,200 to 26,700 ^{14}C yr BP), left a terminal moraine 15 km from the coastline. Outwash filled the main Hoh valley, constructing a fill surface inset below the terraces described above. In addition, meltwater spilled over a low divide into the Cedar Creek drainage (Plate 1) and deposited outwash at the modern coastline (Chapter 2). This outwash buries the Lyman Rapids outwash south of Cedar Creek. Corresponding outwash in the Queets coastal sequence is found only in low terraces at the mouth of the river.

Loess deposition is the final event recorded in the coastal sequence. The loess was likely derived from distal outwash on the then-exposed coastal plain. One to 2.5 m of loess mantles the stratigraphic sequence along the entire coastline, and covers most inland outwash terraces. A radiocarbon date on seeds from subjacent, fine-grained pond sediments south of the Queets River provides a maximum age of $15,180 \pm 230$ ^{14}C yr BP (AA-15380).

NEOTECTONIC DEFORMATION

As reflected in the foregoing discussion of coastal stratigraphy, the Pleistocene strata in the project area have been deformed tectonically. The principal structure is the Kalaloch syncline (Baldwin, 1939), a broad fold reflected in the wave-cut surface, in younger-sequence strata, and in the coastal terrace (Figure 3.2 and Plate 2). Dipping strata in the Steamboat Creek Formation also reflect deformation associated with the syncline. Unequivocal faults have not been observed. However, the south end of the syncline is associated with features suggestive of a thrust fault, and minor offsets appear to cut portions of the stratigraphic sequence between Abbey Island and the Hoh River.

This study focuses on deformation associated with the Kalaloch syncline. The stratigraphic sequence provides chronologic constraint and a time-transgressive view of the deformation, and permits the calculation of deformation rates. These geologically determined deformation rates, in turn, aid understanding geodetically measured deformation rates. The geologic and geodetic rates have similar spatial variability but differing magnitudes, leading to the conclusion that the synclinal deformation is wholly plastic while nearly uniform coastal uplift reflects flexural, interseismic deformation.

KALALOCH SYNCLINE

The Kalaloch syncline is a gentle, asymmetric structure that is evident along a 31-km coastline traverse between the Hoh and Raft rivers. The traverse mostly reflects the actual (as opposed to apparent) cross-sectional geometry of the structure: although the image of the syncline relies almost exclusively on seacliff exposures that are two dimensional in the scale of the traverse, the coastline is nearly perpendicular to the inferred east-northeast-trending axis of the syncline.

The synclinal structure is most perceptible in the pattern of the wave-cut surface and its cover sediments. The surface descends from 30 m altitude to beach level (1 to 2 m altitude) in the 14 km between the Hoh River and Browns Point, lies below beach level in the 13 km between Browns Point and the Whale Creek area, and rises from beach level to 31 m altitude in the 4 km between the Whale Creek area and the Raft River (Figure 3.2 and Plate 2). Overlying beach sand and gravels reflect the syncline in similar fashion.

The southern limb of the syncline dips more steeply than the northern limb, indicating a south-southeast dipping axial plane. The steeply dipping southern limb is

associated with a possible thrust-fault propagation fold affecting strata of the Steamboat Creek Formation (see below).

The seacliff altitudes of the wave-cut surface and cover sediments depend in part on the distance seaward from the associated paleoshoreline. Fortunately, that distance is uniform (1 to 1.5 km) along most of the traverse. Between Beach Trail 5 and Browns Point, however, the seacliff-paleoshoreline distance shortens to approximately zero. Thus, the apparent wave-cut surface altitude, relative to adjacent areas, is inflated (see Figure 3.8 and associated discussion of lateral correlations). That disparity is accounted for in the calculation of deformation rates.

The syncline is also reflected in the exposure pattern of the younger sequence. Lyman Rapids outwash in the Kalaloch area is exposed on both limbs of the syncline, having subsided below beach level in the axial zone (Figure 3.10). Gradients of the tops of outwash units south of the Hoh River are likely inflated by deformation on the north limb of the syncline (Figures 3.3 and 3.5) because the depositional gradient and deformational inclination are additive. In contrast, outwash surface gradients are likely deflated south of the Queets River (Figure 3.13), where the southerly depositional gradient opposed the subsequent, down-to-the-north deformation on the south limb of the syncline. Finally, the terrace formed by the silt/peat/local gravel sequence in the axial zone of the syncline (Figure 3.10) also reflects the synclinal warping.

Deformation of the Steamboat Creek Formation

Some Steamboat Creek strata exhibit deformation reflective of the Kalaloch syncline. While the structural dip of the wave-cut surface and younger sequence strata are imperceptible at outcrop scale, dips on Steamboat Creek strata are steep enough to be readily observed. In the Destruction Island Viewpoint area (Figures 3.5 and 3.7), the formation is dominated by outwash. One exposure, however, contains a 1-m-thick bed of magnetically reversed overbank sand and silt that dips 8° south (Figure 3.17). Seacliffs within 1.6 km south of the Hoh River (Figure 3.3) expose Steamboat Creek strata that dip as much as 30° south. However, those exceptional dips may be at least partially related to paleo-landsliding. A structural component may also exist, but distinction of the two components is not possible.

Steamboat Creek strata exposed on the south limb of the Kalaloch syncline are more strongly deformed, forming clear angular unconformities with the wave-cut surface and younger sequence strata. North of Whale Creek (Figures 3.14 and 3.16),

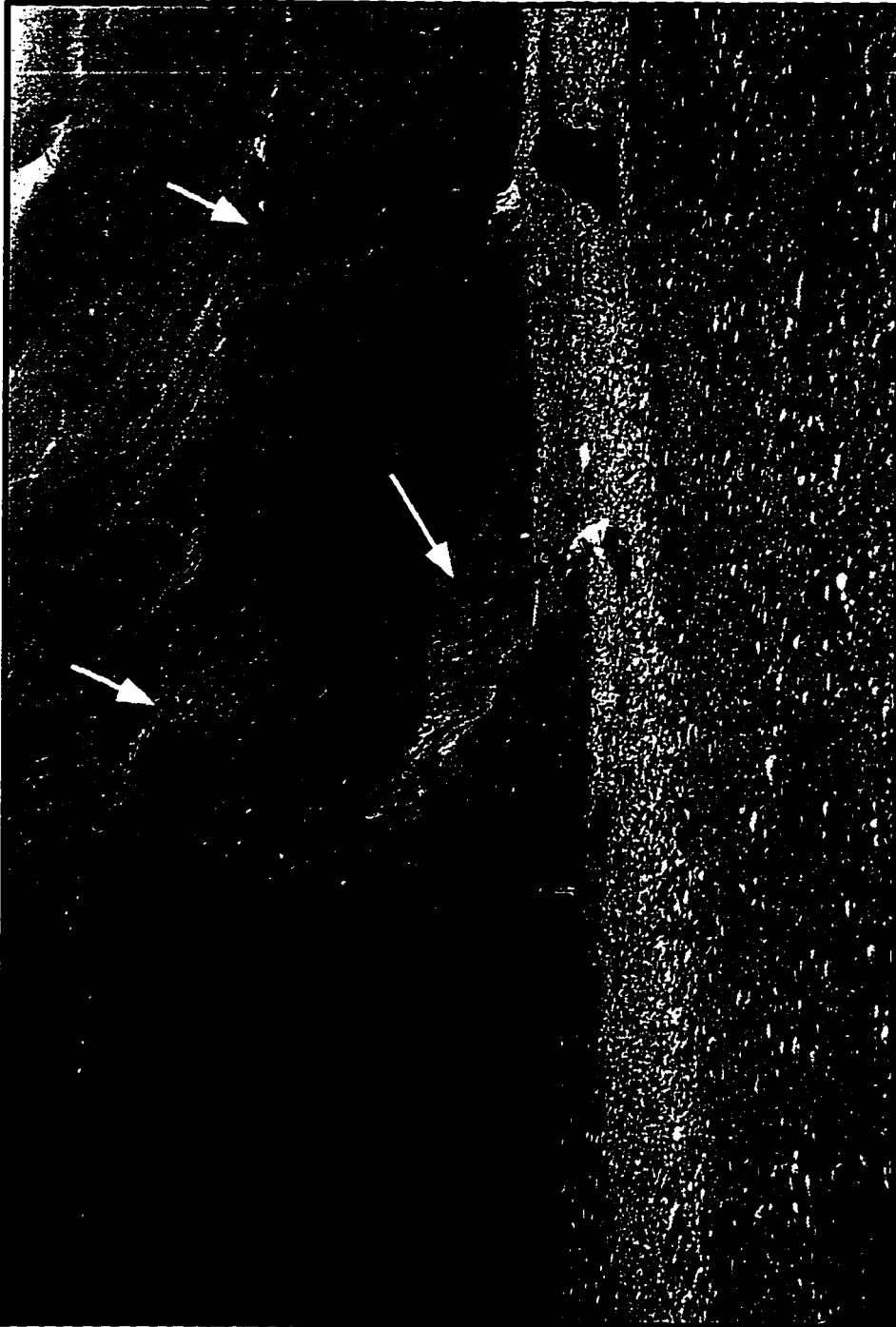


Figure 3.17: Seacliff below Destruction Island Viewpoint. Note south-dipping sand and silt bed (lower arrow) in Steamboat Creek Formation outwash. Wave-cut surface (upper arrows), marked by boulder lag, truncates outwash at 11 m altitude.

the strata reappear above beach level dipping 11° north (Figure 3.18). Dips in the Whale Creek area range from 15° north to 26° south and appear to reflect a gentle, west-northwest-trending anticline in the Steamboat Creek Formation. Finally, an exposure 0.8 km south of Whale Creek displays northerly dips of Steamboat Creek strata that increase progressively from 18° to nearly 90° over a distance of 80 m (Figure 3.19). These relationships suggest the presence of a thrust fault at depth (see below).

DEFORMATION RATES

The stratigraphic and chronologic data described in the first half of this chapter constrain deformation rates for the Kalaloch syncline. Those rates can aid understanding of geodetically measured deformation and help to explain similar synclinal structures recognized along the Cascadia convergent margin.

The most detailed contouring of geodetic uplift rates (Holdahl et al., 1987; Savage et al., 1991) shows areas of uplift minima and maxima in coastal Washington state (Figure 3.20). Uplift rates reach a maximum of more than 3.2 mm/yr on the northwestern part of the Olympic Peninsula, while uplift minima encompass Willapa Bay, Gray's Harbor, and a portion of the central Olympic coast. The latter uplift minimum is centered on Kalaloch, and is coincident with the Kalaloch syncline (Figure 3.21). If these detailed data are accurate, they show that the Kalaloch syncline is an active structure. The coincidence of geologically and geodetically recorded data permit useful comparisons between deformation on widely differing time scales.

The buried wave-cut surface provides the most reliable datum for deformation-rate calculation. The rates calculated for the wave-cut surface are applied to altitudes of Steamboat Creek strata to constrain secular deformation rates. The north and south limbs of the syncline are quite different in terms of deformation style and the quality of geologic and geodetic data; therefore, the two limbs are treated separately.

Age of the Wave-cut Surface: Summary of Evidence

The age of the buried wave-cut surface is critical to deformation rate calculations. Thus, it is worthwhile to summarize pertinent evidence from this and other studies.

West and McCrumb (1988) and P. McCrory (personal communication, 1996) correlate the local, buried wave-cut surface with IS 5a wave-cut terraces at Willapa Bay and in Oregon (Whiskey Run terrace). The principal bases for these correlations are:



Figure 3.18: Seacliff 0.3 km north of Whale Creek. Note north-dipping beds of Steamboat Creek Formation at base, truncated by wave-cut surface (lower arrow). Upper arrow marks beach sediment/outwash contact

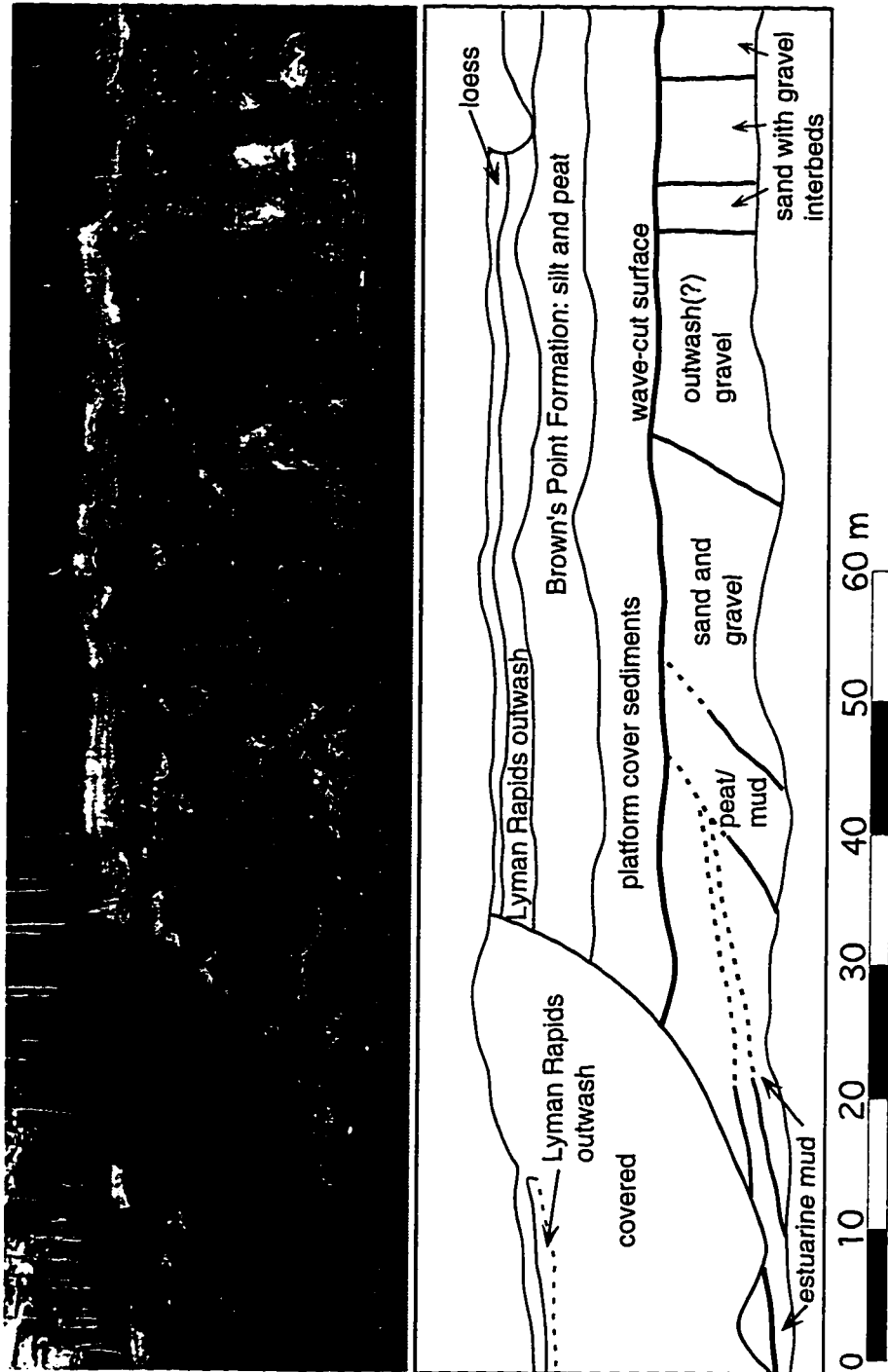


Figure 3.19: Seacliff 0.8 km south of Whale Creek, exposing strongly deformed Steamboat Creek Formation sediments (below wave-cut surface). Note progressively steepening dips on Steamboat Creek Formation strata from left to right (north to south, shown with solid and dashed bedding lines). Sketched irregularities in wave-cut surface and overlying contacts reflect the perspective of the photograph, not actual irregularities. Scale is approximate.

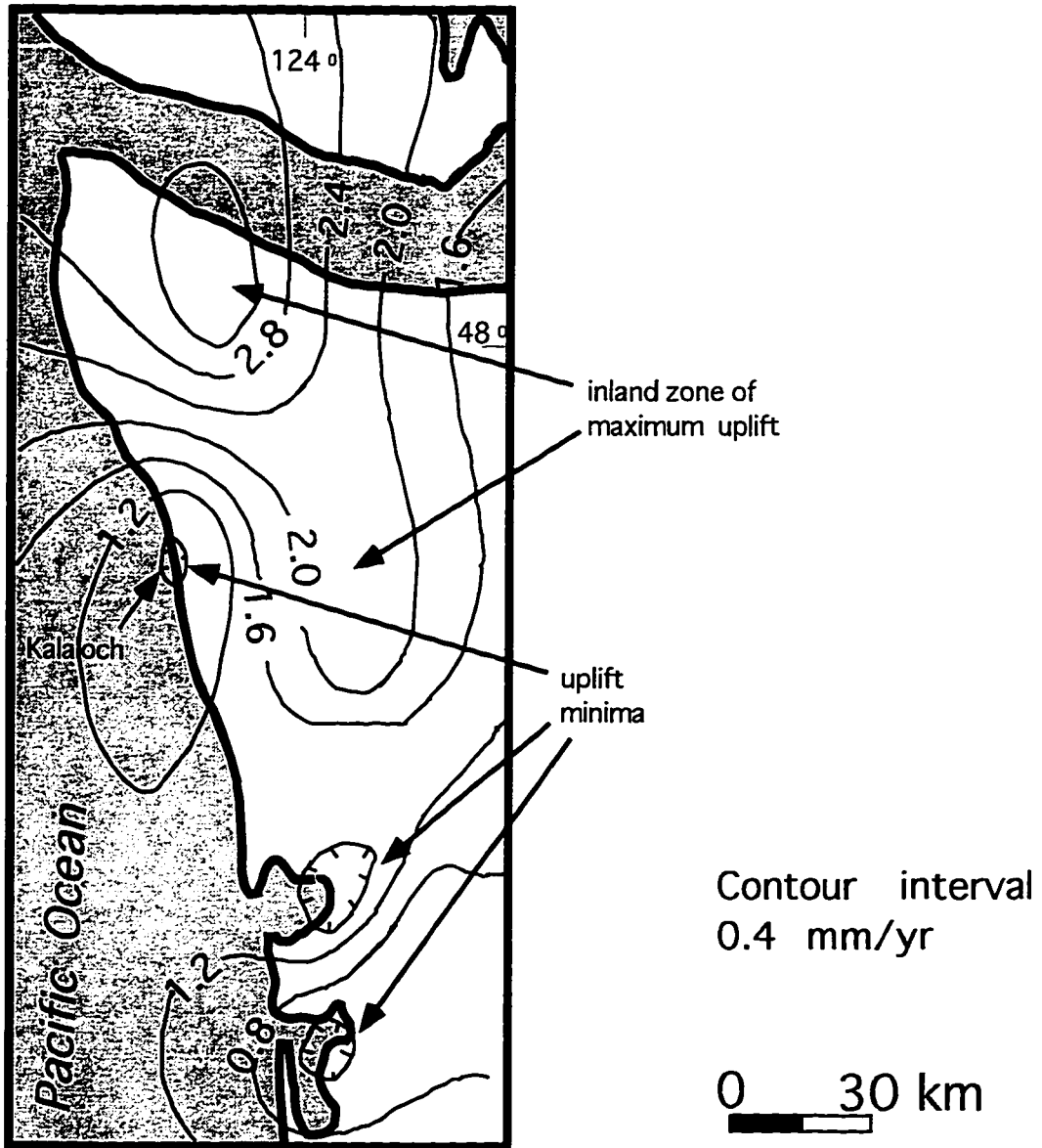


Figure 3.20: Uplift rates (mm/yr) inferred from tide gauges and leveling (after Holdahl et al., 1987, and Savage et al., 1991).

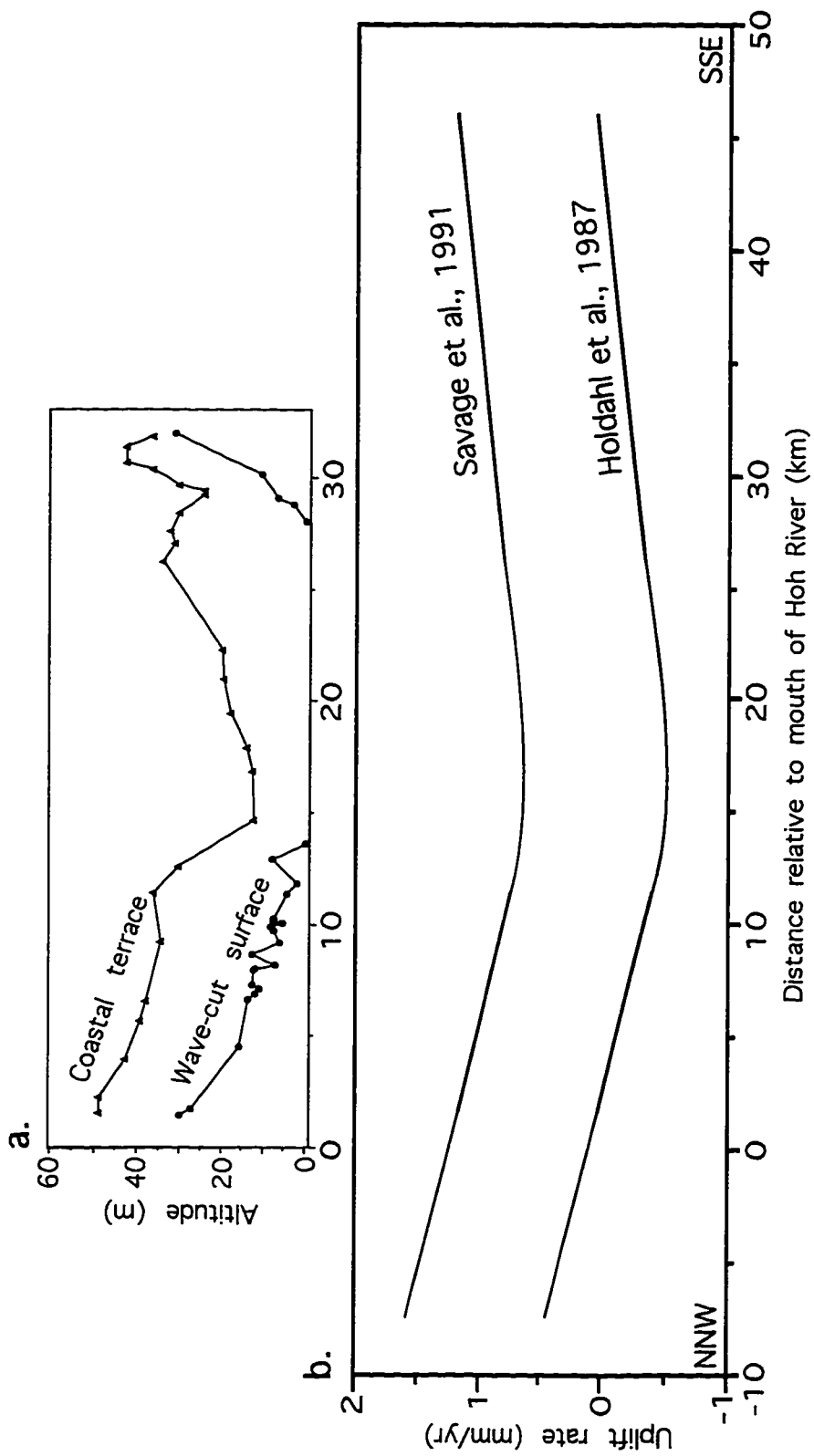


Figure 3.21: a. Observed deformation of buried wave-cut surface and coastal terrace between Hoh and Raft rivers (vertical exaggeration 200X), compared with b. Profile of geotically measured coastal uplift derived from Figure 3.20. Note coincidence of observed deformation and geotectic uplift patterns. Horizontal scale is coincident for both plots. Difference between Savage et al. (1991) and Holdahl et al. (1987) uplift rate plots lies in differing values for eustatic sea-level rise.

1. The buried wave-cut surface has been traced stratigraphically and geomorphically from this study area to Willapa Bay, located 90 km south of the Raft River (P. McCrory, personal communication, 1996). The buried wave-cut surface thus correlates with one correlated to IS 5a via amino-acid racemization data by Kennedy et al. (1982).
2. Heusser (1972) extrapolated sedimentation rates from the upper, radiocarbon-dated portion of his Browns Point section to the lower, undated portion, deriving a 70,000 ^{14}C yr BP age estimate for the basal beach sand and gravel. Thus, the beach sediments and underlying wave-cut surface likely correlate with IS 5a (P. McCrory, personal communication, 1996).

There are concerns with these lines of evidence. First, exposure is limited in some areas (e.g., Copalis Beach, Grays Harbor) between the Raft River and Willapa Bay. Second, correlation may be complicated by structures deforming the Pleistocene stratigraphic and geomorphic sequence. For example, McInelly and Kelsey (1990) and McNeill et al. (1994a) demonstrated that faults and broad folds disrupt terraces and stratigraphic units around Oregon bays. Many of the coastal bays of Oregon and Washington are associated with synclines mapped on the continental shelf (Goldfinger et al., 1992; McNeill et al., 1994b). Thus, correlations between Willapa Bay and the project area may be confounded by such structures, particularly where exposure is poor. Third, Heusser (1972) stated that his basal-sediment age estimate is conservative, and that abundant peat in the lower portion of the section suggests slower sedimentation rates. In fact, Heusser's pollen-derived temperature curve can be plausibly reinterpreted (Figure 2.7) to represent sedimentation through the last interglaciation (i.e., IS 5d through 5a) as well as the last glacial cycle (IS 4 through 2).

The buried wave-cut surface is interpreted here as an IS 5e feature. Thermoluminescence dates, done on an experimental basis for this sequence, suggest an IS 7 age. However, the stratigraphy does not support such an interpretation, and the dates themselves suggest incomplete zeroing of the thermoluminescence signal at the time of deposition (see above). Interpretation of the wave-cut surface as an IS 5e, rather than as an IS 5c or 5a feature is based on the following lines of evidence:

1. At Destruction Island Viewpoint (Figure 3.7) and elsewhere, the wave-cut surface cover sediments are overlain by 1 to 4 m of organic-rich sediments (including peat) and paleosols. These sediments yielded pollen indicative of interglacial coastal

vegetation (Florer, 1972). The time required to deposit interglacial sediment and form soils before deposition of Lyman Rapids outwash suggests that the wave-cut surface might have formed during IS 5e or 5c, but not during IS 5a.

2. A similar argument can be made for sediments exposed between the Queets River and Whale Creek. The cover sediments (beach sand and gravel) are cut by a gravel-filled channel (Figure 3.13), which is itself capped by silt and peat. The silt and peat thicken northward to two, 3- to 4- m thick beds, separated by gravel and containing peat and in-situ stumps. Those beds are overlain by Lyman Rapids outwash. Considerable time was required, after wave-cut surface formation, to form these features.
3. The permanent deformation rates implied by an IS 5c or 5a wave-cut surface age are not supported by morphology or stratigraphy in the Destruction Island Viewpoint area. An IS 5a age implies that an IS 5e surface, if present, would lie at ca. 51 m altitude, only a few meters below the Whale Creek outwash terrace cut by the paleoshoreline 1.5 km inland (Plate 1). A wave-cut feature is not present at that altitude. An IS 5c age for the seacliff wave-cut surface implies that an IS 5e wave-cut surface would lie at ca. 37 m altitude. Southeast of Destruction Island Viewpoint, Steamboat Creek incises the coastal sequence at that elevation, and no evidence of a second wave-cut surface is exposed.

Thus, the bulk of the local stratigraphic evidence supports an IS 5e age for the buried wave-cut surface. An IS 5c age cannot be conclusively ruled out, however. Therefore, deformation rates are calculated assuming both IS 5e and 5c ages.

North Limb of Syncline

The quality of geologic data on the north limb of the syncline is enhanced there by extensive exposures and an easily recognized and measured wave-cut surface. Numerous wave-cut surface altitudes have been measured (Figure 3.21). The quality of coastal geodetic data is also likely to be highest in this area. The releveling survey route (Holdahl et al., 1987) follows U.S. Highway 101 through the western Olympic Peninsula; only between the Queets and Hoh Rivers is the highway near the coastline. Thus the north limb of the syncline between Browns Point and the Hoh River is the only portion of the structure in which geodetic data coincide closely with a well-exposed and easily measured wave-cut surface.

Uplift rates have been calculated using the following procedures based on the accompanying rationales:

1. Measure the altitude of the wave-cut surface in the seacliff.
2. Project the wave-cut surface altitude landward to the paleoshoreline (Figure 3.22) in order to determine the altitude of the buried shoreline angle (the point where wave-cut surface and seacliff meet). The altitude of the shoreline angle at the time of platform formation approximates the altitude of the sea level highstand to within ± 2 m (Wright, 1970; Trenhaile, 1980). Use platform gradients from Bradley and Griggs (1976).
 - a. Use gradient of 0.02 for the 600-m-wide, inner portion of the platform .
 - b. Use gradient of 0.005 for the remainder of the platform width (outer portion).
3. Correct for the difference between modern eustatic sea level and that of the last-interglacial highstand.
 - a. Interpretation of marine terraces on stable coastlines suggests that early last-interglacial (IS 5e) sea level was 3 to 11 m higher than modern sea level (Mesolella et al., 1969; Veeh and Chappell, 1970; Bloom et al, 1974; Dodge et al., 1983). The average of these estimates, ca. 6 m above modern sea level (Muhs et al., 1992), is used here.
 - b. Interpretation of marine oxygen isotope records (Shackleton, 1987) suggests negligible difference between IS 5e and modern sea level and no correction.
 - c. Muhs et al. (1992) indicate that IS 5c sea level was 1 m below modern sea level.
4. Divide altitude of shoreline angle by 125,000 yr or 105,000 yr (approximate ages of IS 5e and IS 5c, respectively) to yield uplift rate in $\text{m}/10^3 \text{ yr}$ (mm/yr).

Potential errors in this analysis arise from three sources: 1) errors in measuring the wave-cut surface altitude (± 3 m) ; 2) divergence of the actual platform gradient from the assumed gradients (± 6 m?) ; and 3) errors in the estimated interglacial eustatic sea level (± 1 m?). Together, these potential errors likely account for less than 12.5 m error in altitude, which is equivalent to 0.1 mm/yr error in the IS 5e uplift rates.

Figure 3.23a shows the results of the deformation rate calculations for the north limb of the syncline and compares the calculated deformation rates with the geodetically recorded deformation rates from Figures 3.20 and 3.21. The northward increase in deformation rates reflects the tilting of the north limb of the syncline.

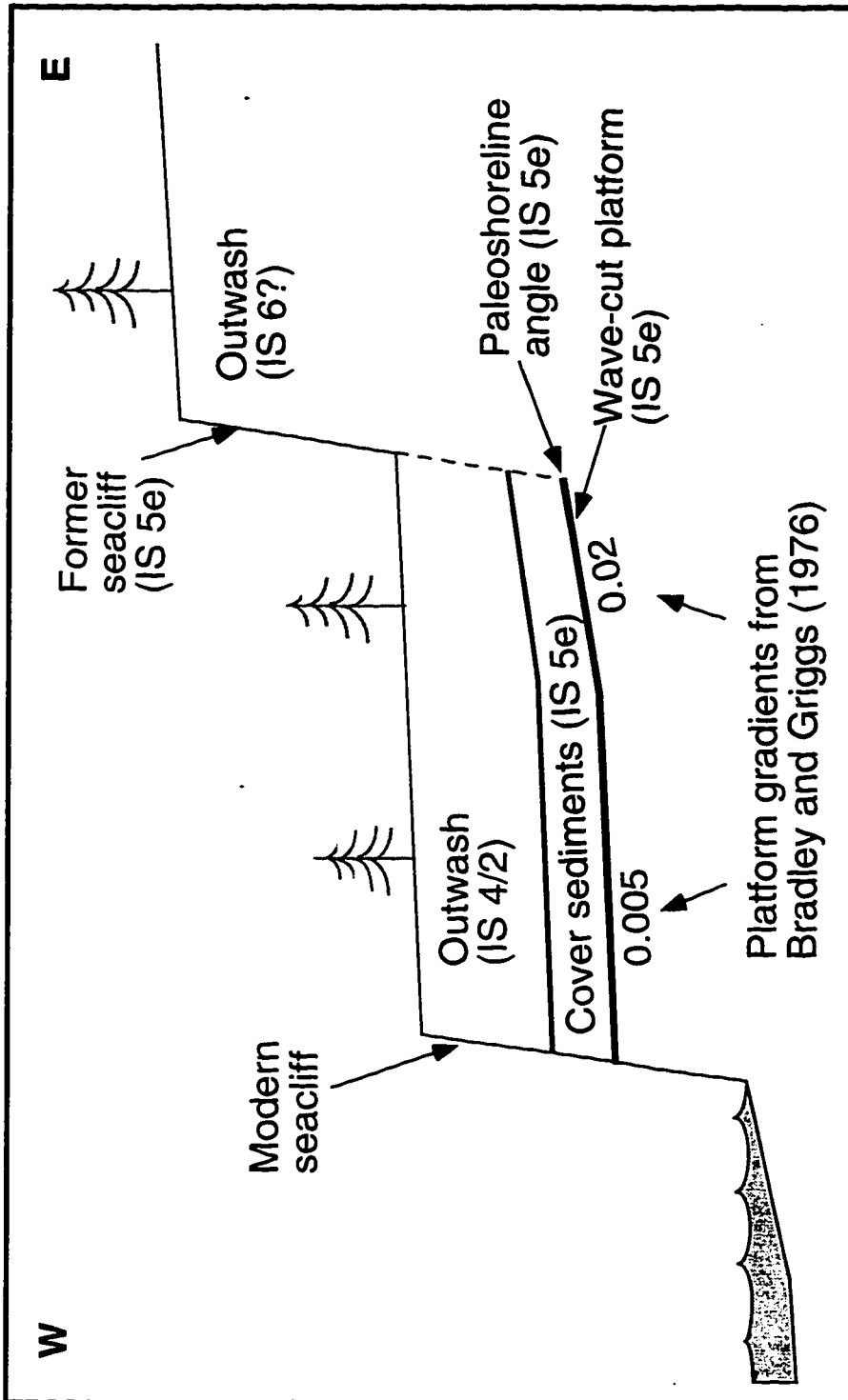


Figure 3.22: Schematic cross-section showing projection of wave-cut surface, as measured in modern seacliff, to paleoshoreline. Projection procedure estimates altitude of wave-cut surface at the paleoshoreline angle, which corresponds with contemporary mean low sea level. Horizontal and vertical scales vary with location on the coastline.

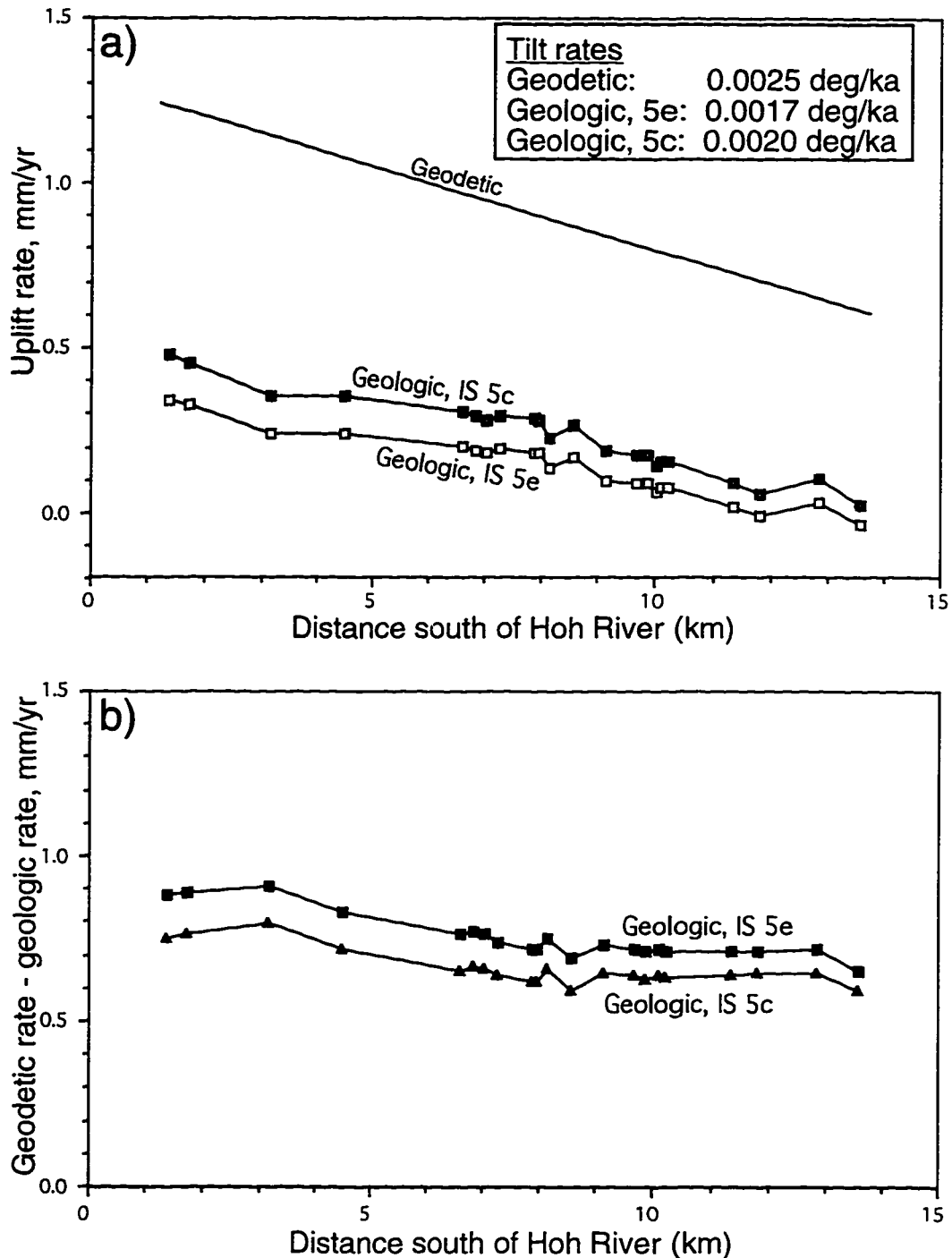


Figure 3.23: Uplift rate comparisons for north limb of the Kalaloch syncline. a) comparison of geologic rates (this study) with geodetic rates from Savage (1991). IS 5e uplift rate calculations assume IS 5e sea level was 6 m higher than modern sea level. If IS 5e sea level equaled modern sea level (Shackleton, 1987), IS 5e uplift rates would be 0.048 mm/yr greater than rates shown. b) difference between geodetic and geologic rates, equivalent to flexural component of geodetic rates.

The most striking aspect of this deformation rate comparison is the marked difference in magnitude between the geologic and geodetic rates (Figure 3.23b). Because differencing removes the permanent component of the modern deformation, the residual plotted in Figure 3.23b represents the flexural (elastic) component of the geodetic uplift rates. The comparison shows that this portion of the coastline is experiencing 0.6 to 0.9 mm/yr of flexural, interseismic deformation that should be recovered during the next seismic event. The remainder of the geodetically measured uplift is expressed as permanent rock uplift.

The spatial variability reflected in the two types of rates is very similar. That is, uplift rates increase northward at similar rates. Corresponding tilt rates are 0.0017 degrees/ 10^3 yr (IS 5e geologic), 0.0020 degrees/ 10^3 yr (IS 5c geologic), and 0.0025 degrees/ 10^3 yr (geodetic). The close correspondence of these tilt rates is surprising, given the strongly contrasting time scales and methods by which the rates were recorded and calculated. Their similarity indicates that the spatial variability in geodetic rates is reflected wholly in the geologic structure. Conversely, the similarity of tilt rates suggests that the synclinal deformation lacks an elastic component, i.e., that it grows at a constant rate unaffected by seismic events.

South Limb of Syncline

Unfortunately, neither the geologic nor geodetic data are as reliable for the south limb of the Kalaloch syncline as for the north limb. The geodetic leveling line turns inland near the Queets River, so the coastal geodetic data are less reliable for the area in which the wave-cut surface is exposed. Furthermore, landslide activity between Whale Creek and the Raft River renders intact stratigraphic exposures uncommon. The altitude of only four points on the wave-cut surface have been measured.

Figures 3.24a and 3.24b compare geologic uplift rates for the south limb with corresponding geodetic rates. The uplift rates increase southward, reflecting the steep gradient on the wave-cut surface (Figure 3.14). As with the north limb, geodetic rates are much greater than geologic rates, supporting the interpretation of a significant flexural, interseismic component. In contrast with the north limb, the corresponding tilt rates are substantially different. The geologic uplift rates represent a greater tilt rate. The cause of the disparity may be a local fold that affects the stratigraphic sequence (see below), inflating geologic uplift rates.

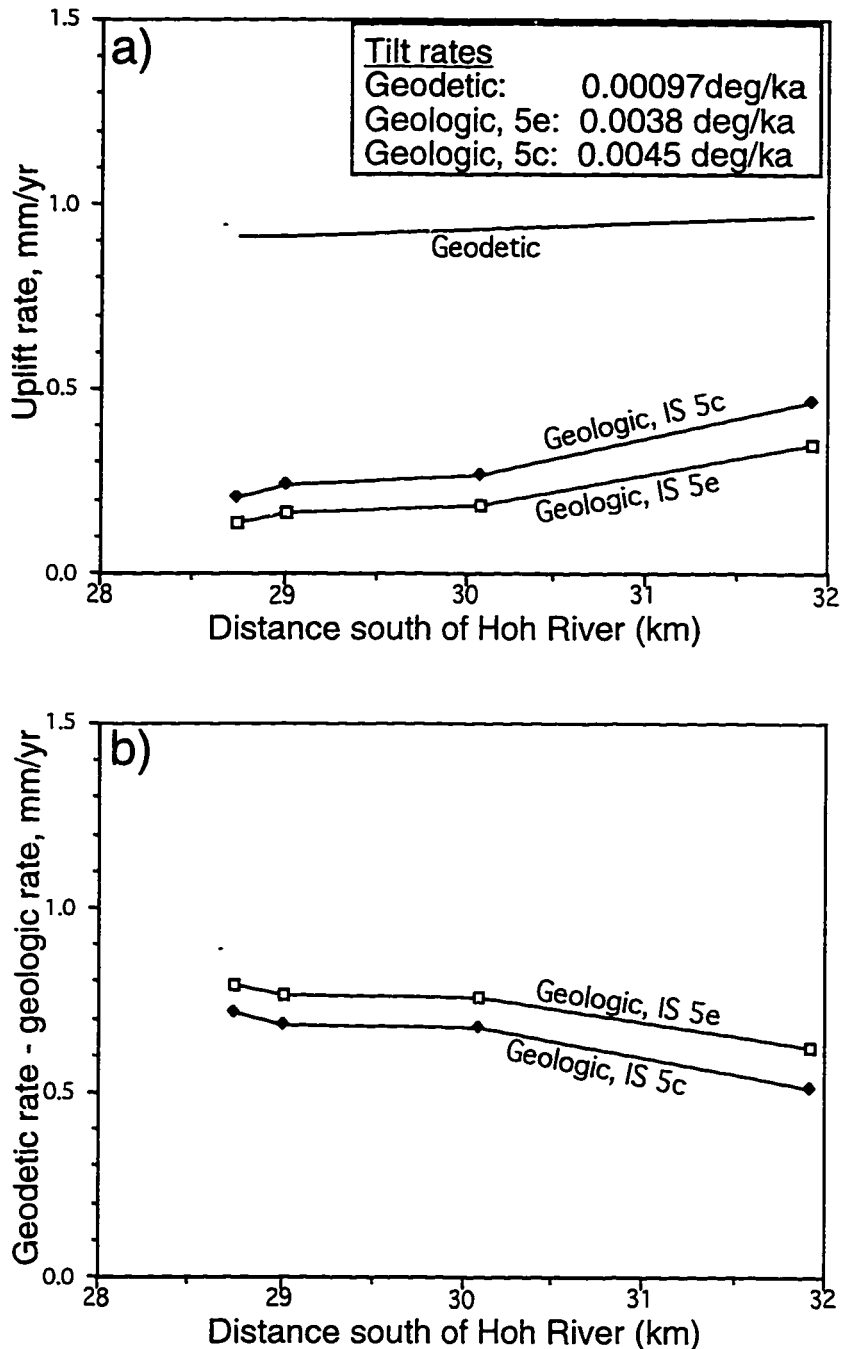


Figure 3.24: Uplift rate comparisons for south limb of the Kalaloch syncline. a) Comparison of geologic rates (this study) with geodetic rates from Savage (1991). IS 5e uplift rate calculations assume IS 5e sea level was 6 m higher than modern sea level. If IS 5e sea level equaled modern sea level (Shackleton, 1987), IS 5e uplift rates would be 0.048 mm/yr greater than rates shown. b) Difference between geodetic and geologic rates, equivalent to flexural component of geodetic rates. Note that horizontal scale is different than in Figure 3.23

DISCUSSION

The deformation rate comparisons indicate that the geodetic uplift measurements are dominated by a flexural component. According to the comparisons the coastal area is experiencing 0.6 to 0.9 mm/yr of transient, flexural uplift—short-term strain accumulation that should be recovered as coseismic subsidence in a megathrust earthquake. In a broader study covering much of the Oregon portion of the Cascadia margin, Kelsey et al. (1994) also found that geodetic uplift rates largely reflect short-term strain accumulation. Their measured geologic uplift rates range from 0.03 to 0.34 mm/yr, very similar to the range of Olympic geologic uplift rates described here. On portions of the Oregon Coast, however, the flexural component is much greater than on the Olympic Coast. Flexural uplift rates there are as high as 4.5 mm/yr, which is as much as an order of magnitude larger than the flexural component on the central Olympic Coast. The Olympic flexural rates are comparable to only one section of the Oregon coast. The ratio of geologic to geodetic uplift rates in Kelsey et al.'s (1994) study ranged from 0.01 to 0.08 (with one anomalous ratio of 4.9 in an area of late Quaternary faulting), compared with 0.12 to 0.33 on the north limb of the Kalaloch syncline. These ratio contrasts largely reflect the contrast in the flexural component, as geologic uplift rates are quite similar in the two areas. The comparison suggests that while the Olympic Coast is experiencing substantial flexural strain accumulation, the accumulation is much less than that along portions of the Oregon Coast. As noted, Kelsey et al. (1994) studied uplift rates over a much longer stretch of coast than has this study; therefore, the comparisons should be viewed with caution.

The described contrasts in coastal flexural uplift may reflect a broader locked zone between the North American and Juan de Fuca plates in the Olympic coast region. Hyndman and Wang (1995) used thermal models, fit to horizontal and vertical geodetic data, to estimate the widths of locked and transition zones on the plate boundary (the transition zone links the shallow, locked zone with the deeper, continuously sliding zone). They concluded that the locked and transition zones are wider across the Olympic Peninsula (85 and 75 km, respectively) than across other portions of the margin (35 to 60 km locked zone). The broader Olympic locked and transition zones are related to a gentler dip on the subducting plate and consequent higher heat flow. The broad locked zone resulting from the model reflects an inland zone of geodetically constrained uplift (Mitchell et al., 1994) that is greater than the coastal uplift (Figure 3.20).

Secular Uplift Rates

The 105,000- and 125,000-yr-averaged geologic uplift rates described above cannot have been maintained over much longer time periods. As noted, three samples of magnetically reversed sediment have been collected from the Steamboat Creek Formation. These samples suggest that parts of the Steamboat Creek Formation were deposited more than 780,000 yr BP (Baksi et al., 1992). If these sediments were deposited near sea level, they should now lie at least ca. 220 to 350 m above sea level if the calculated deformation rates had been maintained since their deposition. Their current position near sea level suggests that secular uplift is approximately zero, and that they have experienced subsidence, in addition to the current uplift, during more than 780,000 yr since their deposition. The inferred variability of uplift rates likely reflects the variable dynamics of accretionary wedge deformational processes.

POSSIBLE ORIGINS OF THE KALALOCH SYNCLINE

This study has focused on documenting the Kalaloch syncline and its deformation rates, rather than its origin. A few comments can be made regarding its origin, however. On a broad scale, this syncline and others on the Cascadia margin reflect accretionary wedge processes. Goldfinger et al. (1992) speculated that the northeast-trending synclines and associated strike-slip faults have resulted from block rotations caused by oblique convergence between the well-coupled Juan de Fuca and North American plates. They suggested that nonelastic deformation of the upper plate might act to absorb a portion of the force of plate convergence.

On a local scale, features associated with the Kalaloch syncline provide clues to its origin. As noted, Steamboat Creek Formation strata in the Whale Creek area are strongly deformed. Their deformation likely reflects the same processes that have gently deformed the wave-cut surface and younger sequence, but the deformation is discernible at outcrop scale because the older strata have been subjected to those processes over an extended time. Two structures can be discerned in the Whale Creek area. A gentle anticline deforms Steamboat Creek strata near Whale Creek. A more dramatic structure affects Steamboat Creek strata 0.8 km south of Whale Creek. Although intact intervening exposures are lacking, the strata there are interpreted (by superposition) to be older than those affected by the anticline. As noted (Figure 3.19), dips on glacial and nonglacial strata increase progressively southward from 18° to 90°

over the 80-m extent of the exposure. The older strata dip more steeply. The geometry of the structure suggests a fault-propagation fold at the tip of a thrust fault (e.g., Suppe, 1985), the upper portion of the fold having been beveled off during formation of the wave-cut surface. The progressively steeper dips suggest that the fault was active through the period in which the strata were deposited.

The inferred fault-propagation fold also appears to have deformed the wave-cut surface and younger sequence. The wave-cut surface exhibits its steepest slope between Whale Creek and the Raft River (Figure 3.16), rising from approximately 0 m to 31 m altitude over 4 km. Furthermore, the coastal terrace reaches an anomalously high altitude of 52 m in the area south of the fold structure. It thus appears that this structure has been active through the time represented by the stratigraphic sequence, and may still be active. Conceivably the inferred thrust fault and related forces are responsible for broader deformation expressed as the Kalaloch syncline.

Alternatively, the south limb of the Kalaloch syncline may be controlled by diapiric forces. Diapiric intrusions of melanged Hoh lithic assemblage bedrock have been described in the region (e.g. Rau, 1973, 1980). The diapiric activity creates melanges of sandstone and siltstone blocks in an intensely sheared clay and siltstone matrix. Melange of the Hoh lithic assemblage has been mapped in the area between the fold structure described above and the Raft River (Rau, 1975). The steeply dipping Steamboat Creek strata, the unusually steep wave-cut surface, and the elevated coastal terrace might all be controlled by an upward diapiric force. Such an interpretation, however, requires long-term diapiric activity, does not adequately explain the anticline in the Whale Creek area, and says little about the rest of the synclinal structure.

SUMMARY

This study has documented coastal sedimentation and deformation for a unique portion of the Cascadian margin. Details and complexities of the interglacial-glacial transition have been revealed, as have varying influences on sedimentation along the coastline. The Kalaloch syncline is similar to other structures documented along the Cascadia subduction zone, but its subaerial exposure and stratigraphic record permit discernment of the deformational processes involved.

The coastal stratigraphy and geomorphology between the Hoh and Raft rivers have resulted from an interplay of glacial-interglacial environmental changes and tectonic deformation. Glacial-interglacial cycles have produced alternating episodes of glacial-

fluvial inundation and marine transgression, which have alternately caused aggradation and erosion in the coastal zone. During glaciations, broad outwash fans were constructed at river mouths. Those fans are preserved as thick outwash units in coastal exposures. Away from river mouths, sedimentation was dominated by delivery of sediment from adjacent uplands. Evidence of at least four glaciations is preserved in the coastal sequence—two that occurred more than 780,000 yr BP, and two since the last interglaciation. A presumed IS 6 glaciation is recorded in the inland geomorphic sequence (Whale Creek drift, Chapter 2), but associated sediments are lacking in the coastal stratigraphic sequence.

Tectonic deformation has affected the entire coastal sequence. The wave-cut surface and younger sequence are gently deformed, while the Steamboat Creek Formation exhibits deformation discernible at outcrop scale. Deformation rate comparisons show that 20th century coastal uplift is dominated by flexure. Deformation of the Steamboat Creek Formation and younger strata in the Whale Creek area suggests that the Kalaloch syncline may be associated with an active, hidden thrust fault.

FUTURE RESEARCH

The most pressing needs for coastal research include improved chronologic control, collection of stratigraphic and structural data north of the present study area, and collection of new geodetic data throughout the area. The potential for radiocarbon dating of the coastal sequence described here has been largely exhausted. Much of the sequence is too old for radiocarbon dating or, at best, pushes the limits of the method. The portion of the sequence whose age is within the reasonable limits of the method has been sufficiently dated for the purposes of understanding the overall stratigraphic framework. Infrared-stimulated luminescence dating might yield better age constraint on parts of the younger sequence too old for radiocarbon dating, on the wave-cut surface and its cover sediments, and on the younger portions of the Steamboat Creek Formation. Finally, additional paleomagnetic analysis of Steamboat Creek Formation sediments from the Whale Creek and Hoh River areas may help to constrain their ages better within broad limits.

The coastal areas between the Hoh River and Cape Flattery deserve close study. Geodetic uplift rates are higher in those areas (Savage et al., 1991; Holdahl et al., 1987; Figure 3.20) than in the area described herein, and it remains to be shown whether geologic uplift rates spanning the last 125,000 years show similar relationships to the

geodetic rates. The coastline between the Hoh River and LaPush is, unfortunately, dominated by bedrock hills; thus, stratigraphic and geomorphic control on the age(s) of the wave-cut surface(s) will be less reliable than between the Hoh and Raft rivers. The glacial/interglacial sequence at LaPush should afford some chronologic control, however.

The reliability of the neotectonic conclusions of this study are tempered by the generalized nature and accuracy of the geodetic data on which they rely. New, global positioning system (GPS)-based geodetic data being collected in the area by Khazaradze et al. (1995; G. Khazaradze, personal communication, 1995) will fill some of this need. Where possible, geodetic data should be collected in areas of known structures, and along the coastline. New data between Browns Point and the Hoh River would help to reconcile geologic and geodetic uplift rates. Data collected on the coastline between the Queets and Raft rivers would help to assess the modern activity of structures on the south limb of the syncline. Finally, collection of geodetic data on Destruction Island would provide a third dimension to the coastal data.

CHAPTER 4
QUATERNARY STRATIGRAPHIC AND GEOMORPHIC EVOLUTION
OF THE WESTERN OLYMPIC PENINSULA

INTRODUCTION

The foregoing glacial geologic and coastal stratigraphic studies provide the basis for a synthesis of the area's Quaternary stratigraphic and geomorphic history. That history has been influenced by the advance and retreat of mountain glaciers, the rise and fall of sea level (coupled with the concomitant advance and retreat of the shoreline), and subduction zone deformation. The apparent relative contributions of those processes differ between coastal and river valley environments. Therefore, the two realms are considered separately in the ensuing discussion.

INTERACTION BETWEEN QUATERNARY GLACIAL CYCLES AND TECTONIC DEFORMATION

Glaciation and tectonic deformation are clearly intertwined in the large-scale geomorphic evolution of the Olympic Peninsula. Accretionary wedge deformation has uplifted the Olympic Mountains and provided glacier habitat, while unroofing by glacial erosion has likely enhanced accretionary wedge uplift (Brandon, 1994). In the lower western valleys and coastal zone, however, glacial deposition has exerted a much stronger influence on geomorphic and stratigraphic evolution than has Quaternary tectonic deformation. Furthermore, available evidence suggests that the two processes have not substantially influenced one another.

The apparent relative influences of glaciers, sea level, and tectonism on geomorphic and stratigraphic evolution vary between coastal and river-valley settings. River-valley evolution appears largely influenced by glacier fluctuations, with sea-level fluctuations having relatively minor effects. Quaternary tectonism has had little apparent effect there—the river mouths occupy the higher portions of the Kalaloch syncline (Chapter 3), and there is no evidence to suggest that the rivers are significantly influenced by the deformation. In the coastal zone, influences of tectonism, glacier fluctuations, and sea-level fluctuations can be discerned. Thus, apparent significant effects of tectonism and sea-level fluctuation are limited to the coastal zone. This perception may be colored in part by the nature of the observable records: extensive stratigraphic exposure in the coastal zone provides for ready examination of tectonic and

oceanic influences, whereas the extensive geomorphic record and spotty exposure of the river valleys favor recognition of glacial processes. The lack of cross-structure stratigraphy and geomorphology in the river valleys limits investigation of tectonic influences.

GEOMORPHIC AND STRATIGRAPHIC EVOLUTION OF THE RIVER VALLEYS THROUGH THE LAST INTERGLACIAL-GLACIAL CYCLE

Valley evolution can be best discerned for the last interglacial-glacial cycle, and that record likely applies to earlier interglacial-glacial cycles as well. The last cycle includes an IS 5e (or IS 5c) sea-level highstand (Chapter 3) and six discernible glacier advances and readvances into the lower valleys (Chapter 2). For purposes of this discussion, the Lyman Rapids glacier advance is assumed to have occurred during IS 4 or IS 3. Although an IS 5b age is conceivable (Chapter 2), stratigraphic evidence favors the former interpretation.

THE LAST INTERGLACIATION (IS 5)

The last interglaciation was a time of dominant shoreline retreat and valley excavation in the project area (Figure 4.1a). During IS 5e (or possibly 5c, see Chapter 3) the shoreline retreated inland past the location of the modern shoreline in most areas between the Hoh and Raft river mouths. The resulting paleoshoreline is preserved as diffuse scarps near the mouths of the Hoh, Queets and Raft river valleys, separating Whale Creek and Lyman Rapids/Hoh Oxbow outwash terraces (Plate 1). The paleoshoreline lies ca. 1.5 km or less inland. The wave-cut terrace (now buried) that lay seaward of the IS 5e shoreline stabilized, receiving only small amounts of sediment from adjacent uplands and older outwash terraces (Chapter 3). The shoreline remained seaward of the modern shoreline during later parts of the interglaciation (i.e., IS 5d through 5a).

The rivers eroded preexisting drift in wide swaths during IS 5d through 5a. In the Hoh valley, sediments and landforms of Whale Creek and Wolf Creek drift have been observed only at the outer edge of the valley mouth. Although small volumes of older sediment locally may underlie drift of the last glacial cycle, the river removed most of the older sediment prior to deposition of Lyman Rapids drift. In the Queets valley, the river similarly eroded a broad reach of the valley, but large areas of Whale Creek and Wolf Creek drift are preserved on the coastal plain.

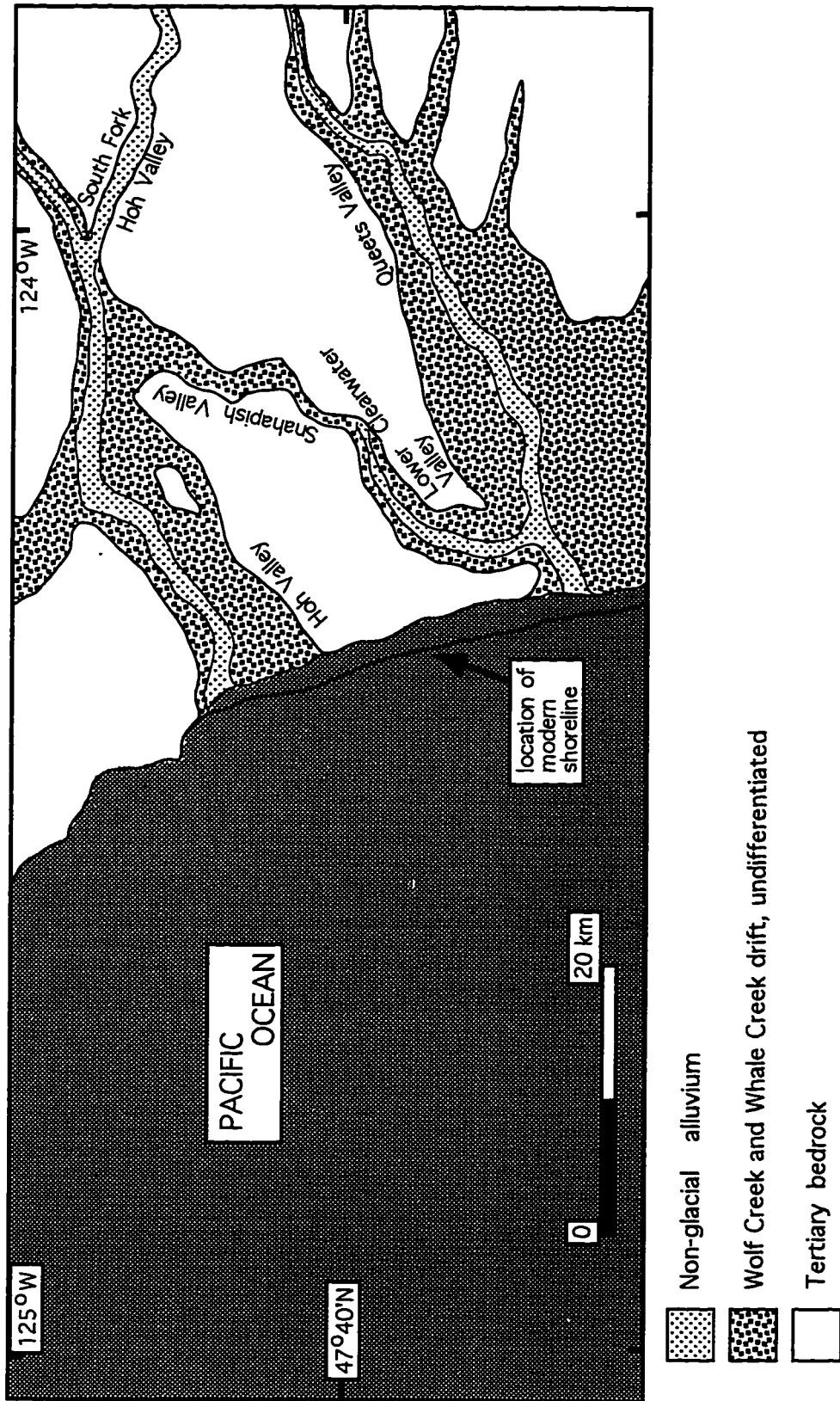


Figure 4. 1a: Schematic map of project area ca. 125,000 yr BP (IS 5e), showing inferred distribution of sediment types. Note that IS 5e shoreline is a short distance landward of the modern shoreline location.

Wide swaths of the lower valleys were apparently cleared of preexisting drift prior to the onset of the last glacial cycle (Figure 4.1b). The Lyman Rapids glaciation then began the process of valley filling. This view of valley evolution, in which all erosion is thought to have been fluvial, ignores possible glacial erosion during the last glacial cycle. While such subsequent glacial erosion cannot be discounted, the outwash-till sequences in the middle Hoh valley (Figure 2.4) clearly indicate that the downvalley portion of the glacier advanced over its own outwash during the Hoh Oxbow Ø, I, and/or II advances. Thus, the glacier was largely depositing sediment, not eroding it, in its downvalley ablation zones. The Queets valley stratigraphic sequence indicates similar processes during the Lyman Rapids I and Hoh Oxbow I advances.

THE LAST GLACIAL CYCLE (IS 4 THROUGH IS 2)

The previously excavated portions of the lower valleys were progressively filled with drift during successive advances of the last glacial cycle. The Hoh valley glacier advanced to the Lost Creek area during the Lyman Rapids glaciation (Figure 2.1, Plate 1), constructing a massive terminal moraine and filling the lower valley with outwash (Figure 4.2a). A second glacier lobe constructed a moraine south of a prominent bedrock outlier south of the Hoh Oxbow and built a fan that merged with the main valley train near Pins Creek. Upon crossing the IS 5e shoreline scarp, the meltwater streams were able to migrate laterally and construct a broad fan on the extensive plain exposed by lowered sea level. A third glacier lobe advanced to the current Hoh-Bogachiel divide, and its outwash likely influenced the stratigraphic and geomorphic evolution of the Bogachiel valley.

In the Queets valley, the glacier advanced to Lyman Rapids, constructing a broad moraine across that portion of the coastal plain (Figure 4.2a, Plate 1). Meltwater streams filled the previously excavated downvalley area with outwash, and constructed a broad fan (similar to that at the Hoh valley mouth) beyond the IS 5e shoreline scarp. Lyman Rapids basal till and advance outwash are exposed upvalley of the terminal moraine (Chapter 2). As in the case of later Hoh valley advances, it is clear from such deposits that the downvalley portion of the glacier advanced over its own outwash.

Moraine-dammed lakes filled both valleys following the Lyman Rapids glaciation (Figure 4.2b). Silt-dominated lacustrine sediment partially filled the areas upvalley from the moraines. In the Hoh valley, the lake persisted for nearly 30,000 yr

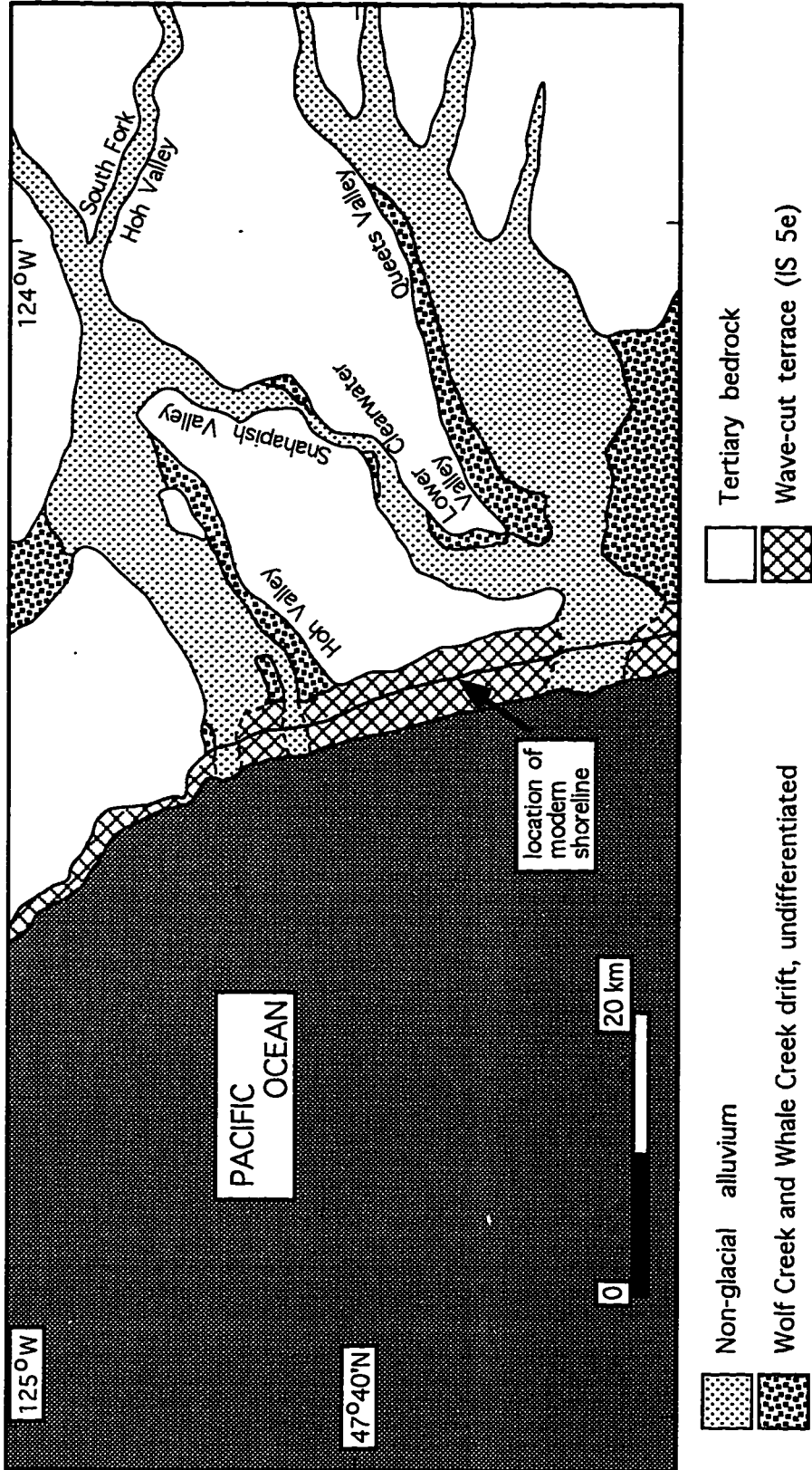


Figure 4.1b: Schematic map of project area prior to Lyman Rapids advance (ca. 80,000 yr BP; IS 5a), showing inferred distribution of sediment types and geomorphic features. Shoreline position inferred from IS 5a sea-level estimate of 5 m below modern (Muhs et al., 1992). Note IS 5e wave-cut terrace exposed by relatively low IS 5a sea level. If the Lyman Rapids glacier advance occurred during IS 5b (Chapter 2), this figure would represent conditions ca. 105,000 yr BP (IS 5c). Note broad portions of Hoh and Queets valleys in which preexisting drift was removed prior to the Lyman Rapids advance.

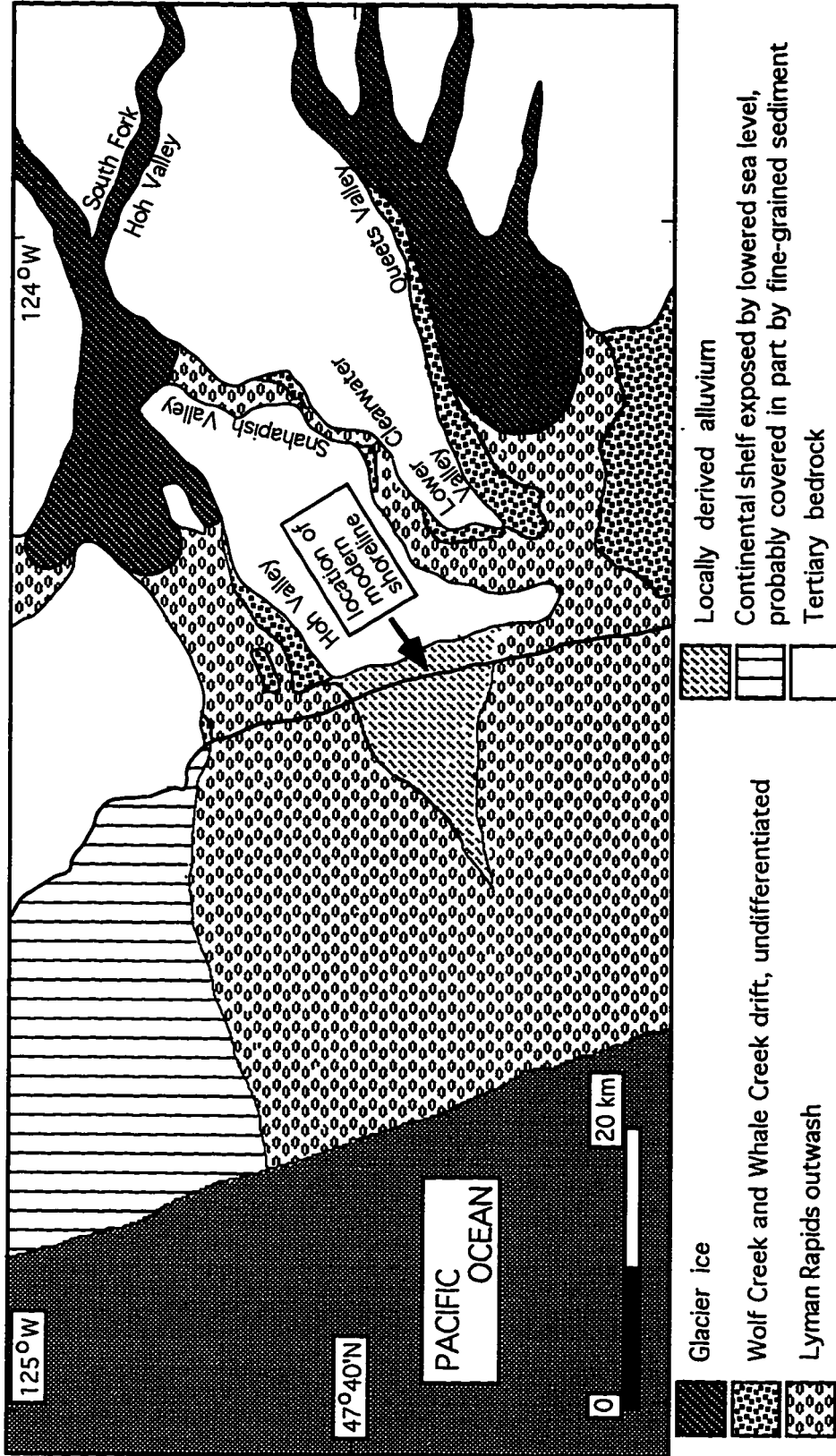


Figure 4.2a: Schematic map of project area at peak of Lyman Rapids advance, showing inferred distribution of glacier ice, sediment types, and geomorphic features. Shoreline position is inferred from IS 4 sea-level estimate of ca. 80 m below modern (Shackleton, 1987). Note broad area of continental shelf exposed by relatively low sea level. As discussed in Chapter 2, the Lyman Rapids advance may have occurred during early or middle Wisconsin time (> ca. 52,000 14C yr BP; IS 4 or IS 3) or late in the last interglaciation (i.e., IS 5b). If the advance occurred during IS 3 or IS 5b, sea level would have been higher than during IS 4 and the inferred shoreline consequently landward of that shown.

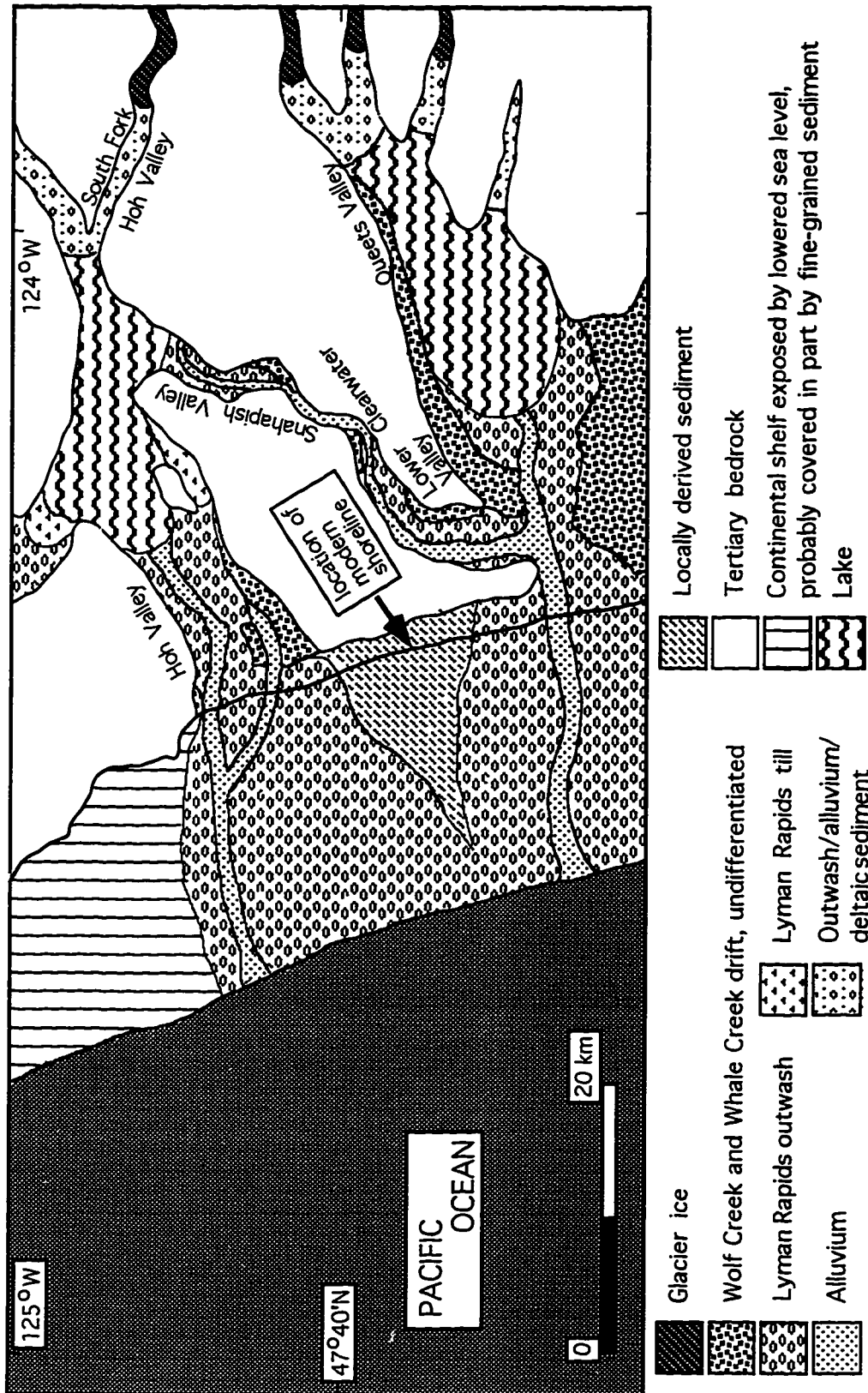


Figure 4.2b: Schematic map of project area ca. 40,000 yr BP (IS 3, pre-Hoh Oxbow \emptyset advance), showing inferred distribution of glacier ice, lakes, sediment types, and geomorphic features. Shoreline position inferred from IS 3 sea-level estimate of ca. 49 m below modern (Shackleton, 1987). Note broad area of continental shelf exposed by relatively low IS 3 sea level. Locations of glacier termini are speculative.

(ca. 65,000 to 39,000 ¹⁴C yr BP). The duration of the Queets valley lake cannot be specified with existing data.

The ca. 39,000 ¹⁴C yr BP Hoh Oxbow Ø advance continued the valley-filling process. This advance is documented only in the Hoh valley, but likely occurred in the Queets valley as well. The glacier advanced to an undetermined limit between Awful Creek and the Hoh Oxbow, depositing 10 to 20 m of advance outwash and 4 m of till, now exposed at Awful Creek and High Banks (Figure 2.4, sections 1 and 2). A valley train likely filled the lower Hoh valley, inset between Lyman Rapids landforms, but no evidence of it has been observed.

The ca. 29,000 to 26,000 ¹⁴C yr BP Hoh Oxbow I advance (Figure 4.2c) was the most extensive of middle and late Wisconsin time (IS 3 and 2) and played a major role in the stratigraphic and geomorphic evolution of the valleys. In the Hoh valley, the glacier overrode Hoh Oxbow Ø sediments and landforms, depositing a thick sedimentary sequence (Figure 2.4) and constructing extensive landforms. A prominent moraine was constructed in the Hoh Oxbow area (Plate 1). A second moraine lies to the south, behind a bedrock outlier. Meltwater streams filled the main valley with outwash, inset between Lyman Rapids landforms, and overtopped a low divide near Braden Creek similarly to fill the Cedar Creek valley. Outwash fans extended beyond the modern shoreline from the mouths of both valleys. In the Queets valley, the Hoh Oxbow I glacier advanced to the Sams River area (Plate 1), where it constructed a prominent, valley-damming moraine. A valley train filled the valley below, inset between Lyman Rapids landforms. The valley train is broad (3 to 5 km) upvalley from Lyman Rapids, but is only 1- to 2-km wide downvalley where bordered by Lyman Rapids I outwash terraces. A small fan likely extended beyond the modern shoreline.

The ca. 20,000 ¹⁴C yr BP Hoh Oxbow II advance had a relatively small impact on the geomorphic and stratigraphic evolution of the valleys. In the Hoh valley, the glacier constructed a moraine near Awful Creek (Plate 1) and a narrow valley train. The glacier appears to have reoccupied the till surface constructed during the Hoh Oxbow I advance, and meltwater discharged largely into a narrow valley entrenched into that surface. A Hoh Oxbow II advance is not documented in the Queets valley, although such an advance may have been largely responsible for construction of the broad lacustrine fan-delta surface upvalley from the Hoh Oxbow I moraine (Plate 1, Chapter 2).

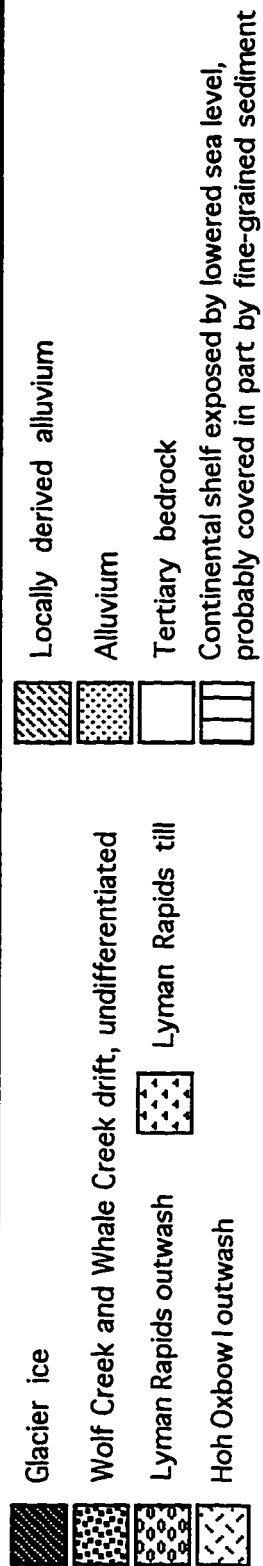
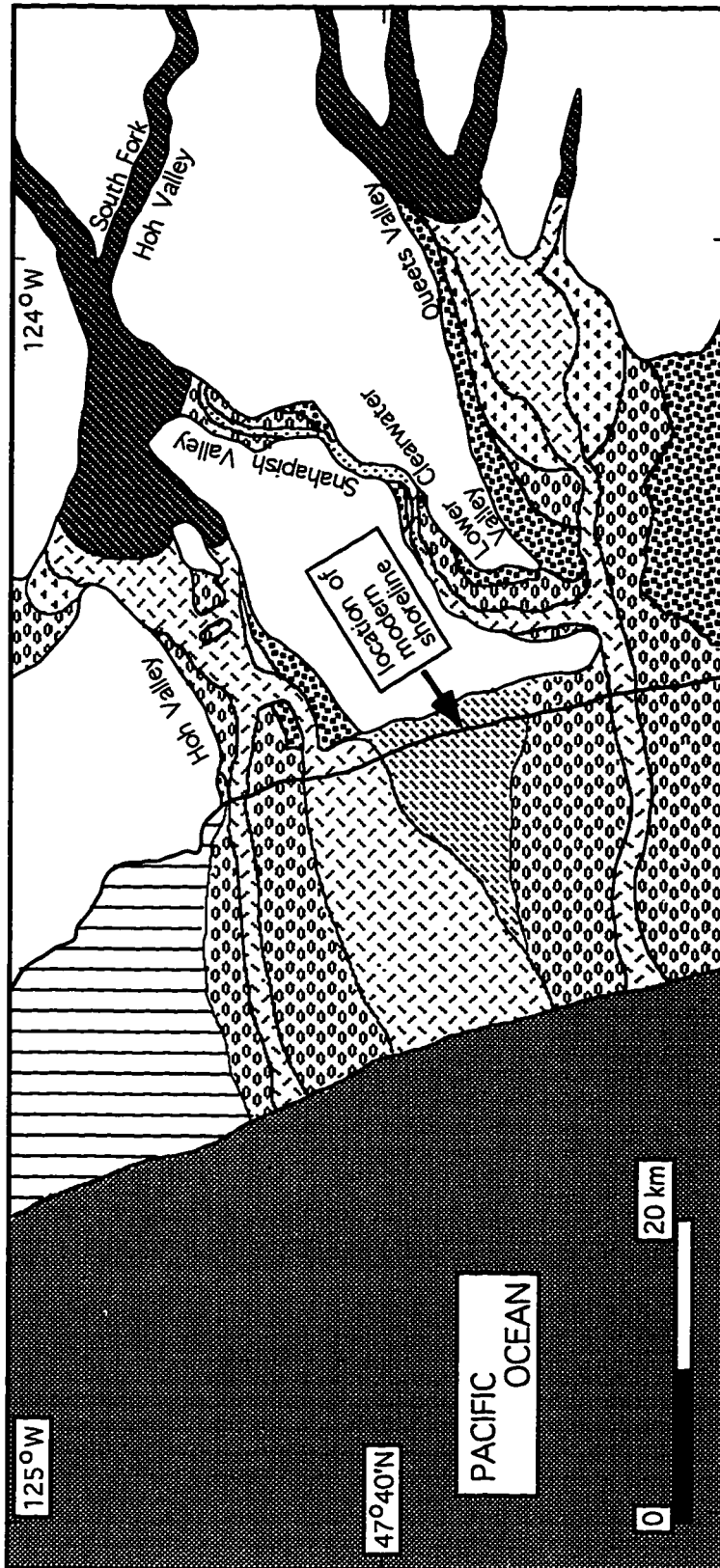


Figure 4.2c: Schematic map of project area ca. 27,000 yr BP (IS 3, Hoh Oxbow I advance), showing inferred distribution of glacier ice, sediment types, and geomorphic features. Shoreline position inferred from 27 ka sea-level estimate of ca. 49 m below modern (Shackleton, 1987). Note broad fan of Hoh Oxbow I outwash at the mouth of Cedar Creek valley near the Hoh valley mouth.

Two subsequent advances, represented by the Twin Creeks drift, completed the valley-filling process in the Hoh drainage. The ca. 18,270 ¹⁴C yr BP Twin Creeks I advance (Figure 4.2d; Plate 1) resulted in moraines in both the main Hoh and South Fork valleys. A valley train extended a short distance (3 km) down the main Hoh valley. A largely erosional surface, resulting from regrading of previously deposited outwash and till, extended to the coastline. The Twin Creeks II advance, documented only in the South Fork Hoh valley, also resulted in a moraine and narrow, largely erosional outwash terraces. Neither of the Twin Creeks advances is documented in the Queets valley, probably because the extensive post-Hoh Oxbow I lake precluded construction of glacial landforms.

Valley evolution has thus been characterized by interglacial excavation and glacial filling. Excavation likely was accomplished by meandering rivers at times of high sea level/transgressive shorelines and reduced sediment load. Valley filling was accomplished through a succession of generally less-extensive glacier advances that constructed moraines progressively farther upvalley and filled progressively narrower erosional trenches between older outwash terraces. Aggradation by braided streams occurred under conditions of high sediment load. The influence of low sea level on valley filling appears limited. The most extensive and thickest outwash aggraded during times of moderately low sea level [ca. 50 to 100 m below modern at 65,000 and 29,000 ¹⁴C yr BP (Shackleton, 1987)]. Conversely, the largely erosional character of the ca. 18,000 ¹⁴C yr BP Twin Creeks I outwash surface may be partly a result of the extreme low sea level of the last glacial maximum and more restricted extent of glaciers.

GEOMORPHIC AND STRATIGRAPHIC EVOLUTION OF THE COASTAL ZONE THROUGH THE LAST INTERGLACIAL-GLACIAL CYCLE

The coastal stratigraphic sequence preserves a particularly clear record of the last interglacial-glacial cycle (IS 5 through IS 2). As discussed in Chapter 3, contrasting records are preserved in two distinct sedimentologic realms. Near river mouths, deposition was largely episodic, resulting in prominent outwash units and discontinuous interglacial/interstadial units. The area between the two river mouths is isolated from outwash deposition, and a more continuous record of local sedimentation is preserved (Figures 4.2a-d).

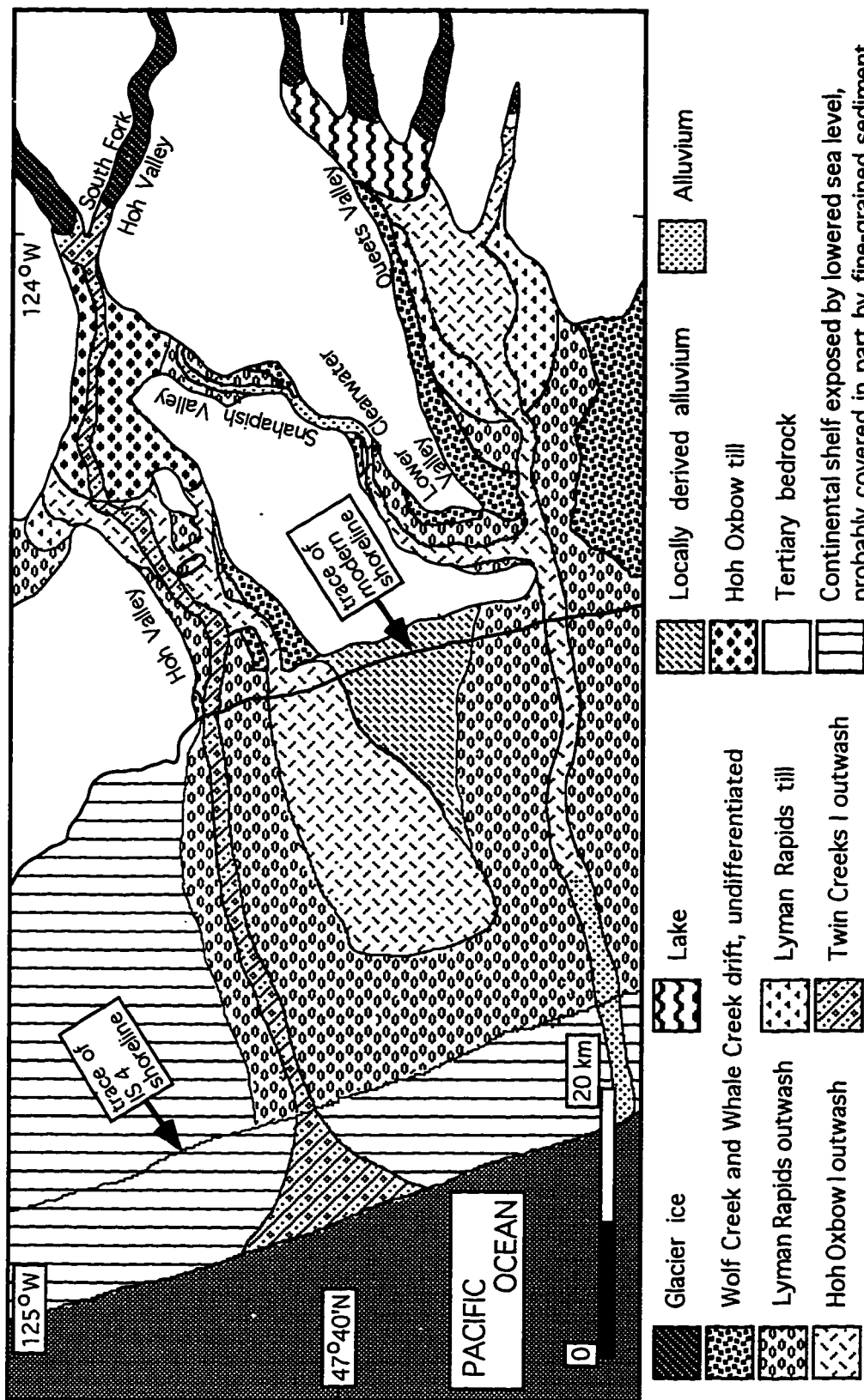


Figure 4.2d: Schematic map of project area ca. 18,000 yr BP (IS 2, Twin Creeks I advance), showing inferred distribution of glacier ice, lakes, sediment types, and geomorphic features. Shoreline position inferred from 18 ka sea-level estimate of ca. 120 m below modern (Shackleton, 1987). Note narrow area of Hoh valley filled with Twin Creeks I outwash, as well as the lake occupying the upper Queets valley. Twin Creeks outwash has not been identified in the lower Queets valley.

THE LAST INTERGLACIATION (IS 5)

The IS 5e (or 5c) sea-level highstand cut a prominent shoreline into Whale Creek drift, ca. 1.5 km inland from the modern shoreline (Figure 4.1a, Plate 1). The IS 5e shoreline separated Whale Creek outwash terraces and older landforms from the wave-cut surface (now buried) subsequently exposed by falling sea level. That surface, an associated boulder-cobble lag, and several meters of sand and gravel beach sediment form the base of the coastal stratigraphic sequence.

The coastal terrace exposed by falling sea level was apparently maintained through the remainder of the last interglaciation (Figure 4.1b). Low sea level (relative to the IS 5e highstand), and slow uplift on the limbs of the Kalaloch syncline probably precluded reoccupation by marine water during the IS 5c and 5a highstands. Low-gradient streams deposited fine sediment from adjacent uplands, and peat accumulated, and thin soils formed (Figure 3.7, Plate 2). An indeterminate amount of shoreline recession may have occurred during those highstands.

THE LAST GLACIAL CYCLE (IS 4 THROUGH IS 2)

During the Lyman Rapids glaciation, broad outwash fans were built at the mouths of both river valleys (Figure 4.2a). Narrow (1.5 km) strips of those outwash fans are preserved as coastal terraces between the modern and IS 5e shorelines (Plate 1), and the outwash gravel dominates the coastal stratigraphic sequence near the river mouths (Plate 2). Migration of meltwater streams southward from the Hoh valley mouth and northward from the Queets valley mouth may have been enhanced by the sloping limbs of the Kalaloch syncline. Between Kalaloch and Beach Trail 5, little outwash was deposited. Instead, sedimentation was dominated by deposition of fine sediment by low-gradient streams originating in adjacent uplands (Browns Point Formation, Chapter 3).

Little sediment accumulated on coastal outwash terraces between the Lyman Rapids and Hoh Oxbow I glaciations. Coastal outwash deposition during the Hoh Oxbow Ø glaciation was probably limited to the entrenched river valleys and now-submerged portions of the continental shelf. Less than 1 m of sediment accumulated in the Destruction Island Viewpoint area (Figure 3.7), and about 6 m accumulated in an abandoned channel near the modern mouth of Whale Creek (Figure 3.14). Between Kalaloch and Beach Trail 5, slow deposition of locally derived sediment and peat continued (ca. 4 m total). Continued tectonic deformation raised the limbs of the

Kalaloch syncline, which likely led to further entrenchment of the Hoh and Queets river mouths and further isolated the Kalaloch-Beach Trail 5 area from subsequent outwash deposition.

During the Hoh Oxbow I glaciation (ca. 27,000 ^{14}C yr BP; Figure 4.2c), most outwash deposition was again limited to the entrenched river valleys and the then-exposed continental shelf. Small terraces and thin outwash units are preserved at the mouths of both rivers. However, an outwash fan was also constructed at the mouth of Cedar Creek, and Hoh Oxbow I outwash was deposited atop the Lyman Rapids outwash terrace south of there. That outwash reached the Beach Trail 4 area, but the Kalaloch-Beach Trail 5 zone was still dominated by slow deposition of locally derived sediment.

Coastal outwash deposition during subsequent glacier advances (Hoh Oxbow II, Twin Creeks I and II) was also limited to valley mouths. This limited deposition is chiefly a result of less-extensive glacier advances (and consequent greater river distance to the coastline), but may have been influenced by tectonically enhanced river-mouth entrenchment. Slow sedimentation continued during this time in the Kalaloch-Beach Trail 5 area; the sequence-capping loess was apparently deposited after 15,200 ^{14}C yr BP.

The coastal geomorphic and stratigraphic evolution thus reflected an interplay of glacial deposition, sea-level fluctuation, and tectonic deformation. Tectonic deformation appears to have had relatively minor influences on sedimentation, but has strongly influenced the modern exposure of the stratigraphic sequence and the morphology of the coastal terrace.

THE HOLOCENE AND THE FUTURE

Since the end of the last glaciation, stratigraphic and geomorphic evolution have been dominated by valley excavation, shoreline retreat, and slow coastal tectonic deformation. In the Hoh valley, approximately a third of the valley width occupied by landforms of the last glaciation has been excavated, leaving a 1- to 1.5-m wide inner valley. The inner Queets valley has been eroded to a similar degree. Low fluvial terraces, presumed by Fonda (1974) to have originated during Little Ice Age glacier advances, occupy large areas of the inner valleys. Shoreline retreat, resulting from rising sea level, has advanced to within 1.5 km of the IS 5e shoreline, and tectonic

deformation has increased stratigraphic and geomorphic dips on the limbs of the Kalaloch syncline.

These processes continue, and will likely persist through the rest of the current interglaciation. Tectonic deformation will continue to enhance the Kalaloch syncline through future seismic cycles. Lateral fluvial erosion will continue to widen the valleys and prepare them for the next major glacier advance. Coastal erosion will continue, and shoreline retreat may reach to or behind the IS 5e paleoshoreline. Thus, the processes are cyclic, and their extant stratigraphic and geomorphic expression is largely a function of the time of observation within the cycles.

LIST OF REFERENCES

- Adams, J., 1990, Paleoseismicity of the Cascadia subduction zone: evidence from turbidites off the Oregon-Washington margin: *Tectonics*, v. 9, p. 569-583.
- Ando, M., and Balasz, F.I., 1979, Geodetic evidence for aseismic subduction of the Juan de Fuca plate: *Journal of Geophysical Research*, v. 84, p. 3023-3028.
- Arnold, R., 1906, Geological reconnaissance of the coast of the Olympic Peninsula, Washington: *Geological Society of America Bulletin*, v. 17, p. 451-468.
- Atwater, B.F., 1987, Evidence for great Holocene earthquakes along the outer coast of Washington State: *Science*, v. 236, p. 942-944.
- Atwater, B.F., 1992, Geologic evidence for earthquakes during the past 2000 years along the Copalis River, southern coastal Washington: *Journal of Geophysical Research*, v. 97, p. 1901-1919.
- Baksi, A.K., Hsu, V., McWilliams, M.O., and Farrar, E., 1992, $(40)\text{Ar}/(39)\text{Ar}$ dating of the Brunhes-Matuyama geomagnetic field reversal: *Science*, v. 256, p. 356-357.
- Baldwin, E.M., 1939, Late-Cenozoic diastrophism along the Olympic Coast [M.S. Thesis]: State College of Washington, 47 p.
- Barnosky, C.W., 1984, Late Pleistocene and early Holocene environmental history of southwestern Washington State, U.S.A.: *Canadian Journal of Earth Sciences*, v. 31, p. 619-629.
- Bierman, P.R., and Gillespie, A.R., 1994, Evidence suggesting that methods of rock-varnish cation-ratio dating are neither comparable nor consistently reliable: *Quaternary Research*, v. 41, p. 82-90.
- Bigelow, P.K., 1987, The petrology, stratigraphy, and basin history of the Montesano Formation, south-western Washinton and southern Olympic Peninsula [M. S. Thesis]: Western Washington University, 263 p.
- Bloom, A.L., Broecker, W.W., Chappell, J.M.A., Matthews, R.K., and Mesolella, K.J., 1974, Quaternary sea level fluctuations on a tectonic coast: *Quaternary Research*, v. 4, p. 185-205.
- Bond, G., Heinrich, H., Broecker, W., Labeyrie, L., McManus, J., Andrews, J., Huon, S., Jantschik, R., Clasen, S., Simet, C., Tedesco, K., Klas, M., Bonani, G., and Ivy, S., 1992, Evidence for massive discharges of icebergs into the North Atlantic ocean during the last glacial period: *Nature*, v. 360, p. 245-249.
- Bond, G., Broecker, W., Sigfus, J., McManus, J., Labeyrie, L., Jouzel, J., and Bonani, G., 1993, Correlations between climate records from North Atlantic sediments and Greenland ice: *Nature*, v. 365, p. 143-147.

- Booth, D.B., 1987, Deglaciation along the southern margin of the Cordilleran Ice Sheet, *in* W. F. Ruddiman and H. E. Wright, J., eds., *North America and Adjacent Oceans during the Last Deglaciation*: Geological Society of America, p. 71-90.
- Boyer, S.E., and Lingley, W.S., 1991, Structure and kinematics of the Olympic subduction complex, NW Washington, and implications for mechanical models of accretionary prisms: [abstract]: Geological Society of America, *Abstracts with Programs*, v. 23, no. 6, p. 428.
- Bradley, W.C., and Griggs, G.B., 1976, Form, genesis, and deformation of central California wavecut platforms: *Geological Society of America Bulletin*, v. 87, p. 433-449.
- Brandon, M.T., and Calderwood, A.R., 1990, High-pressure metamorphism and uplift of the Olympic subduction complex: *Geology*, v. 18, p. 1252-1255.
- Brandon, M.T., and Vance, J.A., 1992, Tectonic evolution of the Cenozoic Olympic subduction complex, Washington State, as deduced from fission track ages for detrital zircons: *American Journal of Science*, v. 292, p. 565-636.
- Brandon, M.T., 1994, Accretion, deformation, and exhumation at sediment-rich subduction zones of the northeast Pacific Basin (abstract): *Geological Society of America Abstracts with Programs*, v. 26, no. 7, p. 29.
- Carson, R.J., 1970, Quaternary geology of the south-central Olympic Peninsula, Washington [Ph.D. Dissertation]: University of Washington, 67 p.
- Clague, J.J., Armstrong, J.E., and Mathews, W.H., 1980, Advance of the late Wisconsin Cordilleran ice sheet in southern British Columbia since 22,000 yr b.p.: *Quaternary Research*, v. 13, p. 322-326.
- Clark, D.H., Clark, M.M., and Gillespie, A.R., 1994, Debris-covered glaciers in the Sierra Nevada, California, and their implications for snowline reconstructions: *Quaternary Research*, v. 41, p. 139-153.
- Colman, S.M., and Pierce, K.L., 1983, Correlation of Quaternary glacial sequences in the western United States based on weathering rinds and related studies, *in* Mahaney, W.C., ed., *Correlation of Quaternary Chronologies*: *Geobooks*, p. 437-453.
- Colman, S.M., and Pierce, K.L., 1986, Glacial sequence near McCall, Idaho: weathering rinds, soil development, morphology, and other relative age criteria: *Quaternary Research*, v. 25, p. 25-42.
- Cong, S., and Ashworth, A.C., 1996, in press, Palaeoenvironmental interpretation of middle and late Wisconsinan fossil coleopteran assemblages from western Olympic Peninsula, Washington: *Journal of Quaternary Science*.

- Crosson, R.S., and Owens, T.J., 1987, Slab geometry of the Cascadia subduction zone beneath Washington from earthquake hypocenters and teleseismic converted waves: *Geophysical Research Letters*, v. 14, p. 824-827.
- Dariento, M.E., and Peterson, C.D., 1990, Episodic tectonic subsidence of late Holocene salt marshes, northern Oregon coast, central Cascadia margin, U.S.A.: *Tectonics*, v. 9, p. 1-22.
- Dariento, M.E., 1991, Late Holocene paleoseismicity along the northern Oregon coast [Ph.D. dissertation]: Portland State University, 148 p.
- Dodge, R.E., Fairbanks, R.G., Benninger, L.K., and Maurrasse, F., 1983, Pleistocene sea levels from raised coral reefs of Haiti: *Science*, v. 219, p. 1423-1425.
- Dorn, R.I., Turrin, B.D., Jull, A.J.T., Linick, T.W., and Donahue, D.J., 1987, Radiocarbon and cation-ratio ages for rock varnish on Tioga and Tahoe morainal boulders of Pine Creek, eastern Sierra Nevada, California, and their paleoclimatic implications: *Quaternary Research*, v. 28, p. 38-49.
- Easterbrook, D.J., 1986, Stratigraphy and chronology of Quaternary deposits of the Puget lowland and Olympic Mountains of Washington and the Cascade Mountains of Washington and Oregon, *in* Sibrava, V., Bowen, D.Q., and Richmond, G.M., eds., *Quaternary glaciations in the northern hemisphere: Quaternary Science Reviews*, p. 145-159.
- Florer, L.E., 1972, Quaternary paleoecology and stratigraphy of the sea cliffs, western Olympic Peninsula, Washington: *Quaternary Research*, v. 2, p. 202-216.
- Forman, S.L., and Ennis, G., 1992, Limitations of thermoluminescence to date waterlain sediments from glaciated fiord environments of western Spitsbergen, Svalbard: *Quaternary Science Reviews*, v. 11, p. 61-70.
- Gillespie, A., and Molnar, P., 1995, Asynchronous maximum advances of mountain and continental glaciers: *Reviews of Geophysics*, v. 33, p. 311-364.
- Goldfinger, C., Kulm, L.D., Yeats, R.S., Applegate, B., Mackay, M.E., and Moore, G.F., 1992, Transverse structural trends along the Oregon convergent margin--implications for Cascadia earthquake potential and crustal rotations: *Geology*, v. 20, p. 141-144.
- Grousset, F.E., Labeyrie, L., Sinko, J.A., Cremer, M., Bond, G., Duprat, J., Cortijo, E., and Huon, S., 1993, Patterns of ice-rafted detritus in the glacial North Atlantic: *Paleoceanography*, v. 8, p. 175-182.
- Gosse, J.C., Klein, J., Evenson, E.B., Lawn, B.R., Middleton, R., 1995, Beryllium-10 dating of the duration and retreat of the last Pinedale glacial sequence: *Science*, v. 268, p. 1329-1333.
- Haase, P.C., 1987, Glacial stratigraphy and landscape evolution of the north-central Puget Lowland, Washington [M. S. Thesis]: University of Washington, 73 p.

- Halstead, E.C., 1968, The Cowichan ice tongue, Vancouver Island: *Canadian Journal of Earth Sciences*, v. 5, p. 1409-1415.
- Heaton, T.H., and Kanamori, H., 1984, Seismic potential associated with subduction in the northwestern United States: *Bulletin of the Seismological Society of America*, v. 74, p. 933-941.
- Heine, J.T., 1996, Late-glacial climate change on Mt. Rainier volcano, Washington (abstract): *American Quaternary Association Abstracts*, p. 82.
- Heinrich, H., 1988, Origin and consequences of cyclic ice rafting in the northeast Atlantic Ocean during the past 130,000 years: *Quaternary Research*, v. 29, p. 142-152.
- Heusser, C.J., 1964, Palynology of four bog sections from the western Olympic Peninsula, Washington: *Ecology*, v. 45, p. 23-40.
- Heusser, C.J., 1972, Palynology and phytogeographical significance of a late Pleistocene refugium near Kalaloch, Washington: *Quaternary Research*, v. 2, p. 189-201.
- Heusser, C.J., 1973, Environmental sequence following the Fraser advance of the Juan de Fuca lobe, Washington: *Quaternary Research*, v. 3, p. 284-306.
- Heusser, C.J., 1974, Quaternary vegetation, climate, and glaciation of the Hoh River Valley, Washington: *Geological Society of American Bulletin*, v. 85, p. 1547-1560.
- Heusser, C.J., 1978, Palynology of Quaternary deposits of the lower Bogachiel River area, Olympic Peninsula, Washington: *Canadian Journal of Earth Sciences*, v. 15, p. 1568-1578.
- Heusser, C.J., Heusser, L.E., and Streeter, S.S., 1980, Quaternary temperatures and precipitation for the north-west coast of North America: *Nature*, v. 286, p. 702-704.
- Hicock, S.R., Hebda, R.J., and Armstrong, J.E., 1982, Lag of the Fraser glacial maximum in the Pacific Northwest: pollen and macrofossil evidence from western Fraser Lowland, British Columbia: *Canadian Journal of Earth Sciences*, v. 19, p. 288-296.
- Holdahl, S.R., Martin, D.M., and Stoney, W.M., 1987, Methods for combination of water level and leveling measurements to determine vertical crustal motions, *in* *Proceedings of Symposium on Height Determination and Recent Crustal Movement in Western Europe*: Dumler Verlag, Bonn, p. 373-388.
- Holdahl, S.R., Faucher, F., and Dragert, H., 1989, Contemporary vertical crustal motion in the Pacific northwest, *in* Cohen, S.C. and Vanicek, P., eds., *Slow deformation and transmission of stress in the earth*: Geophysical Monograph 40: American Geophysical Union, p. 17-29.

- Hyndman, R.D., and Wang, K., 1993, Thermal constraints on the zone of major thrust earthquake failure: the Cascadia subduction zone: *Journal of Geophysical Research*, v. 98, p. 2039-2060.
- Hyndman, R.D., and Wang, K., 1995, The rupture zone of Cascadia great earthquakes from current deformation and the thermal regime: *Journal of Geophysical Research*, v. 100, p. 22133-22154.
- Imbrie, J., Hays, J.D., Martinson, D.G., McIntyre, A., Mix, A.C., Morley, J.J., Pisias, N.G., Prell, W.L., and Shackleton, N.J., 1984, The orbital theory of Pleistocene climate: Support from a revised chronology of the marine ^{18}O record, *in* Berger, A.L. et al., eds., *Milankovitch and Climate, Part 1*: p. 269-305.
- Kaufman, D.S., Forman, S.L., Lea, P.D., and Wobus, C.W., 1996, Age of pre-late-Wisconsin glacial-estuarine sedimentation, Bristol Bay, Alaska: *Quaternary Research*, v. 45, p. 59-72.
- Kelsey, H.M., Engebretson, D.C., Mitchell, C.E., and Ticknor, R.L., 1994, Topographic form of the Coast Ranges of the Cascadia Margin in relation to coastal uplift rates and plate subduction: *Journal of Geophysical Research*, v. 99, p. 12245-12255.
- Kelsey, H.M., Ticknor, R.L., Bockheim, J.G., and Mitchell, C.E., 1996, Quaternary upper plate deformation in coastal Oregon: *Geological Society of America Bulletin*, v. 108, p. 843-860.
- Kennedy, G.L., Lajoie, K.R., and Wehmiller, J.F., 1982, Amino-stratigraphy and faunal correlations of late Quaternary marine terraces, Pacific coast, U.S.A.: *Nature*, v. 299, p. 545-547.
- Khazaradze, G., Qamar, A., and Dragert, H., 1995, Permanent GPS network in Washington (abstract): *EOS*, v. 76, no. 46, p. 150.
- Kulm, L.D., Goldfinger, C., and Yeats, R.S., 1993, Oblique convergence and active strike slip faults of the Cascadia subduction zone, Washington margin (abstract): *EOS*, v. 74, p. 200.
- Kvenvolden, D.A., Blunt, D.J., and Clifton, H.E., 1979, Amino-acid racemization in Quaternary shell deposits at Willapa Bay, Washington: *Geochimica et Cosmochimica Acta*, v. 43, p. 1505-1520.
- LaChapelle, E.R., 1960, *The Blue Glacier Project, 1959 and 1960*: Seattle, Washington, University of Washington, Department of Meteorology and Climatology, 54 p.

- LaChapelle, E.R., 1963, Recent variations in the regime of glaciers in western Washington, *in* Meier, M.F., ed., The glaciers of Mount Rainier; International Union of Geodesy and Geophysics Glacier Study Tour, September 2-5, 1963: Unpublished guidebook, on file at U.S. Geological Survey Project Office - Glaciology, p. 3-5.
- Mackin, J.H., 1941, Glacial geology of the Snoqualmie-Cedar area, Washington: *Journal of Geology*, v. 49, p. 449-481.
- Martinson, D.G., Pisias, N.G., Hays, J.D., Imbrie, J., Moore, T.C., and Shackleton, N.J., 1987, Age dating and the orbital theory of the ice ages: development of a high-resolution 0 to 300,000-year chronostratigraphy: *Quaternary Research*, v. 27, p. 1-29.
- McCrary, P.A., 1992, Quaternary deformation along the Washington margin of the Cascadia subduction zone: evidence from the Raft River area (abstract): *Geological Society of America Abstracts with Programs*, v. 24, no. 5, p. 69.
- McCrary, P.A., 1994a, Quaternary crustal shortening along the central Cascadia subduction margin, Washington (abstract): *Geological Society of America Abstracts with Programs*, v. 26, no.7, p. 523.
- McCrary, P.A., 1994b, Late Quaternary Thrust Faulting Along the Cascadia Margin, Washington: Implications for Partitioning of Strain (abstract): *EOS*, v. 75, no.44, p. 622.
- McInelly, G.W., and Kelsey, H.M., 1990, Late Quaternary tectonic deformation in the Cape Arago-Bandon region of coastal Oregon as deduced from wave-cut platforms: *Journal of Geophysical Research*, v. 95, p. 6699-6713.
- McNeill, L., Goldfinger, C., Kulm, L., and Yeats, R., 1994a, Deformation of Quaternary marine terraces in the Siletz Bay region of Oregon (abstract): *Proceedings of the Oregon Academy of Sciences*, v. 30, p. 38.
- McNeill, L., Goldfinger, C., Kulm, L., and Yeats, R., 1994b, Tectonics of the Washington continental margin, Cascadia subduction zone (abstract): *Geological Society of America Abstracts with Programs*, v. 26, no.7, p. 523.
- McNeill, L., Piper, K.A., Goldfinger, C., and Kulm, L., 1995, Detachment faulting on the Cascadia continental shelf: active extension in a compressional regime? (abstract): *EOS*, v. 76, no. 46, p. 534.
- Mesolella, K.J., Matthews, R.K., Broecker, W.S., and Thurber, D.L., 1969, The astronomical theory of climatic change: Barbados data: *Journal of Geology*, v. 77, p. 250-274.
- Mitchell, C.E., Vincent, P., Weldon, R.J., and Richards, M., 1994, Present-day vertical deformation of the Cascadia margin, Pacific Northwest, U.S.A.: *Journal of Geophysical Research*, v. 99, p. 12257-12278.

- Moore, J.L., 1965, Surficial geology of southwestern Olympic Peninsula [M.S. Thesis]: University of Washington, 63 p.
- Muhs, D.R., Rockwell, T.K., and Kennedy, G.L., 1992, Late Quaternary uplift rates of marine terraces on the Pacific coast of North America, southern Oregon to Baja California Sur: *Quaternary International*, v. 15/16, p. 121-133.
- Nelson, A.R., 1992, Holocene tidal-marsh stratigraphy in south-central Oregon-- Evidence for localized sudden submergence in the Cascadia subduction zone: *Society for Sedimentary Geology (SEPM) Special Publication 48*, p. 287-301.
- Pazzaglia, F.J., and Brandon, M.T., in review, Tectonic implications of fluvial terraces along the Clearwater River, Olympic Mountains, Washington: submitted to *Tectonics*.
- Phillips, F. M., Zreda, M. G., Elmore, D., Sharma, P., 1993, Evidence for a connection between dynamic behavior of the Laurentide ice sheet and mountain glaciation in western North America: *EOS*, v. 74, p.360.
- Porter, S.C., 1975, Equilibrium-line altitudes of late Quaternary glaciers in the Southern Alps, New Zealand: *Quaternary Research*, v. 5, p. 27-47.
- Porter, S.C., 1976, Pleistocene glaciation in the southern part of the North Cascade Range, Washington: *Geological Society of America Bulletin*, v. 87, p. 61-75.
- Porter, S.C., 1977, Present and past glaciation threshold in the Cascade Range, Washington, U. S. A. : topographic and climatic controls, and paleoclimatic implications: *Journal of Glaciology*, v. 18, p. 101-116.
- Porter, S.C., Pierce, K.L., and Hamilton, T.D., 1983, Late Pleistocene mountain glaciation in western United States, *in* Porter, S.C., ed., *Late Quaternary environments of the United States*: University of Minnesota Press, p. 71-111.
- Rau, W.W., 1973, Geology of the Washington coast between Point Grenville and the Hoh River: Washington Department of Natural Resources, Division of Geology and Earth Resources, Bulletin 66, 58 p.
- Rau, W.W., 1975, Geologic map of the Destruction Island and Taholah quadrangles, Washington: Washington Department of Natural Resources, Geology and Earth Resources Division Map GM-13, 1:62,500.
- Rau, W.W., 1980, Washington coastal geology between the Hoh and Quillayute Rivers: Washington Department of Natural Resources, Division of Geology and Earth Resources, Bulletin 72, 58 p.
- Riddihough, R.P., 1984, Recent plate movements of the Juan de Fuca plate system: *Journal of Geophysical Research*, v. 89, p. 6980-6994.
- Savage, J.C., Lisowski, M., and Prescott, W.H., 1991, Strain accumulation in western Washington: *Journal of Geophysical Research*, v. 96, p. 14493-14507.

- Shackleton, N.J., 1987, Oxygen isotopes, ice volume and sea level: Quaternary Science Reviews, v. 6, p. 183-1990.
- Spicer, R.C., 1986, Glaciers in the Olympic Mountains, Washington [M. S. Thesis]: University of Washington, 157 p.
- Suppe, J., 1985, Principles of structural geology: Englewood Cliffs, NJ, Prentice-Hall, Inc., 537 p.
- Swanson, T.W., 1994, Application of ^{36}Cl dating based on the deglaciation history of the Cordilleran ice sheet in Washington and British Columbia (abstract): Geological Society of America Abstracts with Programs, v. 26, no. 7, p. 512.
- Tabor, R.W. and Cady, W.M., 1978a, The structure of the Olympic Mountains, Washington - analysis of a subduction zone: U. S. Geological Survey Professional Paper 1033, 38 p.
- Tabor, R.W., and Cady, W.M., 1978b, Geologic Map of the Olympic Peninsula: U.S. Geological Survey Map I-994, 1:125,000.
- Thackray, G.D., and Pazzaglia, F.J., 1994, Quaternary stratigraphy, tectonic geomorphology, and fluvial evolution of the Western Olympic Peninsula, Washington, *in* Swanson, D.A. and Haugerud, R.A., eds., Geologic field trips in the Pacific Northwest: 1994 Geol. Soc. Am. Ann. Mtg., p. 2A-1 - 2A-30.
- Thompson, R.S., Whitlock, C., Bartlein, P.J., Harrison, S.P., and Spaulding, W.G., 1993, Climatic changes in the western United States since 18,000 yr B.P., *in* Wright, Jr., H.E., Kutzbach, J.E., Webb III, T., Ruddiman, W.F., Street-Perrott, F.A., and Bartlein, P.J., eds., Global climates since the last glacial maximum: University of Minnesota Press, p. 468-513.
- Trenhaile, A.S., 1980, Shore platforms: a neglected coastal feature: Progress in Physical Geography, v. 4, p. 1-23.
- Veeh, H.H., and Chappell, J., 1970, Astronomical theory of climatic change: support from New Guinea: Science, v. 167, p. 862-865.
- Wagner, H.C., Batatian, L.D., Lambert, T.M., and Tomsen, J.H., 1986, Preliminary geologic framework studies—continental shelf and upper continental slope off southwestern Washington: Washington Division of Geology and Earth Resources, Open File Report 86-1.
- Wagner, H.C., and Tomsen, J.H., 1987, Geologic framework within the Strait of Juan de Fuca, 1:250,000: Washington Division of Geology and Earth Resources, Open File Report 87-1.
- Waite, R.B., and Thorson, R.M., 1983, The Cordilleran ice sheet in Washington, Idaho, and Montana, *in* Porter, S.C., ed., Late Quaternary Environments of the United States: University of Minnesota Press, p. 53-70.

- West, D.O., and McCrumb, D.R., 1988, Coastline uplift in Oregon and Washington and the nature of Cascadia subduction zone tectonics: *Geology*, v. 16, p. 169-172.
- Whitlock, C., 1992, Vegetational and climatic history of the Pacific Northwest during the last 20,000 years: implications for understanding present-day biodiversity: *Northwest Environmental Journal*, v. 8, p. 5-28.
- Worona, M.A., and Whitlock, C., 1995, Late Quaternary vegetation and climate history near Little Lake, central Coast Range, Oregon: *Geological Society of America Bulletin*, v. 107, p. 867-876.
- Wright, L.W., 1970, Variation in the level of the cliff/shore platform junction along the south coast of Great Britain: *Marine Geology*, v. 9, p. 347-353.

Glenn David Thackray
Assistant Professor
Department of Geology, Idaho State University
Pocatello, Idaho

Education:

Beloit College: B.S. Geology, 1985; Thesis: Geology of portions of the Jackfish Lake and Basswood Lake West quadrangles, Minnesota (advisor: H.H. Woodard)
University of Oregon: M.S. Geological Sciences, 1989; Thesis: Paleoenvironmental analysis of paleosols and associated fossils in Miocene volcanoclastic deposits, Rusinga Island, western Kenya (advisor: G.J. Retallack)
University of Washington: Ph.D. Geological Sciences, 1996; Dissertation: Glaciation and neotectonic deformation on the western Olympic Peninsula, Washington (advisor: S.C. Porter)

Employment:

<u>Employer</u>	<u>Position</u>	<u>Dates</u>
University of Oregon	Graduate Teaching Fellow/Instructor	1986-1988
Russ Fetrow Engineering, Inc.	Hydrogeologic Consultant	1988-1990
University of Washington	Teaching and Research Assistant	1991-1994
Idaho State University	Assistant Professor	1995-

Publications:

Thackray, G.D. 1994. Fossil nest of sweat bees (Halictinae) from a Miocene paleosol, Rusinga Island, western Kenya. *Journal of Paleontology*, 68:795-800.

Bestland, E.A., G.D. Thackray, and G.J. Retallack. 1995. Cycles of doming and eruption of the Miocene Kisingiri volcano, southwest Kenya. *Journal of Geology*, 103: 598-607.

Thackray, G.D. 1994. Warping of coastal terraces and glacial-interglacial strata, Olympic coast, Washington (abstract). *Proceedings of the Oregon Academy of Sciences* 30:38.

Thackray, G.D. 1994. Extensive Early Wisconsin (Stage 4) Glaciation on the western Olympic Peninsula, Washington (abstract). *Abstracts of the American Quaternary Association Biennial Meeting, Minneapolis, Minnesota*, p. 167.

Thackray, G.D. and F.J. Pazzaglia. 1994. Quaternary stratigraphy, tectonic geomorphology, and fluvial evolution of the western Olympic Peninsula, Washington, *in* D.A. Swanson and R.A. Haugerud, eds., *Geologic Field Trips in the Pacific Northwest*, Geological Society of America Annual Meeting, Seattle, Washington, v. 2, p. A1-29.

Thackray, G.D. 1994. Deformation of Middle and Late Pleistocene strata on the Olympic Coast of Washington (abstract). *Geological Society of America, Abstracts with Programs* 26(7): 523.

Thackray, G.D. 1995. Extent and chronology of glaciation on the western Olympic Peninsula, Washington (abstract). *Geological Society of America, Abstracts with Programs* 27(5): 81.

Thackray, G.D. 1995. Rates of coastal deformation on the Olympic Peninsula, northern Cascadia margin (abstract). *Eos, Transactions of the American Geophysical Union*, 76(46): F534.

Thackray, G.D. and F.J. Pazzaglia. 1996. Quaternary Glaciation and Tectonism on the Western Olympic Peninsula, Washington. *Guidebook for the Friends of the Pleistocene, Third Annual Pacific Northwest Cell Field Conference*.

Thackray, G.D. 1996. Chronology of Middle and Late Wisconsin glacier advances on the Olympic Peninsula, Washington: synchronous with North Atlantic cooling cycles? (abstract). *Geological Society of America, Abstracts with Programs*, 28(7):234.

PLEASE NOTE:

Oversize maps and charts are filmed in sections in the following manner:

LEFT TO RIGHT, TOP TO BOTTOM, WITH SMALL OVERLAPS

The following map or chart has been refilmed in its entirety at the end of this dissertation (not available on microfiche). A xerographic reproduction has been provided for paper copies and is inserted into the inside of the back cover.

Black and white photographic prints (17" x 23") are available for an additional charge.

UMI

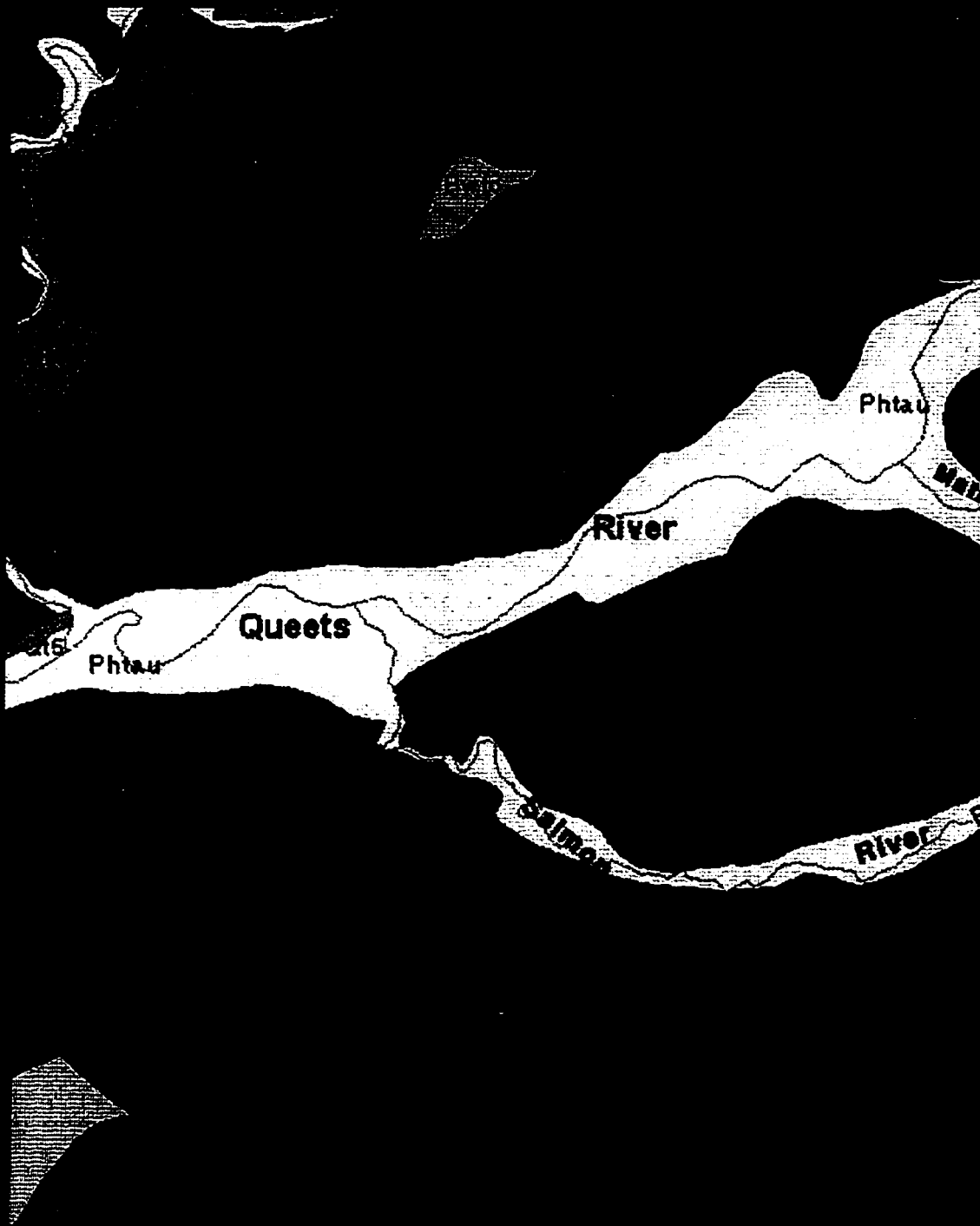


**PLATE 1: QUATERNARY GEOLOGIC MAP
OF THE HOH, QUEETS, AND LOWER
CLEARWATER VALLEYS, WASHINGTON**

0 5 10 km

SCALE 1:100,000

PLEASE NOTE:

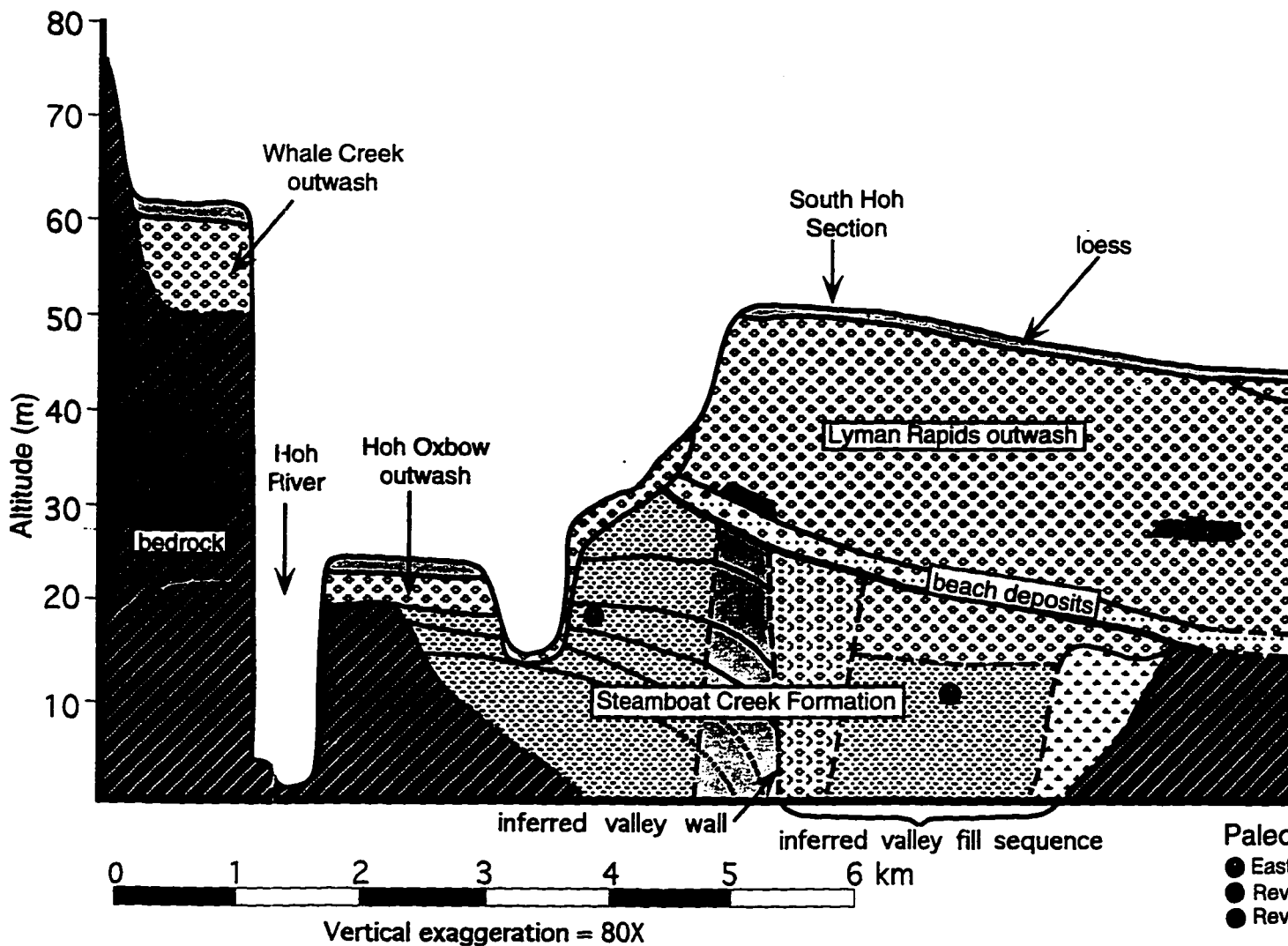
Oversize maps and charts are filmed in sections in the following manner:

LEFT TO RIGHT, TOP TO BOTTOM, WITH SMALL OVERLAPS

The following map or chart has been refilmed in its entirety at the end of this dissertation (not available on microfiche). A xerographic reproduction has been provided for paper copies and is inserted into the inside of the back cover.

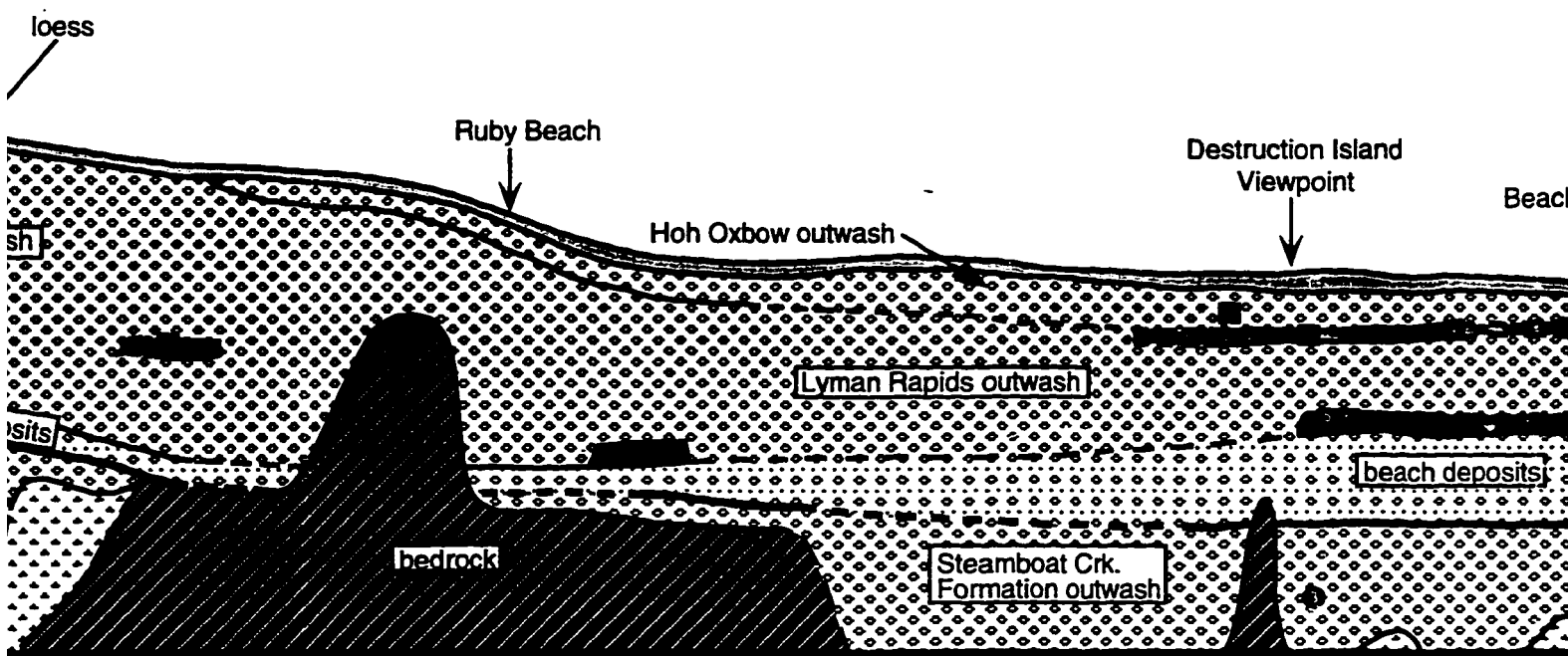
Black and white photographic prints (17" x 23") are available for an additional charge.

UMI



1 3 4 3

Quality of exposure: 5 = continuous exposure, entire section;

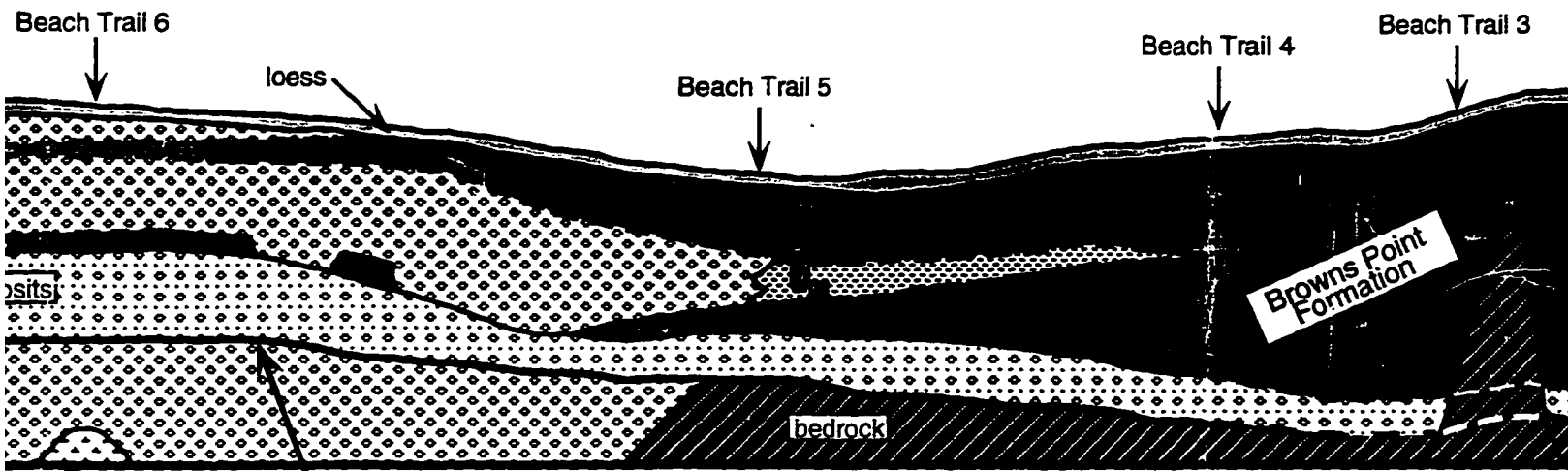


<p>ence</p>	<p>Paleomagnetic polarities</p> <ul style="list-style-type: none"> ● East-directed (excursion) ● Reversed ● Reversed 	<p>Radiocarbon dates</p> <ul style="list-style-type: none"> ■ >49,468 yr BP (AA-18410) ■ 24,422 yr BP (AA- 18401) ■ 36,760 ± 840 yr BP (AA- 15383) ■ 28,352 ± 504 yr BP (AA- 18409) ■ >33,700 yr BP (Florer, 1972) ■ >48,000 yr BP (Florer, 1972)
-------------	--	---

3 | 1 | 3 | 1 | 5 | 2 |

entire section; i = isolated exposures, partial section

PLATE 2: STRA



loess

Beach Trail 6

Beach Trail 5

Beach Trail 4

Beach Trail 3

bedrock

wave-cut surface

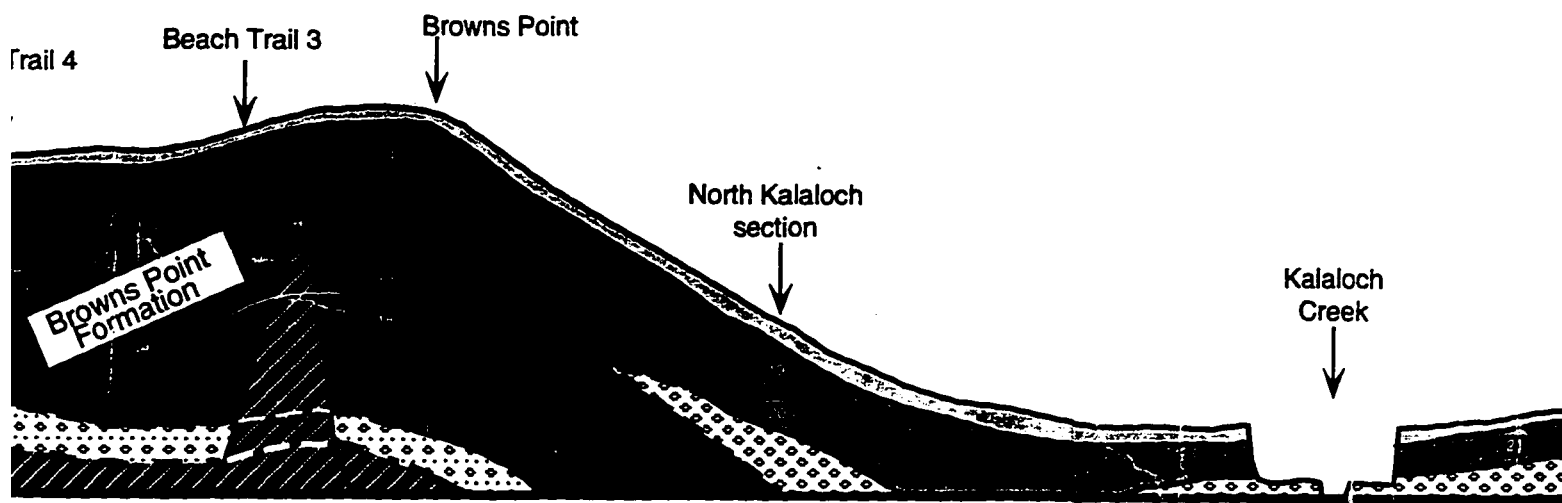
Browns Point Formation

Radiocarbon dates

- 41,600 ± 1500 yr BP (AA- 15375)
- >48,038 yr BP (AA- 16698)
- >49,164 yr BP (AA- 16697)
- 36,120 ± 870 yr BP (AA- 15377)
- 30,560 ± 430 yr BP (AA- 15384)
- 46,659 ± 3366 yr BP (AA- 16695)
- >49,000 yr BP (AA- 15385)
- 16,700 ± 160 yr BP (Heusser, 1972)
- 21,450 ± 300 yr BP (Heusser, 1972)
- 34,100 ± 800 yr BP (Heusser, 1972)
- 42,700 ± 1600 yr BP (Heusser, 1972)
- >47,000 yr BP (Heusser, 1972)
- 30,3
- >49
- 22,4
- 4,57



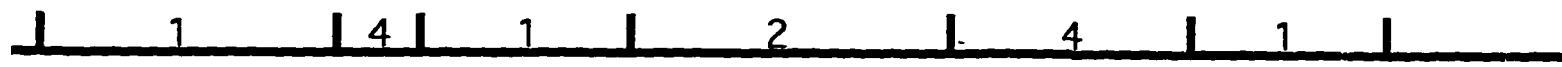
2: STRATIGRAPHIC CROSS-SECTION



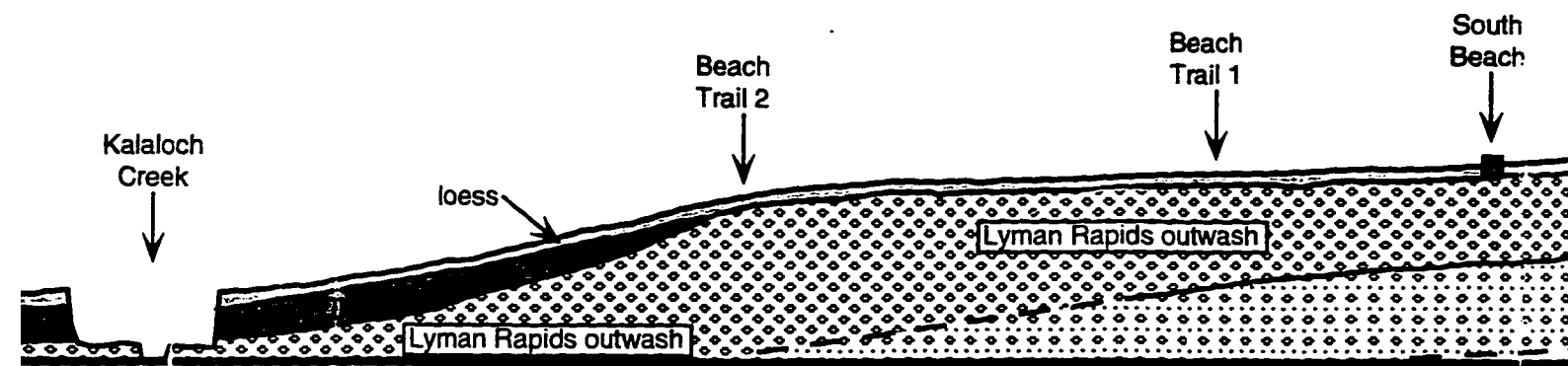
AA- 15385
 r BP (Heusser, 1972)
 r BP (Heusser, 1972)
 r BP (Heusser, 1972)
 yr BP (Heusser, 1972)
 Heusser, 1972)

■ 30,340 ± 260 yr BP (Beta-61321)
 ■ >49,000 yr BP (AA-15379B)
 ■ 22,440 ± 220 yr BP (AA- 15378)
 ■ 4,570 ± 60 yr BP (Beta-62572)

■ glacial silt (distal
 ■ outwash
 ■ loess
 ■ silty/sandy interbe



S-SECTION, HOH RIVER TO RAFT

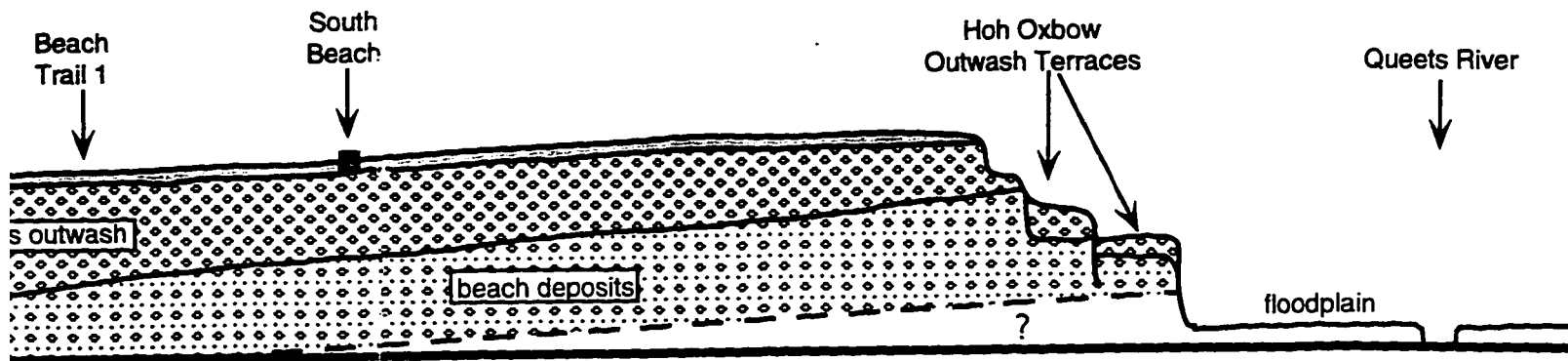


Key to lithology

glacial silt (distal outwash)	BPF-sand/gravel/silt facies	interglacial silt/sand/peat	sand and till
outwash	BPF-silt/sand/peat facies	glacial-lacustrine sand/silt	glacial-m...
loess	BPF-silt/clay/peat facies	eolian sand/silt interbeds	bedrock
silty/sandy interbeds	BPF-clay/peat facies	fluvial gravel and sand	

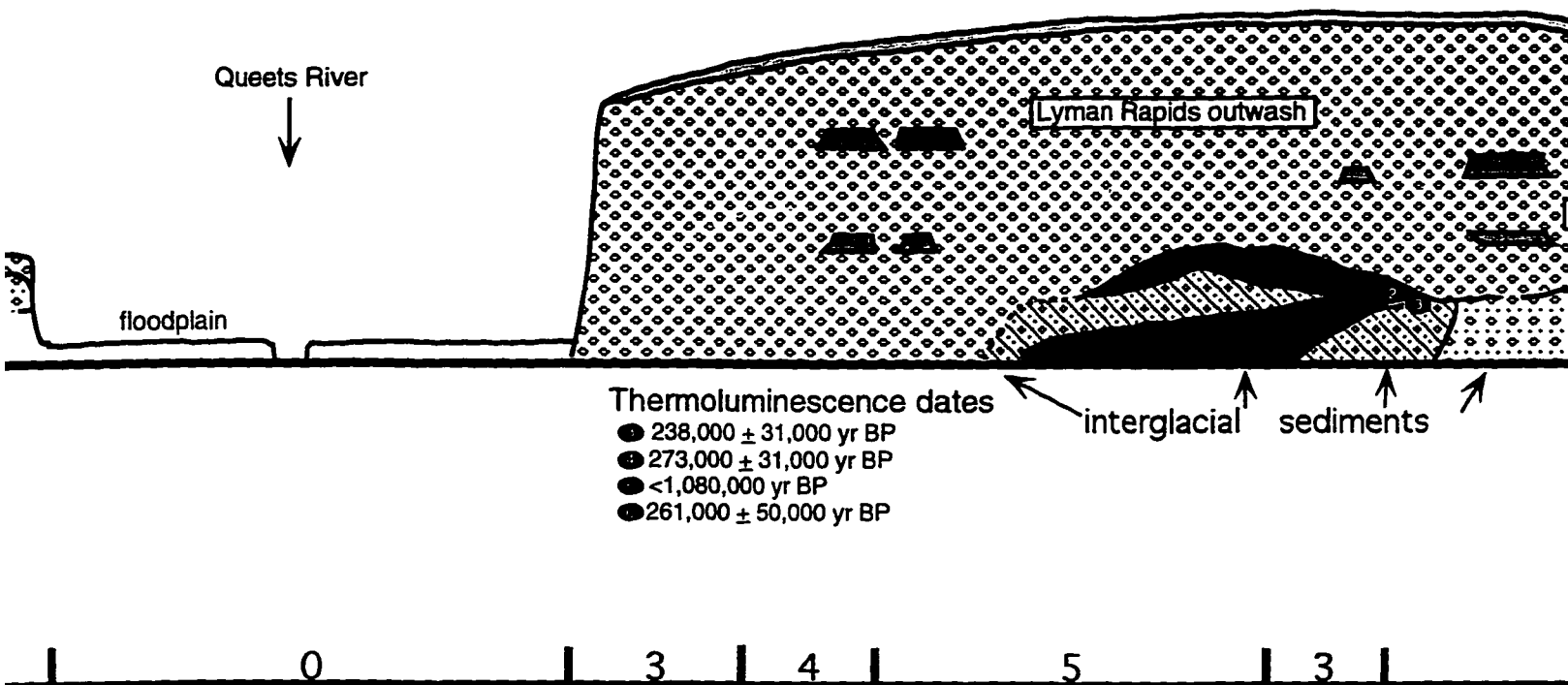
1 4 2

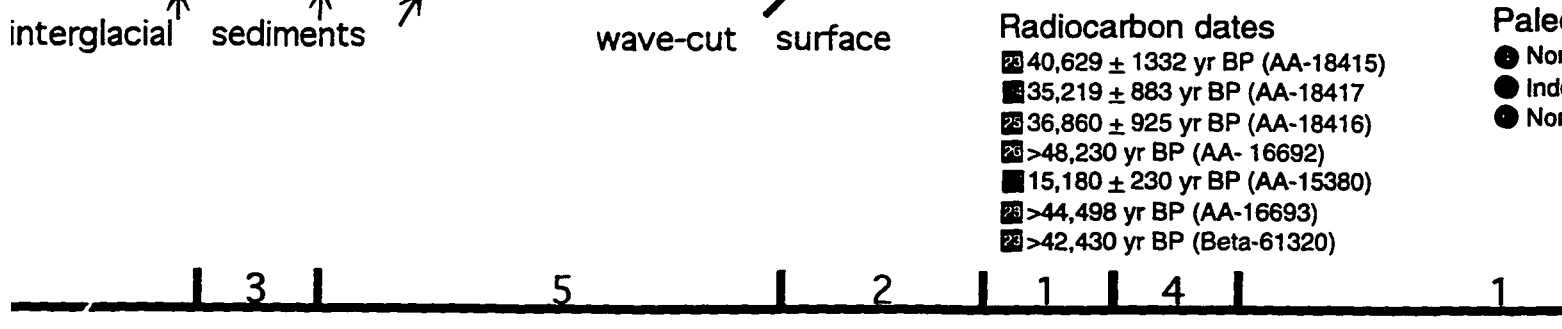
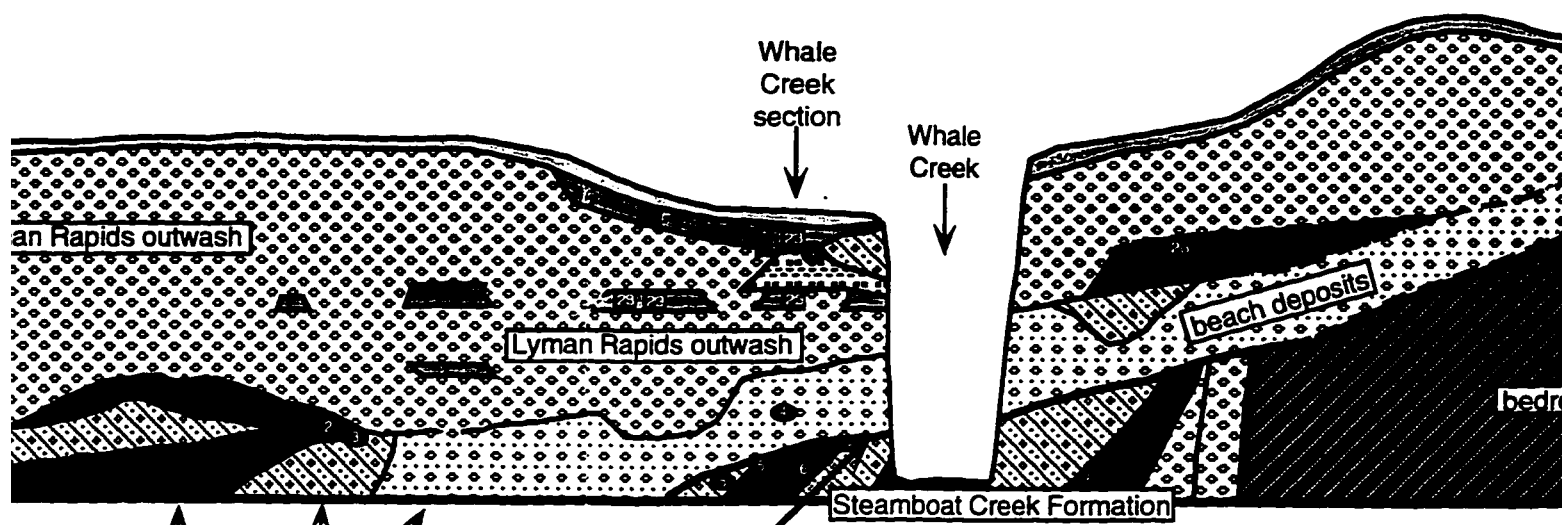
TO RAFT RIVER

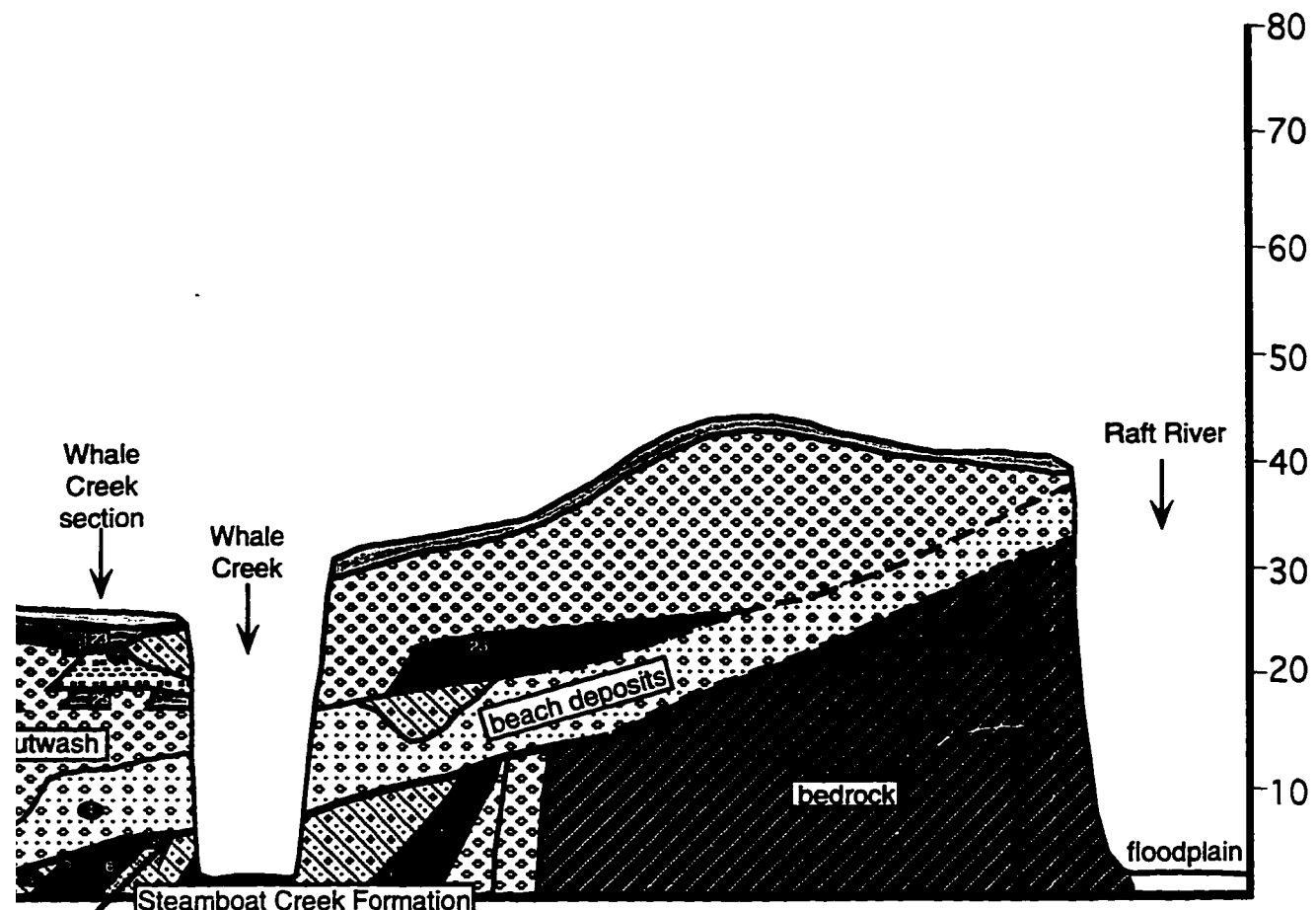


- | | |
|-------------------|----------------------------|
| l silt/sand/peat | sand and gravel beach dep. |
| ustrine sand/silt | till |
| nd/silt interbeds | glacial-marine drift |
| vel and sand | bedrock |









cut surface

- Radiocarbon dates**
- 20 40,629 ± 1332 yr BP (AA-18415)
 - 21 35,219 ± 883 yr BP (AA-18417)
 - 22 36,860 ± 925 yr BP (AA-18416)
 - 23 >48,230 yr BP (AA-16692)
 - 24 15,180 ± 230 yr BP (AA-15380)
 - 25 >44,498 yr BP (AA-16693)
 - 26 >42,430 yr BP (Beta-61320)

- Paleomagnetic polarities**
- Normal
 - Indeterminate
 - Normal

